

FIGURE 14.1.1-2

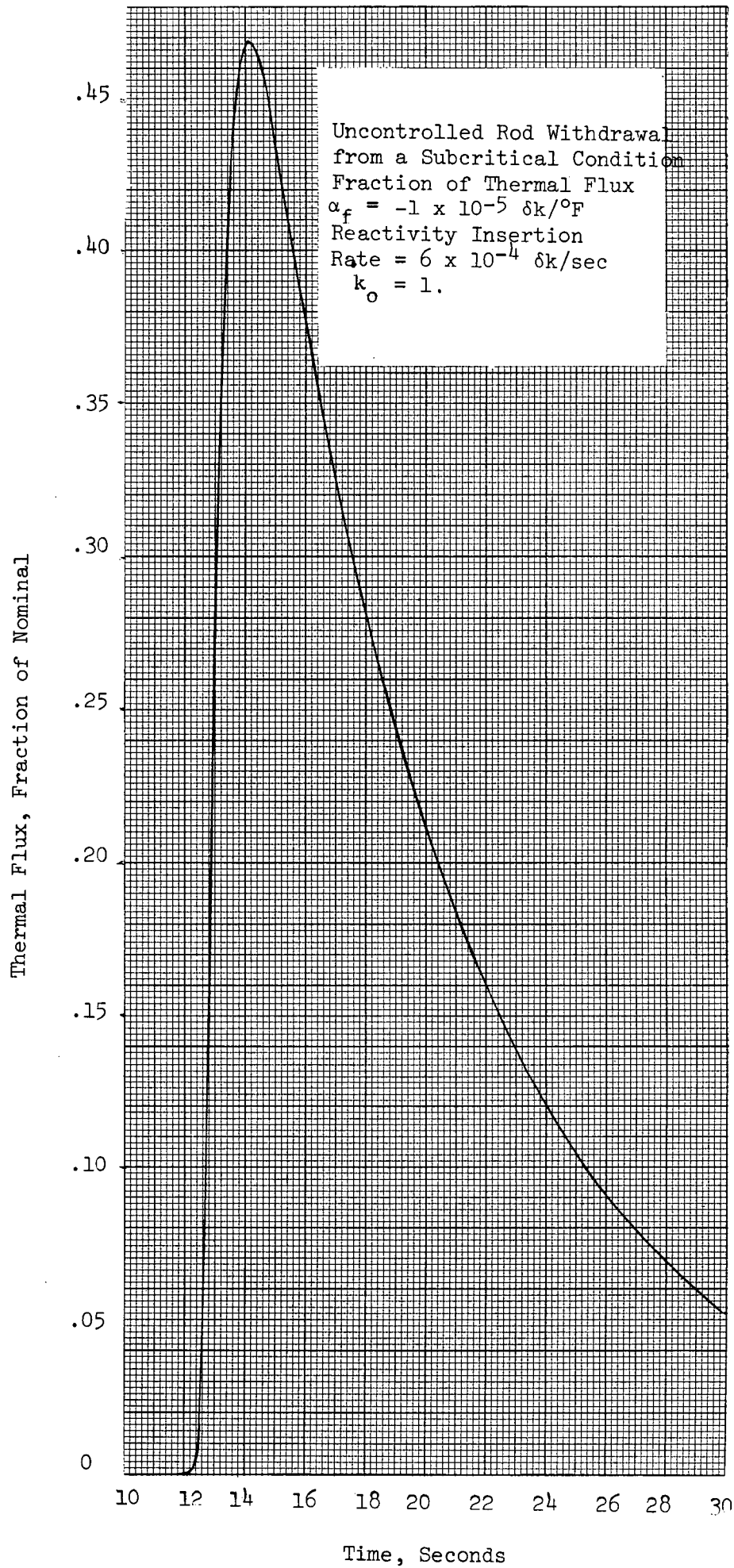


FIGURE 14.1.1-3

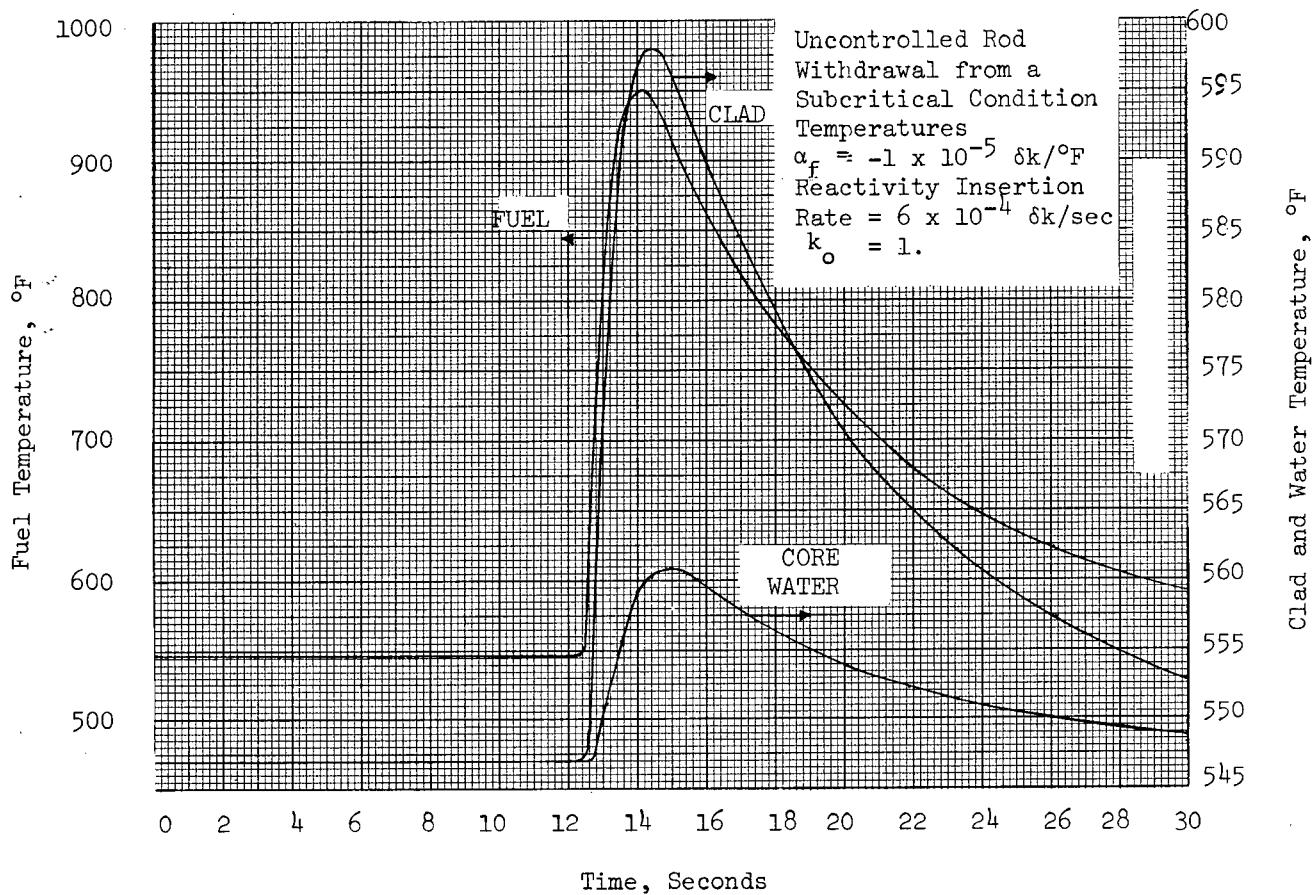


FIGURE 14.1.1-4

14.1.2 UNCONTROLLED RCCA WITHDRAWAL AT POWER

An uncontrolled RCCA withdrawal at a core power of 2244 MW(t) results in an increase in core heat flux. Since the heat extraction from the steam generator remains constant, there is a net increase in reactor coolant temperature. Unless terminated by manual or automatic action, this power mismatch and resultant coolant temperature rise would eventually result in DNB. Therefore, to prevent the possibility of damage to the cladding, the Reactor Protection System is designed to terminate any such transient with an adequate margin to DNB.

The automatic features of the Reactor Protection System which prevent core damage in a rod withdrawal accident at power include the following:

- a) Nuclear power range instrumentation actuates a reactor trip if two out of the four channels exceed an overpower setpoint.
- b) Reactor trip is actuated if any two out of three ΔT channels exceed an overtemperature ΔT setpoint. This setpoint is automatically varied with power distribution, temperature and pressure to protect against DNB.
- c) Reactor trip is actuated if any two out of three ΔT channels exceed an overpower ΔT setpoint. This setpoint is automatically varied with power distribution to ensure that the allowable fuel power rating is not exceeded.
- d) A high pressure reactor trip, actuated from any two out of three pressure channels, is set at a fixed point. This set pressure will be less than the set pressure for the pressurizer safety valves.

- e) A high pressurizer water level reactor trip, actuated from any two out of three level channels, is actuated at a fixed setpoint. This affords additional protection for RCCA withdrawal accidents.

The manner in which the combination of overpower and overtemperature ΔT trips provide protection over the full range of reactivity insertion rates is illustrated in Section 7. Figure 7.2-8 represents the possible conditions of reactor vessel average temperature and ΔT with the design power distribution in a two-dimensional plot. The boundaries of operation defined by the overpower ΔT trip and the overtemperature ΔT trip are represented as "protection lines" on this diagram - the overpower ΔT trip as a line and the overtemperature ΔT trip as a family of sloping lines. The protection lines are drawn to include all adverse instrumentation and setpoint errors, so that under nominal conditions trip would occur well within the area bounded by these lines. A maximum steady state operating condition for the reactor is shown on the figure.

The utility of the diagram just described is in the fact that the operating limit imposed by any given DNB ratio can be represented as a line on this coordinate system. The DNB lines represent the locus of conditions for which the DNBR equals 1.3. All points below and to the left of this line have a DNB ratio greater than this value. The diagram shows that DNB is prevented for all cases if the area enclosed within the maximum protection lines is not traversed by the applicable DNB ratio line at any point.

The region of permissible operation (power, pressure and temperature) is completely bounded by the combination of reactor trips: nuclear overpower (fixed setpoint); high pressure (fixed setpoint); low pressure (fixed setpoint); overpower and overtemperature ΔT (variable setpoints). These trips are designed to preclude a DNB ratio of less than 1.30.

Method of Analysis

The purpose of this analysis is to demonstrate the manner in which the above protective systems function for various reactivity insertion rates from different initial conditions. Reactivity coefficients, initial conditions and effects of control functions govern which protective function occurs first.

Analysis is performed using several digital computer codes. First, the actual core limits are determined employing the W-3 DNB correlation described in Section 3. These limits are shown on Figure 7.2-2. Protection lines, illustrated in Figure 7.2-8 are then selected and incorporated into a transient analysis by a detailed digital simulation of the unit.

In the analysis, the effect of the RCCA movement on core power distribution is considered by its effect of causing a decrease in overtemperature ΔT and overpower ΔT trip setpoints proportionate to the decrease in margin to DNB. This has the effect of causing a reactor trip sooner in the transient.

Results

Figures 14.1.2-1 and 14.1.2-2 show the response of nuclear power, average coolant temperature, pressure, and DNB ratio to a rapid rod withdrawal (5.625×10^{-4} $\delta k/\text{sec}$) accident starting from full load. Initial conditions assumed maximum power and temperature errors. Nominal reactivity coefficients for beginning of core life were assumed. Reactor trip on high nuclear power assumed to be actuated at a conservative value of 118% of nominal occurs in approximately 3 seconds after start of the accident. Since this is rapid with respect to the thermal time constants of the plant, small changes in T_{avg} and pressure result. The minimum DNB ratio is 1.49.

The response of nuclear power, average coolant temperature, pressure and DNB ratio for a slow rod withdrawal (2.5×10^{-5} $\delta k/sec$) from full power is shown in Figures 14.1.2-3 and 14.1.2-4. Reactor trip on overtemperature ΔT trip occurs after approximately 50 seconds. The rise in temperature and pressure is quite large. The minimum DNB ratio reached during the transient is 1.34.

Figure 14.1.2-5 shows the minimum DNB ratio as a function of reactivity insertion rate from initial full power operation. It can be seen that two reactor trip channels provide cover over the whole range of reactivity rates, these are high nuclear flux and overtemperature ΔT trip channels. The cross over point between the two zones of effectiveness occurs when the reactivity rate is 1×10^{-4} $\delta k/sec$. The minimum DNB ratio is never less than 1.34.

For rod withdrawal accidents starting at 80 per cent power, reactor trip occurs because of the activation of one of three different trip channels, namely high pressurizer level, overtemperature ΔT and high nuclear flux as shown in Figure 14.1.2-6. For low reactivity rates, less than 10^{-5} $\delta k/sec$, trip occurs from high pressurize level. For high reactivity rates, greater than 2×10^{-4} $\delta k/sec$, trip occurs from high nuclear flux. Between these two limits the trip is initiated by high ΔT overtemperature trip. The minimum DNB ratio for the range of reactivity rates is greater than 1.30.

Figure 14.1.2-7 shows the minimum DNB ratio as a function of reactivity insertion rate for rod withdrawal accidents starting at 60 per cent power.

The results are very similar to the 80% power case, except that the range over which the overtemperature ΔT trip operates is smaller. The high pressurizer level trip acts sooner than the ΔT overtemperature trip for the lower reactivity rates. The minimum value of DNB ratio for all reactivity rates is 1.32.

Conclusions

In the unlikely event of a control rod withdrawal incident, from full power operation or lower power level, the core and reactor coolant system are not adversely affected since the minimum value of DNB ratio reached is in excess of 1.3 for all rod reactivity rates. Protection is provided by nuclear flux overpower, overtemperature ΔT and high pressurizer level trips. The preceding sections have described the effectiveness of these protection channels.

Transient Response for
Uncontrolled Rod Withdrawal
From Full Power Terminated
by Nuclear Overpower Trip

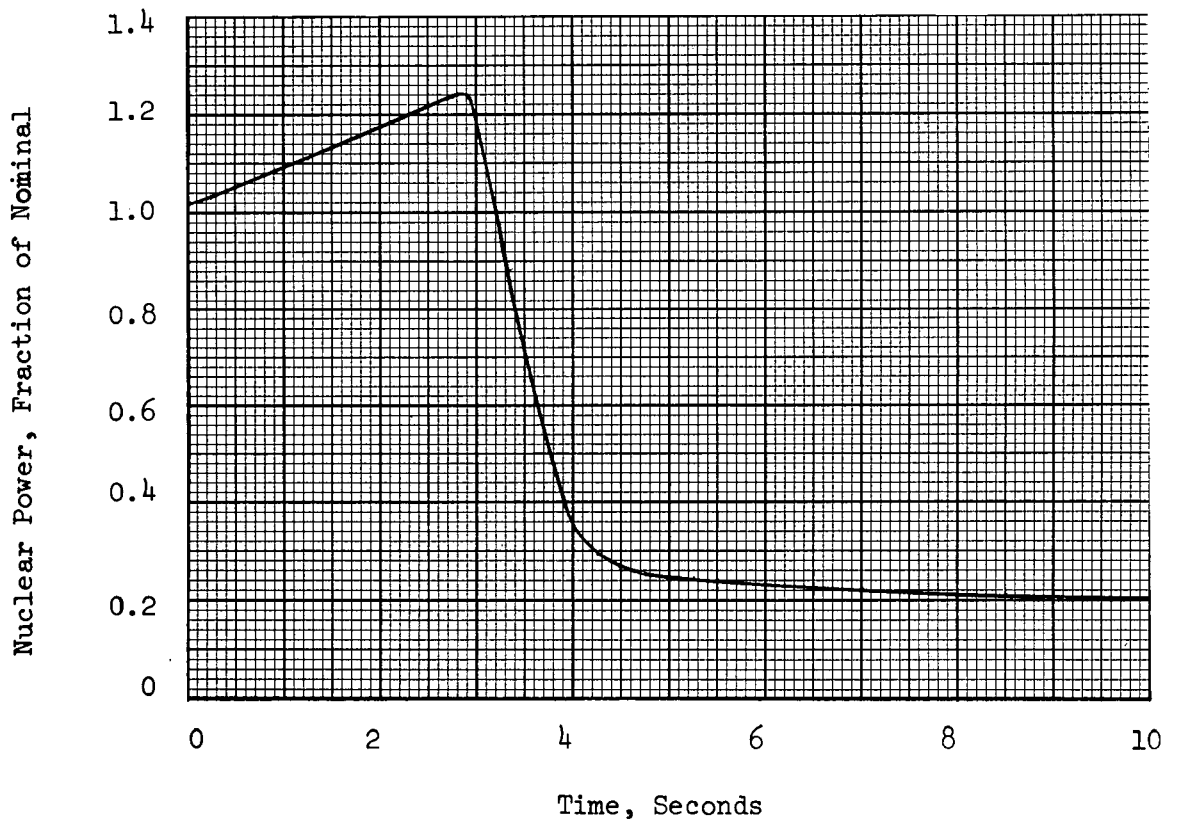
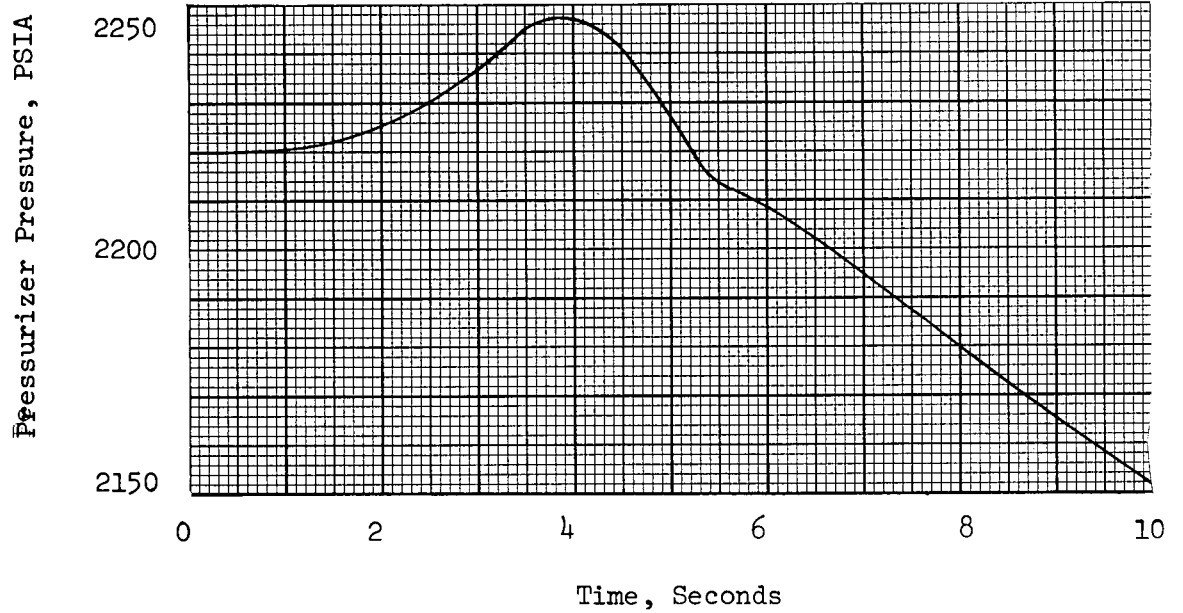


FIGURE 14.1.2-1

Transient Response for
Uncontrolled Rod Withdrawal
from Full Power Terminated
by Nuclear Overpower Trip

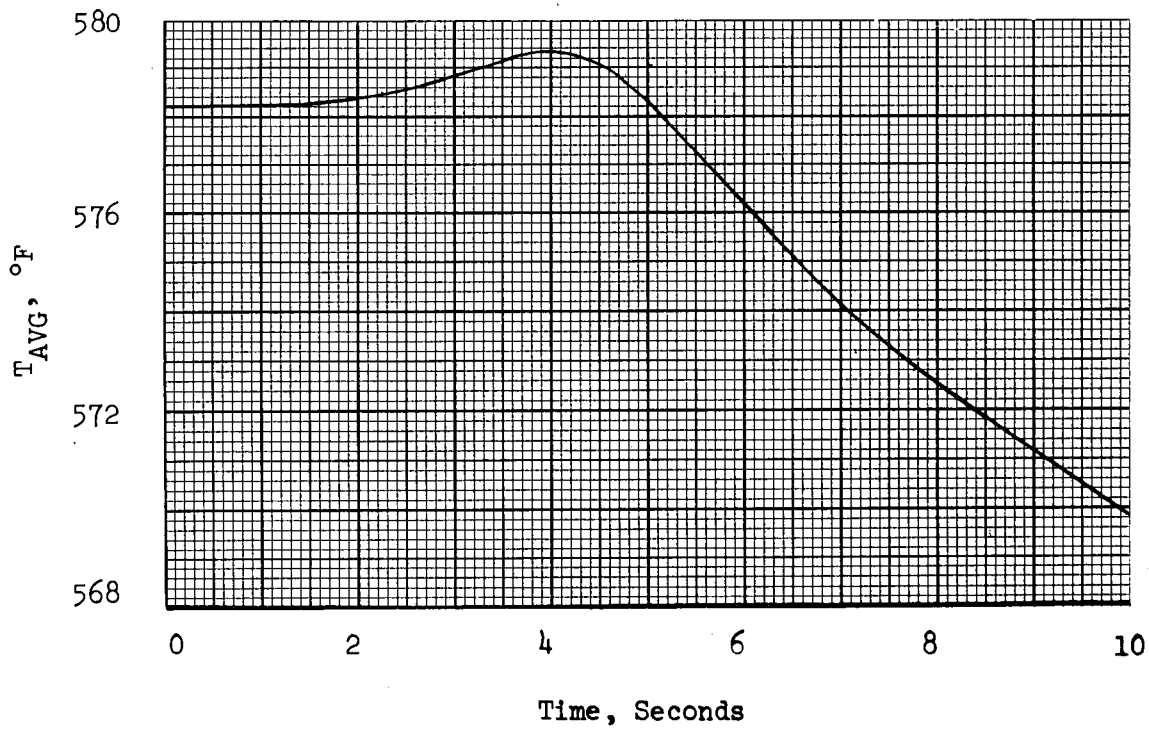
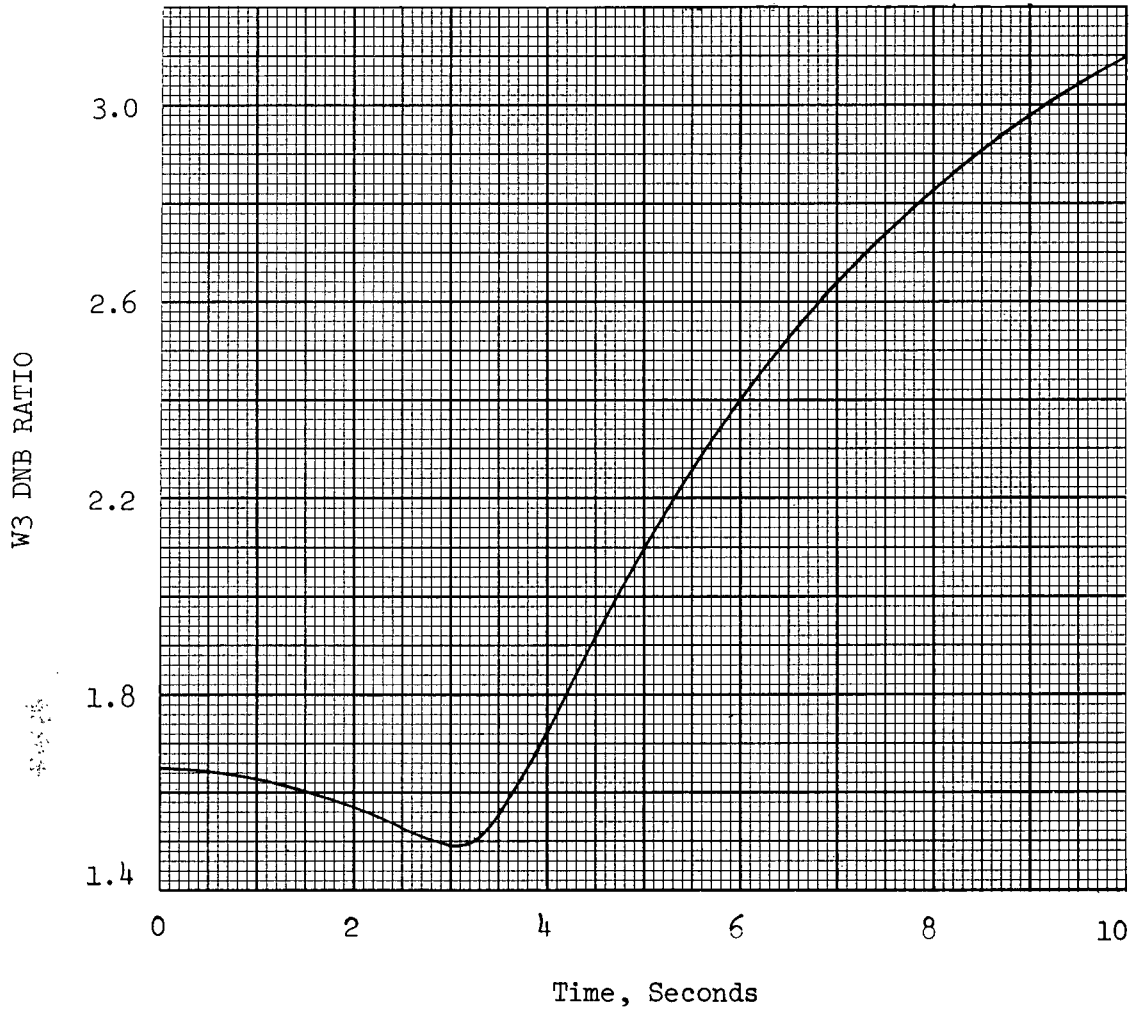


FIGURE 14.1.2-2

Transient Response for Uncontrolled
Rod Withdrawal from Full Power
Terminated by Overtemperature ΔT Trip

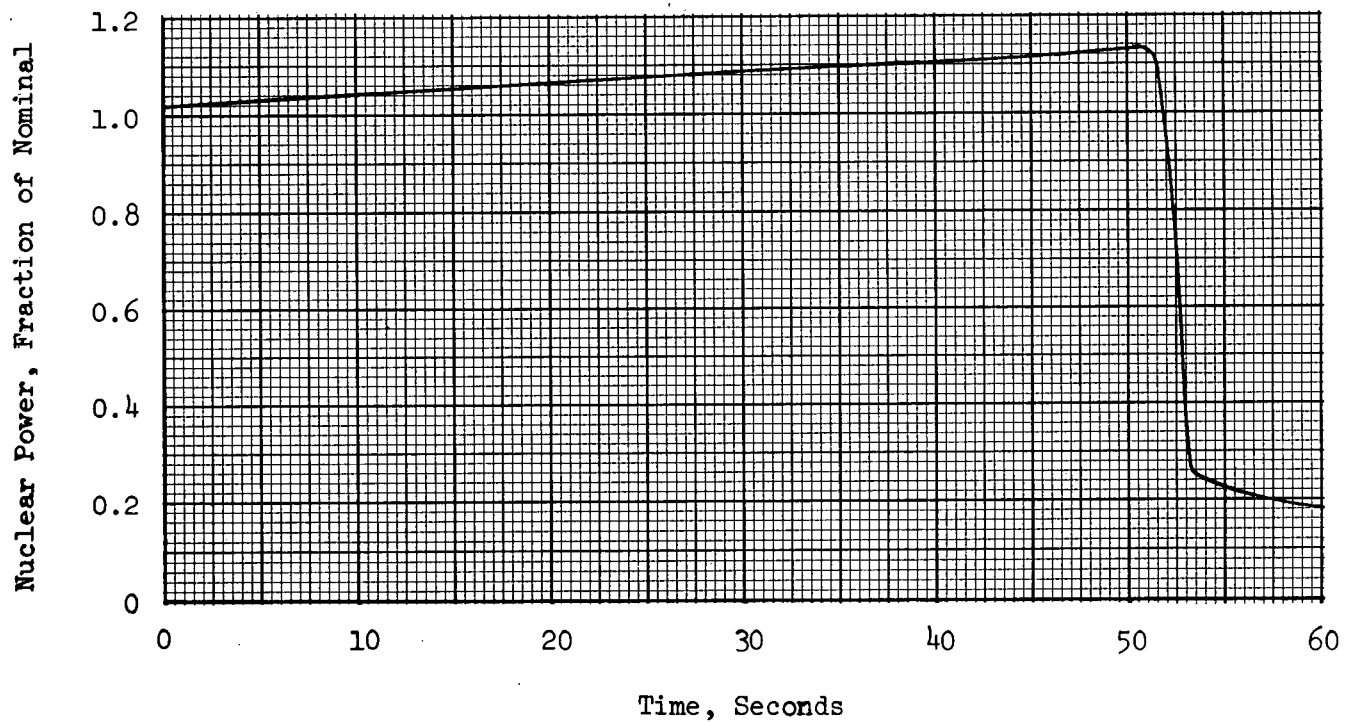
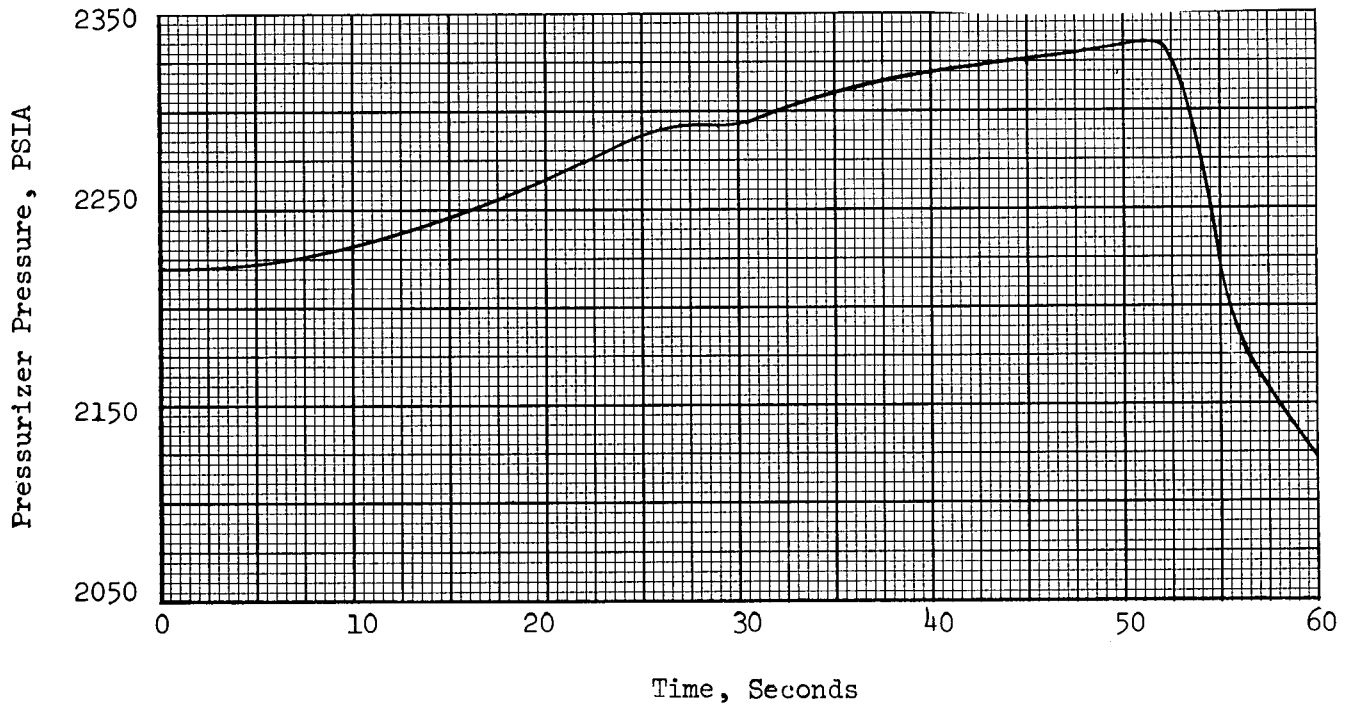


FIGURE 14.1.2-3

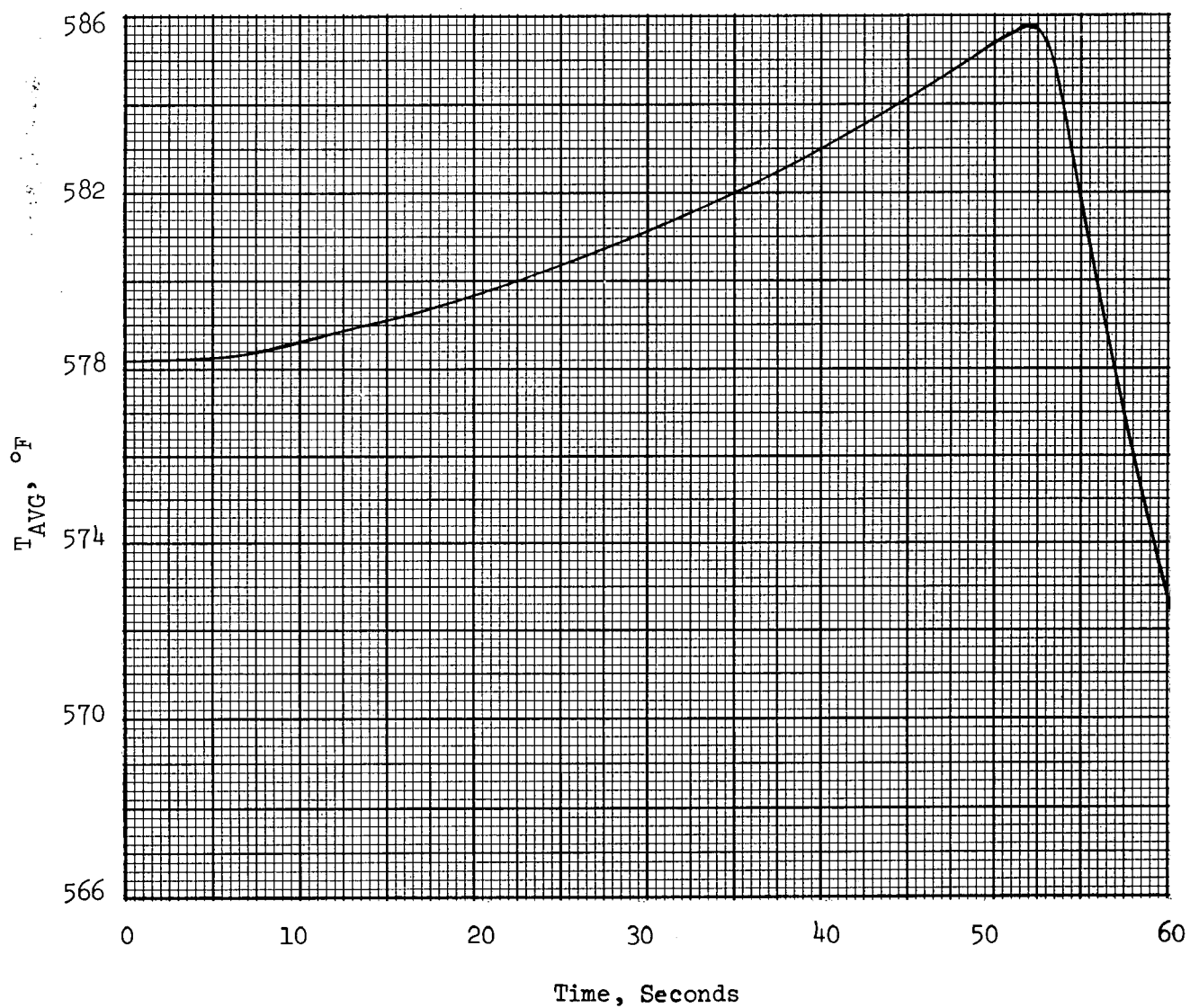
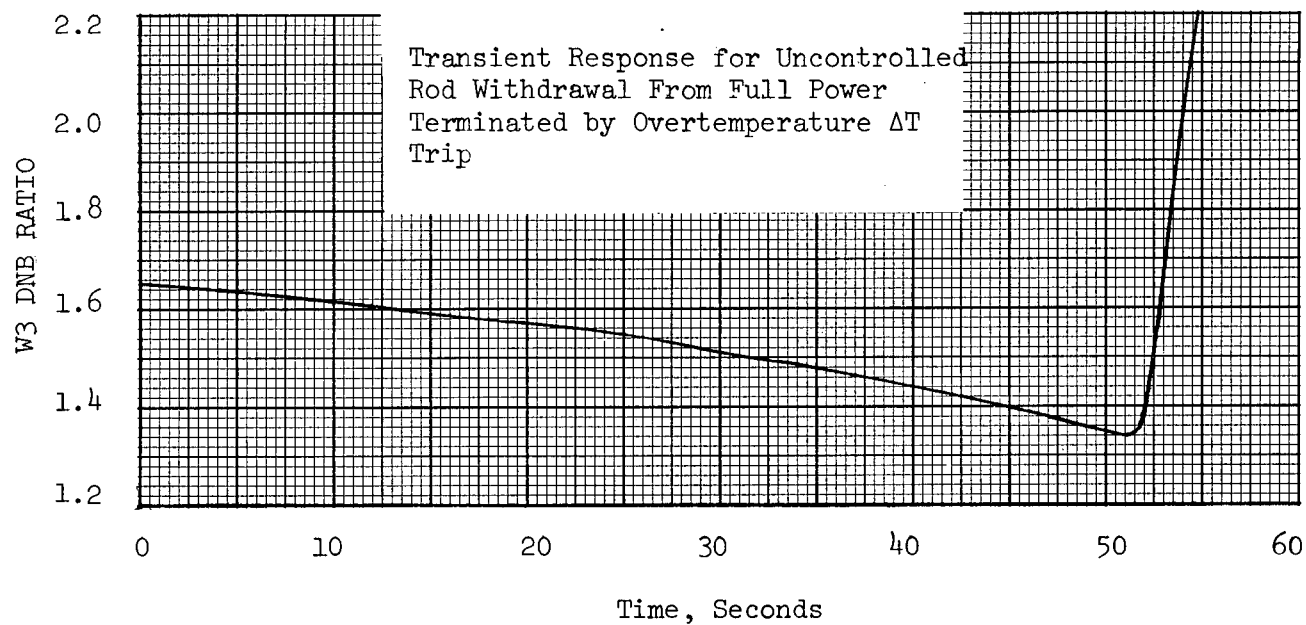


FIGURE 14.1.2-4

Effect of Reactivity Insertion
Rate on Minimum DNB Ratio for
a Rod Withdrawal Accident from
Full Power Conditions

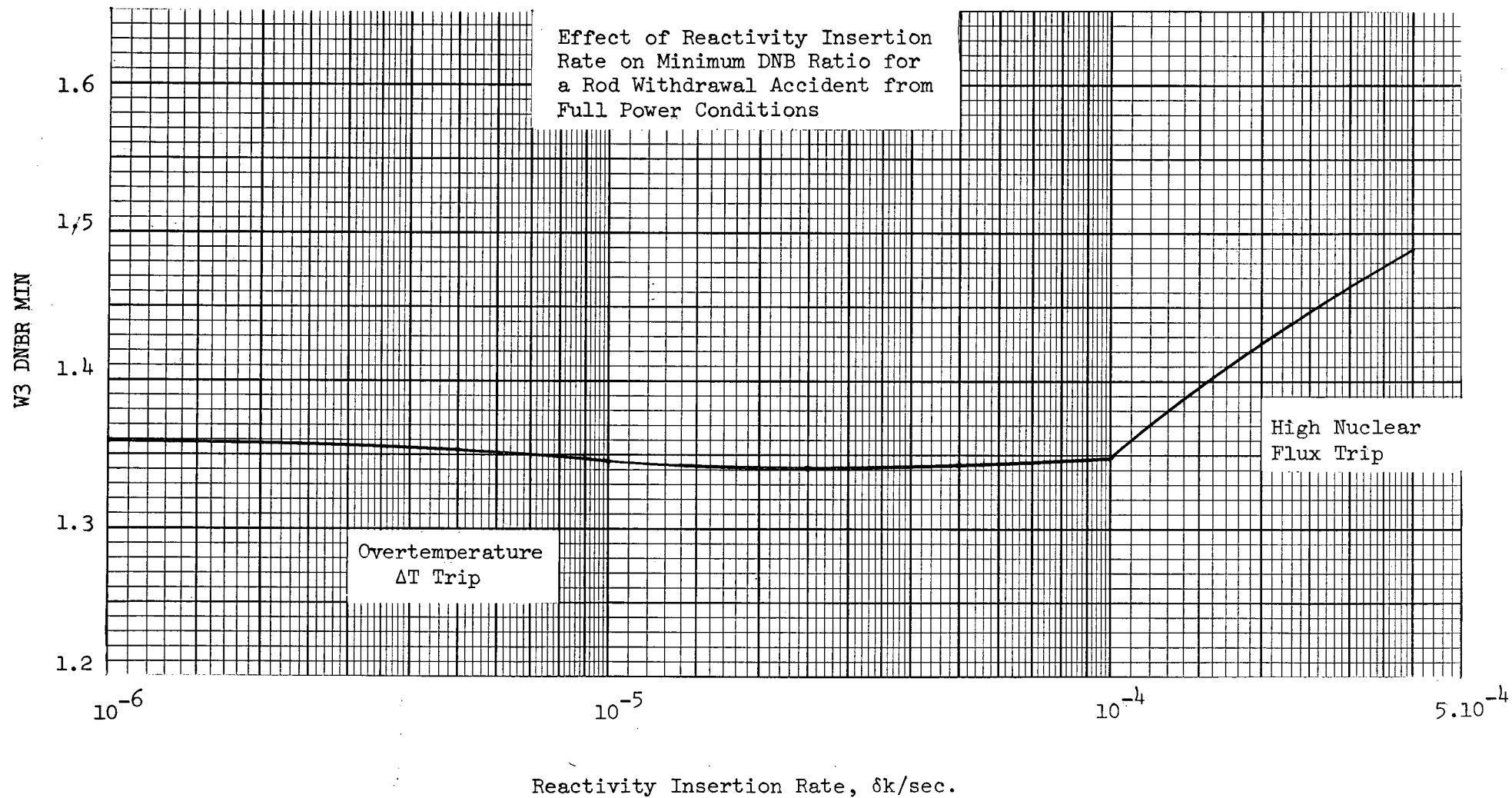


FIGURE 14.1.2-5

FIGURE 14.1.2-6

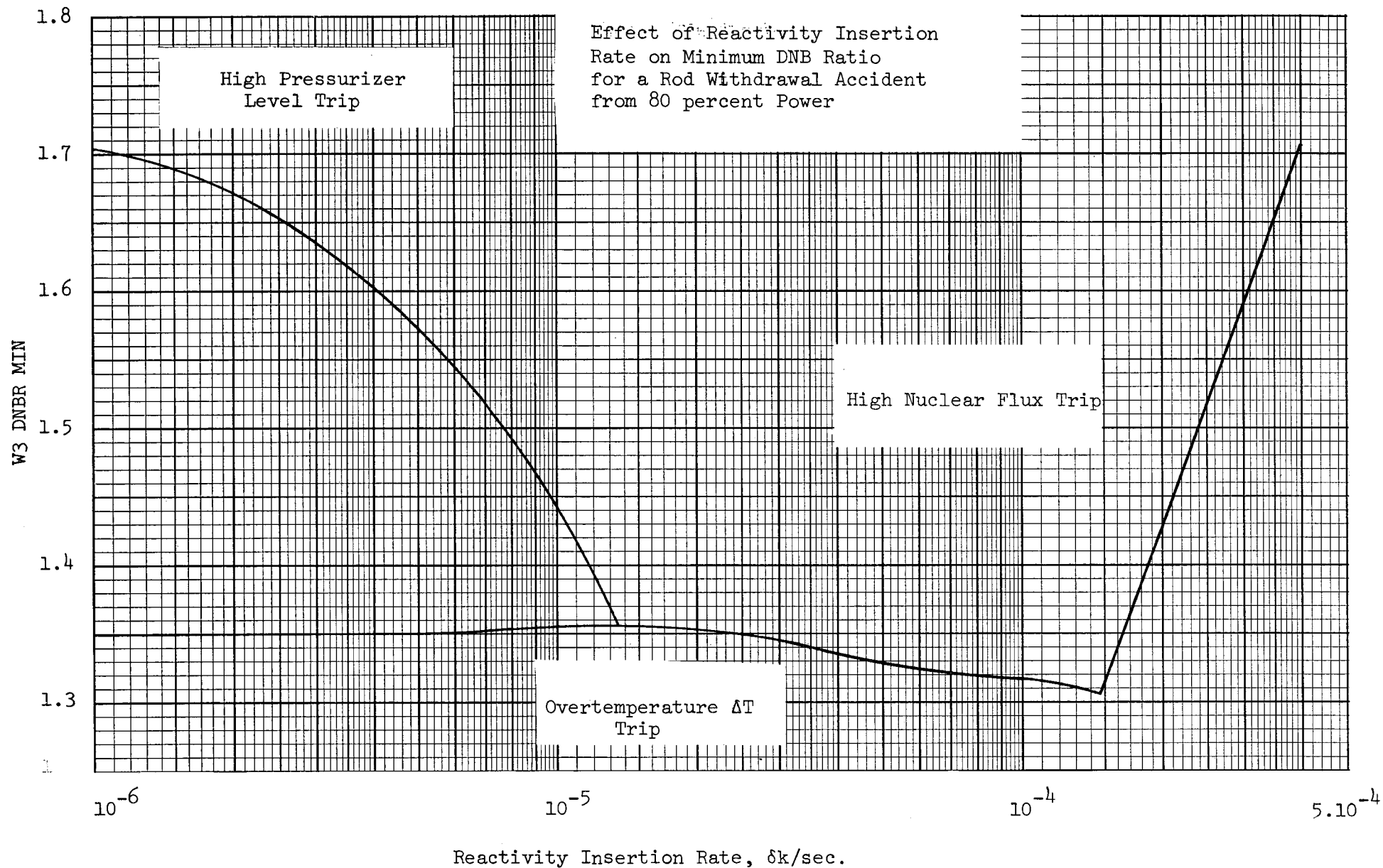
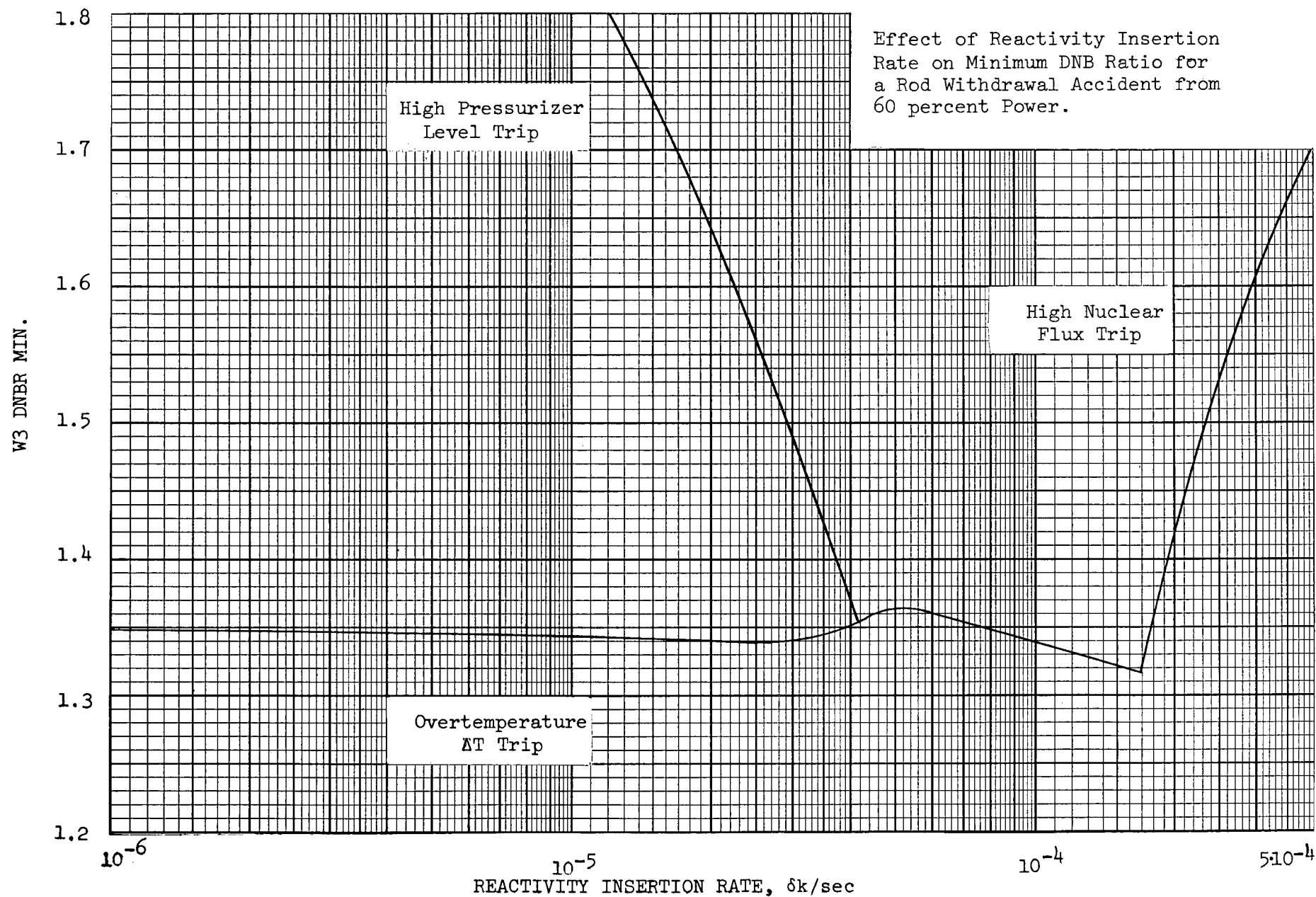


FIGURE 14.1.1.2-7



14.1.3 MALPOSITIONING OF THE PART LENGTH RODS AND XY CONTROL RODS

Part Length Rods

The part length rods are employed to improve the axial power distribution as well as to control potential axial xenon oscillations.⁽¹⁾ A failure of the power supply will not cause these rods to drop into the core. Since the rods are controlled manually, the only malfunctions that can occur are due to operator action or inaction.

The maximum rod speed is 15 in/minute, so that if the operator continuously withdraws the rods erroneously the consequences are less severe than for the full length rod withdrawal cases considered in Sections 14.1.1 and 14.1.2.

When the plant is operating at steady state, the operator is called upon to move the part length rods at intervals of several hours. However, when major load changes occur some administrative control has to be performed to maintain the part length rods within a prescribed allowable region of travel. The instrumentation system provides adequate information for the manual control of the part length rods.

The part length rods may have to be moved periodically (every 3 to 5 hours) to damp out axial xenon oscillations. A period of the order of 24 hours, without control, would be required for the axial oscillations to become serious.

The axial distribution is, however, continuously monitored by the upper and lower sections of out-of-core ion chambers. Out-of-limit signals are generated should the relative readings differ by a preset amount. No alarms are actuated directly by the out-of-limit signals. However, the reactor protection system automatically resets the overpower and overtemperature trip settings to a level consistent with the power distribution. A reduction in the power capability might be necessary until the normal power distribution is restored.

The Control and Protection System automatically initiates a turbine cutback to prevent an unnecessary trip. Thus the Control and Protection System ensures that the core limits are not reached as a result of operator inaction. Once the operator takes the necessary steps to rectify the maldistribution in axial flux, the turbine load can be increased to the previous level.

XY Control Rods

Although it is expected that this core will be stable to XY xenon oscillations for the nominal feedback conditions plus uncertainties, the capability is provided to control any oscillations should they occur.⁽¹⁾

The X-Y control rods are operated manually, one or two selected rods at a time. The control strategy to be employed is to correct for any XY offset greater than ten percent. The XY offset is the ratio of the power in any one quadrant of the core to the average power.

If the XY offset reaches ten percent then the XY control rod, which is located in the quadrant with the power peak, is inserted manually into the core. The rod is left in the core until the xenon has redistributed (4 hours) and then the rod is withdrawn.

The operator is provided with rod position indication for each XY rod. An alarm is actuated when any rod bottom defeat switch is actuated so that an XY rod can be inserted into the core. This defeat switch must be actuated to prevent a load cutback and block an automatic rod withdrawal.

The operator is thus presented with sufficient information to prevent him incautiously inserting an X-Y rod. Should this occur, automatic rod withdrawal is blocked by 1/4 high nuclear power, high ΔT in any two loops or T_{avg} deviation in any single loop. Alarms are sounded in all cases and in the case of the ΔT deviation a load cutback also ensues.

REFERENCE: Section 14.1.3

1. Westinghouse Proprietary, "Power Distribution Control in Westinghouse Pressurized Water Reactors," WCAP-7208 (1968).

14.1.4 ROD CLUSTER CONTROL ASSEMBLY (RCCA) DROP

Dropping of a full length RCCA could occur only when the drive mechanism is de-energized. This would result in a power reduction and an increase in the hot channel factor. If no protective action occurred, the Reactor Control System would restore the power to the level which existed before the incident. This would lead to a reduced safety margin or possibly DNB, depending upon the magnitude of the hot channel factor.

If a RCCA drops into the core during power operation (2244 MWt), it would be detected by either a rod bottom signal device or by the use of the out of core ion chambers.⁽¹⁾ The rod bottom signal device provides an individual position indication signal for each RCCA. Initiation of this signal is independent of lattice location, reactivity worth or power distribution changes inherent with the dropped RCCA. The other independent indication of an RCCA drop is obtained by using the out of core power range channel signals. This rod drop detection circuit is actuated upon sensing a rapid decrease in local flux such as could occur from depression of flux in one region by a dropped RCCA. This detection circuit is designed such that normal load variations do not cause it to be actuated.

A rod drop signal from any rod position indication channel, or from one or more of the four power range channels, initiates protective action by reducing turbine load by a preset adjustable amount and blocking of further automatic rod withdrawal. Either action individually prevents core damage. The turbine runback is redundantly obtained by acting upon the turbine load limit and on the turbine governor control system. The rod stop is also redundantly actuated.

Method of Analysis

The transient following a dropped RCCA accident is determined by a detailed digital simulation of the plant. The dropped rod is assumed to cause a step decrease in reactivity and the core power generation is determined using a point neutron kinetics model. The overall plant response is calculated by simulating the turbine load runback and blocking of automatic rod withdrawal. The analysis is performed for the case in which the load cutback nearly matches the power decrease from the negative reactivity for a dropped rod ($-2.0 \times 10^{-3} \delta k$), and also for the case in which the load cutback is greater than that required to match the worth of the dropped rod ($-1.0 \times 10^{-3} \delta k$). In both cases the load is assumed to be cut back from 100 to 75 per cent of full load at a conservatively slow rate of one per cent per second. The actual amount of load cutback to be used will be determined during initial startup experiments and will be set to match the power reduction caused by the highest worth dropped rod.

The most negative values of moderator and Doppler temperature coefficients of reactivity are used in this analysis resulting in the highest heat flux during the transient. These are a moderator temperature coefficient of $-3.5 \times 10^{-4} \delta k/^{\circ}F$ and a Doppler coefficient of $-1.0 \times 10^{-5} \delta k/^{\circ}F$. A control group worth of $6 \times 10^{-5} \delta k/in$ is assumed as equilibrium conditions are restored.

Results

Figures 14.1.4-1 and 14.1.4-2 illustrate the transient response following a dropped rod of $2.0 \times 10^{-3} \delta k$. The coolant average temperature decreases rapidly initially, then decreases slowly to new equilibrium condition. The peak heat flux following the initial response to the dropped rod is 95 per cent of nominal. At the same time the core average temperature drops by $2^{\circ}F$ and the pressure by 28 psi.

Figures 14.1.4-3 and 14.1.4-4 illustrate the transient response following a dropped rod of $1. \times 10^{-3} \delta k$. Again the coolant average temperature decreases initially, and then increases because of the negative reactivity feedback and the load cutback: The equilibrium temperature will again be achieved in about six minutes. For this case the peak heat flux following the initial response to the dropped rod is 96.5 per cent of nominal. At the same time the core average temperature drops by 1°F and the pressure by 40 psi.

An analysis has been made of the amount of flux tilt that can be tolerated without core damage for the maximum full power operating conditions (2244 MWt power; core water inlet temperature of 550.2°F primary pressure of 2220 psia); a more conservative condition than those mentioned above. The effect of the flux tilt was represented by an increase in the radial heat flux hot channel factor. It was found that this factor could be increased by 12 per cent before reaching a DNB ratio of 1.30. During initial startup experiments, it will be verified that the flux tilt caused by the worst dropped rod, coupled with the thermal flux, coolant temperature, and primary system pressure responses, will not result in a condition of DNB.

Conclusions

Protection for a dropped RCCA is provided by automatic turbine power cutback and blocking of automatic rod withdrawal. The magnitude of the power cutback is to be determined during the initial startup tests. As the analyses presented show, the protection system, in conjunction with the load cutback, protects the core from DNB for a power tilt of 12 per cent at maximum full power conditions, greater than expected for the plant. At the reduced power condition following the rod drop, this allowable tilt will be even greater.

The power tilt will be experimentally determined and the protection system set to maintain a DNBR greater than 1.30.

REFERENCES: Section 14.1.4

1. Westinghouse Proprietary, "Power Distribution Control in Westinghouse Pressurized Water Reactors," WCAP-7208 (1968).

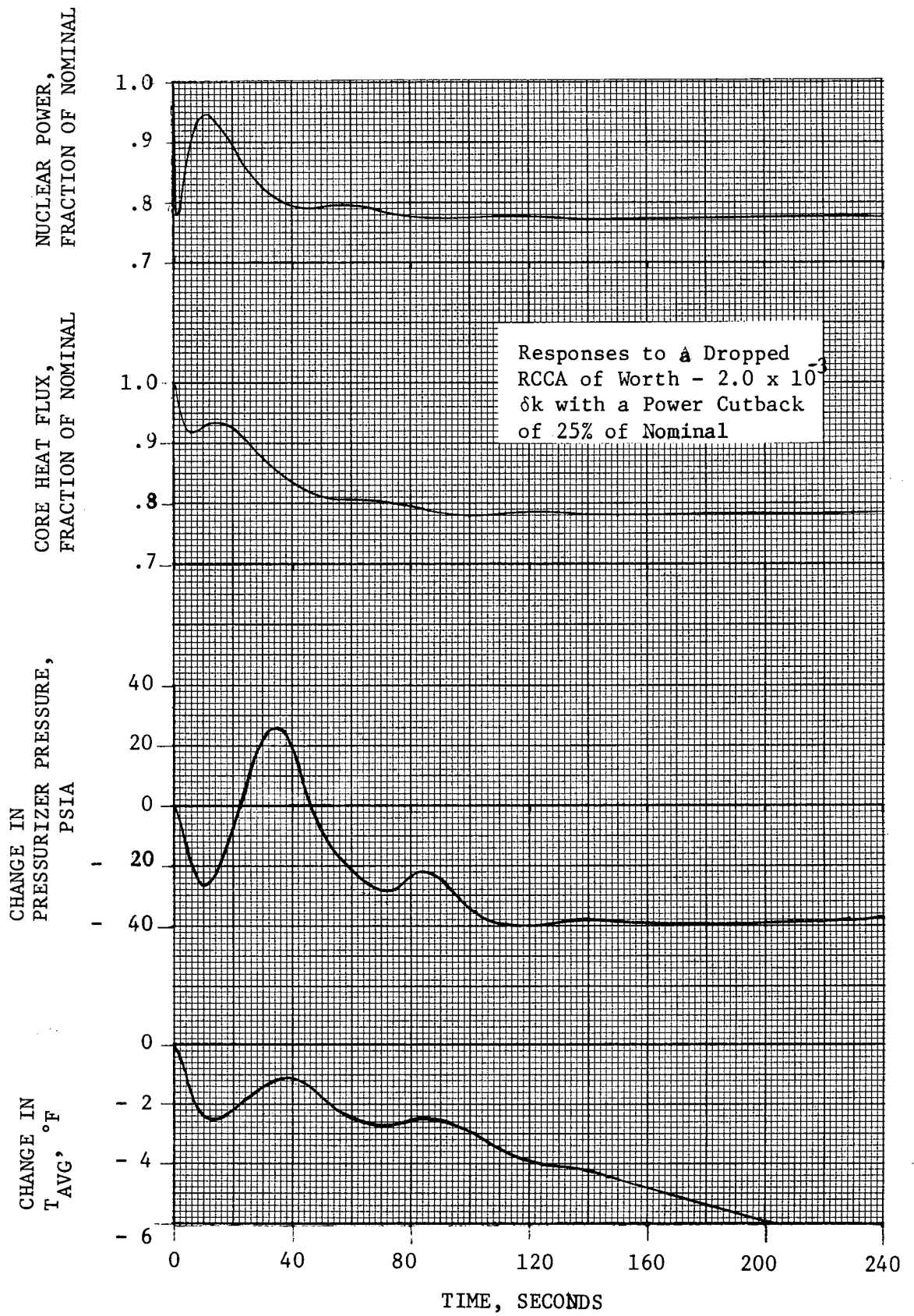


FIGURE 14.1.4-1

Responses to a Dropped RCCA
 of Worth - $2.0 \times 10^{-3} \delta k$ with
 a Power Cutback of 25% of Nominal

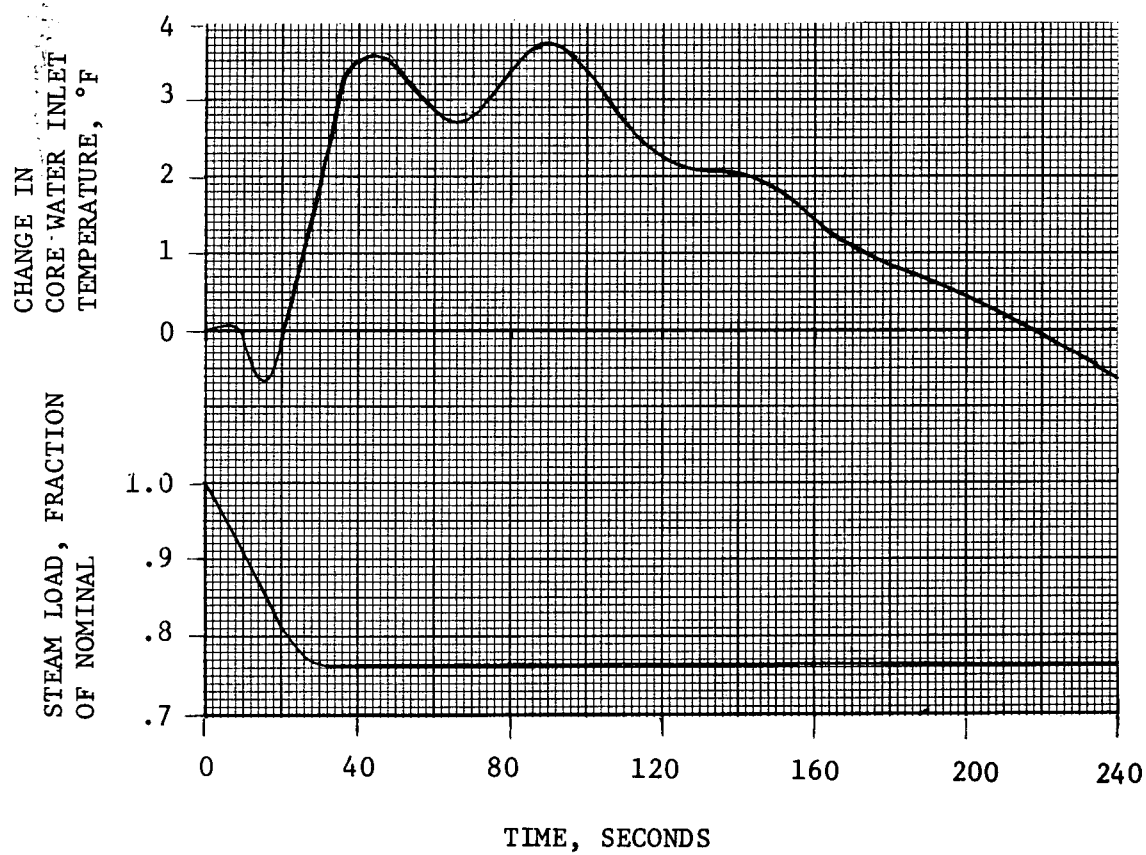


FIGURE 14.1.4-2

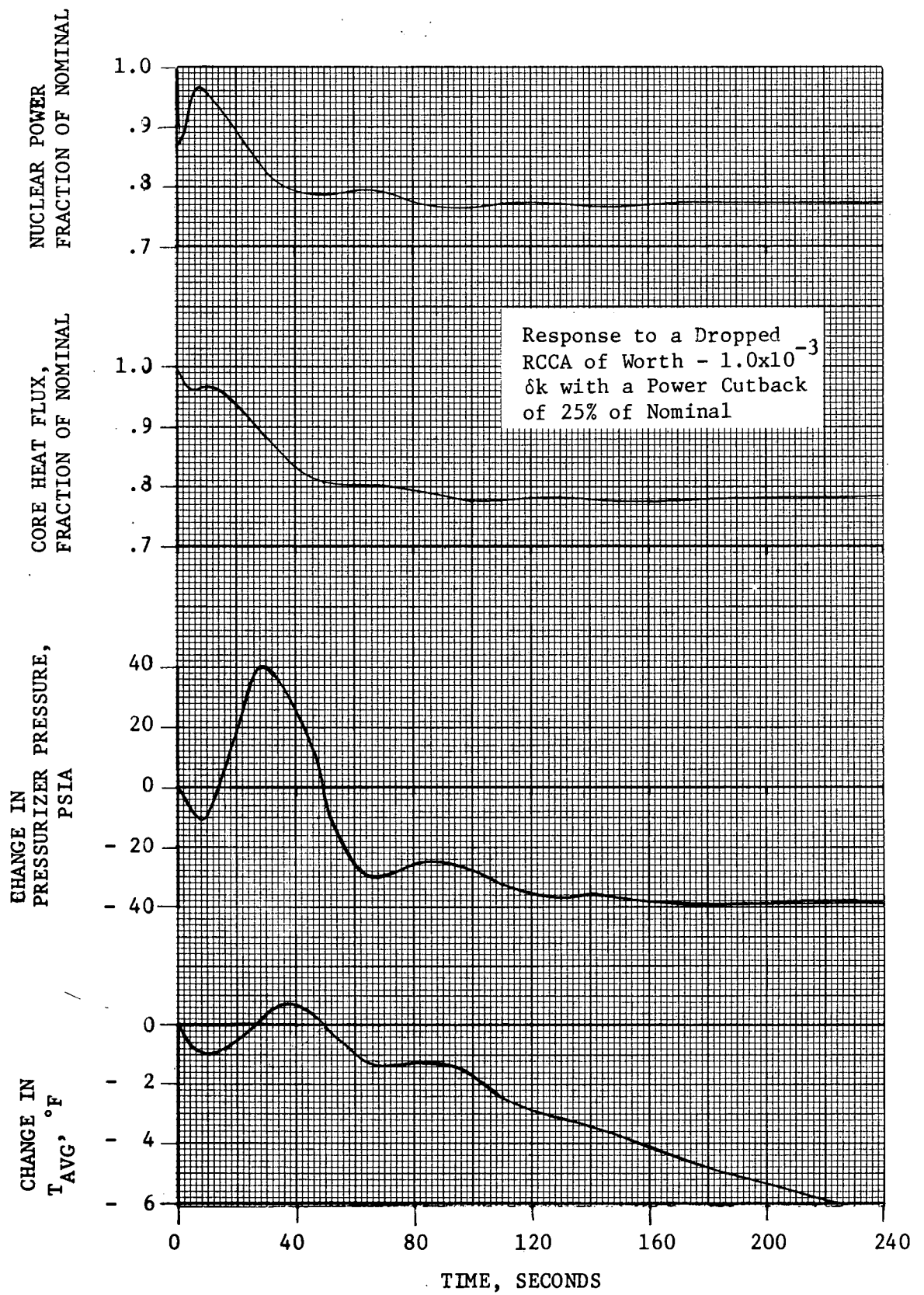


FIGURE 14.1.4-3

Response to a Dropped RCCA
of Worth - $1.0 \times 10^{-3} \delta k$ With
a Power Cutback of 25% of Nominal

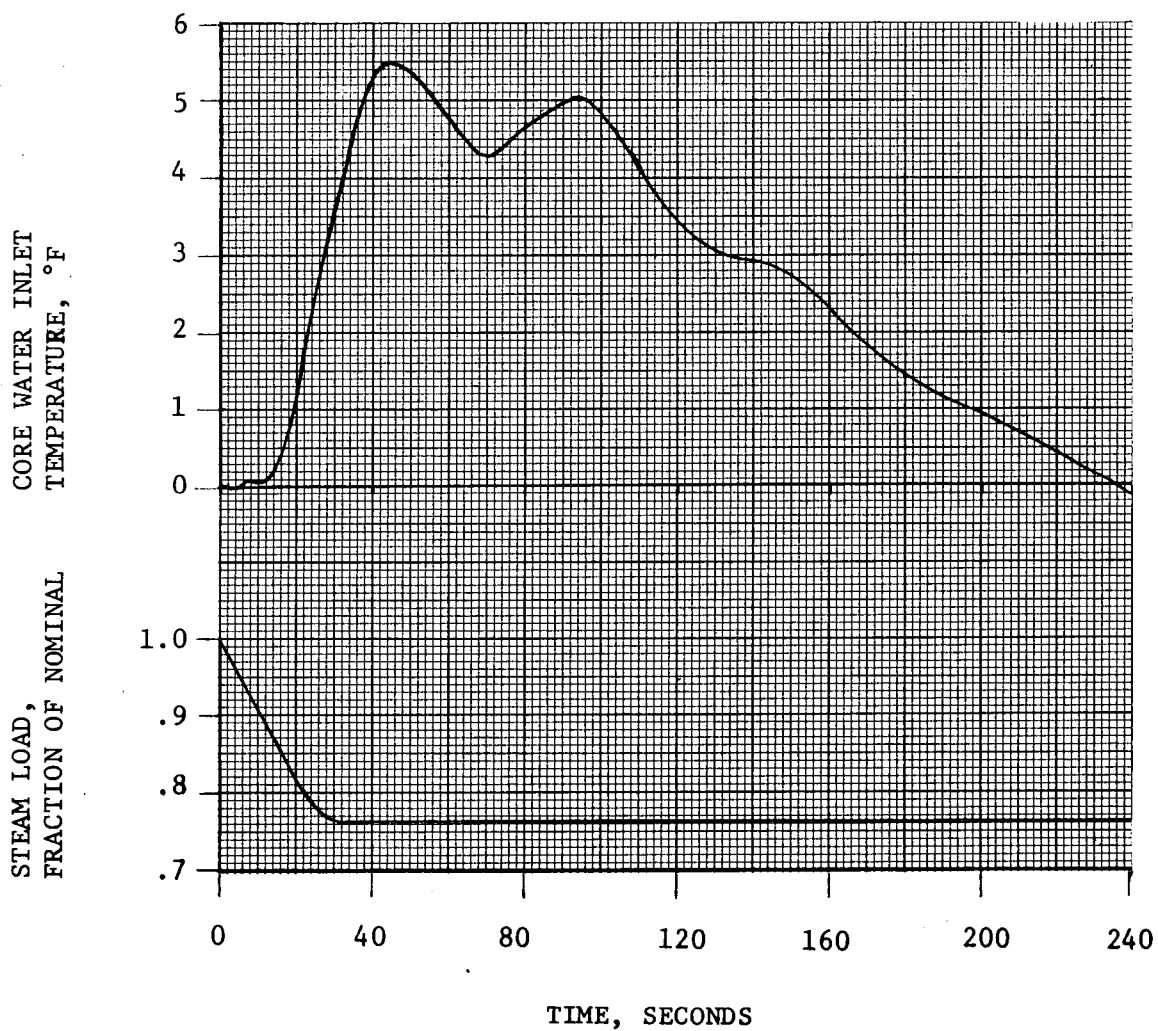


FIGURE 14.1.4-4

14.1.5 CHEMICAL AND VOLUME CONTROL SYSTEM MALFUNCTION

Reactivity can be added to the core with the Chemical and Volume Control System by feeding reactor makeup water into the Reactor Coolant System via the reactor makeup control system. The normal dilution procedures call for a limit on the rate and magnitude for any individual dilution, under strict administrative controls. Boron dilution is a manual operation. A boric acid blend system is provided to permit the operator to match the concentration of reactor coolant makeup water to that existing in the coolant at the time. The Chemical and Volume Control System is designed to limit, even under various postulated failure modes, the potential rate of dilution to a value which, after indication through alarms and instrumentation, provides the operator sufficient time to correct the situation in a safe and orderly manner.

There is only a single, common source of reactor makeup water to the Reactor Coolant System from the reactor makeup water system, and inadvertent dilution can be readily terminated by isolating this single source. The operation of the reactor makeup water pumps which take suction from this tank provides the only supply of makeup water to the Reactor Coolant System. In order for makeup water to be added to the Reactor Coolant System the charging pumps must be running in addition to the reactor makeup water pumps.

The rate of addition of unborated water makeup to the Reactor Coolant System is limited to the capacity of the makeup water pumps. This limiting addition rate is 230 gpm. For totally unborated water to be delivered at this rate to the Reactor Coolant System at pressure, three charging pumps must be operated. Normally only one charging pump and one reactor make-up pump are operating.

The boric acid from the boric acid tank is blended with the reactor makeup water in the blender and the composition is determined by the preset flow rates of boric acid and reactor makeup water on the Reactor Makeup Control. Two separate operations are required. First, the operator must switch from the automatic makeup mode to the dilute mode. Second, the start button must be depressed. Omitting either step would prevent dilution. This makes the possibility of inadvertent dilution very small.

Information on the status of the reactor coolant makeup is continuously available to the operator. Lights are provided on the control board to indicate the operating condition of pumps in the Chemical and Volume Control System. Alarms are actuated to warn the operator if boric acid or demineralized water flow rates deviate from preset values as a result of system malfunction.

To cover all phases of plant operation, boron dilution during refueling, startup, and power operation are considered in this analysis.

Method of Analysis and Results

Dilution During Refueling

During refueling the following conditions exist:

- a) One residual heat removal pump is running to ensure continuous mixing in the reactor vessel,
- b) The valve in the seal water header to the reactor coolant pumps is closed,

- c) The valves on the suction side of the charging pumps are adjusted for addition of concentrated boric acid solution,
- d) The boron concentration of the refueling water is 2500 ppm, corresponding to a shutdown of 16.0 per cent Δk with all control rods in; periodic sampling ensures that this concentration is maintained, and
- e) Neutron sources are installed in the core and BF_3 detectors connected to instrumentation giving audible count rates are installed within the reactor vessel to provide direct monitoring of the core.

A minimum water volume in the Reactor Coolant System of 3200 ft³ is considered. This corresponds to the volume necessary to fill the reactor vessel above the nozzles to ensure mixing via the residual heat removal loop. The maximum dilution flow of 230 gpm and uniform mixing are also considered.

The operator has prompt and definite indication of any boron dilution from the audible count rate instrumentation. High count rate is alarmed in the reactor containment and the main control room. The count rate increase is proportional to the inverse multiplication factor. At 1500 ppm, for example, the core is 3.6 per cent shutdown and the count rate is increased by a factor of 4.4 over the count rate at 2500 ppm.

The boron concentration must be reduced from 2500 ppm to approximately 965 ppm before the reactor will go critical. This would take at least 1.6 hours. This is ample time for the operator to recognize the audible high count rate signal and isolate the reactor makeup water source by closing valves and stopping the reactor makeup water pumps.

Dilution During Startup

Prior to refueling, the Reactor Coolant System is filled with borated (2500 ppm) water from the refueling water storage tank by the charging pumps. Core monitoring is by external BF_3 detectors. Mixing of reactor coolant is maintained by operation of the reactor coolant pumps. Again the maximum dilution flow (230 gpm) is considered. The volume of reactor coolant is approximately 8043 ft^3 which is the volume of the Reactor Coolant System excluding the pressurizer. High source level and all reactor trip alarms are effective.

The minimum time required to reduce the reactor coolant boron concentration to 965 ppm, where the reactor could go critical with all rods in, is about 4.14 hours. Once again, this should be more than adequate time for operator action to the high count rate signal, and termination of dilution flow.

In any case, if continued dilution occurs, the reactivity insertion rate and consequences thereof are considerably less severe than those associated with the uncontrolled rod withdrawal analyzed in Section 14.1.1, Uncontrolled RCCA Withdrawal from a Subcritical Condition.

Dilution at Power

The effective reactivity addition rate for a boron dilution flow of 230 gpm at 575°F is shown as a function of reactor coolant boron concentration on Figure 14.1.5-1. This reactivity addition rate used in this evaluation is $1.1 \times 10^{-5} \text{ } \delta\text{k/sec}$ this is a conservatively high value compared to the expected value at power.

With the reactor in automatic control, at full power, the power and temperature increase from the boron dilution results in the insertion of the control group and a decrease in shutdown margin. A continuation of the

dilution and rod insertion would cause the rods to reach the minimum limit of the rod insertion monitor determined by the maneuvering band ($0.4\% \delta k/k$) and the rod bite ($0.1\% \delta k/k$) in approximately six minutes, Figure 14.1.5-2. Before reaching this point, however, two alarms would be actuated to warn the operator of the accident condition. The first of these, the LOW (rod position) alarm, alerts the operator to initiate normal boration. The other, LOW-LOW alarm, alerts the operator to follow emergency boration procedures. The LOW alarm is set well above the LOW-LOW alarm to provide for sufficient normal boration without the need for emergency procedures.

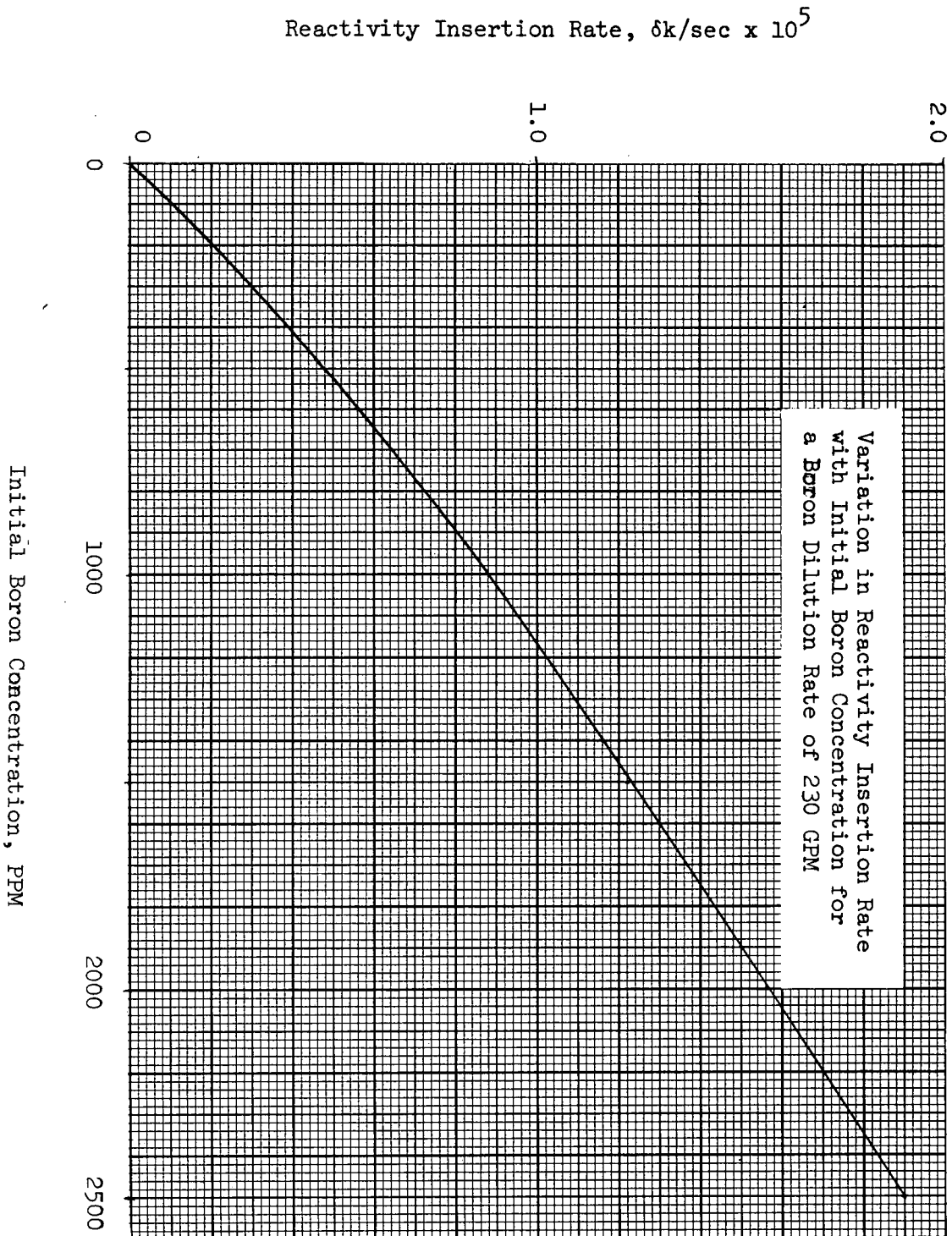
With no boration, it takes approximately 21 minutes before a shutdown margin of one per cent is lost due to dilution. Therefore, plenty of time is available following the alarms for the operator to determine the cause, isolate the reactor water makeup source, and initiate reboration.

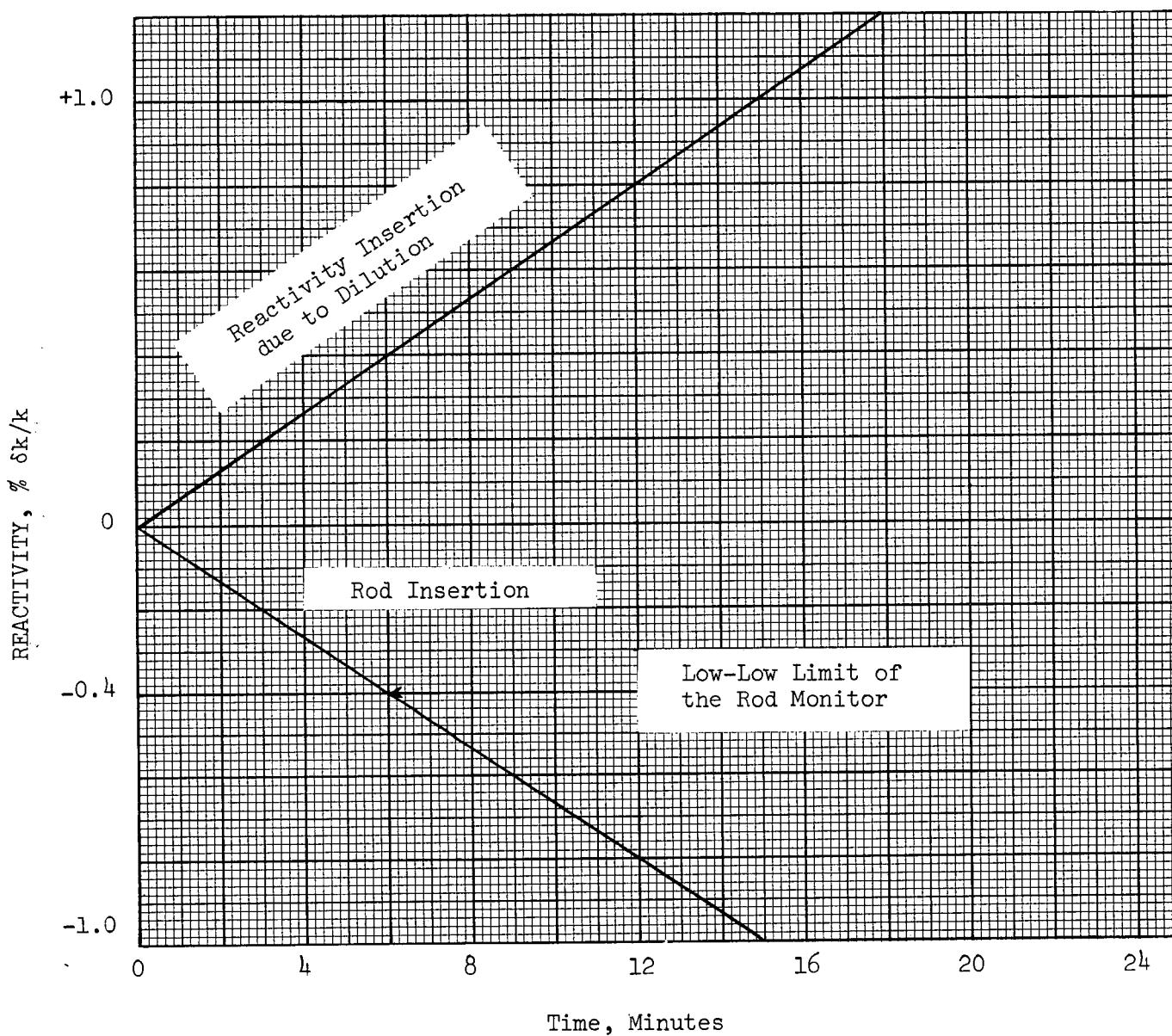
If the reactor is in manual control, and the operator takes no action, power and temperature rise to the overtemperature ΔT trip setpoint in approximately 1.3 minutes. This figure has been obtained by a detailed digital simulation of the unit. Prior to this time the high temperature alarm would be actuated. There are approximately 15 minutes available for the operator to terminate dilution before the reactor can return to criticality following the trip.

Conclusions

Because of the procedures involved in the dilution process, an erroneous dilution is considered incredible. Nevertheless, if an unintentional dilution of boron in the reactor coolant does occur, numerous alarms and indications are available to alert the operator to the condition. The maximum reactivity addition due to the dilution is slow enough to allow the operator to determine the cause of the addition and take corrective action before excessive shutdown margin is lost.

FIGURE 14.1.5-1





Reactivity Insertion
due to Dilution

FIGURE 14.1.5-2

14.1.6 START-UP OF AN INACTIVE REACTOR COOLANT LOOP

Operation of the plant with an inactive loop causes reversed flow through the inactive loop because there are no isolation valves or check valves in the reactor coolant loops.

If the reactor is operated at power in this condition, there is a decrease in the coolant temperature in that loop in comparison with the other loop. The subsequent re-start of the idle reactor coolant pump, without bringing the loop temperature closer to the average temperature would result in the injection of cold water into the core. This cold water causes a rapid reactivity increase.

Assumptions and Method of Analysis

The following assumptions are made:

1. The idle pump on starting accelerates to full flow instantaneously, i.e., no slip and the time to accelerate the pump and coolant are zero.
2. A conservative maximum negative moderator coefficient of $-3.5 \times 10^{-4} \delta k/^{\circ}F$ is assumed.
3. A low Doppler coefficient of $-1.0 \times 10^{-5} \delta k/^{\circ}F$ is taken.
4. A high heat transfer coefficient between the primary and secondary system is assumed for the inactive loop. This implies that the temperature of the water in that part of the inactive loop from the steam generator plenum to the reactor exit plenum is at a temperature equal to the saturation temperature on the secondary side.

5. The core power to flow ratio is taken to be constant at the normal loop operational value.
6. The secondary pressure is taken to be the value corresponding to the above core power.

Account is taken of the delay in the cold water reaching the core from the time the pump is started.

An analog simulation of the complete plant was used to study the ensuing plant transients.

Results

The analog study of the transient behavior of the plant was made at 60% load (1364 MWt). The temperature difference between the water in the active loops and the water in the "hot" leg of the inactive loop is -25°F . The cold water entering the reactor plenum chamber is assumed to mix with the water coming from the active loops. The cold water slug is taken to last for 15 seconds. The temperature coming from all steam generators is assumed to be the same. The delay before the cold slug reaches the inlet to the reactor core is taken to be 4.0 seconds.

The results are shown in Figures 14.1.6-1 through 14.1.6-4. The thermal power buildup up is slow and this leads to the cooling of the primary circuits by the temperature slug. This accounts for the drop in pressurizer pressure and the average temperature.

Conclusions

The results show that for the -25°F change in core inlet temperature, the nuclear power rise does not cause a reactor trip. During the transient, both the primary pressure and the core inlet temperature fall so that there is no significant decrease in DNBR from these effects.

It is expected that the actual transients effects will be less severe, because of alleviating factors which have not been taken into account, e.g., the time constant of the pump is likely to be about 10 seconds. This means that the change in temperature will occur more gradually and that the transient will be less severe.

The conclusion is that the minimum DNBR reached is well in excess of the 1.3 limit value and therefore DNB will not occur during this transient.

START-UP OF AN INACTIVE REACTOR COOLANT LOOP

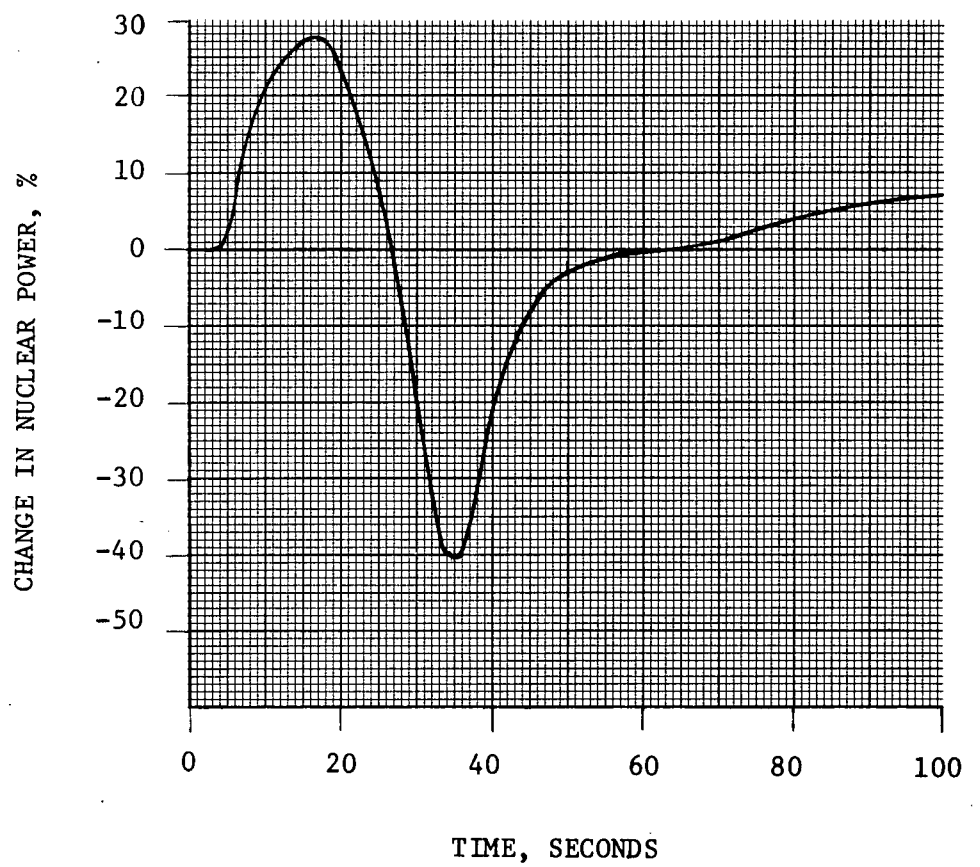


FIGURE 14.1.6-1

START-UP OF AN INACTIVE REACTOR COOLANT LOOP

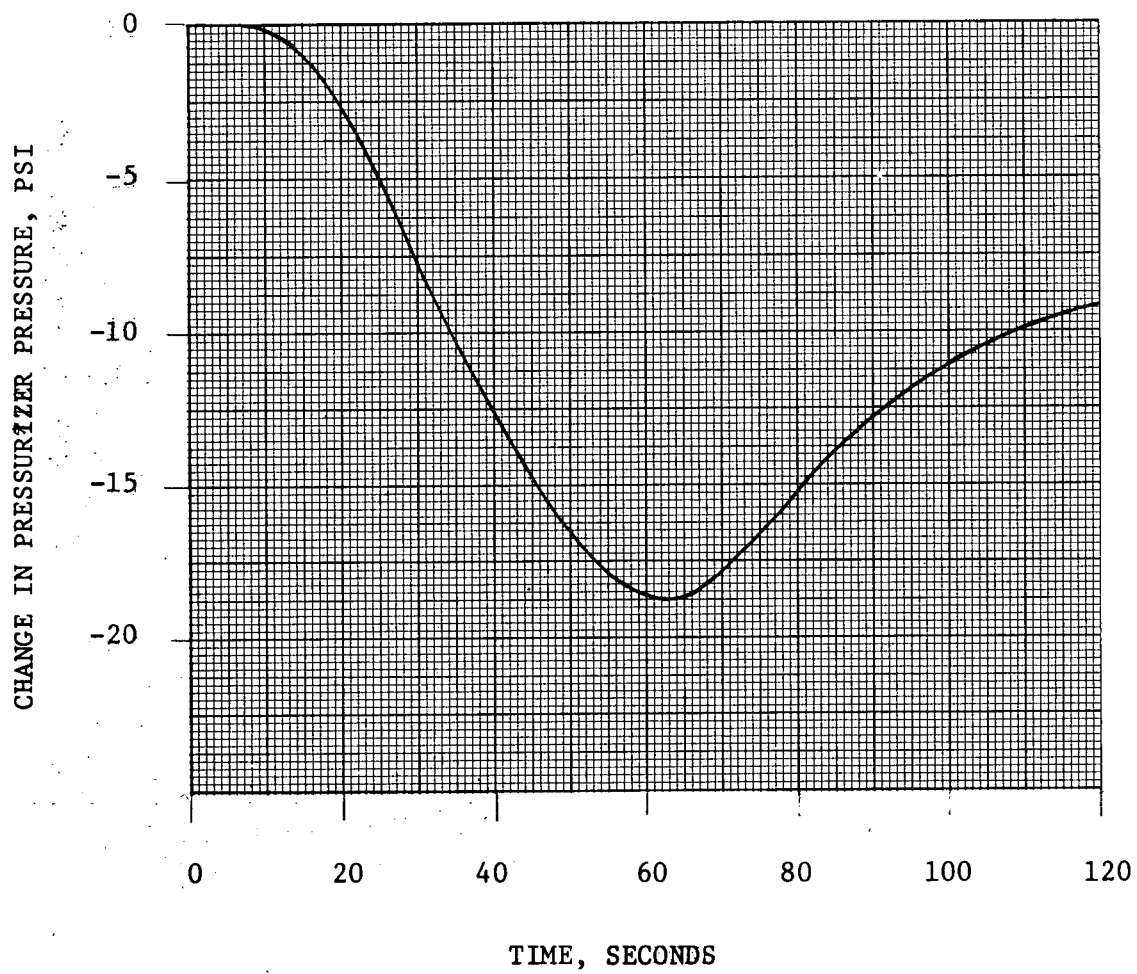


FIGURE 14.1.6-2

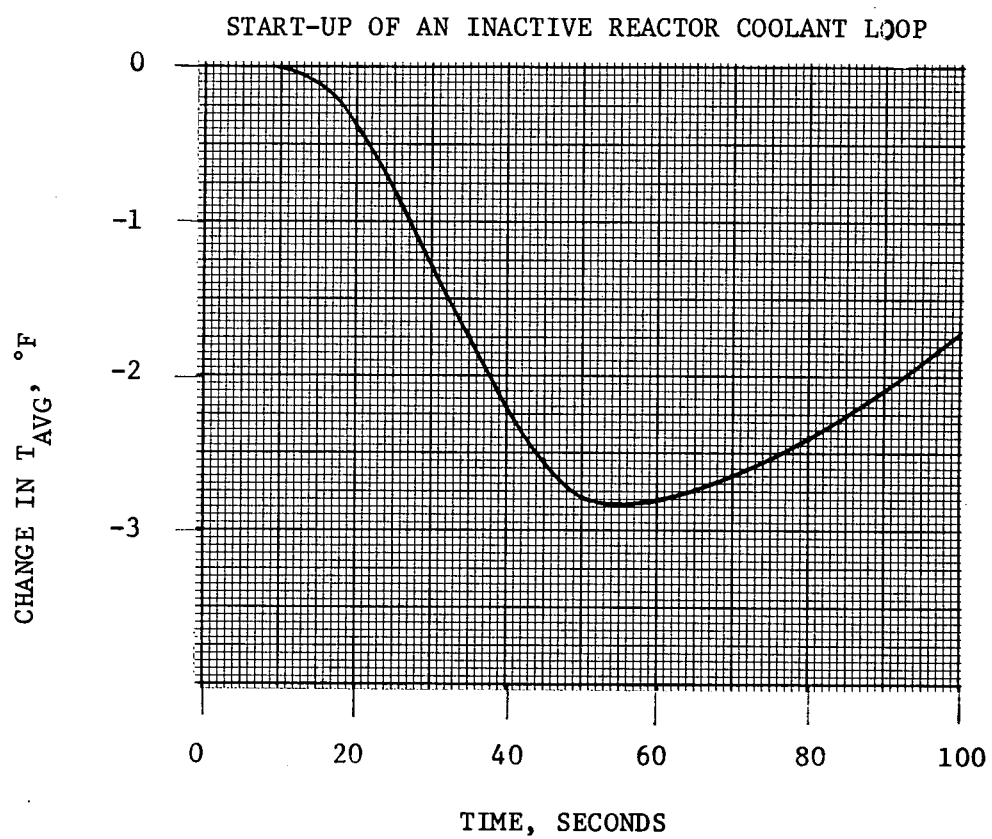


FIGURE 14.1.6-3

START-UP OF AN INACTIVE REACTOR COOLANT LOOP

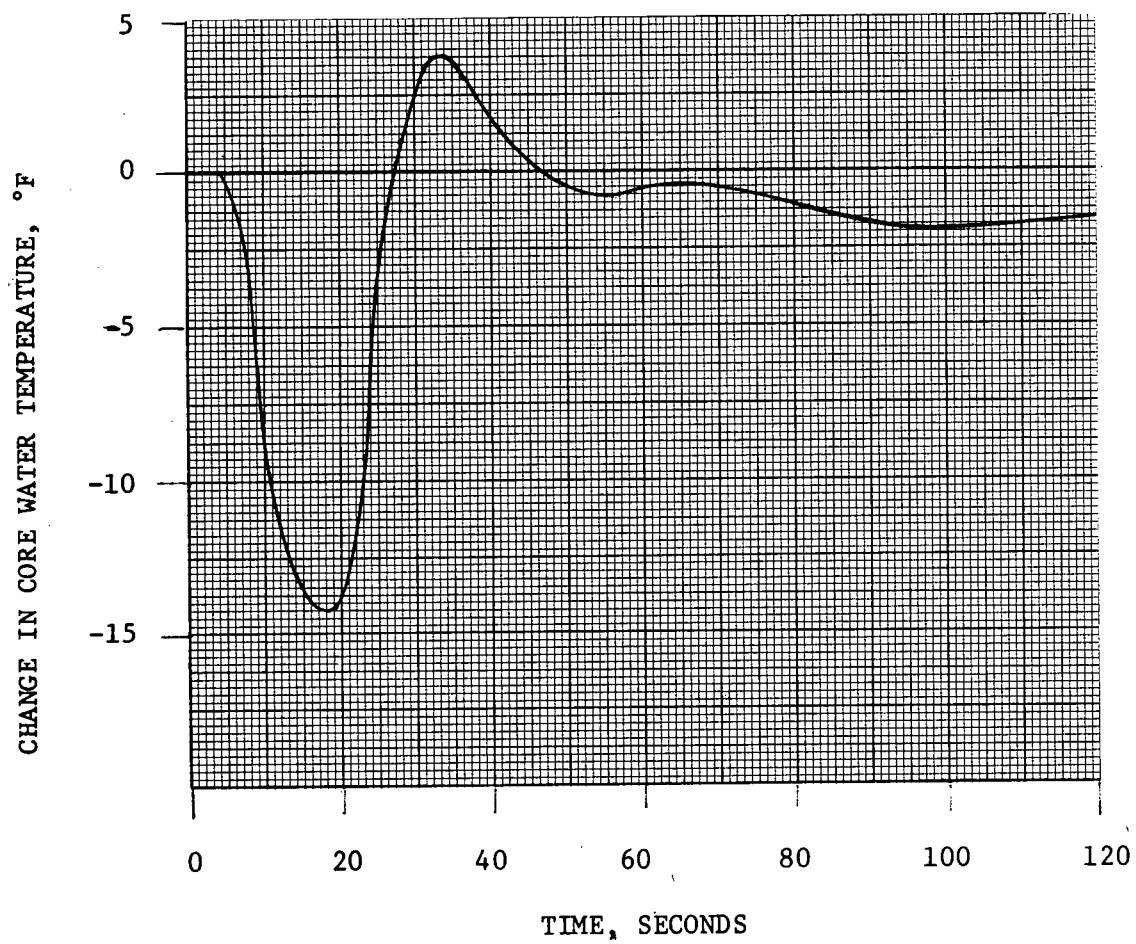


FIGURE 14.1.6-4

14.1.7 REDUCTION IN FEEDWATER ENTHALPY INCIDENT

The reduction in feedwater enthalpy is another means of increasing core power above full power. Such increases are attenuated by the thermal capacity in the secondary plant and in the Reactor Coolant System. The overpower-overtemperature protection (nuclear overpower and ΔT trips) prevents any power increase which could lead to a DNBR less than 1.30.

An extreme example of excess heat removal by the feedwater system is the transient associated with the accidental opening of the feedwater bypass valve which diverts flow around the low pressure feedwater heaters. The function of this valve is to maintain net positive suction head on the main feedwater pump in the event that the heater drain pump flow is lost, e.g., during a large load decrease.

In the event of accidental opening there is a sudden reduction in inlet feedwater temperature to the steam generators. The increased subcooling will create a greater load demand on the primary system which can lead to a reactor trip.

Method of Analysis

Two cases have been analyzed to demonstrate the plant behavior in the event of a sudden feedwater temperature reduction resulting from accidental opening of the bypass valve. The first case was for an uncontrolled reactor with a zero moderator coefficient, since this represents a condition, where the plant has the least inherent transient capability. The second case was for a controlled reactor with a large negative coefficient. These results were obtained by means of a detailed digital simulation of the plant including core kinetics, Reactor Coolant, the Steam and Feedwater Systems. Both transients were assumed to occur from full power (2244 MWt).

Results

Figures 14.1.7-1 and 14.1.7-2 show the transients without automatic control. As expected the pressurizer pressure shows a fairly rapid decrease as the secondary heat extraction exceeds the core power generation. The core power level remains essentially constant at full load. There is an increased margin to DNB because of the accompanying reduction in average temperature. The reactor would not trip. There is a small increase in ΔT as the heat transfer increases through the steam generator.

Figures 14.1.7-3 and 14.1.7-4 illustrate the transients assuming automatic reactor control is functioning. A large negative moderator coefficient is assumed, which acts to increase power. The core power is increasing thus reducing the decrease in coolant average temperature and pressurizer pressure. The steady state conditions are reached with a minimum DNBR greater than 1.59. The plant would actually be tripped from the overpower protection.

Conclusions

Representative transient results for excessive load increases due to cold feedwater addition have been shown which indicate the general behavior, i.e., that a core power increase is accompanied by an average temperature decrease and without a power increase there is a large reduction in coolant average temperature. This has the effect of maintaining considerable margin to a limiting DNBR of 1.30. Core protection for slow increases in plant output in excess of full power is provided by the combination of the overpower-over-temperature protection described in conjunction with the rod withdrawal accident. There is no radioactive release and thus no public hazard in the event of an excessive load increase.

Feedwater Valve Malfunction

During startup and at plant loads below approximately 10%, feedwater to the steam generators is controlled with the feedwater bypass control valves rather than with the main feedwater control valves. Under these conditions the main feedwater control valves are normally in the fully closed position.

Even though the accidental opening of a main feedwater control valve at low load is quite unlikely since the valves are not used at low loads, the reactivity insertion rate at no load following the malfunction of a steam generator main feedwater control valve has been calculated with the following assumptions:

1. A step increase in feedwater flow to one steam generator from 0 to the nominal full load (2200 Mwt) value for one steam generator.
2. The most negative reactivity moderator coefficient at end of life.
3. A constant feedwater temperature of 70°F.
4. Neglect of the heat capacity of the reactor coolant system and steam generator shell metal.
5. Neglect of the energy stored in the fluid of the unaffected steam generators.

The maximum reactivity insertion rate was found to be 3.9×10^{-4} $\Delta k/\text{second}$ which is less than the reactivity insertion rates analyzed in rod withdrawal accidents from a subcritical condition (6×10^{-4} $\Delta k/\text{sec.}$). If the accident occurs with the plant just critical at no load, the reactor may be tripped by the power range flux level trip (low setting) set at approximately 25% or by the source or intermediate range flux level trips. Since the reactivity insertion rate is less than that analyzed for rod withdrawal accidents from

a subcritical condition there is a large margin to DNB. Depending upon the temperature of the feed and the magnitude of the flow the core may not reach the flux level trip setpoints in which case, due to the low core power, there will again be a large margin to DNB.

Continuous addition of cold feedwater after a reactor trip is prevented by:

- a. An interlock which closes all main feedwater control valves by venting the valve actuators following a plant trip if the reactor coolant system temperature is below approximately 554°F.
- b. An interlock which closes the main and bypass feedwater control valves by venting the valve actuators following 2/3 high steam generator level signals in a steam generator. This interlock closes the valves only for the affected steam generator and is redundant down to two solenoids per feedwater control valve which vent the valve actuator.

A continuous cooldown caused by the addition of cold feedwater after a reactor trip is prevented even in the case of a failure in a valve. The reduction of reactor coolant system temperature, pressure, and pressurizer level caused by a cooldown will lead to a safety injection signal on low pressurizer pressure and level. The safety injection signal will trip the main feedwater pumps and close the main and bypass feedwater control valves. This will stop all feedwater even if a valve remains in the fully open position.

OPENING OF FEEDWATER VALVE,
WITHOUT AUTOMATIC REACTOR CONTROL
 $\alpha_{mod} = 0$

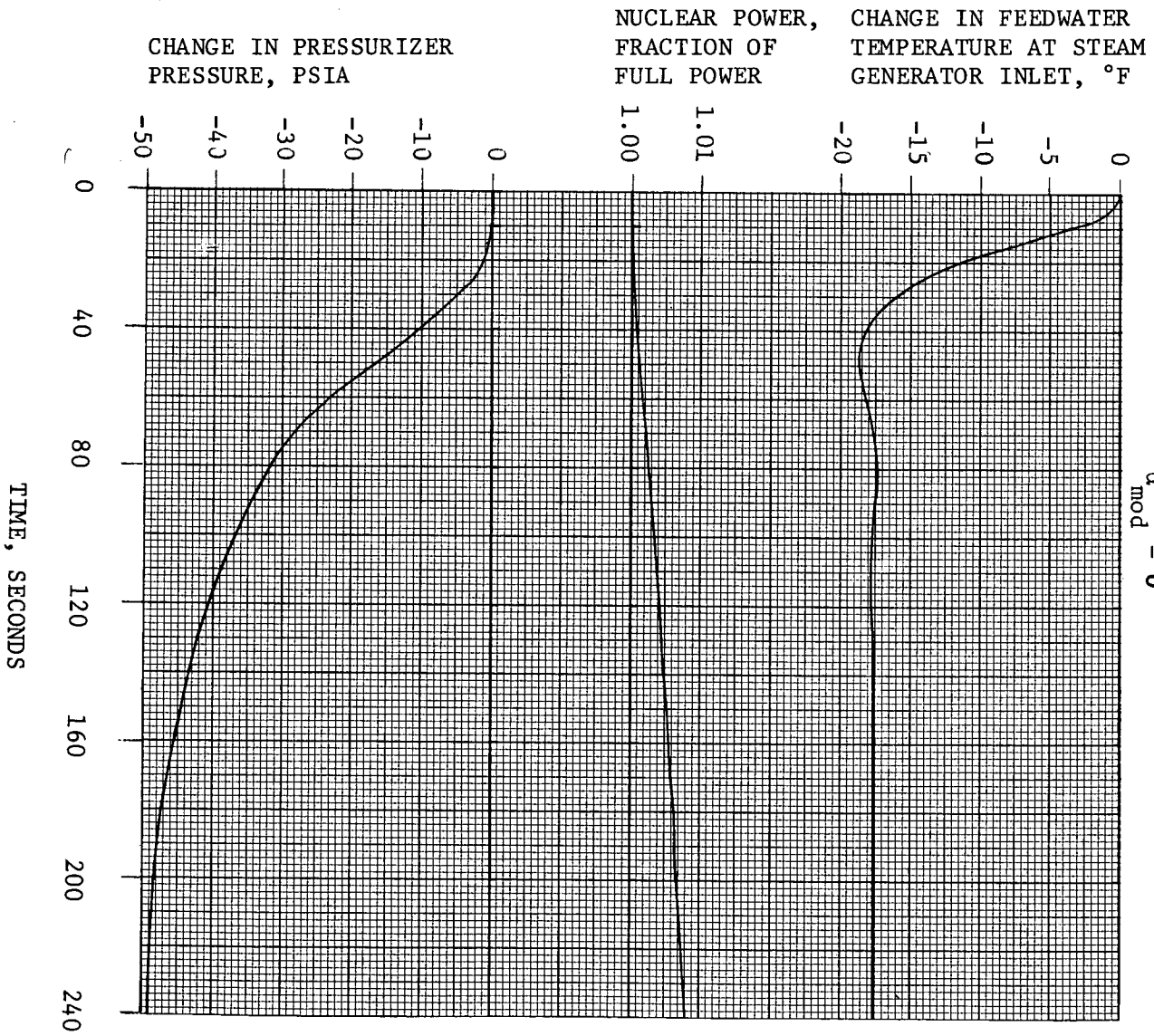


FIGURE 14.1.7-1

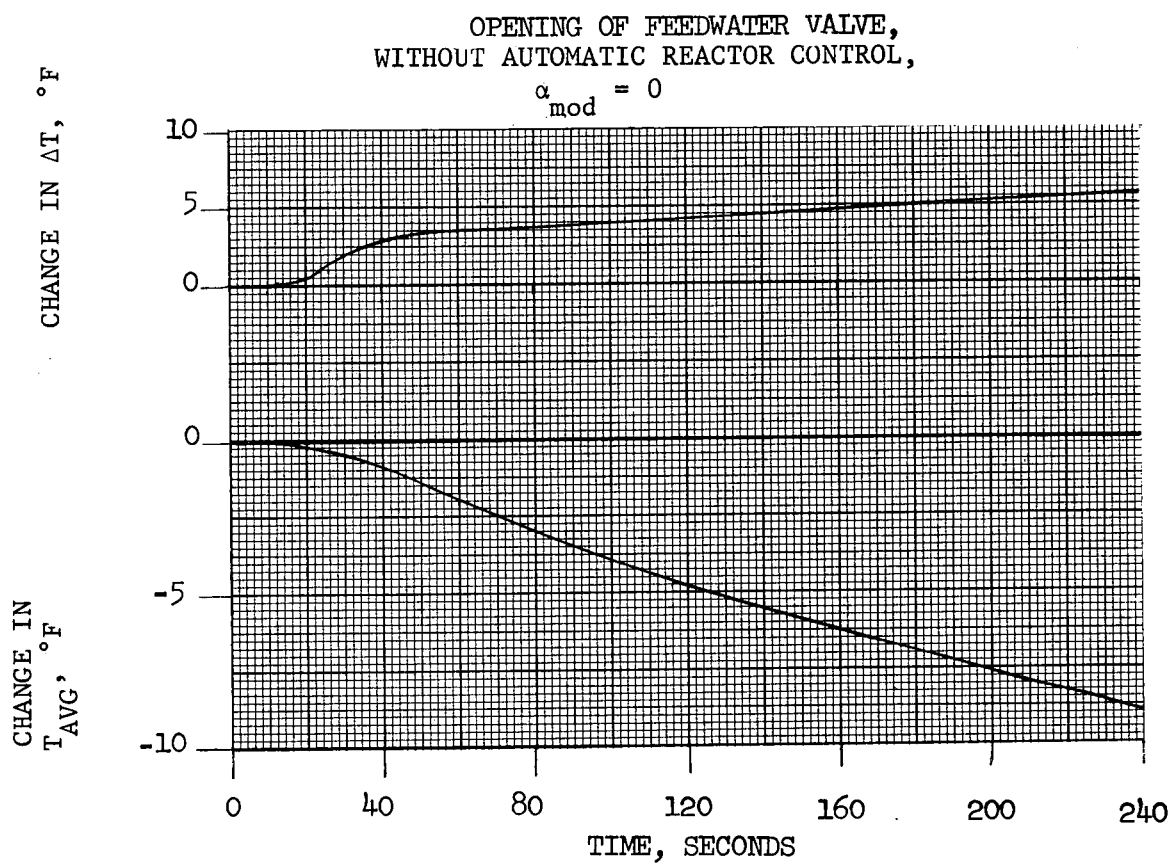


FIGURE 14.1.7-2

OPENING OF FEEDWATER BYPASS VALVE,
WITH AUTOMATIC REACTOR CONTROL,
 $\alpha_{mod} = 3.5 \times 10^{-4} \text{ } \delta k / ^\circ F$

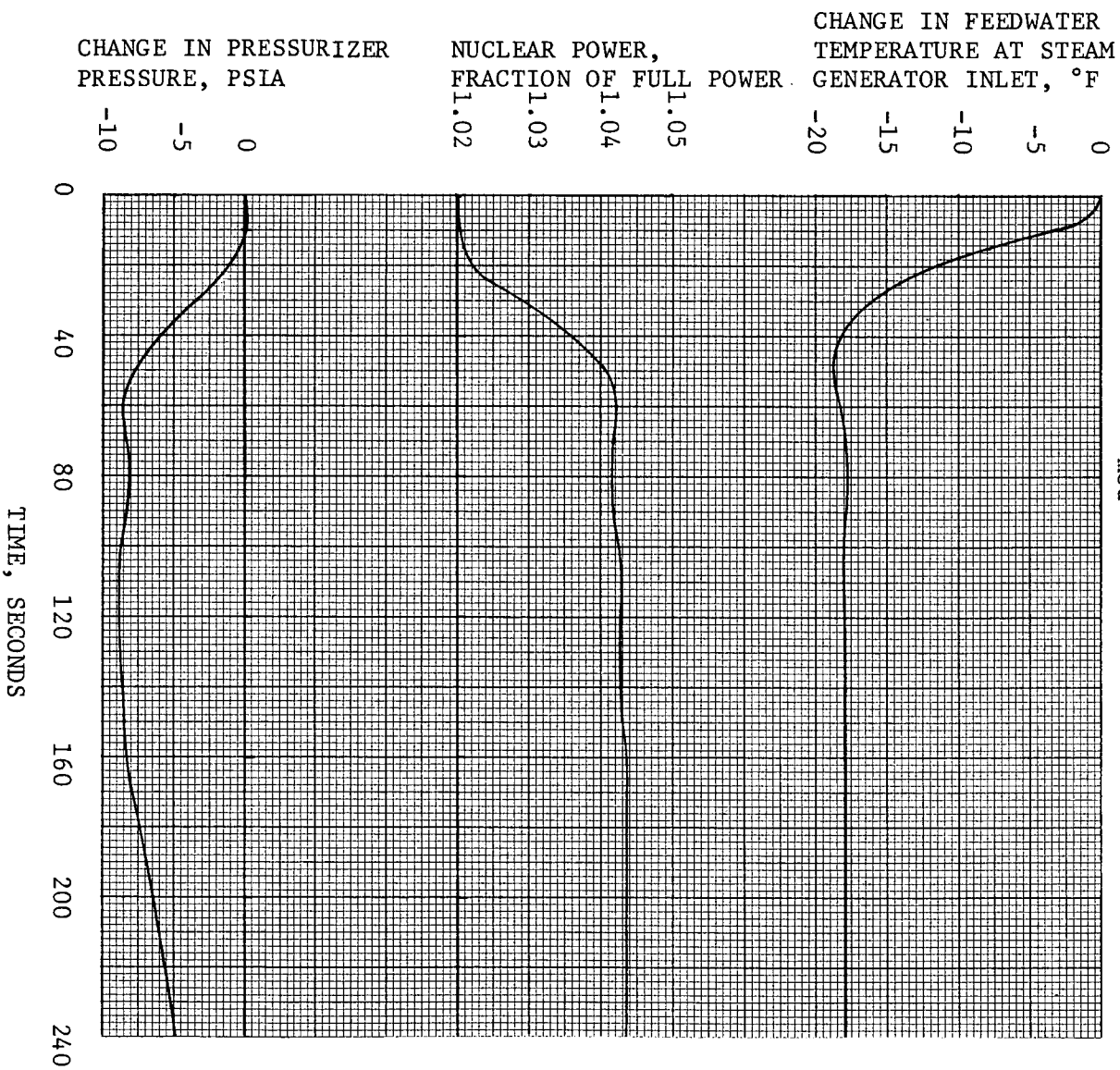


FIGURE 14.1.7-3

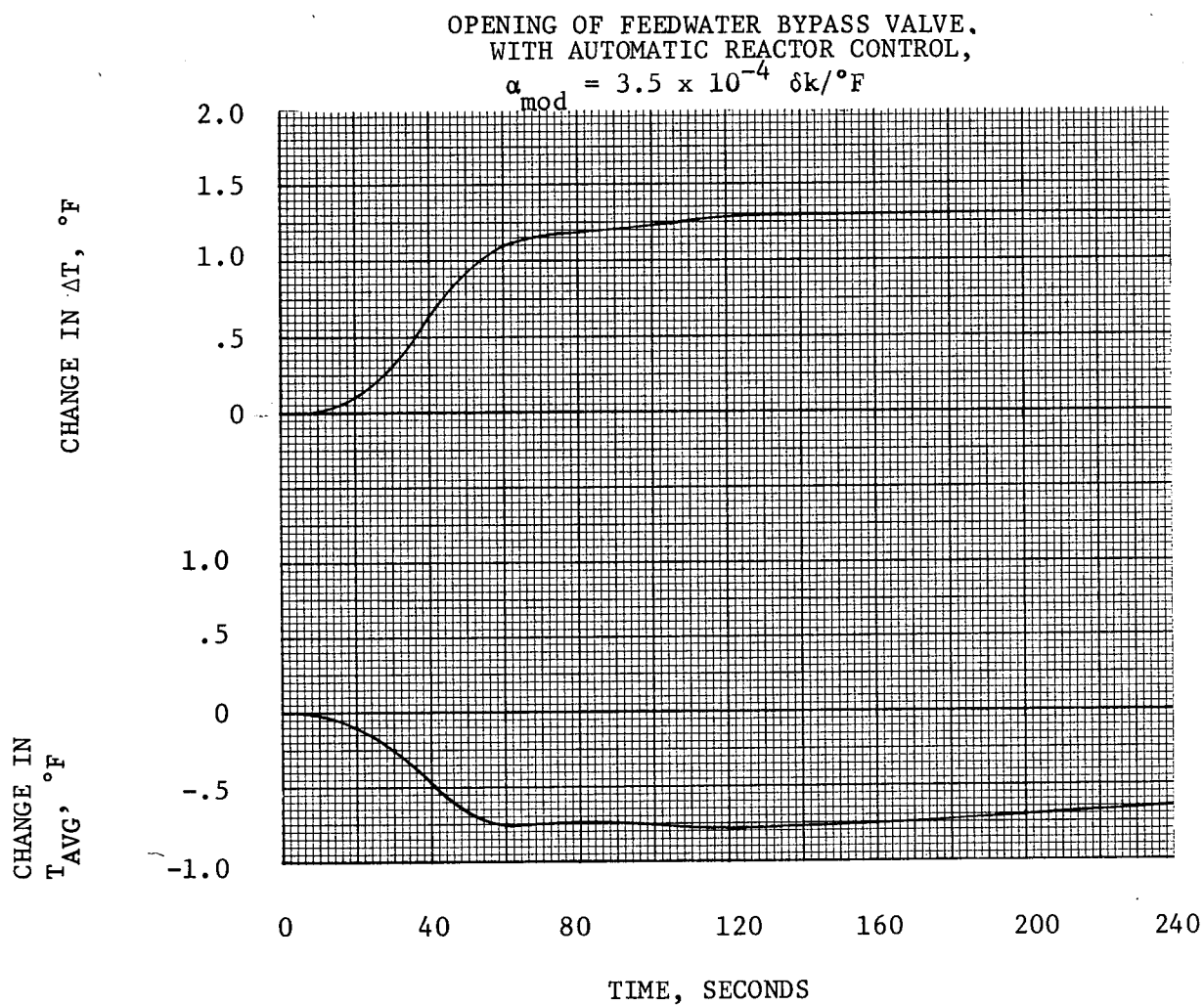


FIGURE 14.1.7-4

14.1.8 EXCESSIVE LOAD INCREASE INCIDENT

An excessive load increase incident is defined as a rapid increase in steam generator steam flow causing a power mismatch between the reactor core power and the steam generator load demand. The reactor control system is designed to accommodate a 20 per cent step load increase and a 15 per cent per minute ramp load increase without a reactor trip in the range of 15 to 95 per cent full power. Any loading rate in excess of these values may cause a reactor trip actuated by the reactor protection system. If the load increase exceeds the capability of the reactor control system, the transient is terminated in sufficient time to prevent the DNBR from going below 1.3 since the core is protected by the combination of the nuclear overpower trip and the overpower- overtemperature trips as discussed in Section 7. An excessive load increase incident could result from either an administrative violation such as excessive loading by the operator or an equipment malfunction such as steam bypass control or turbine speed control.

In case of excessive loading by the operator or by system demand, the turbine load limiter limits maximum turbine load to 100% rated load.

During power operation, steam bypass to the condenser is controlled by signals of reactor coolant conditions, i.e., abnormally high reactor coolant temperature indicates a need for steam bypass. A single controller malfunction does not cause steam bypass because an interlock is provided which blocks the control signal to the valves unless a large turbine load decrease has occurred.

The Reactor Protection System will trip the reactor in time to prevent DNBR less than 1.30, regardless of the rate of load increase for its designed system. Increases in steam load to more than rated load are analyzed as steam line ruptures in Section 14.2.5.

Method of Analysis

Two cases have been analyzed to demonstrate the plant behavior in the event of excessive load increases. These results were obtained by means of a detailed digital simulation of the plant including core kinetics, Reactor Coolant System and the Steam System. Both transients were assumed to occur from full power where the margins to core limits are the smallest. A zero moderator coefficient of reactivity was assumed as this represents the condition where the plant has the least inherent (uncontrolled) transient capability. The results of a 10% step increase in rated turbine load are presented with and without automatic control.

Results

Figure 14.1.8-1 shows the transient without automatic control. As expected, the reactor coolant average temperature and pressurizer pressure show a fairly rapid decrease as the secondary heat extraction exceeds the core power generation. The fixed low pressure trip would occur at about 300 seconds. There is a considerable margin to DNB because of the accompanying large reduction in average temperature. There is a small increase in ΔT as the heat transfer increases through the steam generator. The core power level rises slightly during the transient and reaches 102% after 120 seconds.

Figure 14.1.8-2 and 14.1.8-3 illustrate the transient assuming automatic reactor control is functioning. The core power is increasing thus reducing the rate of decrease in coolant average temperature and pressurizer pressure. With no trip actuation steady state conditions are reached with a minimum DNBR of about 1.30. Protection is provided by the combination overpower- overtemperature protection described in Section 7 and a trip would occur before the limiting DNBR of 1.3 is reached.

Conclusions

Representative transient results for excessive load increases have been shown which indicate the general behavior, i.e., that a core power increase is accompanied by an average temperature decrease and without a power increase there is a larger reduction in coolant average temperature. For this latter case there is a considerable margin to a limiting DNBR of 1.30. Core protection for slow increases in plant output in excess of full power is provided by the combination of the overpower-overtemperature protection described in conjunction with the rod withdrawal accident. There is no radioactive release and thus no public hazard in the event of an excessive load increase.

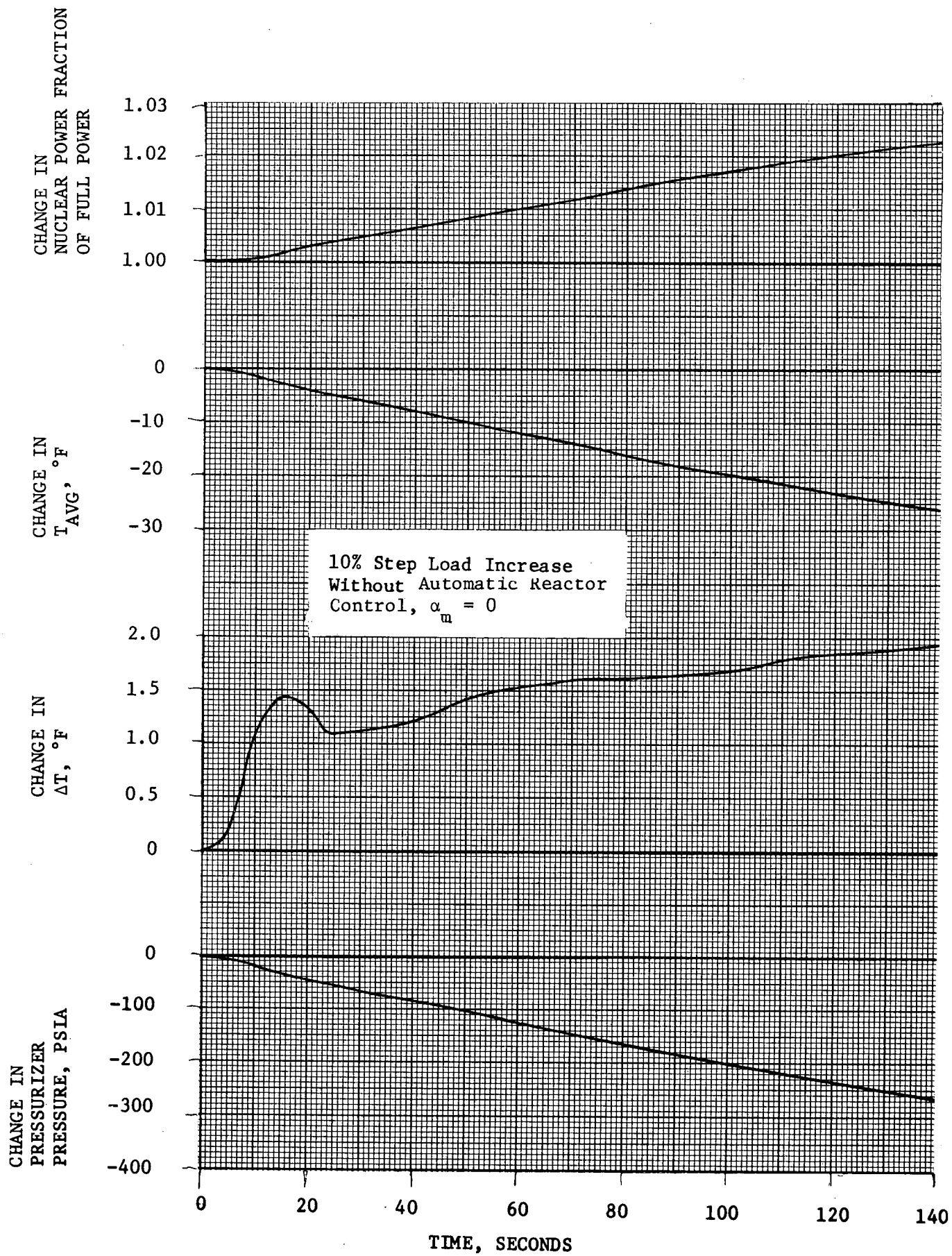


FIGURE 14.1.8-1

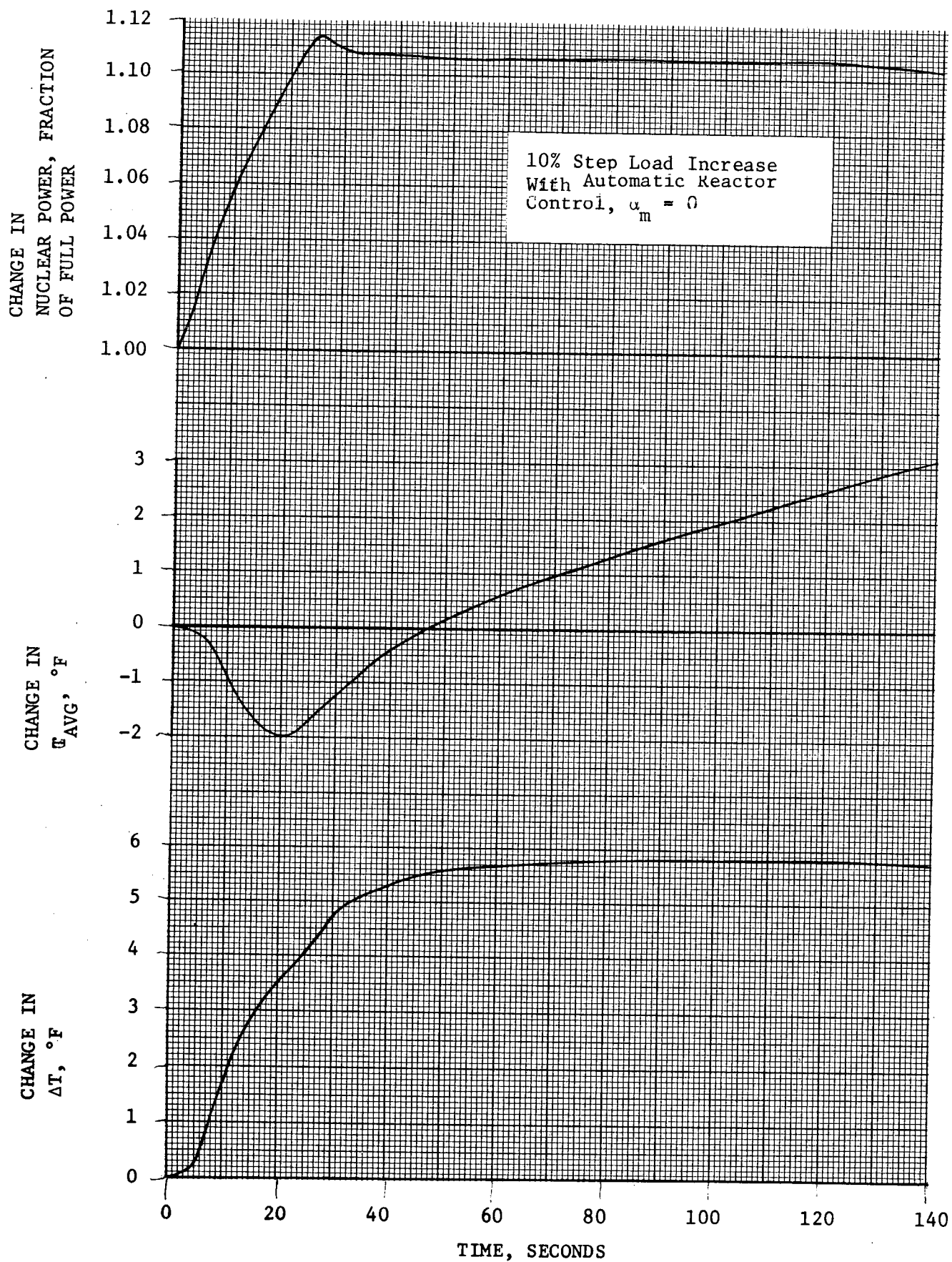


FIGURE 14.1.8-2

10% STEP LOAD INCREASE
WITH AUTOMATIC REACTOR CONTROL
 $\alpha_m = 0$

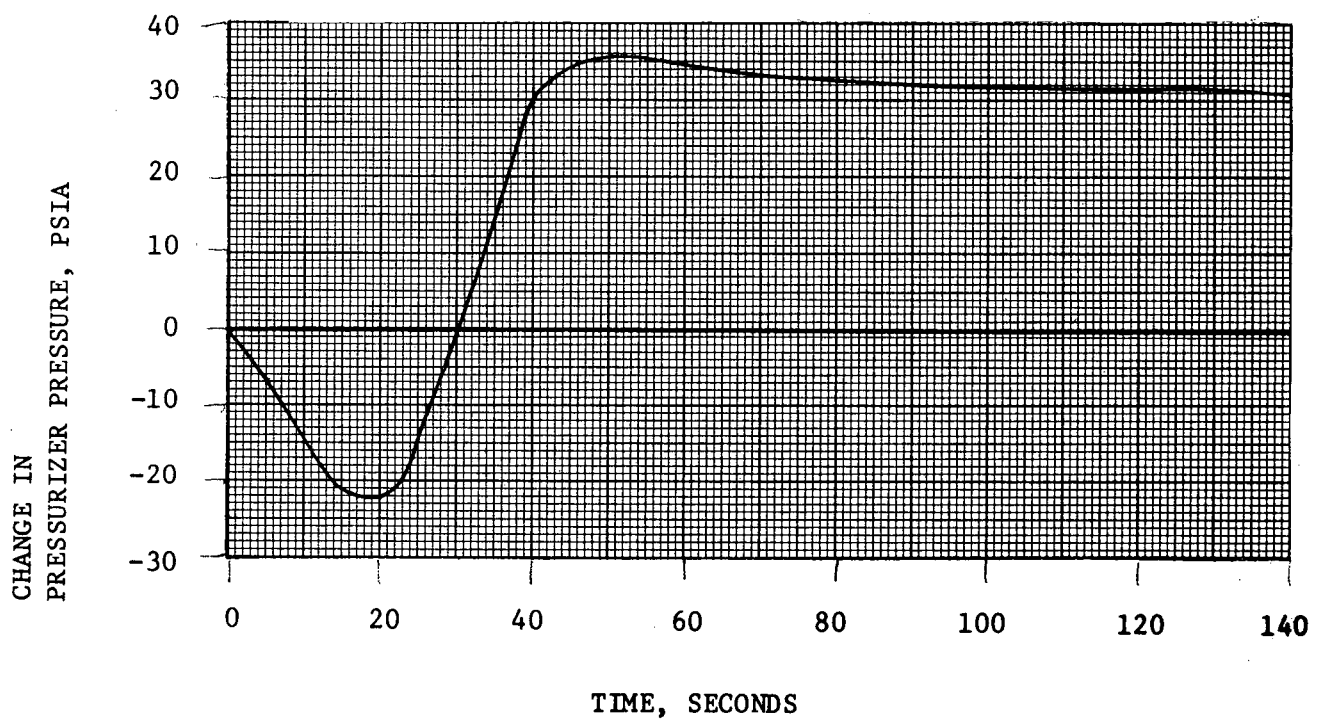


FIGURE 14.1.8-3

14.1.9 LOSS OF REACTOR COOLANT FLOW

Flow Coast-Down Accidents

A loss of coolant flow incident can result from a mechanical or electrical failure in one or more reactor coolant pumps, or from a fault in the power supply to these pumps. If the reactor is at power at the time of the incident, the immediate effect of loss of coolant flow is a rapid increase in coolant temperature. This increase could result in departure from nucleate boiling (DNB) with subsequent fuel damage if the reactor is not tripped promptly. The following trip circuits provide the necessary protection against a loss of coolant flow incident and are actuated by:

- 1) Low voltage or low frequency on pump power supply bus
- 2) Pump circuit breaker opening
- 3) Low reactor coolant flow

These trip circuits and their redundancy are further described in Section 7.2, Reactor Control and Protection System.

Simultaneous loss of electrical power to all reactor coolant pumps at full power is the most severe credible loss-of-coolant flow condition. For this condition reactor trip together with flow sustained by the inertia of the coolant and rotating pump parts will be sufficient to prevent fuel failure, Reactor Coolant System overpressure and prevent the DNB ratio from going below 1.30.

Method of Analysis

The following loss of flow cases are analyzed:

- 1) Loss of three pumps from Reactor Coolant System Heat output of 2200 MWt with three loops operating
- 2) Loss of two pumps from reactor coolant system heat output of 2200 MWt with three loops operating

- 3) Loss of two pumps from reactor coolant system heat output of 1320 MWt with two loops operating

The first case represents the worst credible coolant flow loss. The second and third cases are less severe. Loss of one pump above a preset power level causes a reactor trip by a low flow signal. The power level above which this trip occurs is assumed to be set at 60% of full load. Loss of one pump above 60% of full load is less severe than the second case analyzed since it will trip the reactor earlier and flow coast down is slower. During two loop operation at power the loss of a second single coolant pump activates a reactor trip. This case is a less severe accident than the third case presented.

The normal power supplies for the pumps are the two buses connected to the generator, one of which supplies power to one of the three pumps and the other of which supplies power to two of the three pumps. When a turbine trip occurs, the pumps are automatically transferred to a bus supplied from external power lines, and this pump will continue to supply coolant flow to the core. The simultaneous loss of power to all reactor coolant pumps is a highly unlikely event. Following any turbine trip, where there are no electrical faults which require tripping the generator from the network, the generator remains connected to the network for at least one minute. The reactor coolant pumps remain connected to the generator thus ensuring full flow for one minute after the reactor trip before any transfer is made. Since all the pumps are not on the same bus a single bus fault would not result in the loss of all pumps.

A full plant simulation is used in the analysis to compute the core average and hot spot heat flux transient responses, including flow coastdown, temperature, reactivity, and control rod insertion effects.

These data are then used in a detailed thermal-hydraulic computation to compute the margin to DNB. This computation solves the continuity, momentum, and energy equations of fluid flow together with the W-3 DNB correlation discussed in Section 3.2.2. The following assumptions are made in the calculations:

Initial Operating Conditions

The initial operating conditions, which are assumed to be most adverse with respect to the margin to DNB, are maximum steady state power level, minimum steady state pressure, and maximum steady state inlet temperature:

2200 MWt - 3 loops operating:

Power	$(1.02) (2200 \text{ MWt}) = 2244 \text{ MWt}$
Pressure	$2250 - 30 = 2220 \text{ psia}$
Inlet Temperature	$546.2 + 4 = 550.2^\circ\text{F}$

1320 MWt - 2 loops operating:

Power	$(0.60 + 0.02) (2200 \text{ MWt}) = 1364 \text{ MWt}$
Pressure	$2250 - 30 = 2220 \text{ psia}$
Inlet Temperature	$552.7 + 4 = 556.7^\circ\text{F}$

Reactivity Coefficients

The highest values of the Doppler ($-10 \times 10^{-5} \delta k \text{ F}^{-1}$) and moderator ($0.0 \times 10^{-4} \delta k \text{ F}^{-1}$) temperature coefficients are assumed since these result in the maximum hot spot heat flux during the initial power of the transient, when the minimum DNB ratio is reached.

Reactor Trip

Following the loss of three pumps at power a reactor trip is actuated by either low voltage or the pump circuit breakers since the accident is due to the simultaneous loss of power to all these pumps.

Both the low voltage and circuit breaker trip circuit meet the IEEE 279 criterion and therefore cannot be negated by a single failure.

The time from the loss of power to all pumps to the initiation of control rod motion to shut down the reactor is taken as 1.6 sec, this is a conservative assessment of the delay.

A low flow trip is assumed to be actuated following loss of one or two pumps, since the low flow trip results in a longer delay than the bus undervoltage or breaker trips.

The low flow trip setting is 90 per cent of full flow; the trip signal is assumed to be initiated at 87 per cent of full flow, allowing 3 per cent for flow instrumentation errors. The time from the initiation of low flow signal to initiation of control rod motion is 0.6 sec. Upon reactor trip it is also assumed that the most reactive RCCA is stuck in its fully withdrawn position, hence resulting in a minimum insertion of negative reactivity. The negative reactivity insertion upon trip is conservatively based on a 1 per cent shutdown margin at no load conditions.

Heat Transfer Coefficient

The overall heat conductance between the fuel and the water varies considerably during the transient mostly as a result of the change of fuel gap conductance. A conservatively evaluated overall heat conductance was used in the analysis.

Flow Coastdown

Reactor coolant flow coastdown curves are shown on Figures 14.1.9-1, 14.1.9-2 and 14.1.9-3, these curves are based on high estimates of loop pressure losses.

Results

Figure 14.1.9-4 shows the neutron flux, the average heat flux, and the hot spot heat flux response for the three pump loss from 2200 MWt with three loops operating. Figure 14.1.9-5 shows the DNB ratio as a function of time for this case. A minimum W-3 DNB ratio value of 1.31 is reached 2.25 seconds after initiation of the incident.

Figure 14.1.9-6 shows the transient for loss of two pumps from 2200 MWt with three loops operating and Figure 14.1.9-7 shows the DNB ratio as a function of time for this case. The minimum value of DNB ratio is 1.33 and occurs 2.95 seconds after initiation of the transient.

The transient for loss of two pumps from 1320 MWt with two loops operating at power is shown on Figure 14.1.9-8. The minimum DNB ratio of 1.56 occurs 4.9 seconds after initiation of the transient, as is shown on Figure 14.1.9-8A.

Conclusions

Since DNB does not occur in any loss of coolant flow incident, there is no cladding damage and no release of fission products into the reactor coolant. Therefore, once the fault is corrected, the plant can be returned to service in the normal manner. The absence of fuel failures would, of course, be verified by analysis of reactor coolant samples.

Locked Rotor Accident

A hypothetical transient analysis is performed for the postulated instantaneous seizure of a reactor coolant pump rotor. Flow through the reactor coolant system is rapidly reduced, leading to a reactor trip on a low-flow signal. Following the trip, heat stored in the fuel rods continues to pass into the core coolant, causing the coolant to expand. At the same time, heat transfer to the shell side of the steam generator is reduced, first because the reduced flow results in a decreased tube side film coefficient and then because the reactor coolant in the tubes cools down while the shell side temperature increases (turbine steam flow is reduced to zero upon plant trip). The rapid expansion of the coolant in the reactor core, combined with the reduced heat transfer in the steam generator causes an insurge into the pressurizer and a pressure increase throughout the Reactor Coolant System. The insurge into the pressurizer compresses the steam volume, actuates the automatic spray system, opens the power-operated relief valves, and opens the pressurizer safety valves, in that sequence. The two power-operated relief valves are designed for reliable operation and would be expected to function properly during the accident. However, for conservatism, their pressure-reducing effect is not included in the analysis.

Method of Analysis

The following cases are analyzed:

- 1) Locked Rotor Accident from reactor coolant heat output of 2200 MWt with three loops operating
- 2) Locked Rotor Accident from reactor coolant heat output of 1320 MWt with two loops operating

Initial Conditions

At the beginning of the postulated locked rotor accidents, i.e., at the time the shaft in one of the reactor coolant pumps is assumed to seize, the plant is assumed to be in operation under the most severe steady state operating conditions. The plant is assumed to be operating at 102% of nominal full power, 2200 MWt with three pumps operating, and at 62% of nominal full power with two pumps operating, based on the maximum expected calorimetric error. Inlet temperature is assumed to be 4°F above its programmed value to allow for the 2°F deadband on control rod motion and a maximum temperature error of 2°F (nominal inlet temperature with three pumps operating is 546.2°F and assumed to be 552.7°F with two loops operating). Reactor coolant pressure is conservatively estimated as 30 psi above nominal pressure (2250 psia) to allow for errors in the pressure measurement and control channels.

Evaluation of the Pressure Transient

A digital code was used to determine the peak pressure in the Reactor Coolant System under the postulated accident conditions and to obtain the nuclear power as a function of time which is used later on in the analysis.

After pump seizure, nuclear power is rapidly reduced because of the control rod insertion upon plant trip and void shutdown.

In this analysis, the time from pump seizure to initiation of control rod motion was taken as 0.9 seconds. Shutdown reactivity is conservatively based on a 1 per cent shutdown margin at no load conditions.

No credit was taken for the pressure-reducing effect of the pressurizer relief valves, steam dump and controlled feedwater flow after plant trip. Although these operations are expected to occur and would result in a lower peak pressure, an additional degree of conservatism is provided by ignoring their effect.

The reactor pressurizer safety valves start operating at 2500 psia and their capacity for steam relief is, $29.7 \text{ ft}^3/\text{sec}$.

Evaluation of DNB in the Core During the Accident

Heat flux transients following the pump seizure were evaluated by a detailed digital model with the input of the nuclear power, the pressure and the coolant conditions previously calculated as functions of time. The model is similar to the model incorporated in the LOCTA code but features a larger number of lumps in the fuel. This study used 6 lumps for the fuel and one for the clad.

Calculations of the extent of DNB in the core during the accidents were performed using a multichannel THINC-III model with the heat flux, the coolant flow decay and the coolant conditions calculated as a function of time. Nine concentric channels were used for this study.

In order to estimate the severity of the accident in the core as far as the integrity of the fuel rods are concerned, the thermal behavior of the fuel located at the hot spot after DNB was investigated using the detailed digital model mentioned above with a film boiling heat transfer calculation. Results obtained from an analysis of this "hot spot" condition represent the upper limit with respect to clad temperature, clad melting and zirconium-steam reaction. The steady-state conditions at the hot spot in the core just prior to the accident are shown below:

	<u>three pumps operating</u>	<u>two pumps operating</u>
Heat flux; Btu/hr-ft^2	565,280	343,600
Avg. pellet temp., °F	2510	2130
Avg. clad temp., °F	714	691
System pressure, psi	2220	2220
Coolant mass flow rate, lbs/hr-ft^2	2.32×10^6	1.48×10^6

Film Boiling Coefficient

The following empirical equation was included in the digital program to calculate the film boiling coefficient:

$$\left(\frac{hD}{k}\right)_f = 0.0193 \left(\frac{DG}{\mu}\right)_f^{0.80} \left(\frac{C_p \mu}{k}\right)_f^{1.23} \left(\frac{\rho_g}{\rho_b}\right)^{0.68} \left(\frac{\rho_g}{\rho_l}\right)^{0.068}$$

where $\rho_b = \alpha \rho_g + \rho_l (1-\alpha)$

h = film boiling coefficient, BTU/hr-ft² °F

D = channel equivalent Diameter, ft

k = thermal conductivity of steam BTU/hr-ft °F

G = mass flow rate lbs/hr-ft²

μ = viscosity of steam lb/hr-ft

C_p = specific heat of steam BTU/lb °F

ρ_g = density of steam lbs/ft³

ρ_l = density of water lbs/ft³

α = void fraction

The steam properties are evaluated at film temperature (avg. between wall and bulk temperatures). The program calculates the film coefficient at every time step based upon the actual heat transfer conditions at this time.

The system pressure, bulk density and mass flow rate are an input of the program as a function of time.

For this analysis, the initial values of the pressure and the bulk density were used throughout the transient, since they were the most conservative.

For conservatism, DNB was assumed to start at the beginning of the accident and the heat transfer coefficient between clad and water was reduced suddenly from its steady-state value to 0.7 times the film boiling value at time = 0, without any period of transition boiling. The safety factor of 0.7 was assumed for conservatism in evaluating the film boiling coefficient.

Gap Coefficient

The magnitude and time dependence of the heat transfer coefficient between fuel and cladding has a pronounced influence on the thermal results. The larger the value of this coefficient, the more heat is transferred between pellet and clad. For the first part of the transient, a high gap coefficient produces higher clad temperatures since the heat stored and generated in the fuel pellet tries to redistribute itself in the cooler clad. This effect of the gap coefficient, however, is reversed when the clad temperature exceeds the pellet temperature in cases when zirconium-steam reaction is present.

The effect of the gap coefficient upon the maximum clad temperature during the transient was investigated. Two cases with different initial gap coefficient were considered. The results are depicted in Figure 14.1.9-9. It shows that higher coefficient during the transient results in higher clad temperature. Therefore, high estimated values were used for the transient: 5300 BTU/hr-ft²-°F for the hot spot and 13,200 BTU/hr-ft²-°F for the hot spot with higher initial gap coefficient at 2200 MWt. (3000 BTU/hr-ft²-°F and 10350 BTU/hr-ft²-°F at 1320 MWt).

Zirconium-Steam Reaction

Since it was found that in the worst case examined, the clad temperature exceeded 1800°F, it was necessary to consider the possibility of a zirconium-steam reaction. The zirconium-steam reaction can become significant above this temperature. In order to take this phenomenon into account, the following correlation, which defines the rate of the zirconium-steam reaction, was introduced into the model:

$$\frac{dw^2}{dt} = 33.3 \times 10^6 e^{-\frac{45,500}{1.986T}}$$

where w = amount reacted, mg/cm^2

t = time, sec

T = temperature, °K

The reaction heat is about 1510 cal/gm.

Results

The primary coolant pressure vs. time for a locked rotor accident at 2200 MWt with three loops operating is shown in Figure 14.1.9-10. The peak pressure reached after 4.0 sec, is 2440 psia. The minimum DNB ratio for this case from the W-3 correlation is shown in Figure 14.1.9-11 as a function of time; the worst DNB condition occurs about 2 seconds after the start of the accident.

Figure 14.1.9-12 shows the minimum DNB ratio reached during the accident as a function of number of rods. It can be seen from this figure that less than 10% of the rods reach a DNBR lower than 1.3.

Figure 14.1.9-13 shows the clad temperature transient with zirconium-steam reaction at the hot spots during the accident. The maximum clad temperature is 1810°F. Although zirconium-steam reaction can be detected at 1800°F it produced only a moderate increase in the clad temperature (by 10°F).

Figure 14.1.9-14 through Figure 14.1.9-17 show transient response for a locked rotor accident from 1320 MWt with two loops operating. The peak pressure reaches 2540 psia after 5.0 seconds (see Figure 14.1.9-14). The minimum DNB ratio during the accident as a function of time is depicted in Figure 14.1.9-15.

Figure 14.1.9-16 shows the minimum DNB ratio reached during the accident as a function of the number of rods. It can be seen that less than 10% of the fuel rods reach a DNBR lower than 1.30.

Figure 14.1.9-17 shows the clad temperature transient at the hot spots.

Conclusions

- A) Since the peak pressure reached during the transient is 2540 psia the integrity of the primary coolant system is not endangered and can be considered as an upper limit, because of the conservative assumptions used in the study as given below:
 - 1) Credit was not taken for the negative moderator coefficient
 - 2) It was assumed that the pressurizer relief valves were inoperative
 - 3) The steam dump was assumed to be inoperative.
- B) Less than 10% of the fuel rods exhibited a DNB ratio of less than 1.3.
- C) The peak clad surface temperature of 1810°F, calculated for the hot spot includes the effect of the zirconium-steam reaction (which is still quite small at that temperature). This can also be considered an upper limit since:

- 1) The hot spot was assumed to be in DNB at the start of the accident
- 2) A high gap coefficient was used
- 3) A value of 0.7 times the heat transfer coefficient for film boiling was used in the study and film boiling was assumed to be fully developed from the start of the transient, i.e., no credit was taken for transition boiling.
- 4) The nuclear heat released in the fuel at the hot spot was based on a zero moderator coefficient.

THREE PUMPS LOSS OF FLOW INCIDENT

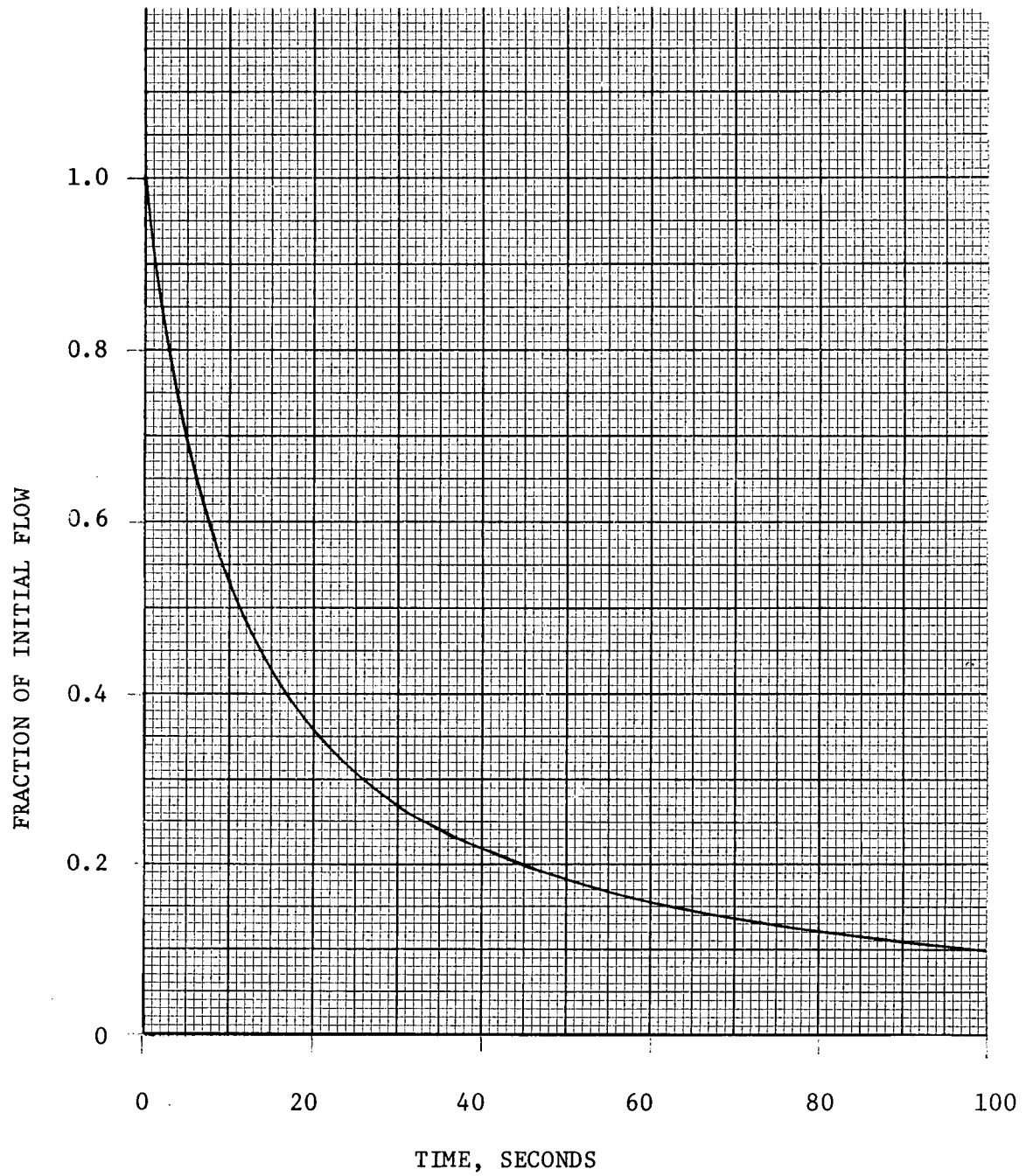


FIGURE 14.1.9-1

TWO PUMPS OUT OF THREE LOSS OF FLOW INCIDENT

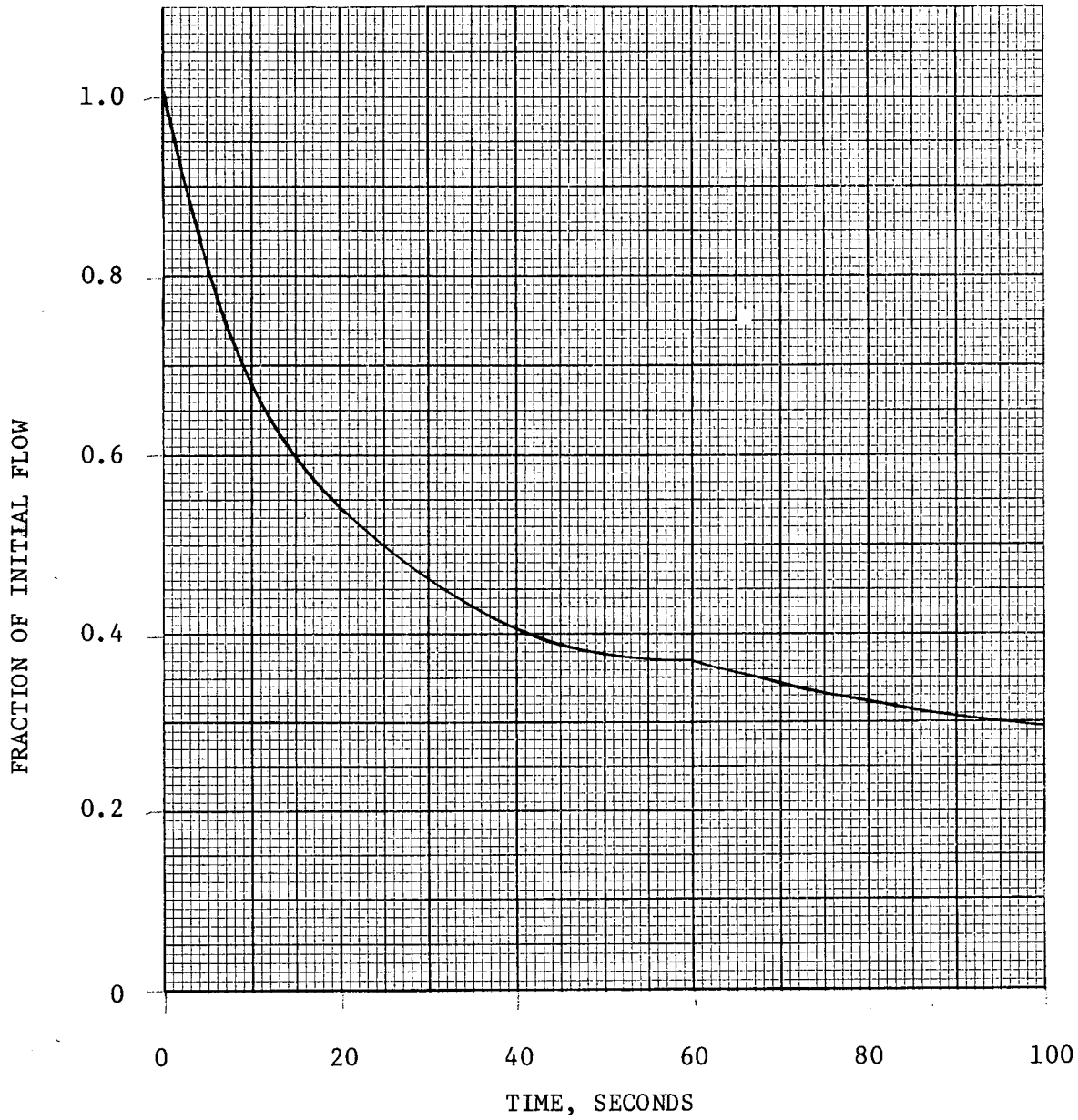


FIGURE 14.1.9-2

TWO PUMPS OUT OF TWO LOSS OF FLOW INCIDENT

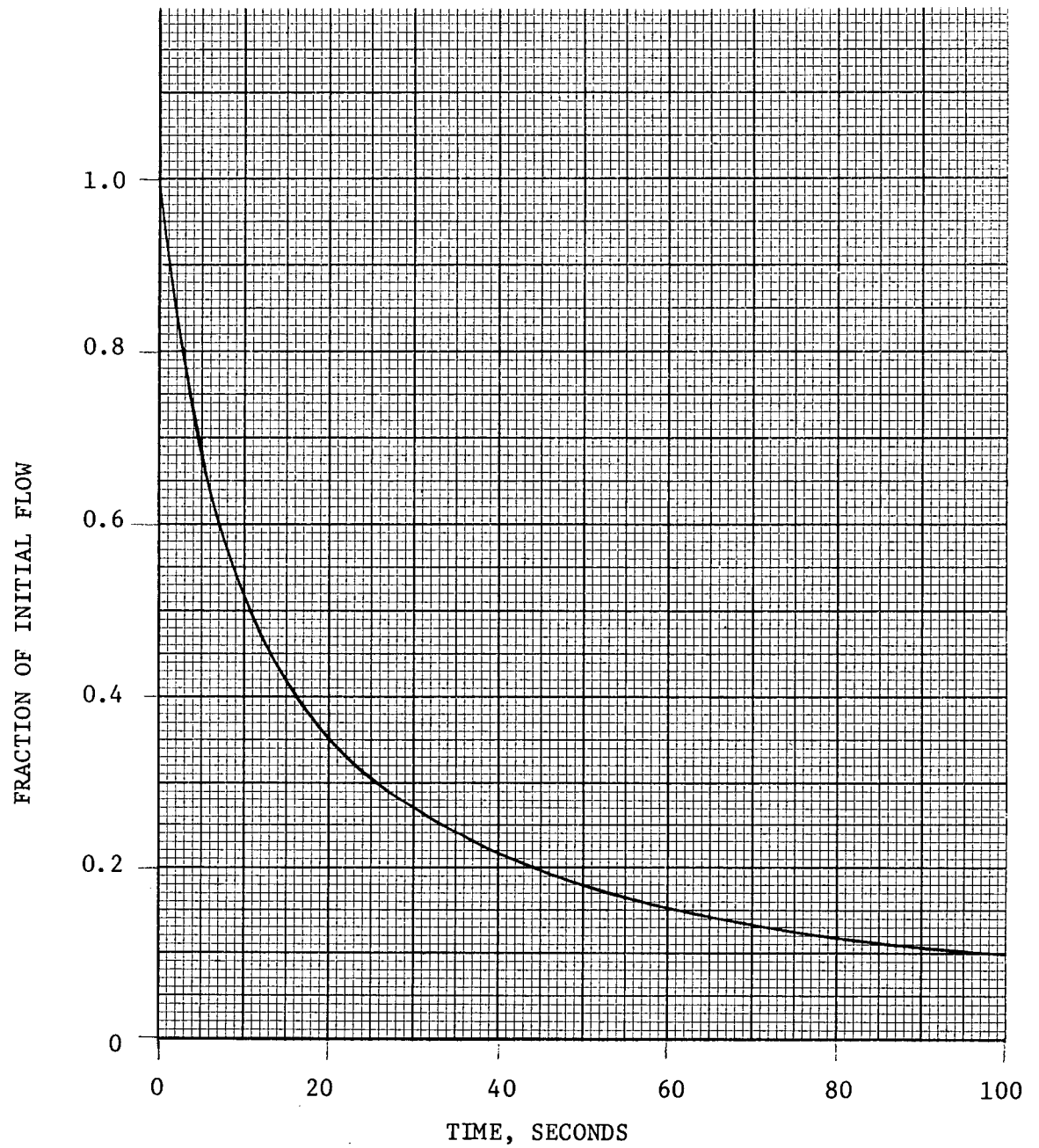


FIGURE 14.1.9-3

THREE PUMPS LOSS OF FLOW INCIDENT

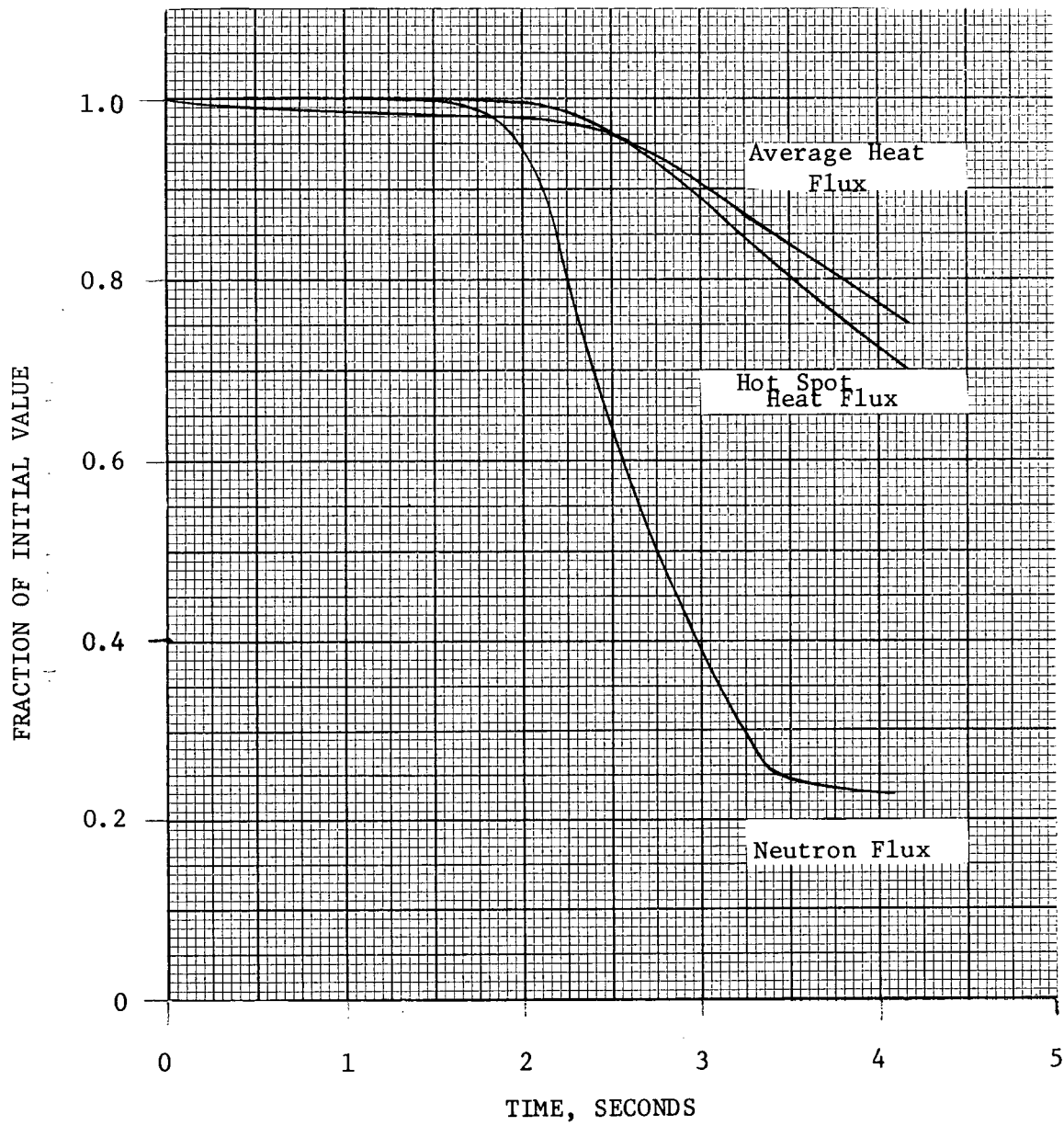


FIGURE 14.1.9-4

THREE PUMPS LOSS OF FLOW INCIDENT

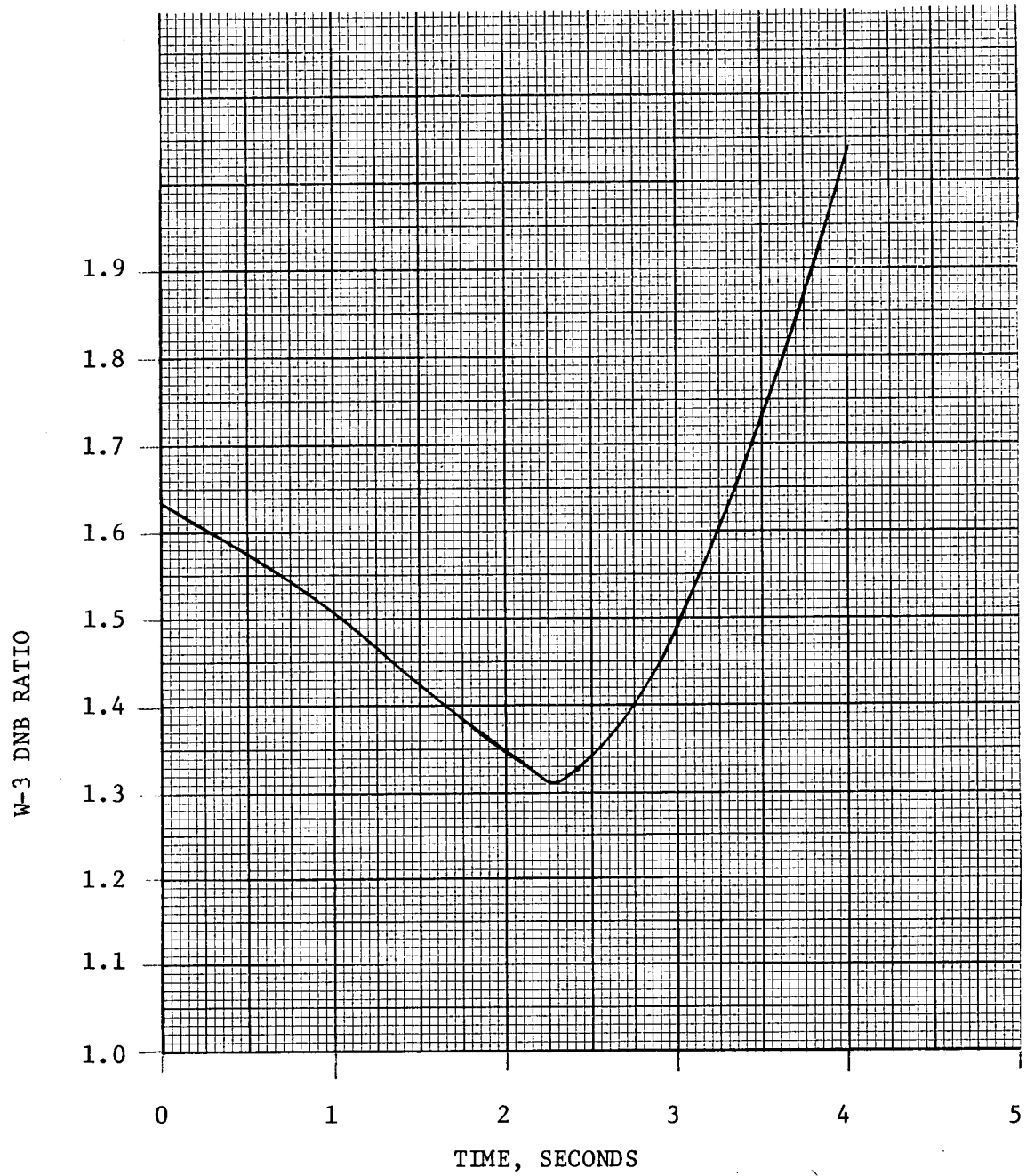


FIGURE 14.1.9-5

TWO PUMPS OUT OF THREE LOSS OF FLOW INCIDENTS

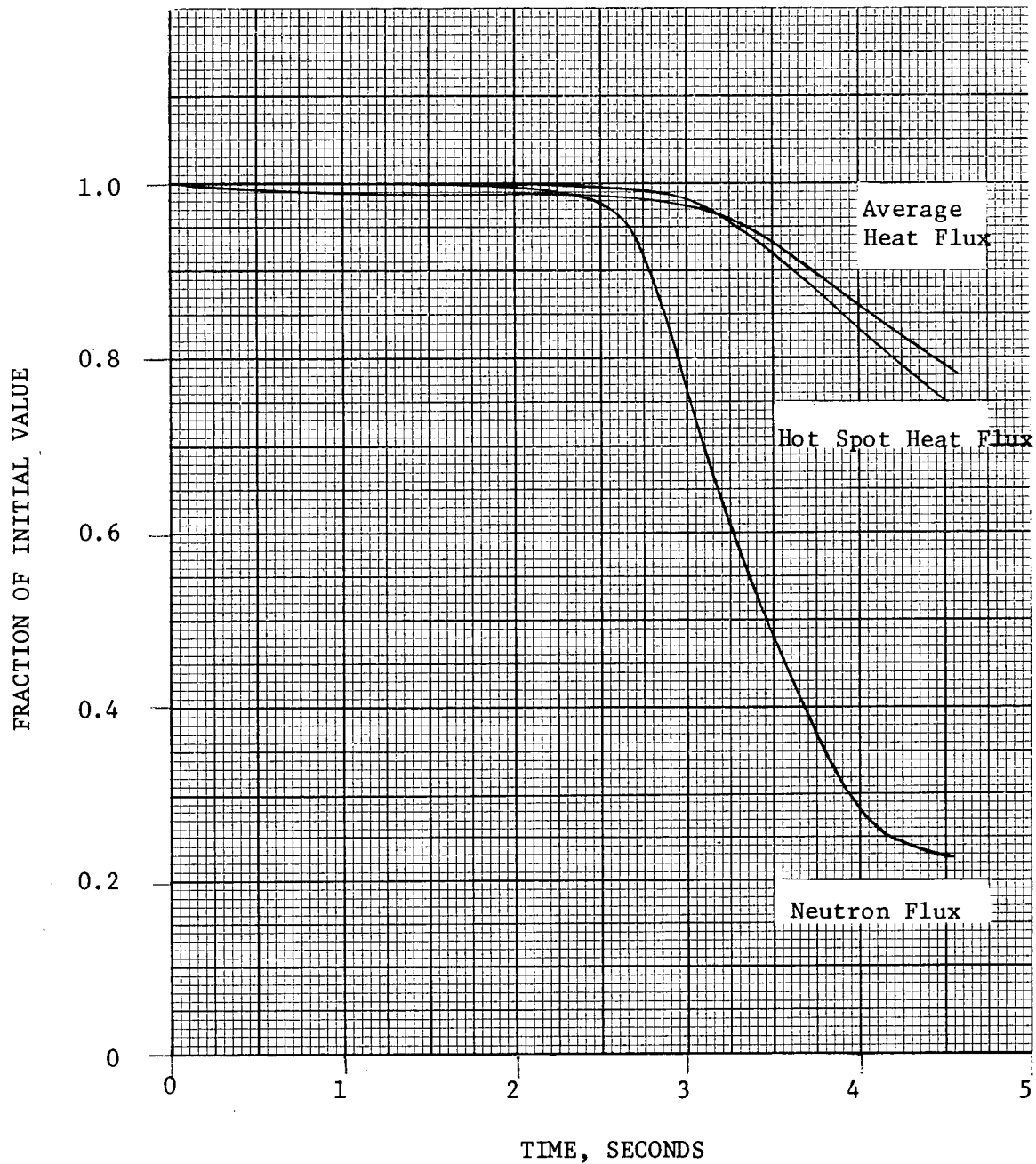


FIGURE 14.1.9-6

TWO PUMPS OUT OF THREE LOSS OF FLOW INCIDENT

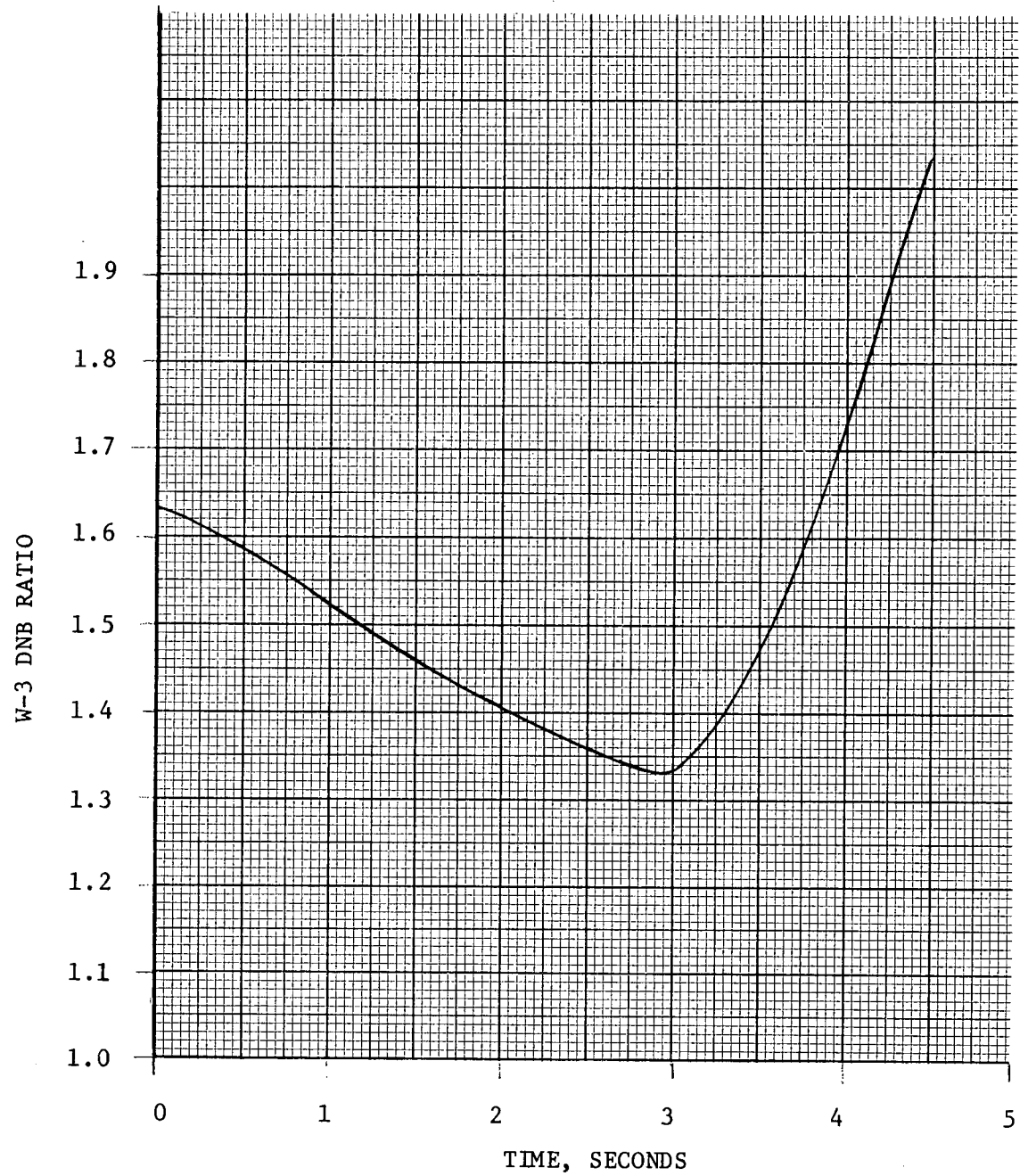


FIGURE 14.1.9-7

TWO PUMPS OUT OF TWO LOSS OF FLOW INCIDENT

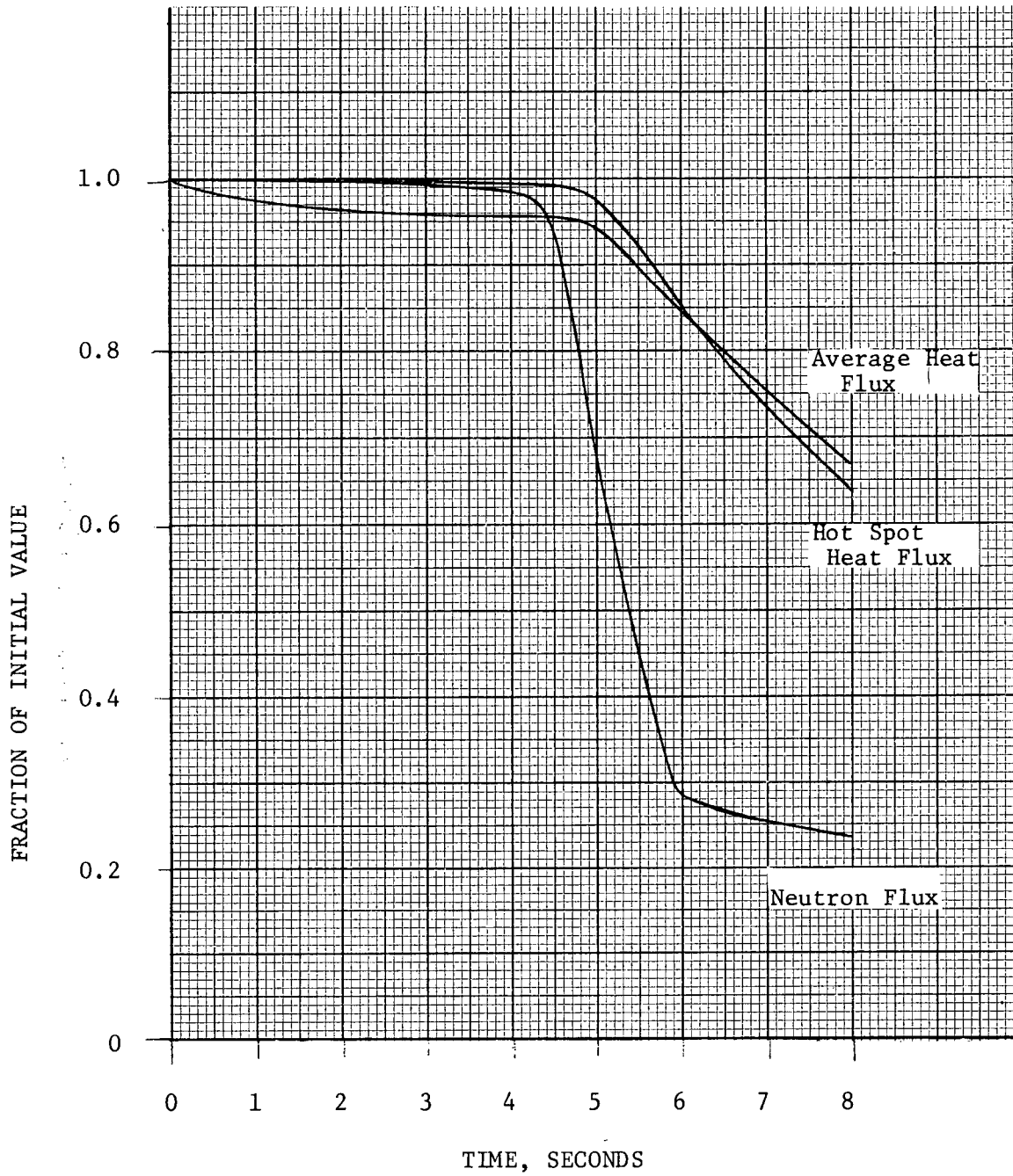


FIGURE 14.1.9-8

TWO PUMPS OUT OF TWO LOSS OF FLOW INCIDENT

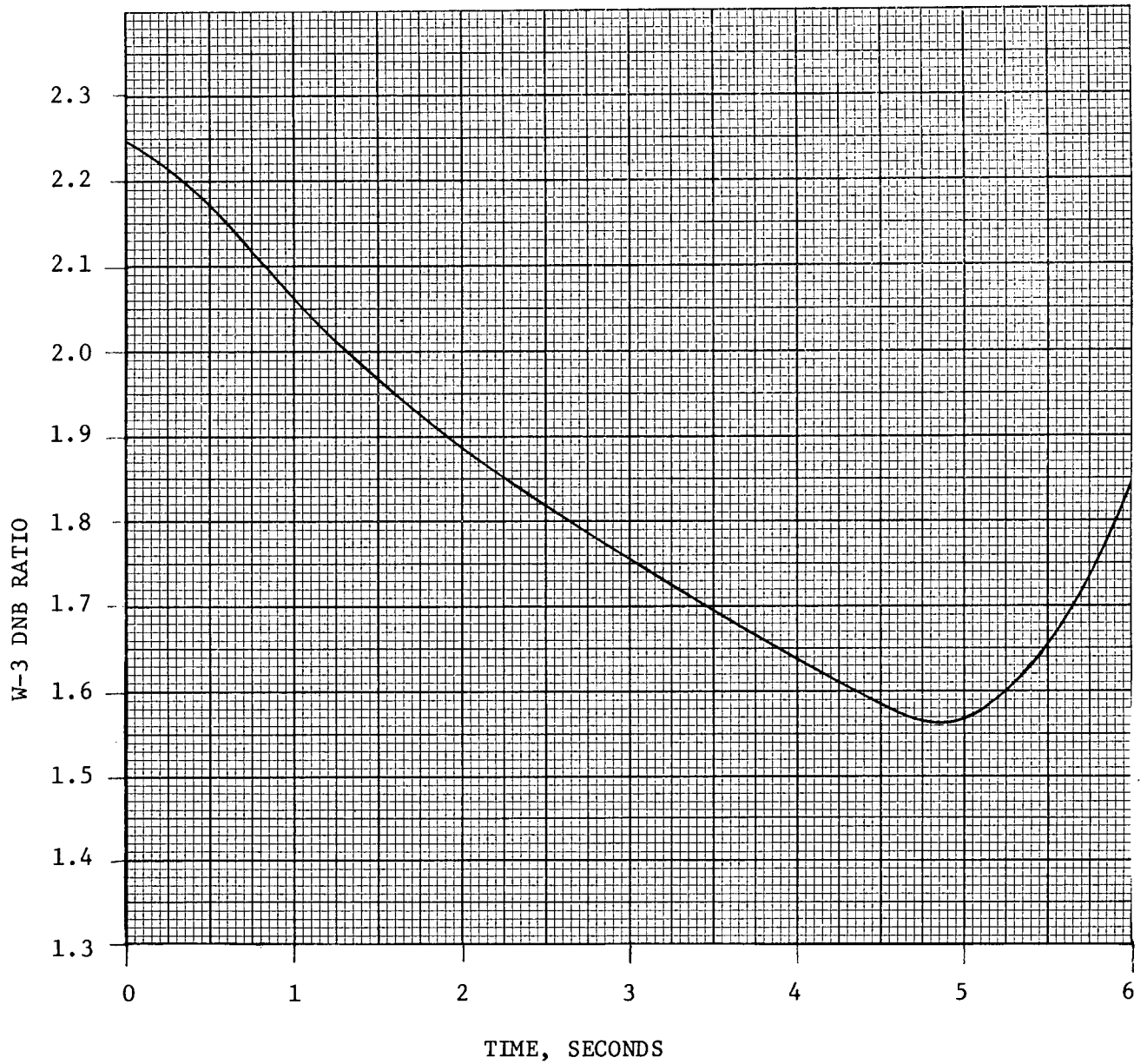


FIGURE 14.1.9=8A.

LOCAL CLAD SURFACE TEMPERATURE vs GAP CONDUCTIVITY

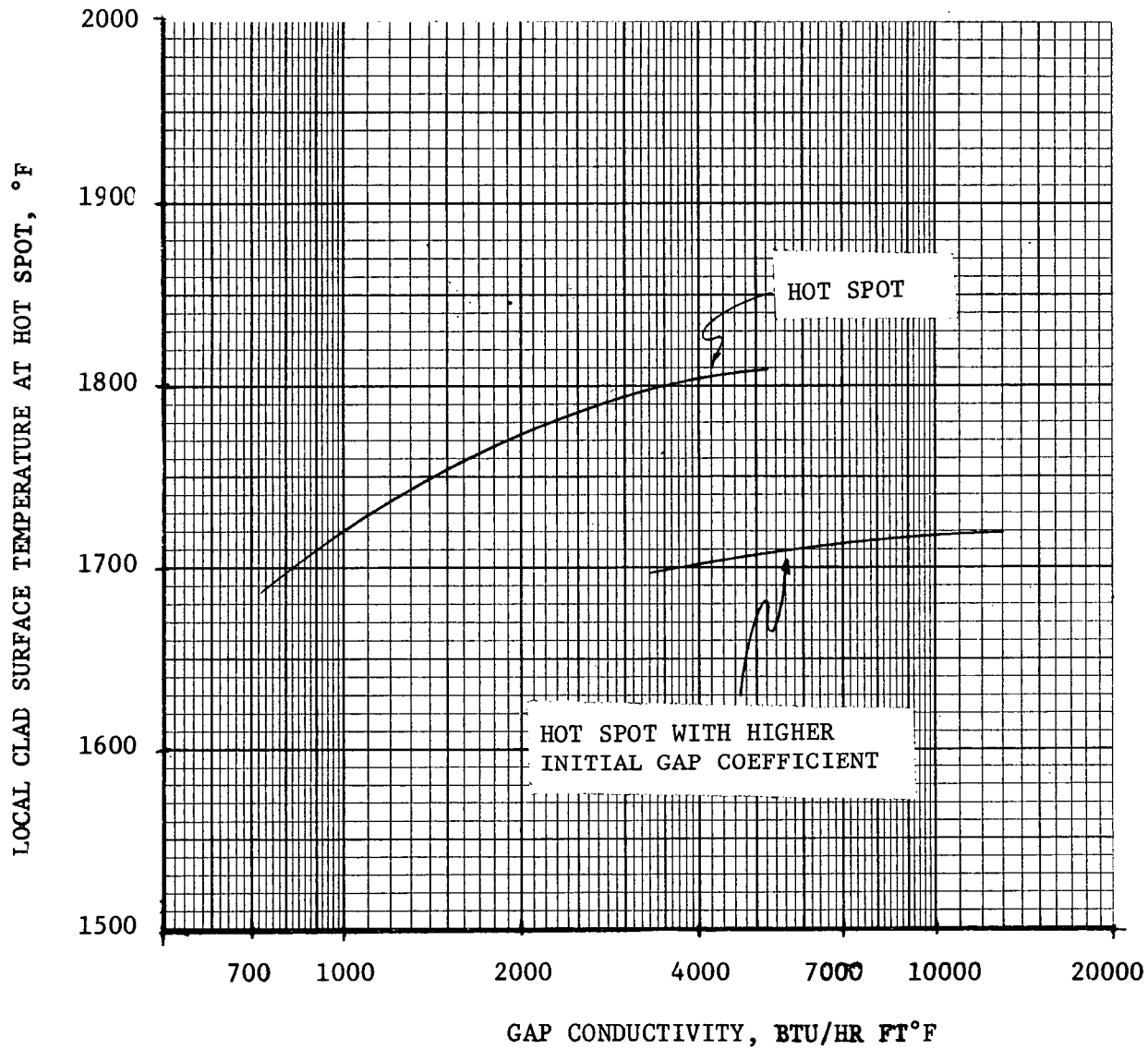


FIGURE 14.1.9-9

LOCKED ROTOR ACCIDENT FROM 2200 MWt WITH THREE
LOOPS OPERATING

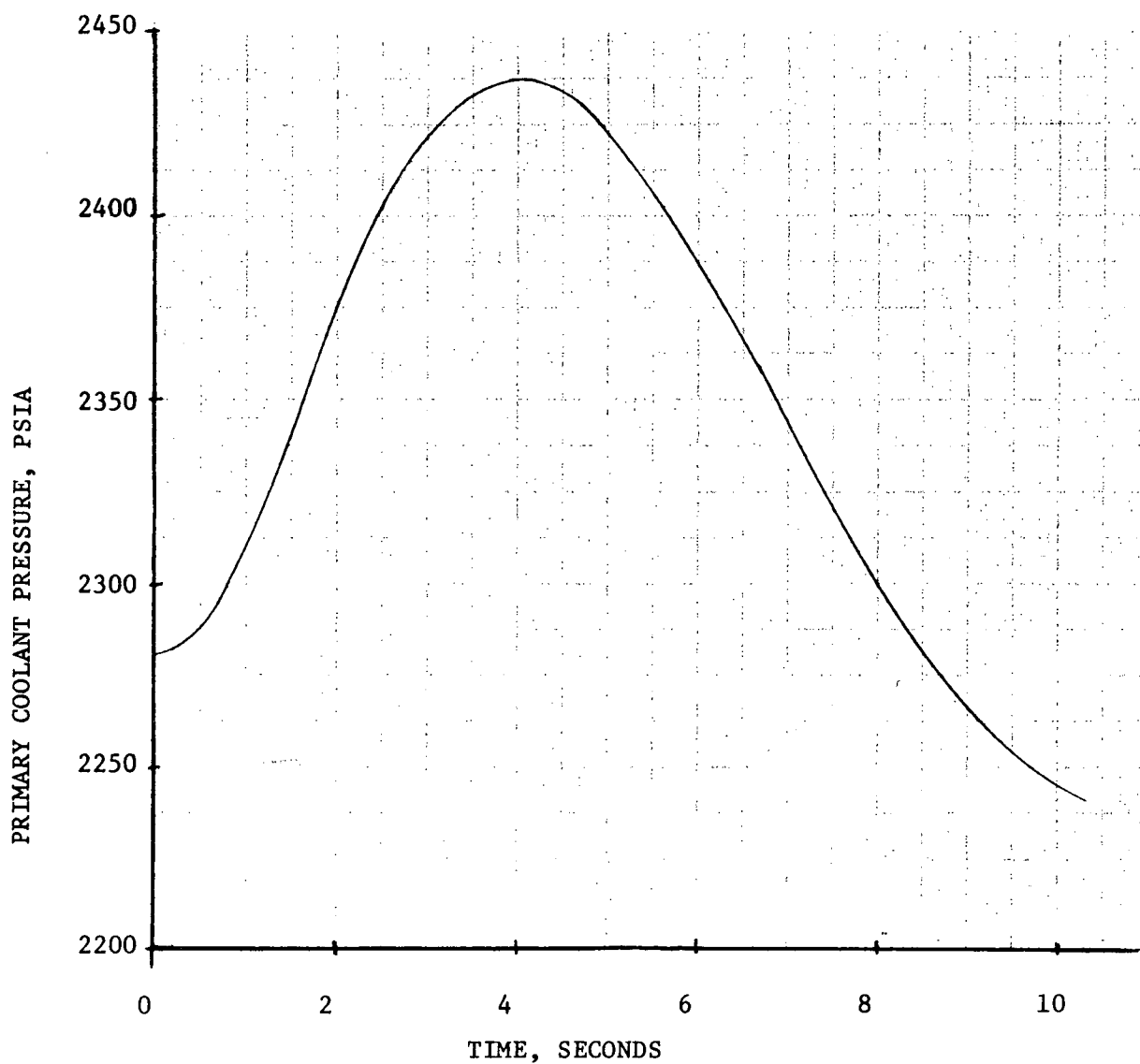


FIGURE 14.1.⁹-10

LOCKED ROTOR ACCIDENT FROM 2200 MWt WITH THREE LOOPS
OPERATING

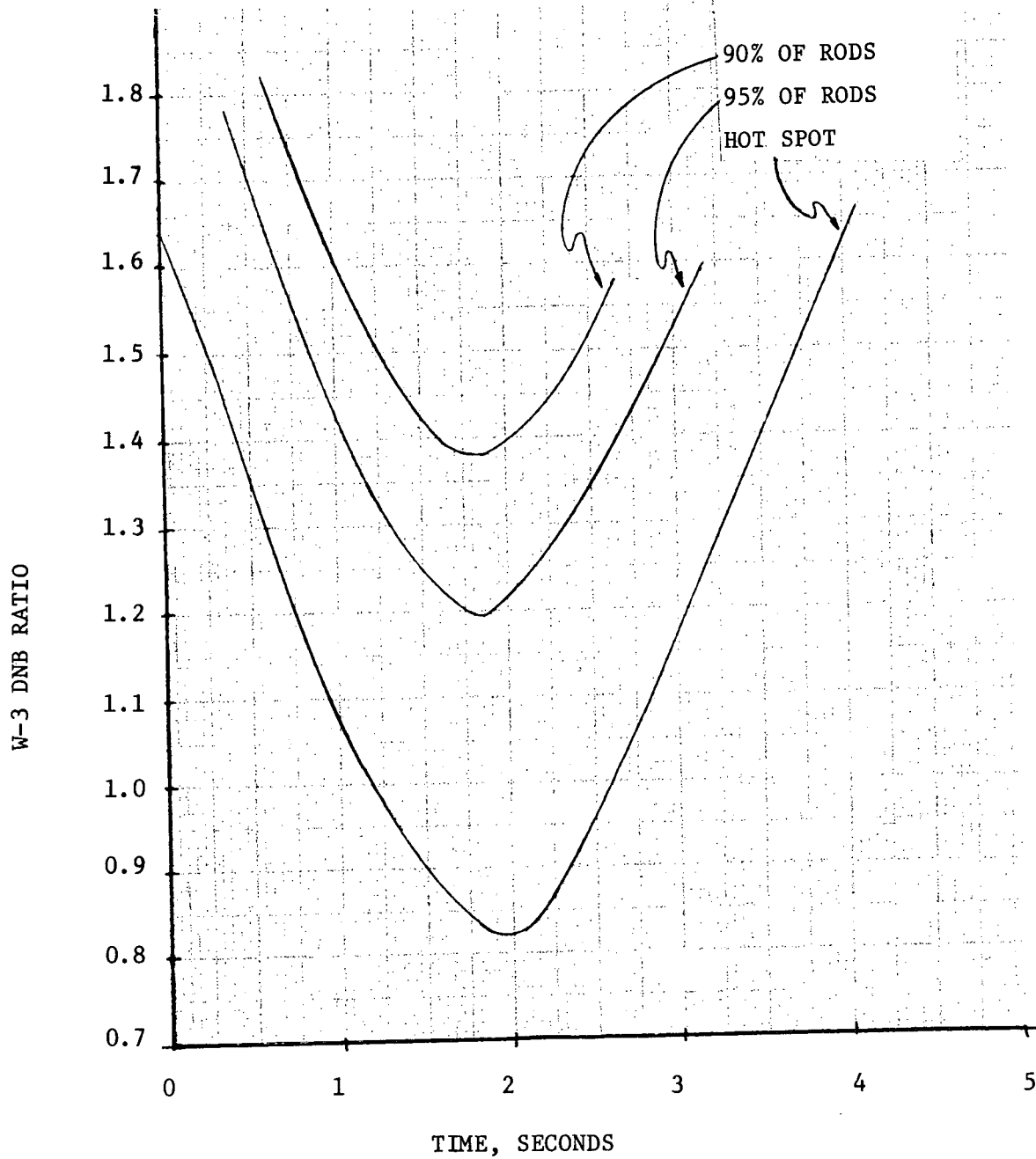


FIGURE 14.1.9-11

LOCKED ROTOR ACCIDENT AT 2200 MWt WITH THREE
LOOPS OPERATING

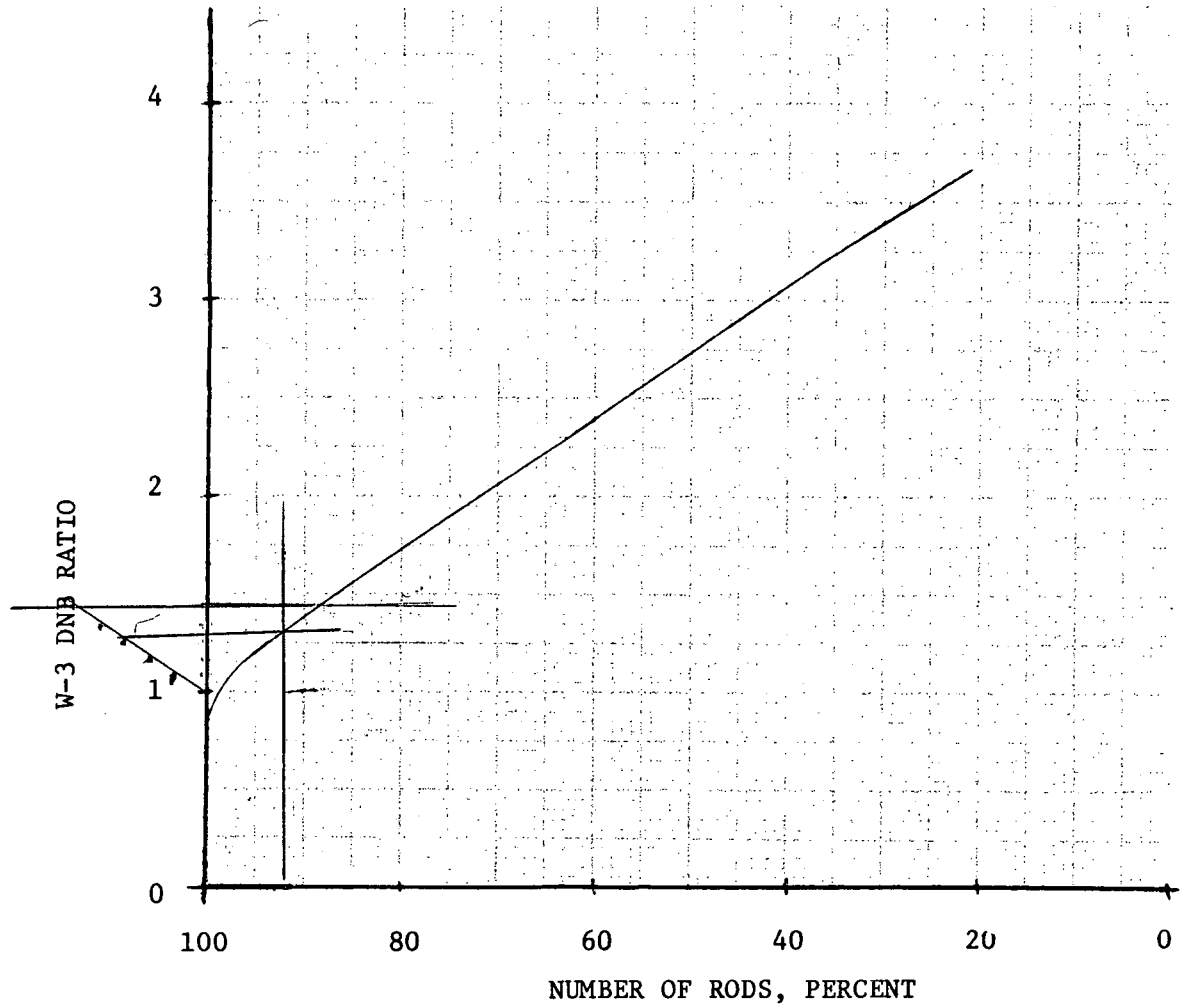


FIGURE 14.1. 9-12

CLAD SURFACE TEMPERATURE vs TIME WITH LOCKED ROTOR
ACCIDENT FROM 2200 MWt WITH THREE LOOPS OPERATING

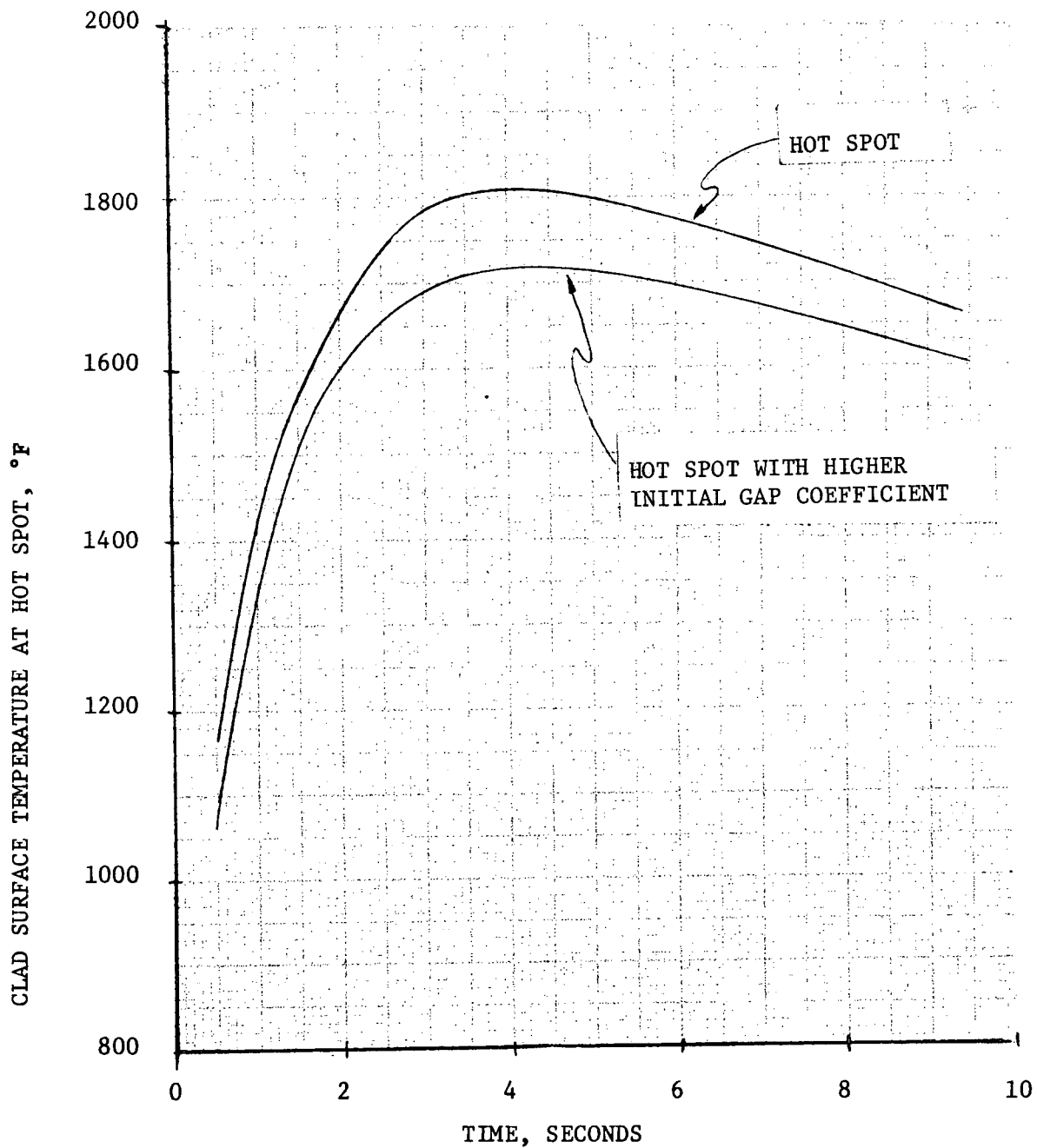


FIGURE 14.1.9-13

LOCKED ROTOR ACCIDENT FROM 1320 MWt WITH TWO LOOPS OPERATING

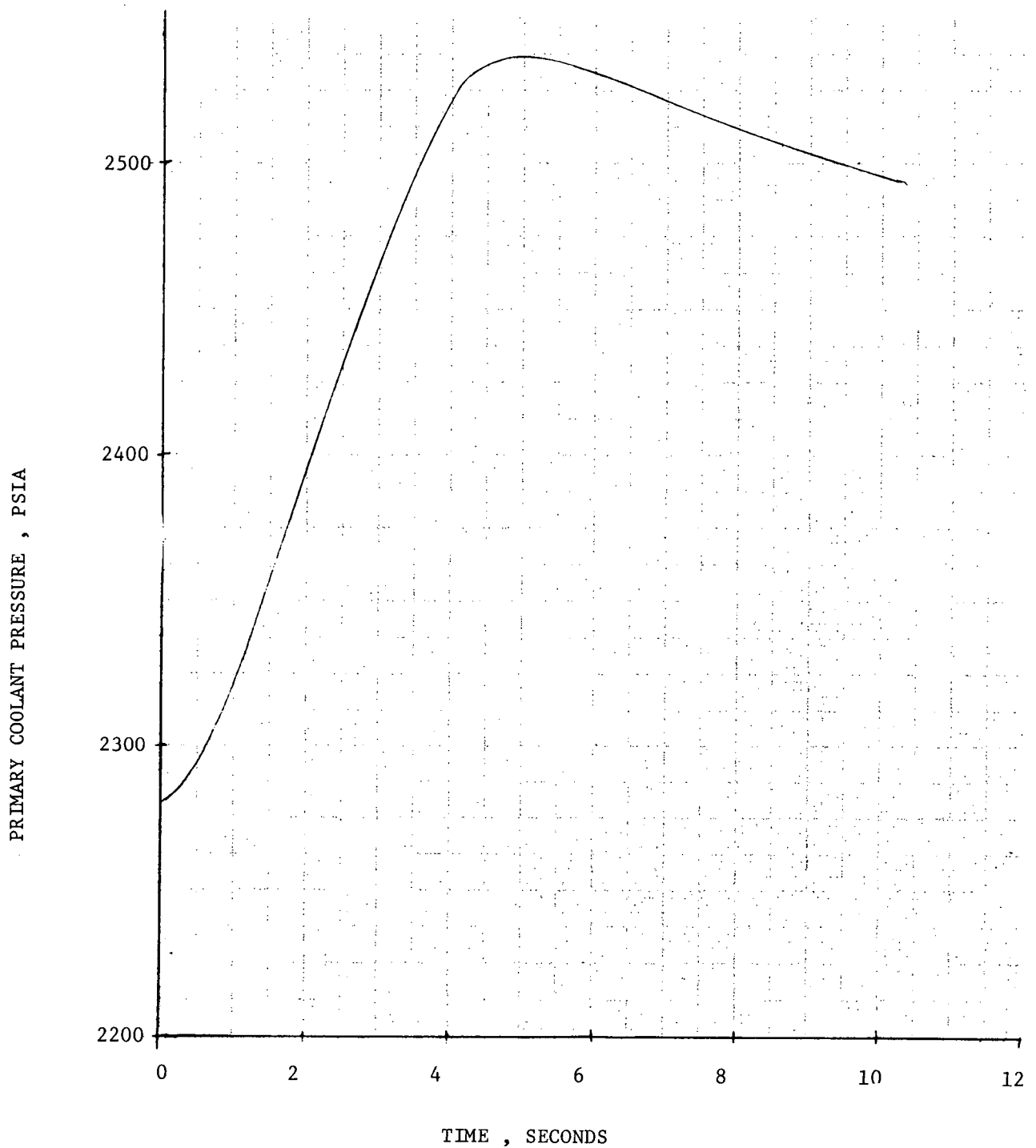
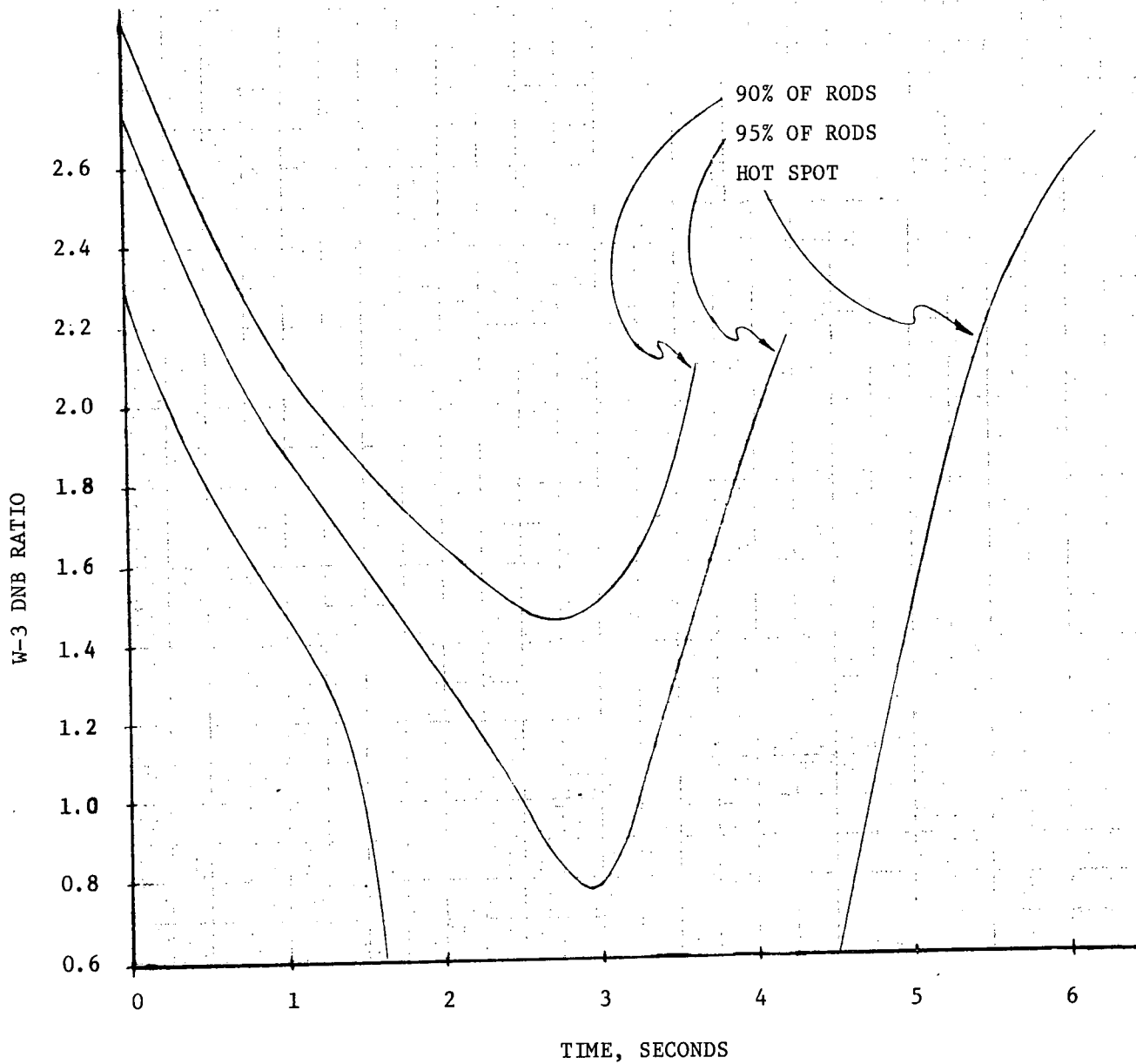


FIGURE 14.1.9-14



LOCKED ROTOR ACCIDENT FROM 1320 MWt WITH TWO LOOPS OPERATING

FIGURE 14.1.9-15

LOCKED ROTOR ACCIDENT FROM 1320 MWt
WITH TWO LOOPS OPERATING

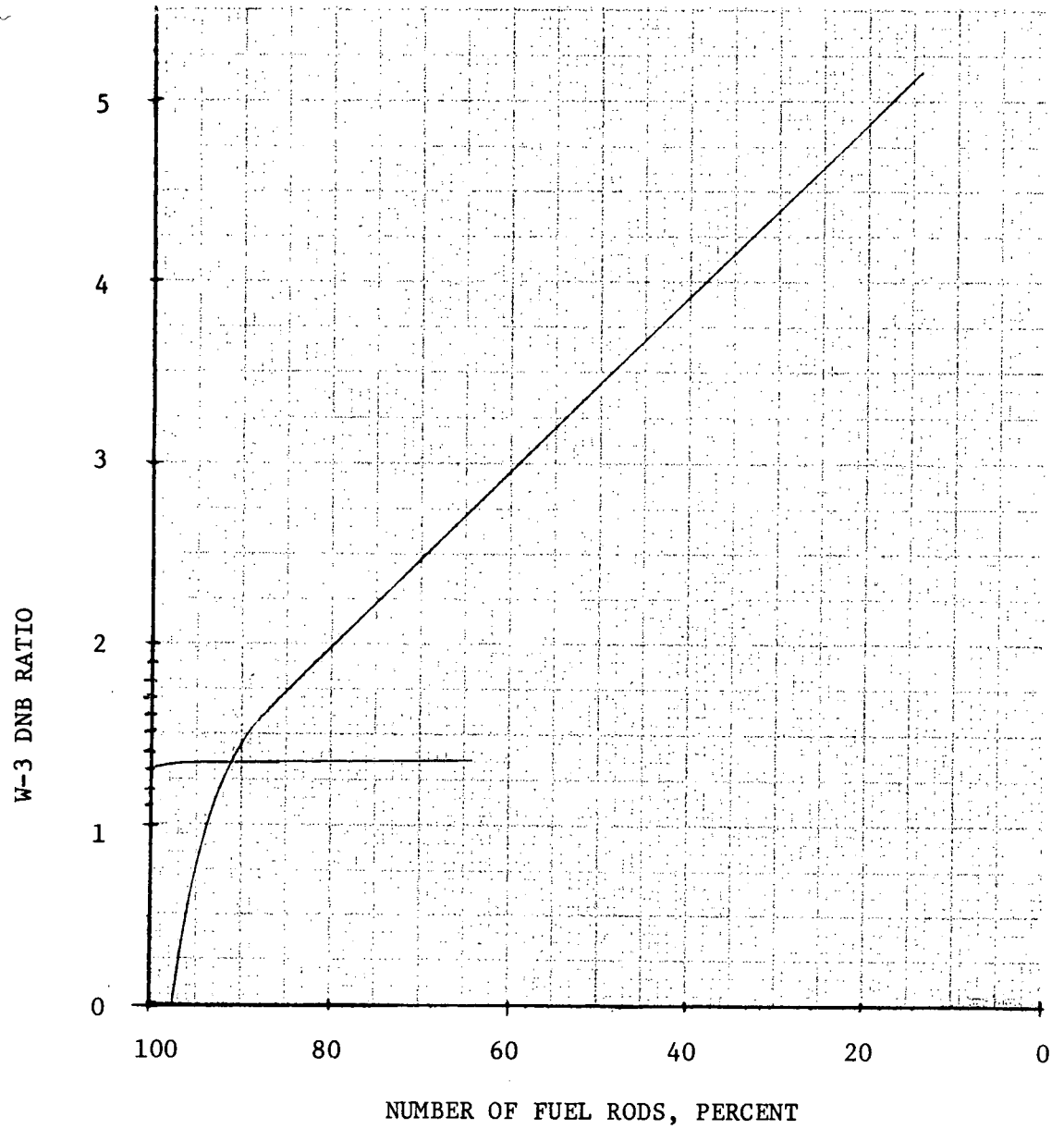


FIGURE 14.1.9-16

CLAD SURFACE TEMPERATURE vs TIME LOCKED ROTOR
ACCIDENT FROM 1320 MWt WITH TWO LOOPS OPERATING

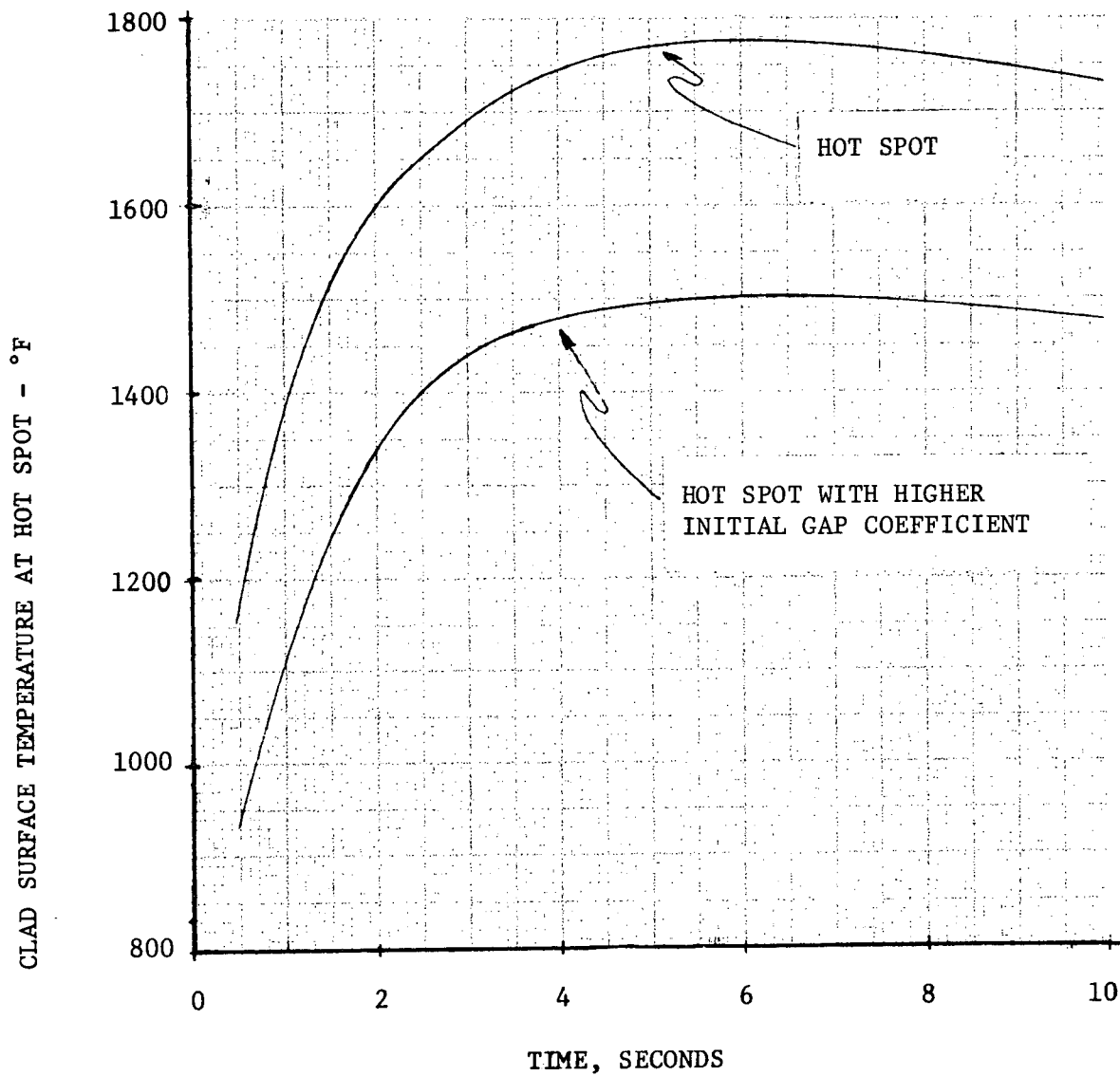


FIGURE 14.1.9-17

14.1.10 LOSS OF EXTERNAL ELECTRICAL LOAD ✓

The loss of external electrical load may result from an abnormal increase in network frequency, or an accidental opening of the main breaker from the generator which fails to cause a turbine trip but causes a rapid large load reduction by the action of the electro-hydraulic turbine control.

The plant is designed to accept a complete loss of export load without actuating a reactor trip. The automatic steam bypass system with 40 percent dump capacity to the condenser and 45% dump capacity to the atmosphere is able to accommodate this abnormal load rejection by reducing the transient imposed upon the reactor coolant system. The reactor power is reduced to the new equilibrium power level at a rate consistent with the capability of the rod control system. The pressurizer relief valves may be actuated, but the pressurizer safety valves and the steam generator safety valves are not actuated in this case.

In the event the steam dump valves fails to open following a large load loss, the steam generator safety valves are actuated and the reactor may be tripped by the high pressurizer pressure signal or the high pressurizer level signal. The steam generator shell side pressure and reactor coolant temperatures increase rapidly. The pressurizer safety valves are sized to protect the reactor coolant system against overpressure without taking credit for the steam bypass system.

The most likely source of a complete loss of load on the Nuclear Steam Supply System is a trip of the turbine-generator. In this case there is a direct reactor trip signal derived from turbine autostop oil pressure (a two out of three signal). Reactor coolant temperatures and pressure do not significantly increase if the steam bypass system and pressurizer pressure control system are functioning properly. However, the plant behavior is also evaluated

for a complete loss of load from full power without a direct reactor trip, primarily to show the adequacy of the pressure relieving devices and also to show that no core damage occurs. The Reactor Coolant System and Steam System pressure relieving capacities are designed to ensure safety of the plant without requiring the automatic rod control pressurizer pressure control and/or steam bypass control systems.

Method of Analysis

The total loss of load transients are analyzed by employing a detailed digital computer program. This code describes the neutron kinetics, decay heat, Reactor Coolant System with pressurizer, steam generators, and the associated steam bypass system and rod control system.

The objectives of this analysis are to determine margins to core protection limits and to establish pressure relieving requirements for the Reactor Coolant and Steam Systems.

Initial Operating Conditions

The initial reactor power, coolant temperatures and pressure are all assumed at maximum values consistent with steady state, full power operation, including allowances for calibration and instrument errors (2244 MWt). This results in the maximum power difference for the load loss, and the minimum margin to core protection limits at the initiation of the total loss of load accident.

Moderator and Doppler Coefficients of Reactivity

The total loss of load is analyzed for both beginning-of-life and end-of-life conditions.

At beginning-of-life the least negative value of moderator coefficient is used with the most negative value of Doppler coefficient. At end-of-life the most negative value of moderator coefficient is used with the most negative value of Doppler coefficient. This results in a least shutdown margin following reactor trip. See Section 3.2.2.

Reactor Control

Two cases are analyzed:

1. The reactor is assumed to be in normal automatic control with the control rods in the minimum incremental worth region.
2. The reactor is assumed to be in manual control. There is no control rod insertion following the accident.

Steam Release

No credit is taken for any of the dump valves openings. The steam generator pressures rise toward the safety valve set point where steam release through safety valves limits secondary steam pressure at the set point.

Pressurizer Spray and Power Operated Relief Valves

Full credit is taken in evaluating margins to DNB for the effect of pressurizer spray and relief valves in reducing or limiting coolant pressure since this may prolong the high pressure reactor trip. A second case is analyzed where no credit is taken for pressure control and pressurizer safety valves may be actuated during the transient.

Results

The transient responses for a total loss of load from full power operation are shown for four cases, two cases for beginning of core life and two cases for end of core life.

Figure 14.1.10-1, -2 and -3 show the transient responses for loss of load accident at beginning of life with zero moderator coefficient. In this transient no credit is taken for steam dump. Full credit is taken for the effect of pressurizer spray and relief valves in reducing or limiting coolant pressure. Credit is also taken for the effect of control rods insertion in reducing the nuclear power to prolong the time to a high pressure trip. It can be seen from the transients that the power operated relief valve capacity is not large enough to limit the pressurizer pressure at 2400 psia and prevent a high pressure trip. The high pressure trip occurs 9.78 seconds after loss of load, and the pressure rises to a maximum of 2441.6 before decreasing. Minimum DNB ratio at the time the pressure trip is actuated, 10.5 seconds after the start of the transient, is 1.61, which is well above the 1.3 design value.

Figures 14.1.10-4, -5 and -6 show the responses for total loss of load at end of life with the most negative moderator coefficient ($-3.5 \times 10^{-4} \delta k/^{\circ}F$). The rest of the plant operating conditions are the same as the case above. The pressurizer pressure increases to 2395 psia initially. The combination of rod insertion, pressurizer spray, and relief valves were able to prevent the pressure from rising above the 2400 psi high pressure trip. The pressure decreases rapidly after about 20 seconds resulting from the large reduction in nuclear power. The increase in coolant average temperature is about 18.5°F. The DNB ratio increases after the trip due to the decrease in nuclear power.

The total loss of load accident was also studied assuming the plant is operating at full power with manual control. There is no control rod insertion following the accident. Operation of the pressurizer spray, relief valves and steam

dump valves are all ignored. The reactor is tripped on the high pressure signal which is set at 2400 psia. Figures 14.1.10-7, -8 and -9 shows the beginning-of-life transients with zero moderator coefficient. The nuclear power remains at constant full power before the reactor is tripped. The peak pressurizer pressure is 2517 psia and maximum surge rate is about 12.6 ft³/sec. This is compared to a pressurizer safety valve capacity of approximately 30.9 ft³/sec. Figures, 14.1.10-10, -11 and -12 are the transients at end of life. The peak pressurizer pressure is 2514 psia and maximum surge rate is about 12.31 ft³/sec.

SV Activation @ 2500 PSIA - say avg surge rate 12.6/2 = 6.3

Conclusions

$$F_{\text{H}_2\text{O}} \text{ expelled} = 4.5 \text{ sec} (6.3) = 28 \text{ ft}^3$$

The analysis indicates that a total loss of load without a direct or immediate reactor trip presents no hazard to the integrity of the Reactor Coolant System and the Steam System. Pressure relieving devices incorporated in the two systems are adequate to limit the maximum pressures. The integrity of the core is maintained by the high pressurizer pressure reactor trip. The minimum DNB ratio is 1.61 for the beginning-of-life case which is well above the 1.3 design value. At end-of-life the DNB ratio during the total loss of load transient is even higher than that for the steady state, full power operating condition.

TOTAL LOSS OF EXTERNAL ELECTRICAL LOAD ACCIDENT

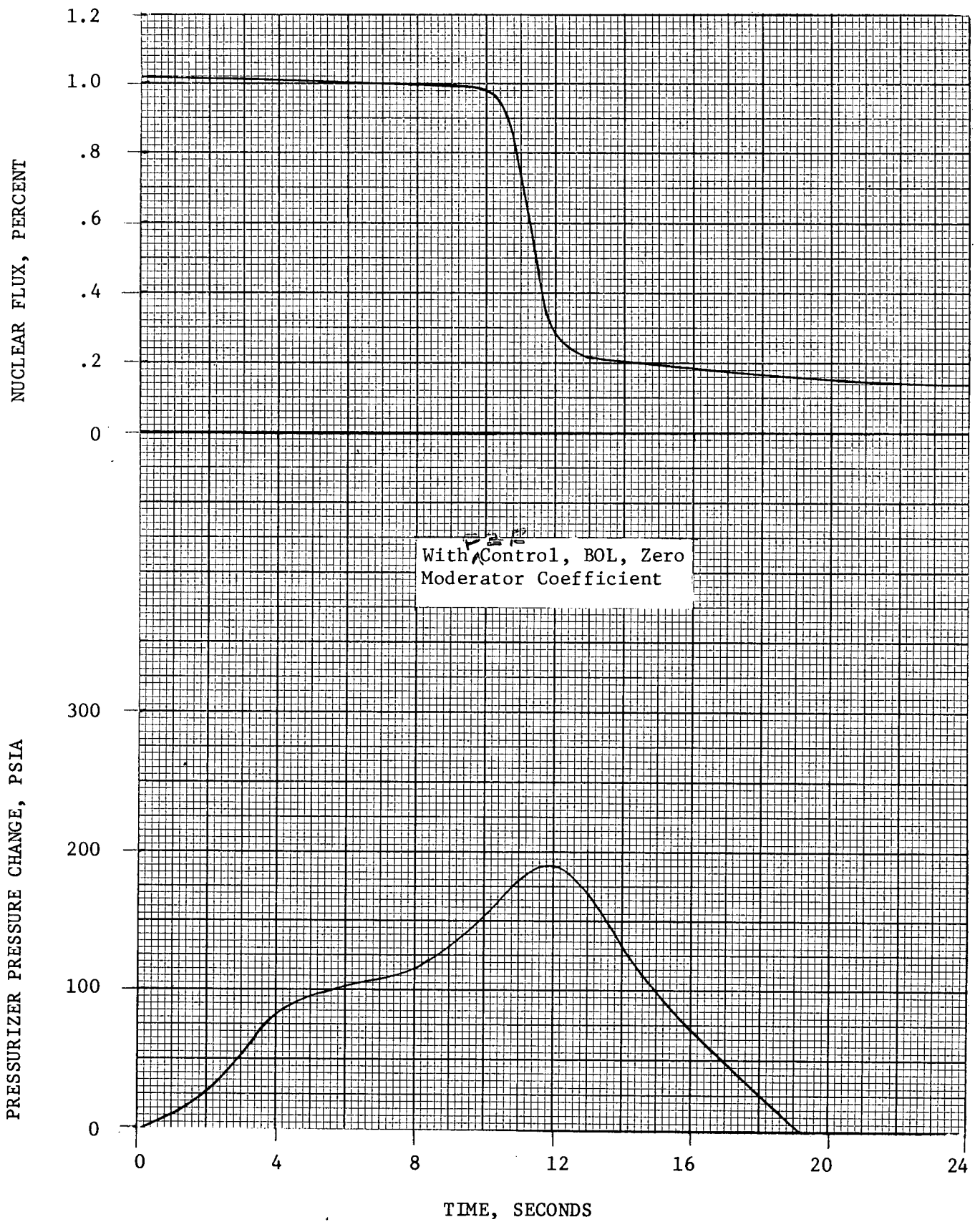


FIGURE 14.1.10-1

TOTAL LOSS OF EXTERNAL ELECTRICAL LOAD ACCIDENT

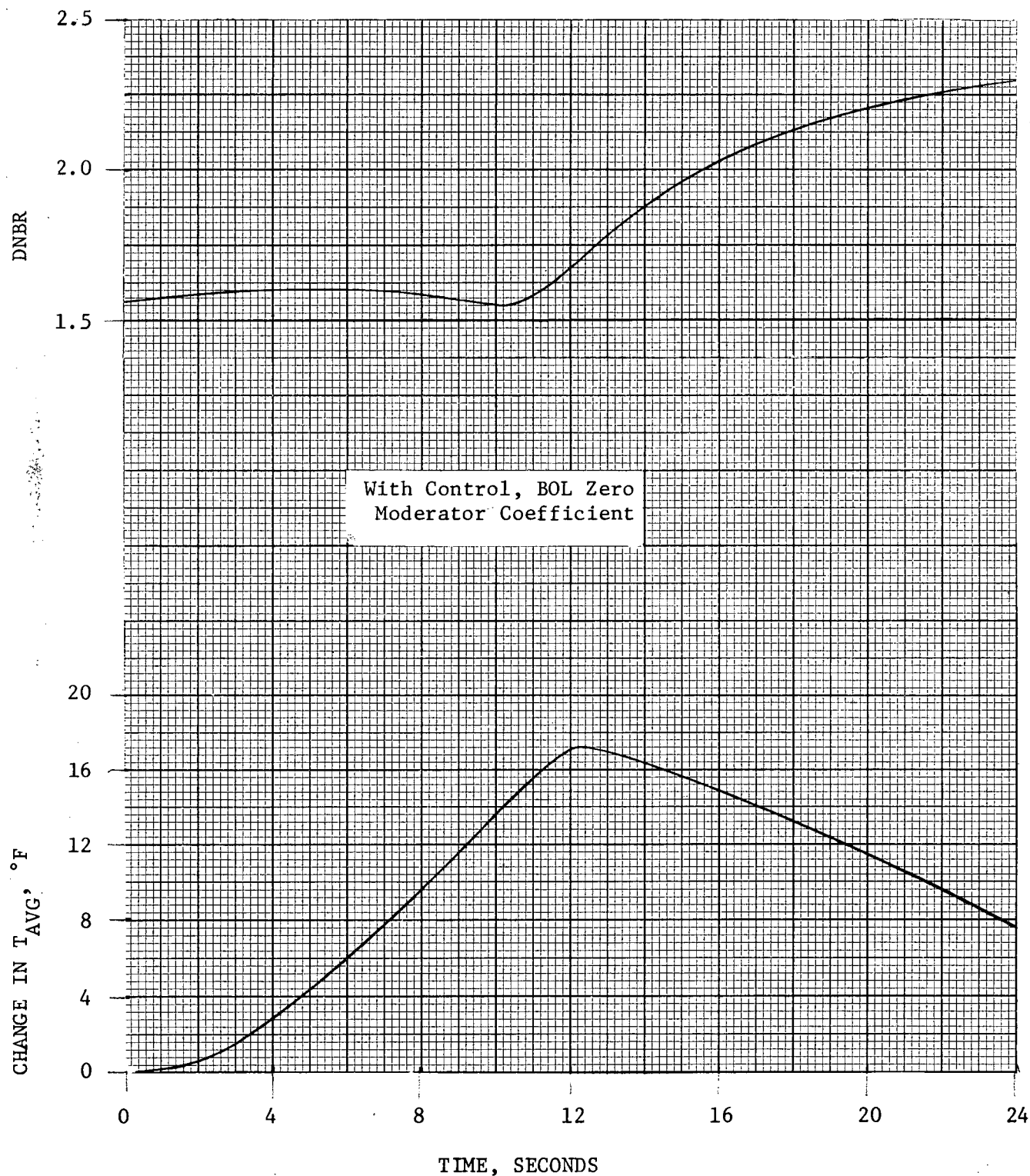


FIGURE 14.1.10-2

TOTAL LOSS OF EXTERNAL ELECTRICAL LOAD ACCIDENT

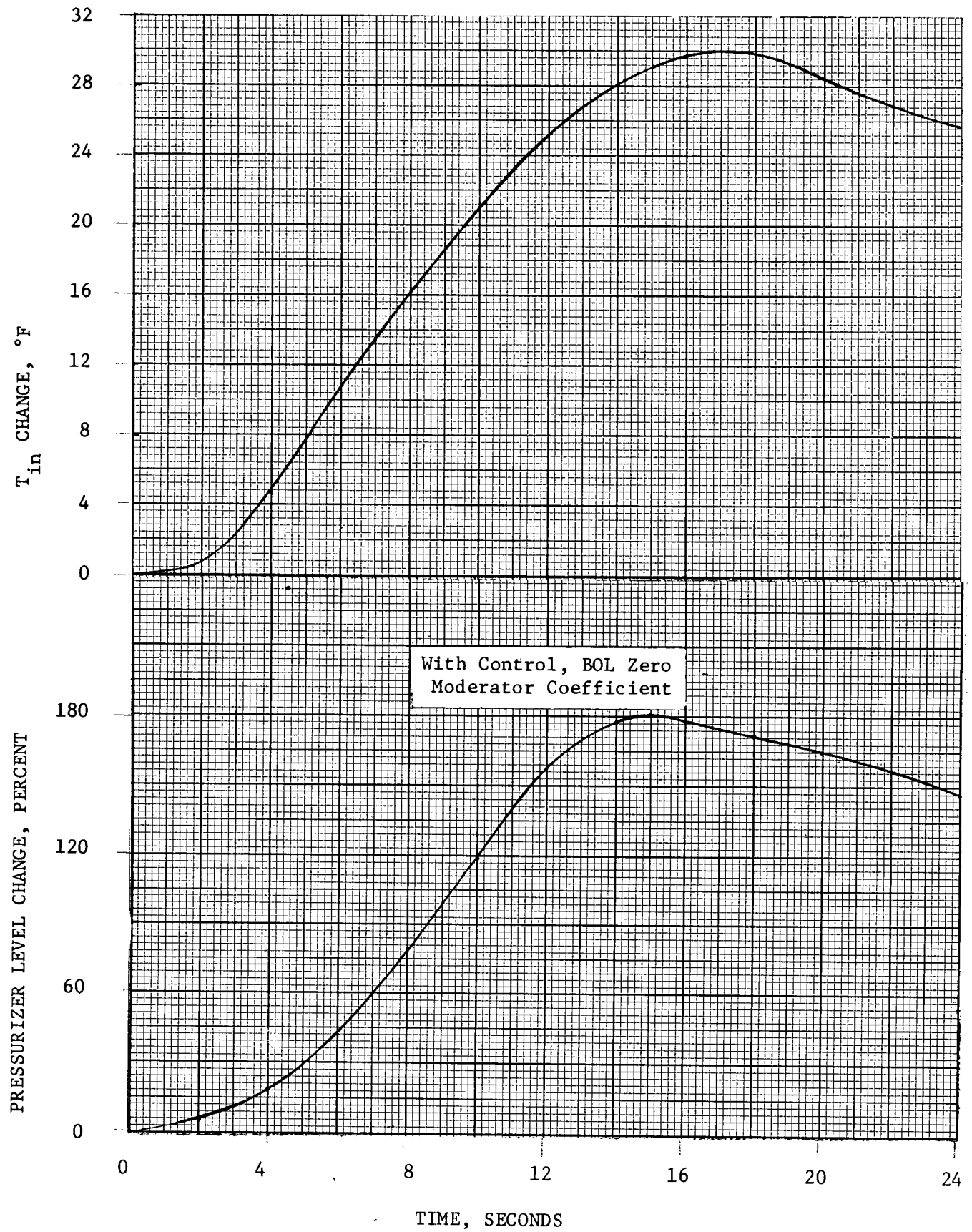


FIGURE 14.1.10-3

TOTAL LOSS OF EXTERNAL ELECTRICAL LOAD ACCIDENT

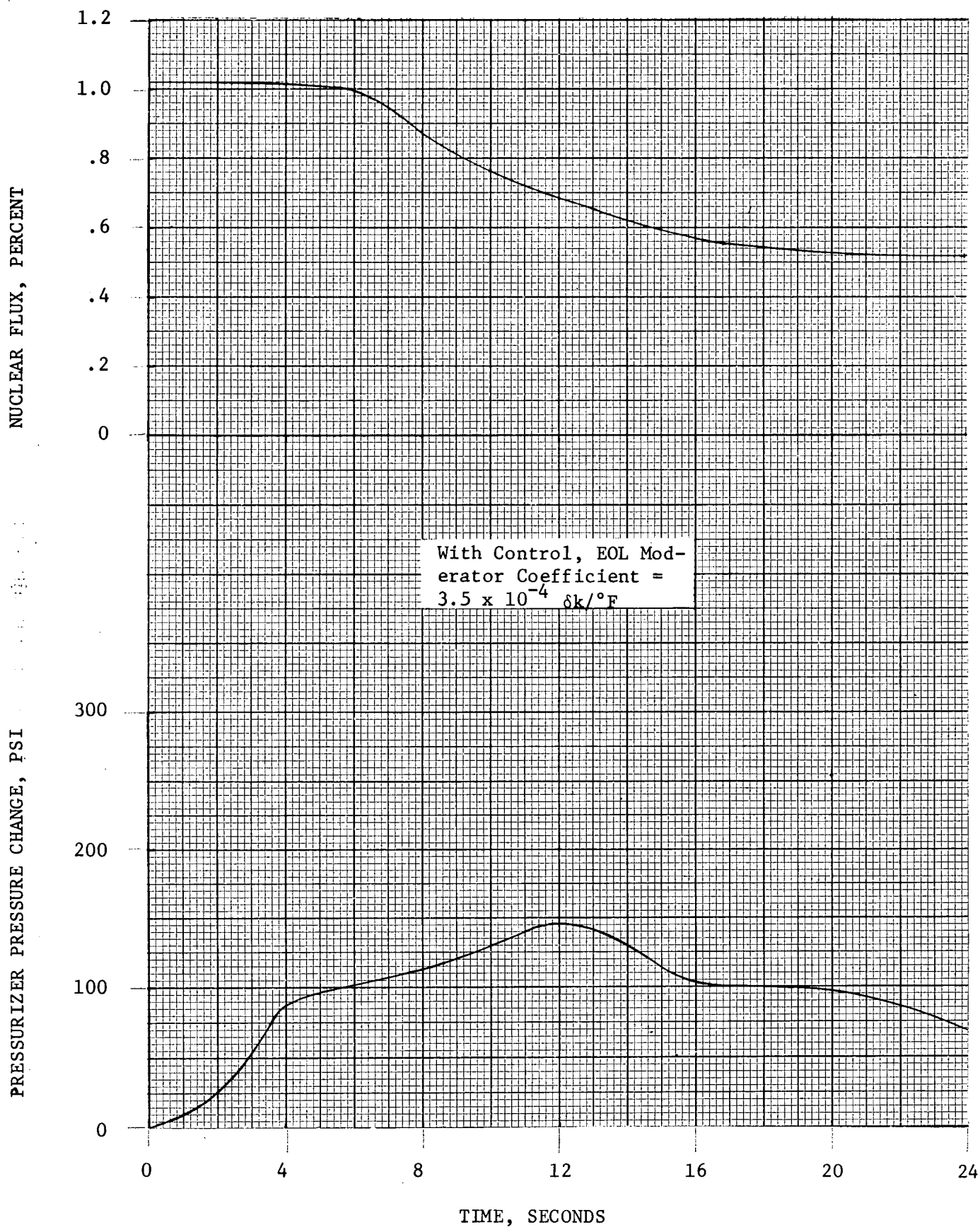


FIGURE 14.1.10-4

TOTAL LOSS OF EXTERNAL ELECTRICAL LOAD ACCIDENT

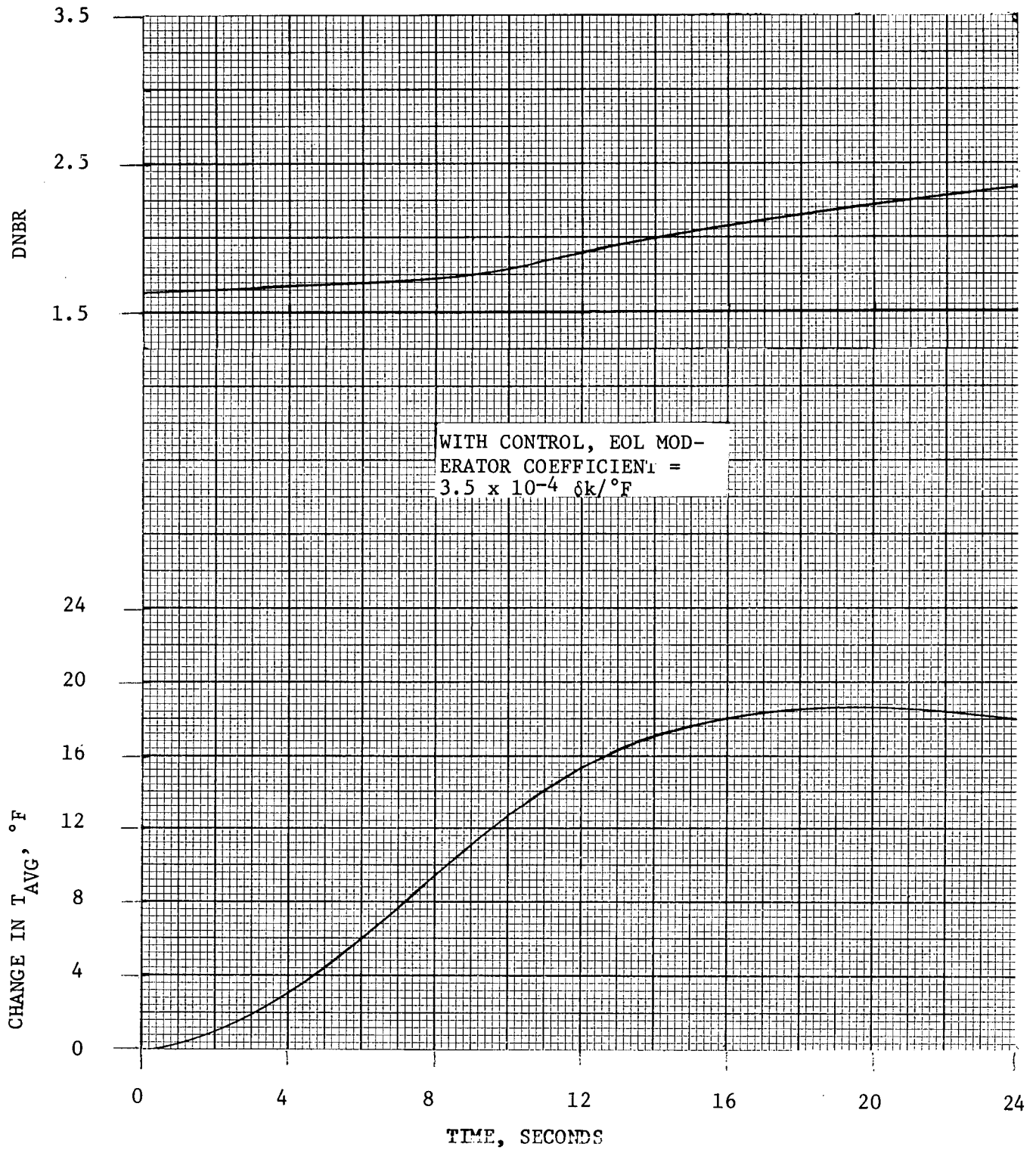


FIGURE 14.1.10-5

TOTAL LOSS OF EXTERNAL ELECTRICAL LOAD ACCIDENT

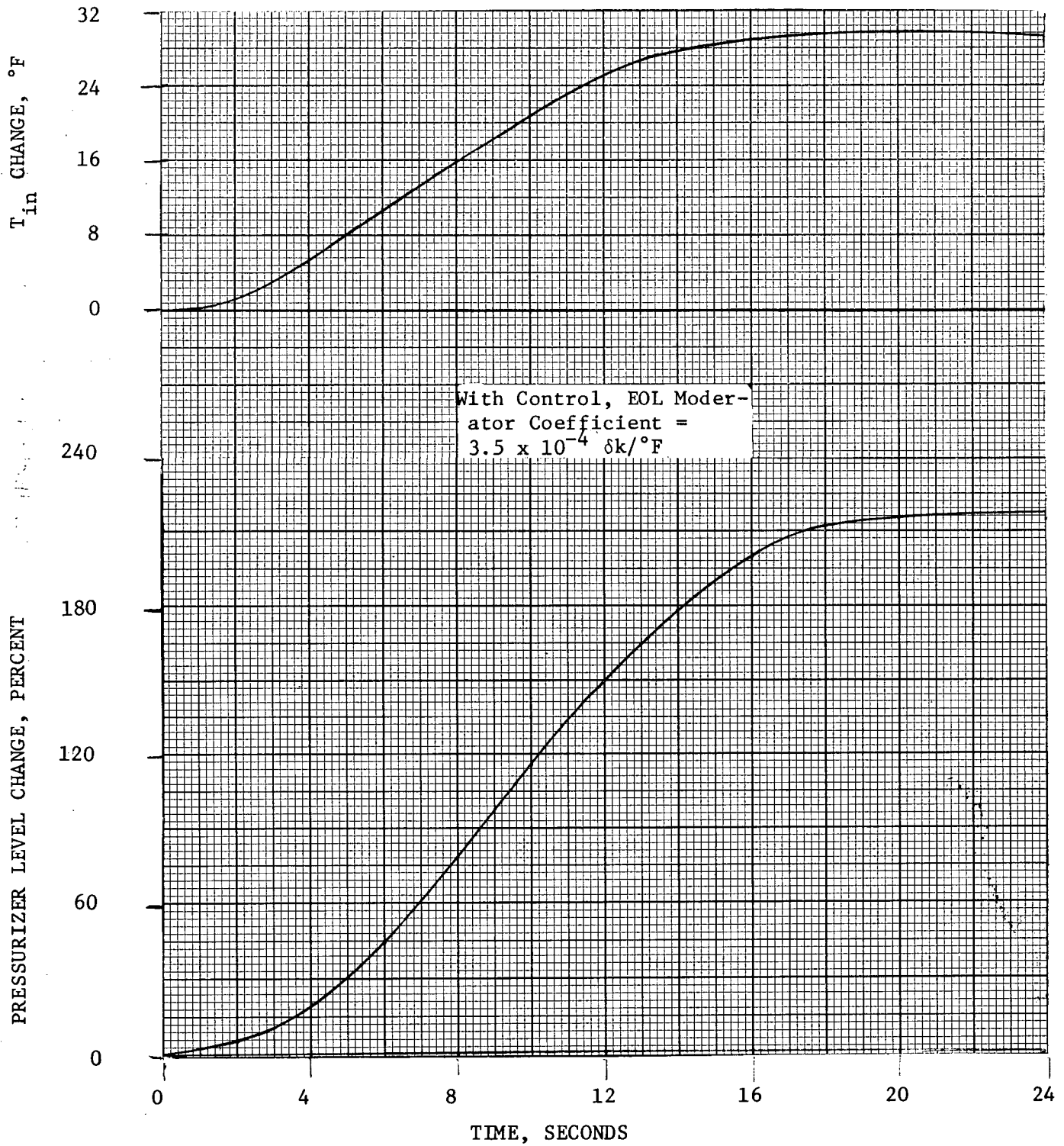


FIGURE 14.1.10-6

TOTAL LOSS OF EXTERNAL ELECTRICAL LOAD ACCIDENT

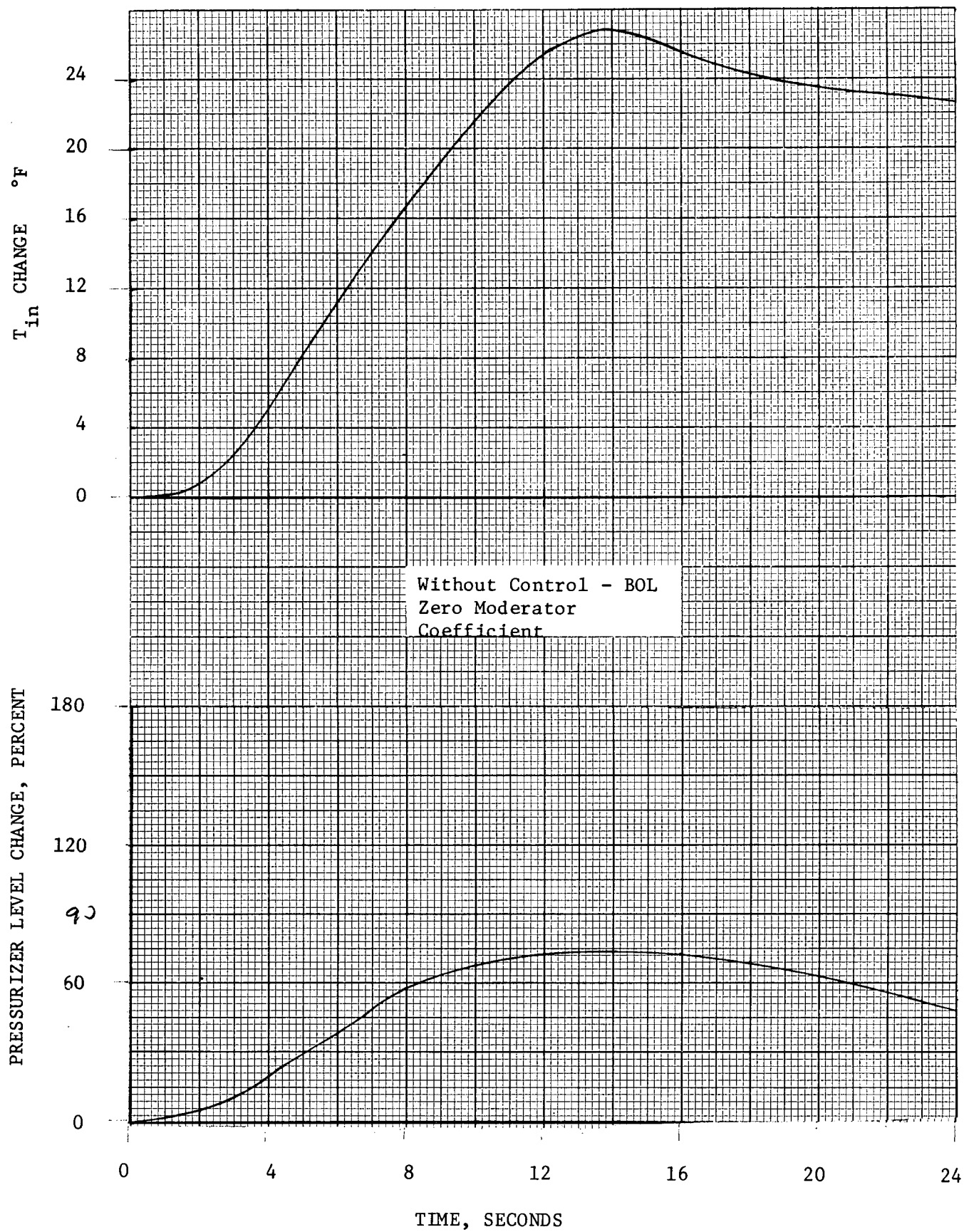


FIGURE 14.1.10-9

TOTAL LOSS OF EXTERNAL ELECTRICAL LOAD ACCIDENT

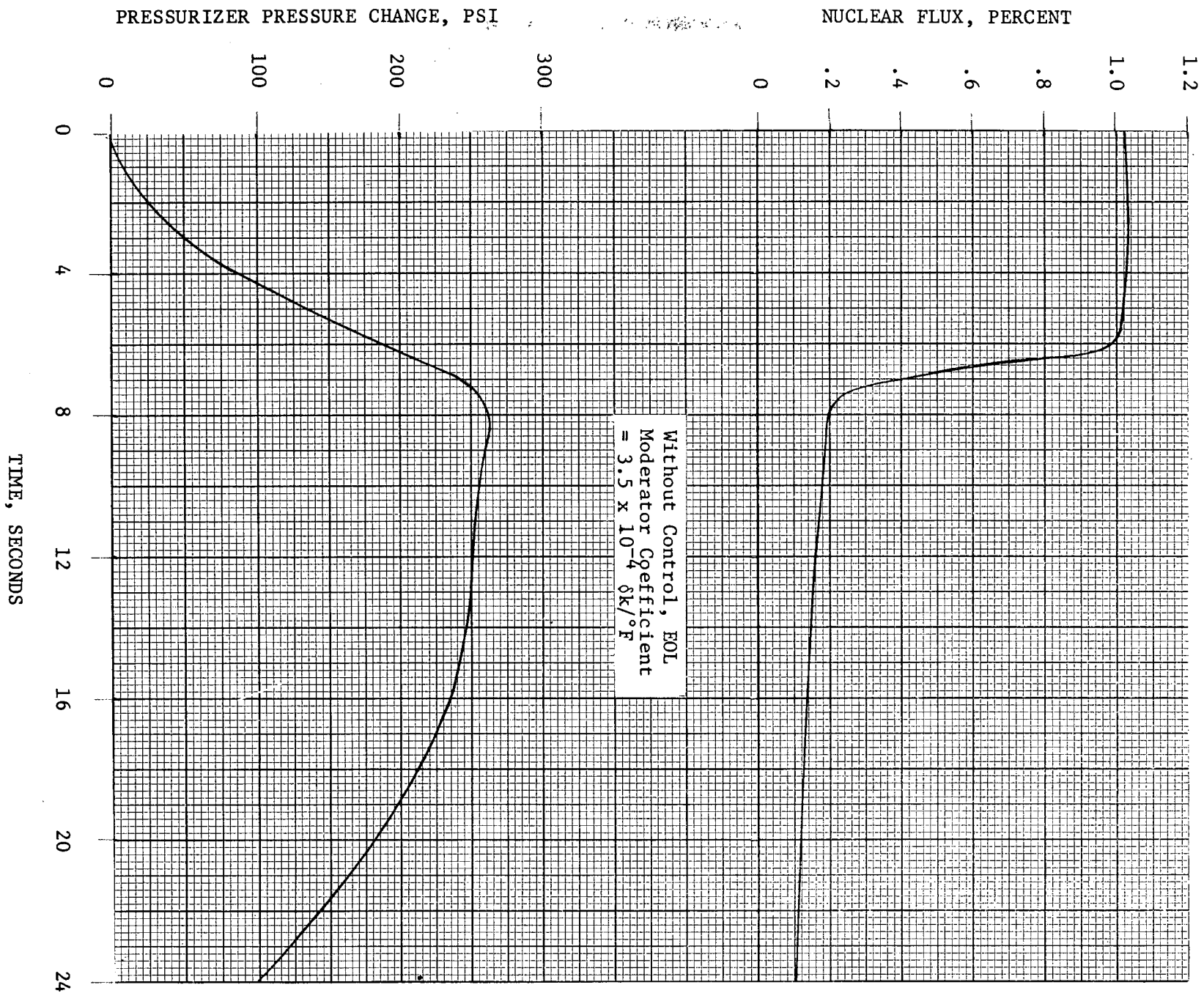


FIGURE 14.1.10-10

TOTAL LOSS OF EXTERNAL ELECTRICAL LOAD ACCIDENT

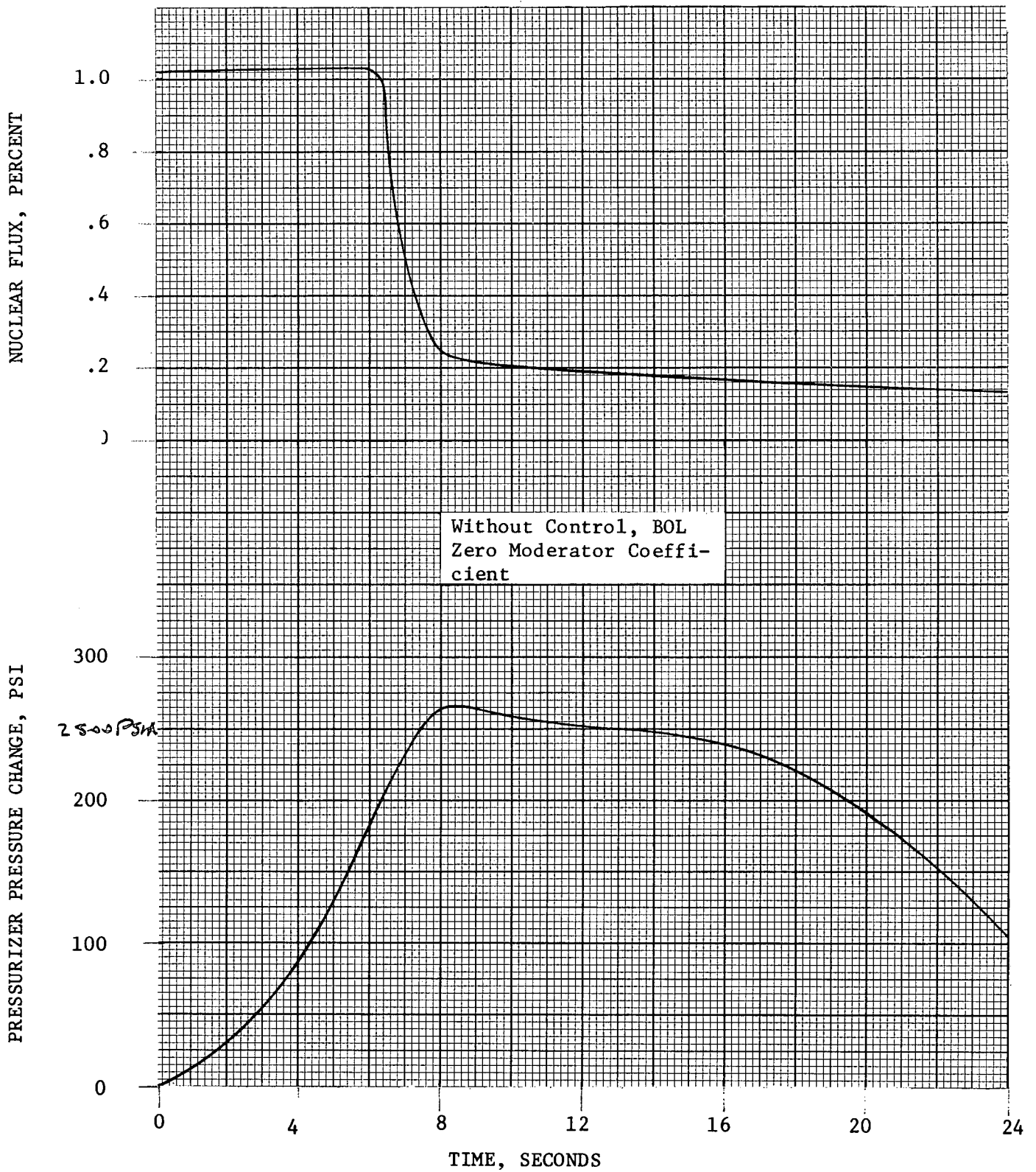


FIGURE 14.1.10-7

TOTAL LOSS OF EXTERNAL ELECTRICAL LOAD ACCIDENT

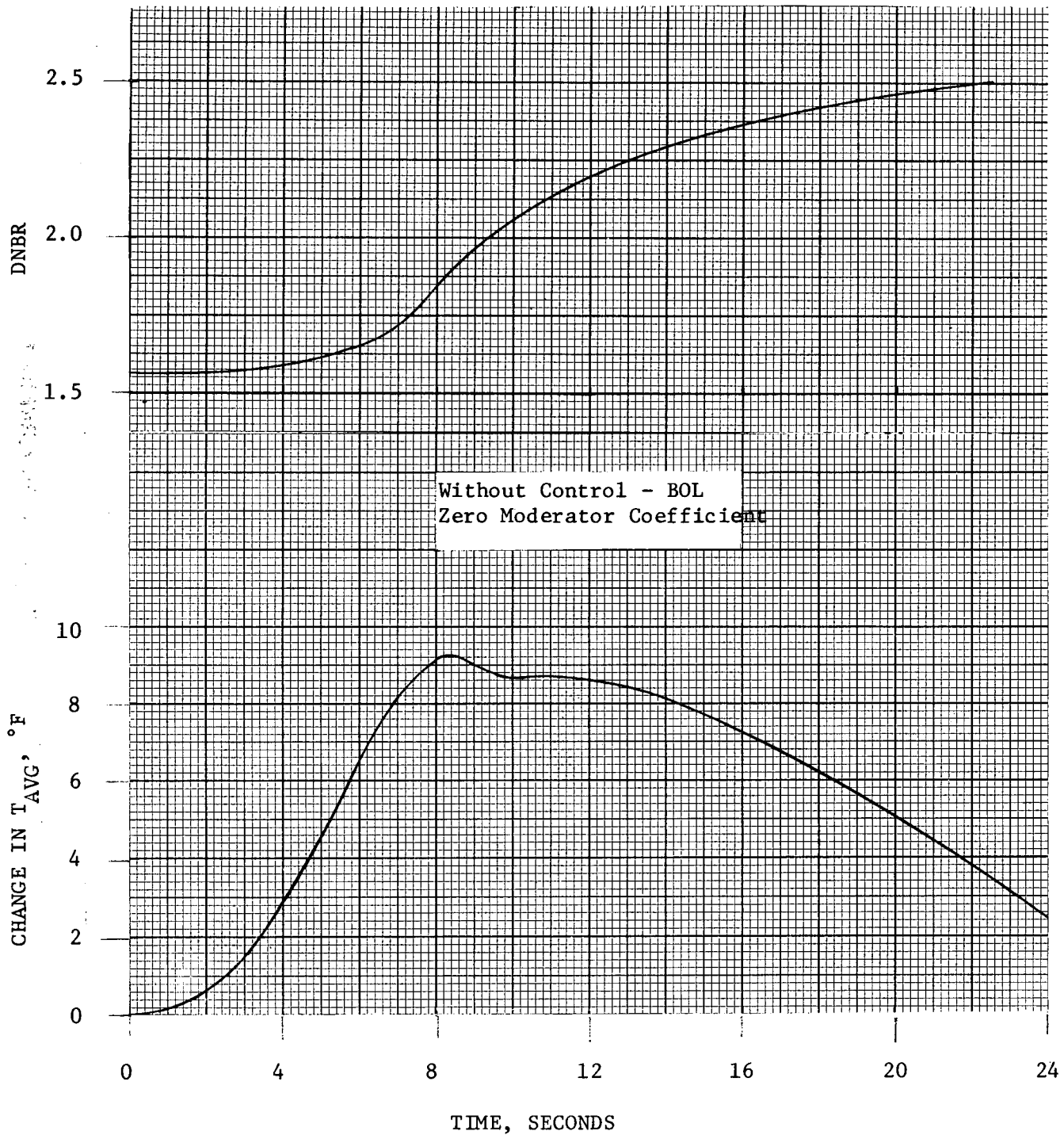


FIGURE 14.1.10-8

TOTAL LOSS OF EXTERNAL ELECTRICAL LOAD ACCIDENT

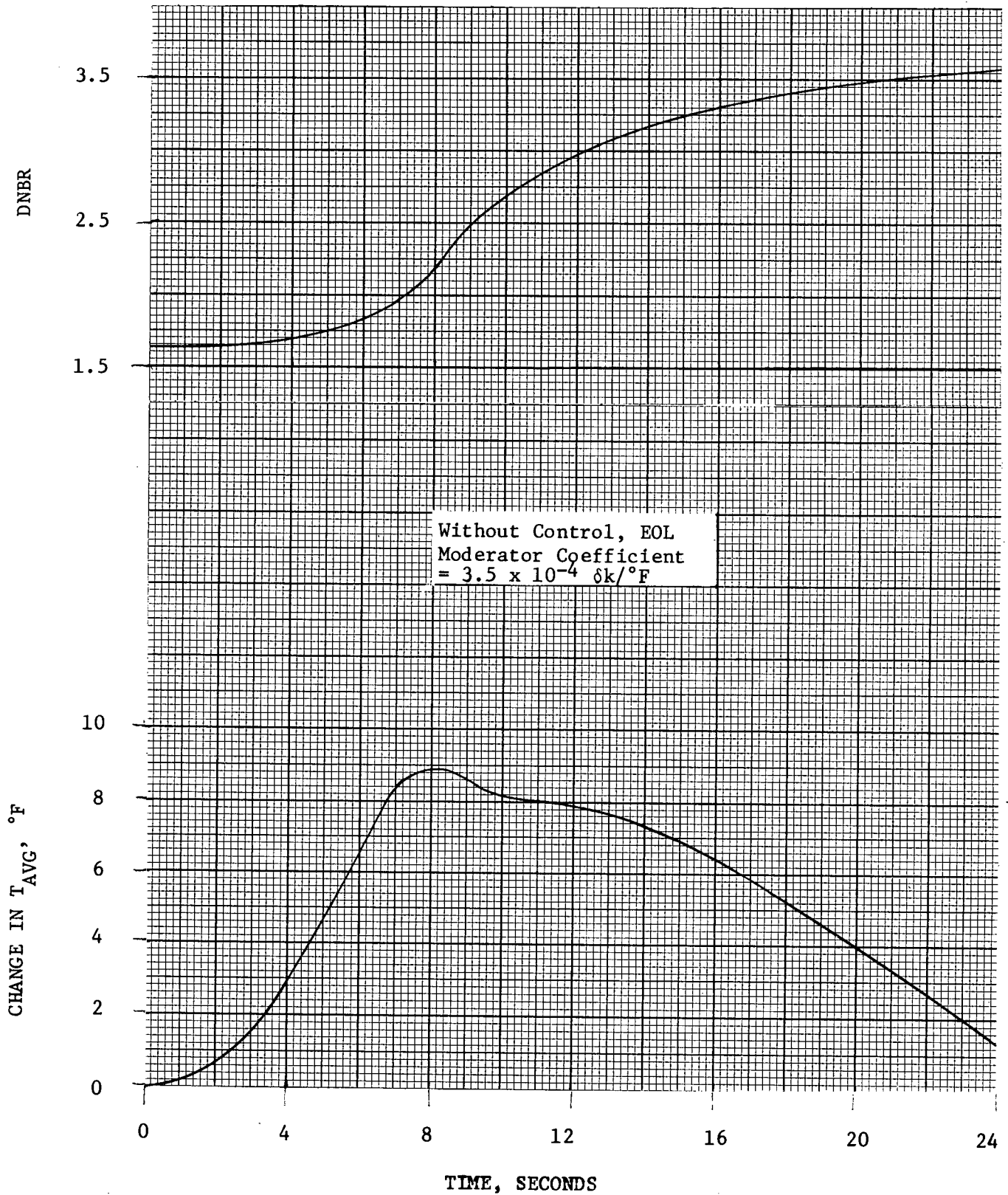


FIGURE 14.1.10-11

TOTAL LOSS OF EXTERNAL ELECTRICAL LOAD ACCIDENT

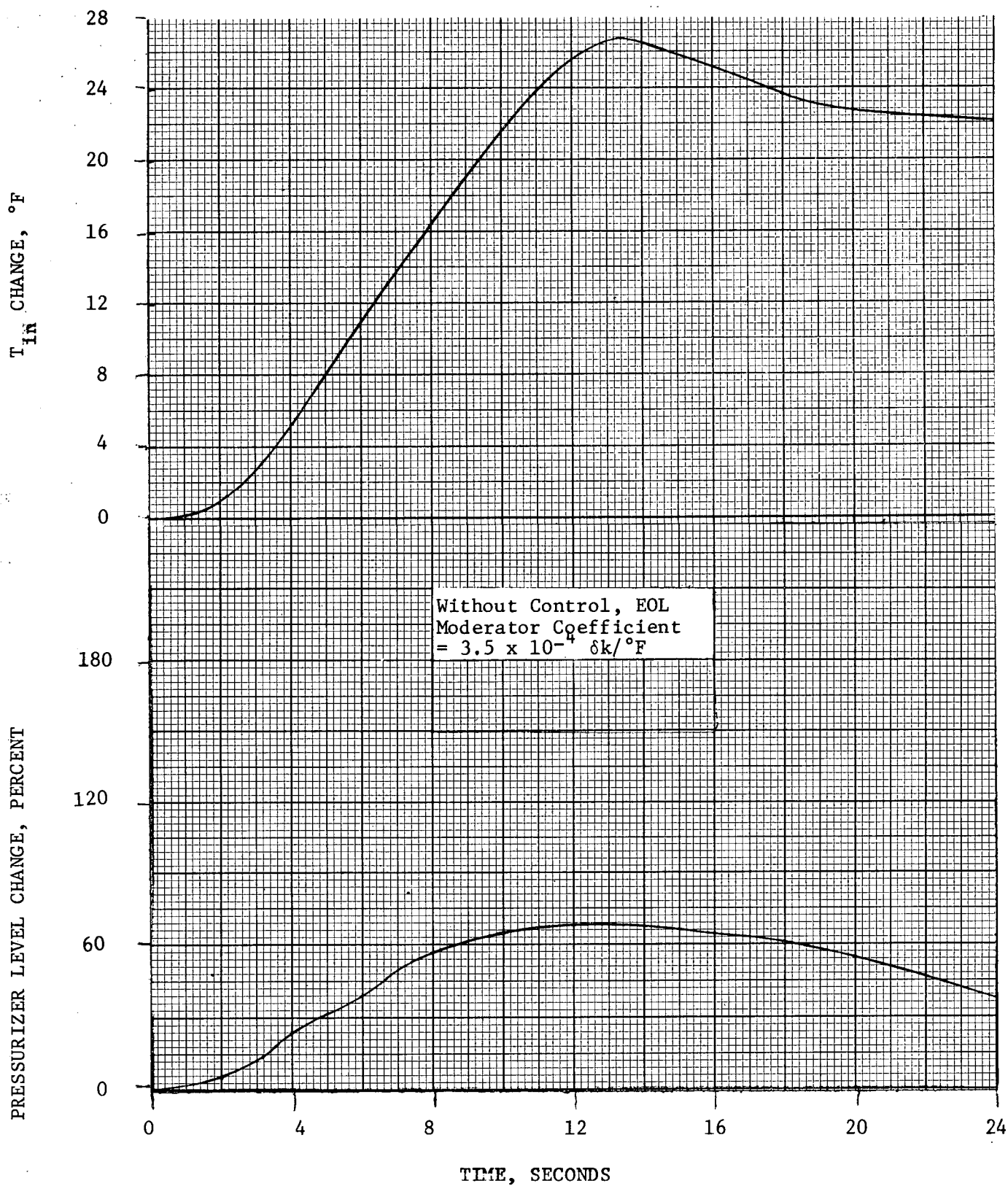


FIGURE 14.1.10-12

14.1.11 LOSS OF NORMAL FEEDWATER

A loss of normal feedwater (from a pipe break, pump failures, valve malfunctions, or loss of outside ac power) results in a reduction in capability of the secondary system to remove the heat generated in the reactor core. If the reactor were not tripped during this accident primary plant damage could possibly occur from a sudden loss of heat sink. If an alternate supply of feedwater were not supplied to the core, residual heat following reactor trip would heat the primary system water to the point where water relief from the pressurizer occurs. Loss of significant water from the Reactor Coolant System could conceivably lead to core damage.

The following provides the necessary protection against a loss of normal feedwater.

- 1) Reactor trip on very low water level in any steam generator
- 2) Reactor trip on steam flow-feedwater flow mismatch in coincidence with low water level in any steam generator.
- 3) Two motor driven auxiliary feedwater pumps (300 gpm each) which are started automatically on:
 - a. Low-Low level in any steam generator, or
 - b. Opening of all feedwater pump circuit breakers, or
 - c. Any Safety Injection signal, or
 - d. Manually, or
 - e. Loss of all A. C. Power.
- 4) One turbine driven pump (600 gpm) which is started automatically on
 - a. Low-low level in 2/3 steam generators, or
 - b. Loss of voltage on both 4160 V. busses, or
 - c. Manually

The motor driven auxiliary feedwater pumps are supplied by the diesel if a loss of outside power occurs and the turbine-driven pump utilizes steam from the secondary systems. The turbine exhausts the secondary steam to the atmosphere. The auxiliary pumps take suction directly from the condensate storage tank for delivery to the steam generators.

3 The above provides considerable backup in equipment and control logic to insure that reactor trip and automatic feedwater flow will occur following any loss of normal feedwater including that caused by a loss of A. C. power.

Method of Analysis

The analysis was performed to show that following a loss of normal feedwater, the auxiliary feedwater system is adequate to remove stored and residual heat to prevent water relief through the pressurizer relief valves.

The following assumptions were made:

- 3
- 1) The initial steam generator water level (in all steam generators) at the time reactor trip occurs is at the very low level, this causes the reactor trip and automatic initiation of the auxiliary feedwater flow. The initial water level is assumed to be at the lower narrow range level tap.
 - 2) The plant is initially operating at 102% of 2300 MWt.
 - 3) A heat transfer coefficient in the steam generators assuming reactor coolant system natural circulation.
- 3

Conclusion

3

The loss of normal feedwater does not result in any adverse condition in the core, because it does not result in water relief from the pressurizer relief or safety valves, nor does it result in uncovering the tube sheets of the steam generators being supplied with water.

TRANSIENT RESPONSE FOLLOWING A LOSS OF NORMAL
FEEDWATER WITH ONE 300 GPM AUXILIARY FEED PUMP
DELIVERING TO TWO STEAM GENERATORS BEGINNING
AT ONE MINUTE.

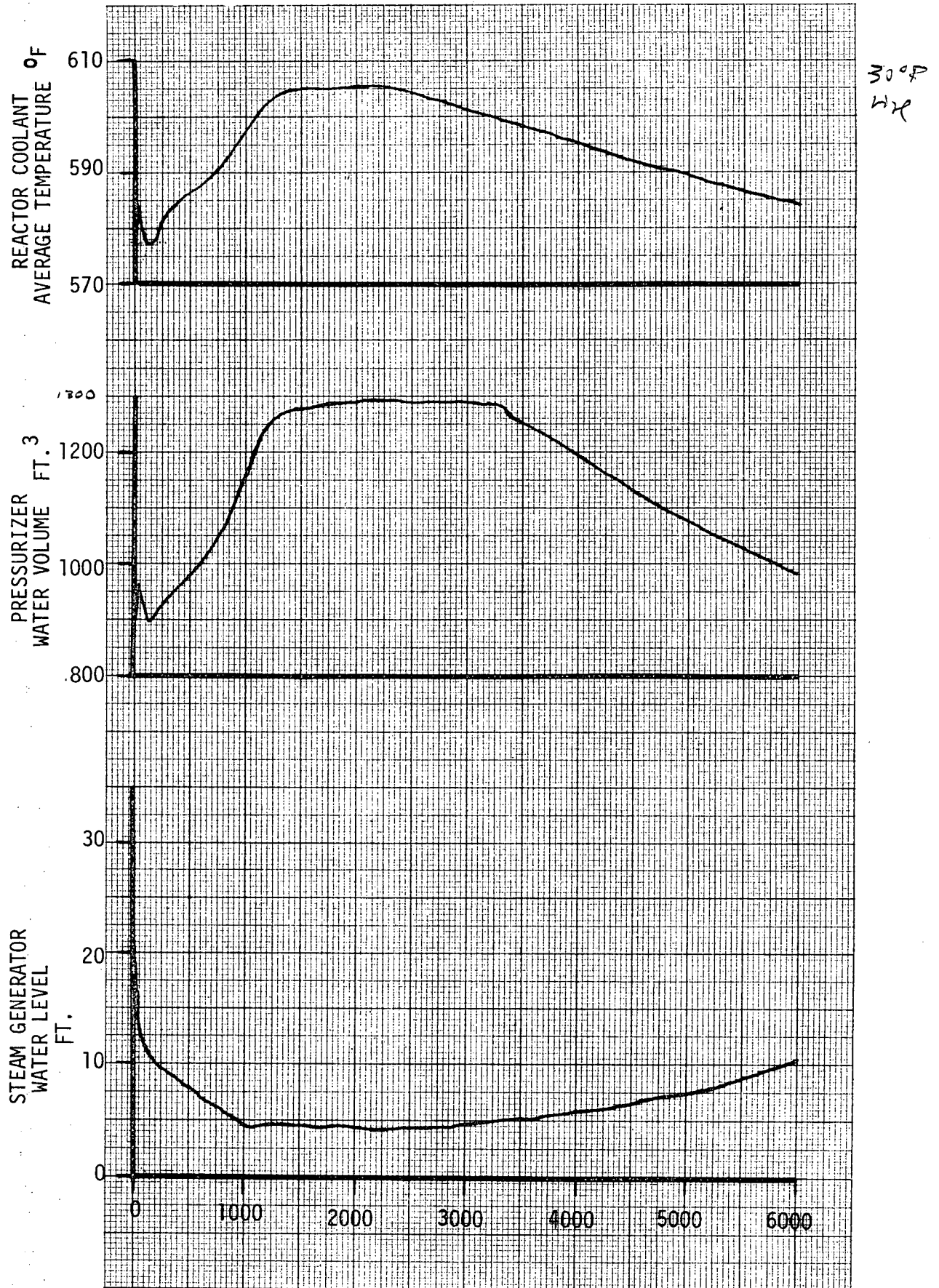


FIGURE 14.1.11-1

14.1.12 Loss of A.C. Power

The consequences of a break in the connections to the main grid system, i.e., a loss of A.C. power, is analyzed below. There are two possibilities; 1) that the loss of connections occurs without a consequent steam turbine trip and 2) that the loss of outside power to the plant leads to a subsequent turbine trip.

Without Turbine Trip

The H. B. Robinson Unit #2 is designed to accept a loss of export A.C. power so that the only load on the turbine/alternator is the auxiliary load. It is designed to accept this load from full power reduction, without the turbine overspeeding and tripping off the line. During the transient the Reactor changes load at its maximum rate. The difference between the steam generated and the steam consumed by the turbine is dumped either into the main condenser or to atmosphere. These two dumps together act as a short term load allowing the reactor to reduce power without tripping.

Method of Analysis

A detailed digital power simulating the whole nuclear power plant was used in the analysis. The program simulated the following components: the Reactor and its control system, the Steam Generator and the feed control, the Turbine, the Feedwater system and the Dump control system.

For the study two cases were considered the first case was with a zero moderator temperature coefficient and the second case was with a moderator temperature coefficient of $-3.5 \times 10^{-4} \delta k/^{\circ}F$. A Doppler coefficient of $-1.0 \times 10^{-5} \delta k/^{\circ}F$ was used in both cases together with a rod rate of $6 \times 10^{-5} \delta k/in.$

Results

Figures 14.1.12-1 and 14.1.12-2 illustrates the transient response following a loss of outside power at the beginning of life (zero moderator coefficient).

Figures 14.1.12-3 and 14.1.12-4 illustrate the response following the loss of outside power at the end of life moderate coefficient equal to -3.5×10^{-4} $\delta k/^\circ F$. It can be seen that the nuclear power reaches its new equilibrium value slightly faster for the zero moderator case.

Conclusion

The margin to trip increases throughout the transient and the DNB ratio is never less than the value at full load, hence there is a sufficient margin over the limiting DNBR of 1.30. There is no radioactive release and thus no public hazard as a result of the loss of A.C. without turbine trip.

With Turbine Trip

In the unlikely event of the turbine tripping upon the loss of A.C. power, there will be a loss of power to the station auxiliaries, via the main reactor coolant pumps, the feedwater pumps, etc. The events following a loss of A.C. power with turbine trip are described in the sequence below.

- a) Plant vital instruments are supplied by the emergency power sources.
- b) As the steam system pressure subsequently increases, the steam system power relief valves are automatically opened to the atmosphere. Steam bypass to the condenser is not available because of loss of the circulating water pumps.
- c) As the steam flow rate through the power relief valves may not be sufficient, the steam generator self-actuated safety valves may temporarily lift to augment the steam flow until the rate of heat dissipation is sufficient to carry away the sensible heat of the fuel and coolant above no-load temperature plus the residual heat produced in the reactor.

- d) As the no-load temperature is reached, the steam system power relief valves are used to dissipate the residual heat and to maintain the plant at the hot shutdown condition.

The auxiliary steam turbine driven feedwater pumps are started upon the loss of normal feedwater supply. The turbine utilizes steam from the secondary system to drive the feedwater pump to deliver makeup water to the steam generators. The turbine driver exhausts the secondary steam to the atmosphere. The electric motor driven auxiliary feedwater are supplied power by the diesel generators. The pumps take suction directly from the condensate storage tank for delivery to the steam generators.

The steam driven feedwater pump can be tested at any time by admitting steam to the turbine driver. The auxiliary feedwater control valves and power relief valves can be operationally tested whenever the plant is at hot shutdown and the remaining valves in the system are operationally tested when the turbine driver and pump are tested.

Method of Analysis

The analysis was performed using a digital code to show that upon loss of all A.C. power to the station auxiliaries, the auxiliary feedwater system is sufficient to remove stored and residual heat without reactor coolant temperature rise leading to water relief through pressurizer relief valves.

The following assumptions are made:

1. The initial steam generator water level (in all steam generators) at the time loss of all A.C. power occurs is at the conservatively low level of 3 ft below the normal water level.
2. The plant is initially operating at 102% of 2300 MWt.
3. A conservative core residual heat generation based upon long term operation at the initial power level preceeding the trip.

4. An auxiliary feedwater flow of 600 gpm is available in at least 5 minutes.
5. Two steam generators are fed with auxiliary feedwater.
6. Secondary system steam relief through the self-actuated safety valves.
7. After normal steam generator level is established, auxiliary feedwater flow is controlled to maintain the water level.

Results

Figure 14.1.12-5 shows plant transient response following loss of all A.C. power to the station auxiliaries.

At the time of complete loss of off-site power and turbine trip, there is a rapid reduction of steam generator water level. This is due to the reduction of steam generator void fraction on the secondary side and because steam flow continues after normal feedwater stops. During the first five minutes, the level drops to about 35% of normal. By the end of this time flow is established from the auxiliary feedwater pump and further reduction of water level is small. The capacity of the auxiliary feedwater system is enough to prevent the water level in the steam generators from receding below the lowest level within the indicator range during the transient. This prevents the tube sheet from becoming uncovered at any time during the transient. As shown by the loss of normal feedwater analysis (Section 14.1.11) there is no water discharge from the pressurizer valves for the case where only one motor-driven auxiliary feedwater pump is available one minute after the accident. Thus any single auxiliary feedwater pump is sufficient for plant protection.

Normal water level is recovered in 60 minutes in the steam generators which receive feed.

The reactor operator in the control room can monitor the steam generator water level and control the feedwater flow with remote operated auxiliary feedwater control valves.

Upon the loss of power to the reactor coolant pumps, coolant flow necessary for core cooling and the removal of residual heat is maintained by natural circulation in the reactor coolant loops. The natural circulation flow was calculated using analytical method based on the conditions of equilibrium flow and maximum loop flow impedance. The model has given results within 15% of the measured flow values obtained during natural circulation tests conducted at the Yankee-Rowe plant and has also been confirmed at San Onofre and Connecticut Yankee. The natural circulation flow ratio as a function of reactor power is given in Table 14.1.12-1.

Conclusion

The loss of A.C. power to the station auxiliaries does not cause any adverse condition in the core, since it does not result in water relief from the pressurizer relief or safety valves neither does it result in the tube sheets of the steam generators, supplied with water, being uncovered.

TABLE 14.1.12-1

NATURAL CIRCULATION REACTOR COOLANT FLOW
VS REACTOR POWER

<u>Reactor Power % Full Power</u>	<u>Reactor Coolant Flow % Nominal Flow</u>
12.0	7.0
10.0	6.6
3.5	4.6
3.0	4.3
2.5	4.0
2.0	3.7
1.5	3.3
1.0	2.9

10

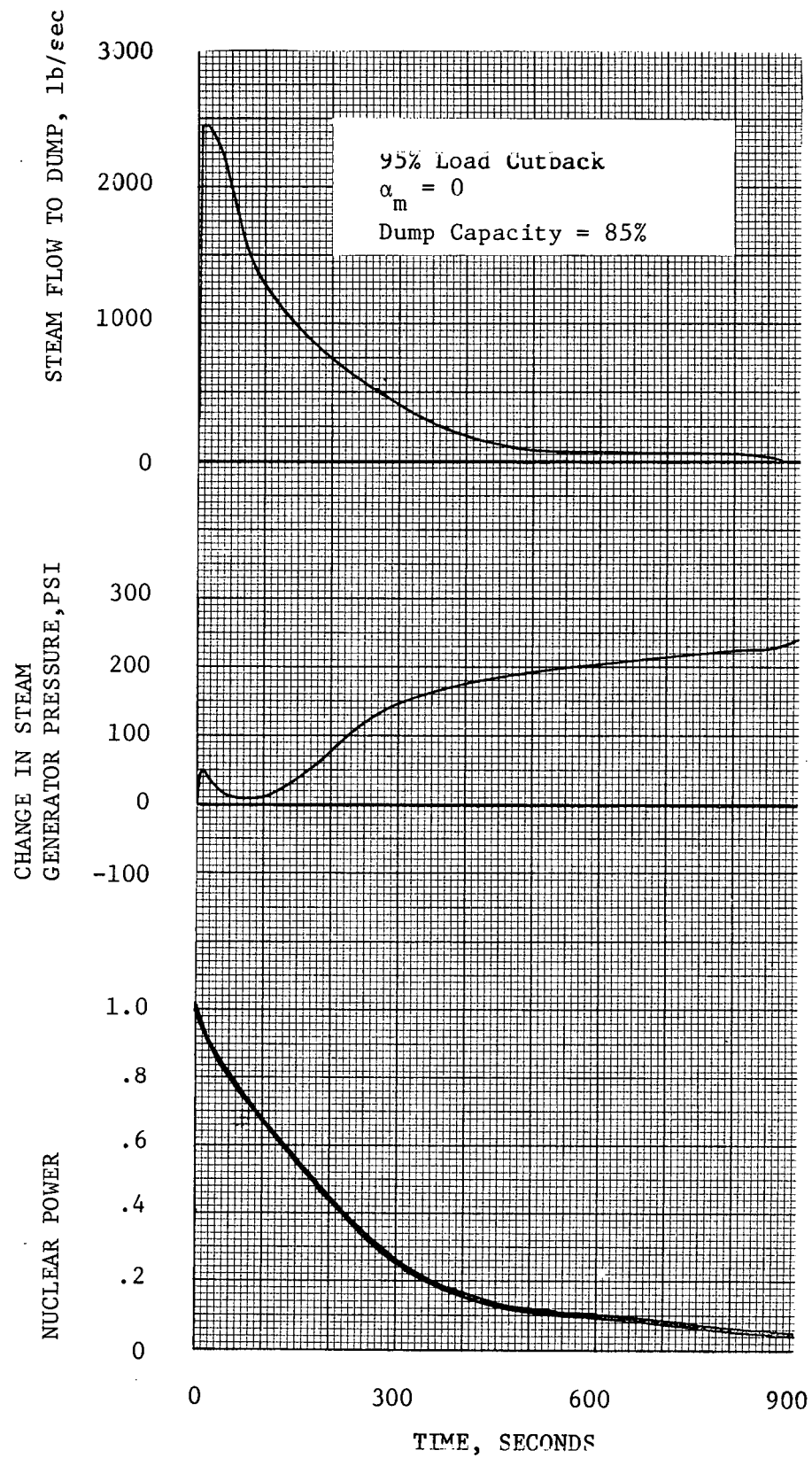


FIGURE 14.1.12-1

95% Load Cutback
 $\alpha_m = 0$
Dump Capacity = 85%

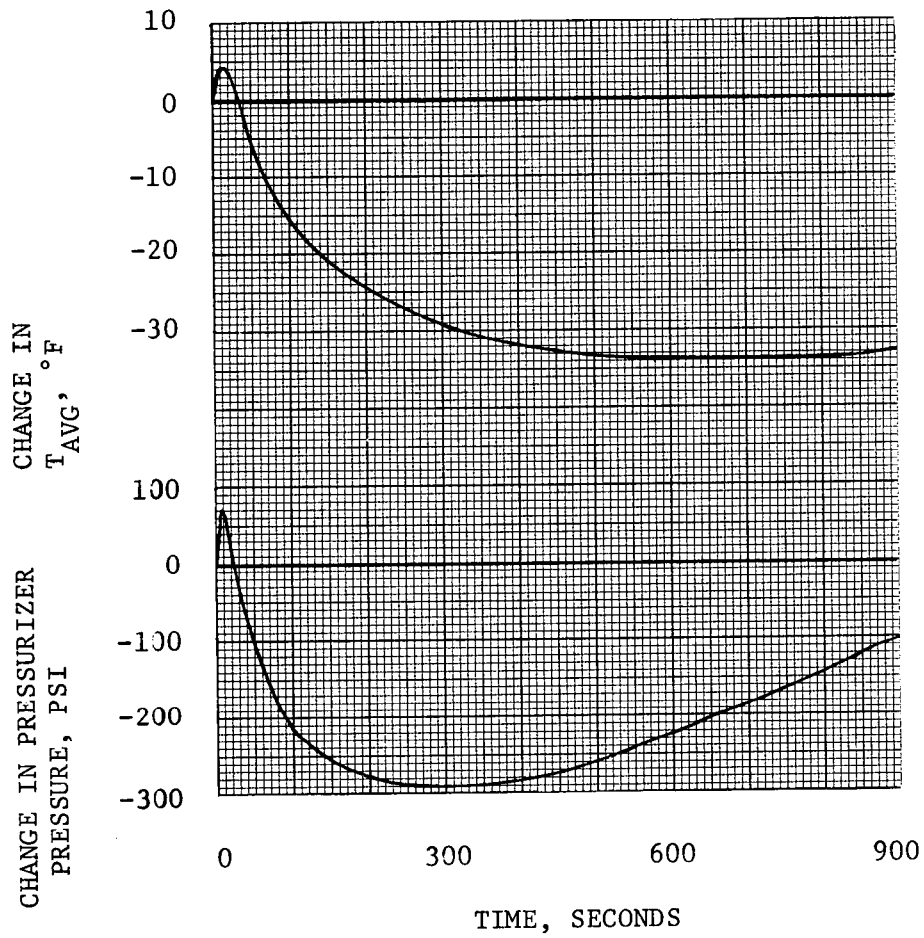


FIGURE 14.1.12-2

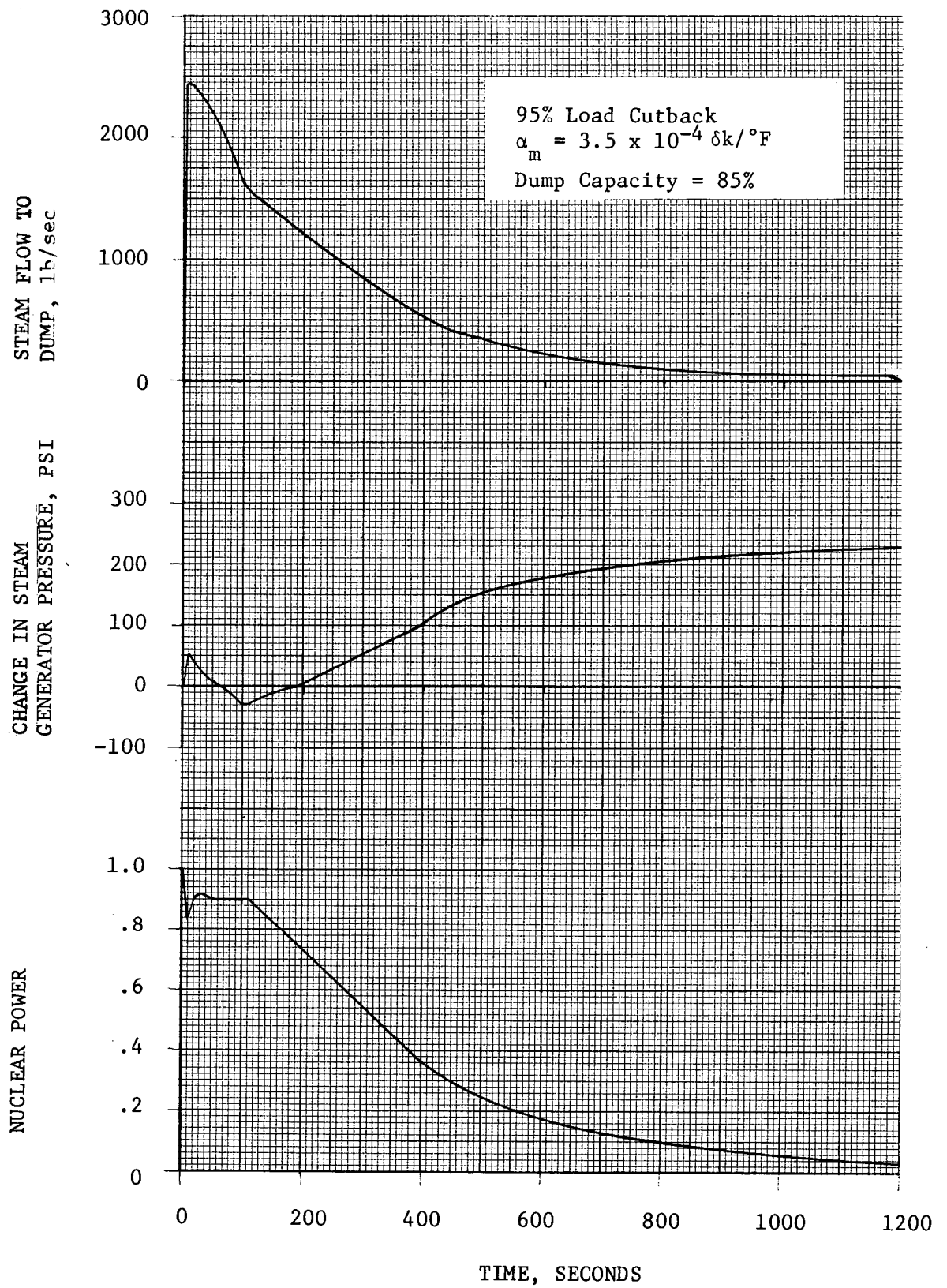


FIGURE 14.1.12-3

95% Load Cutback
 $\alpha_m = -3.5 \times 10^{-4} \delta k / ^\circ F$
85% Dump Capacity

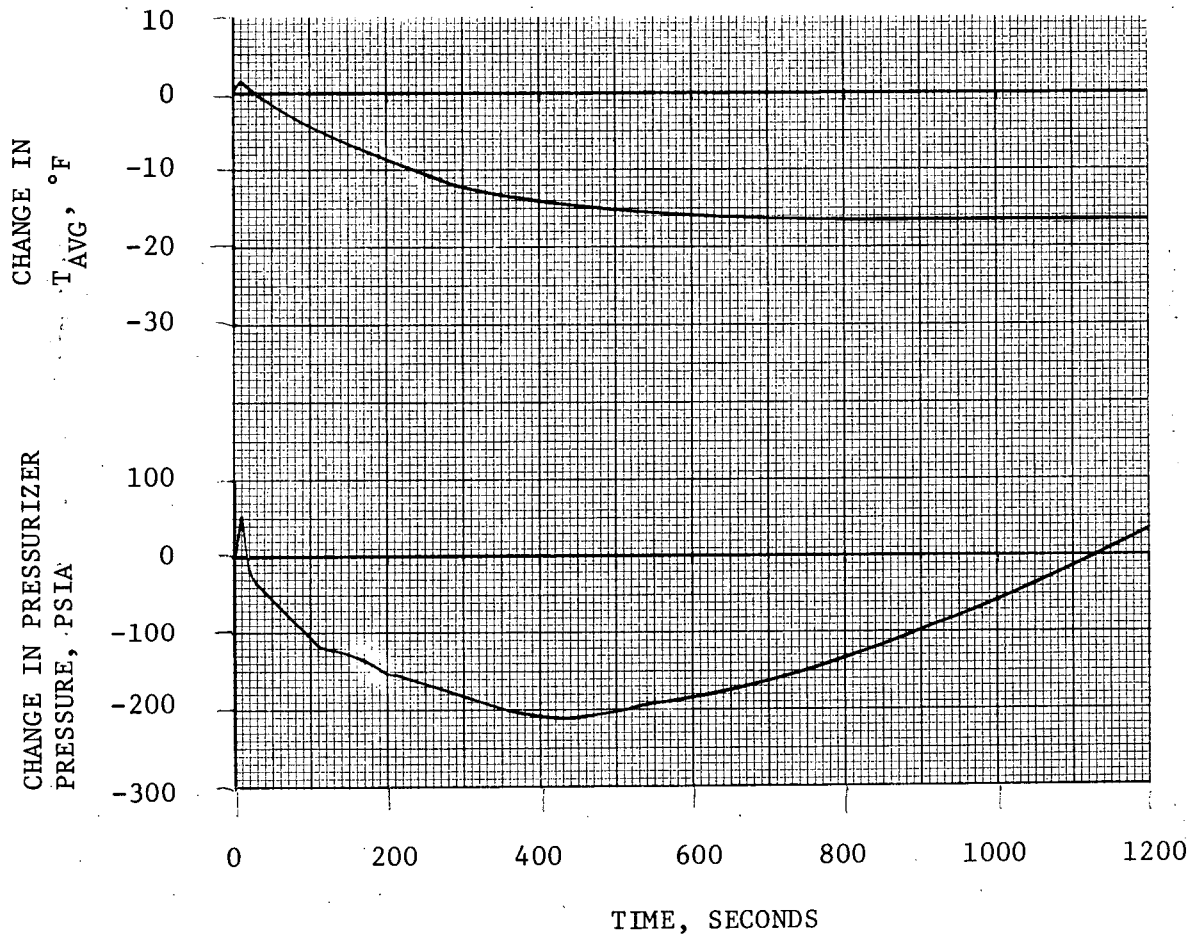


FIGURE 14.1.12-4

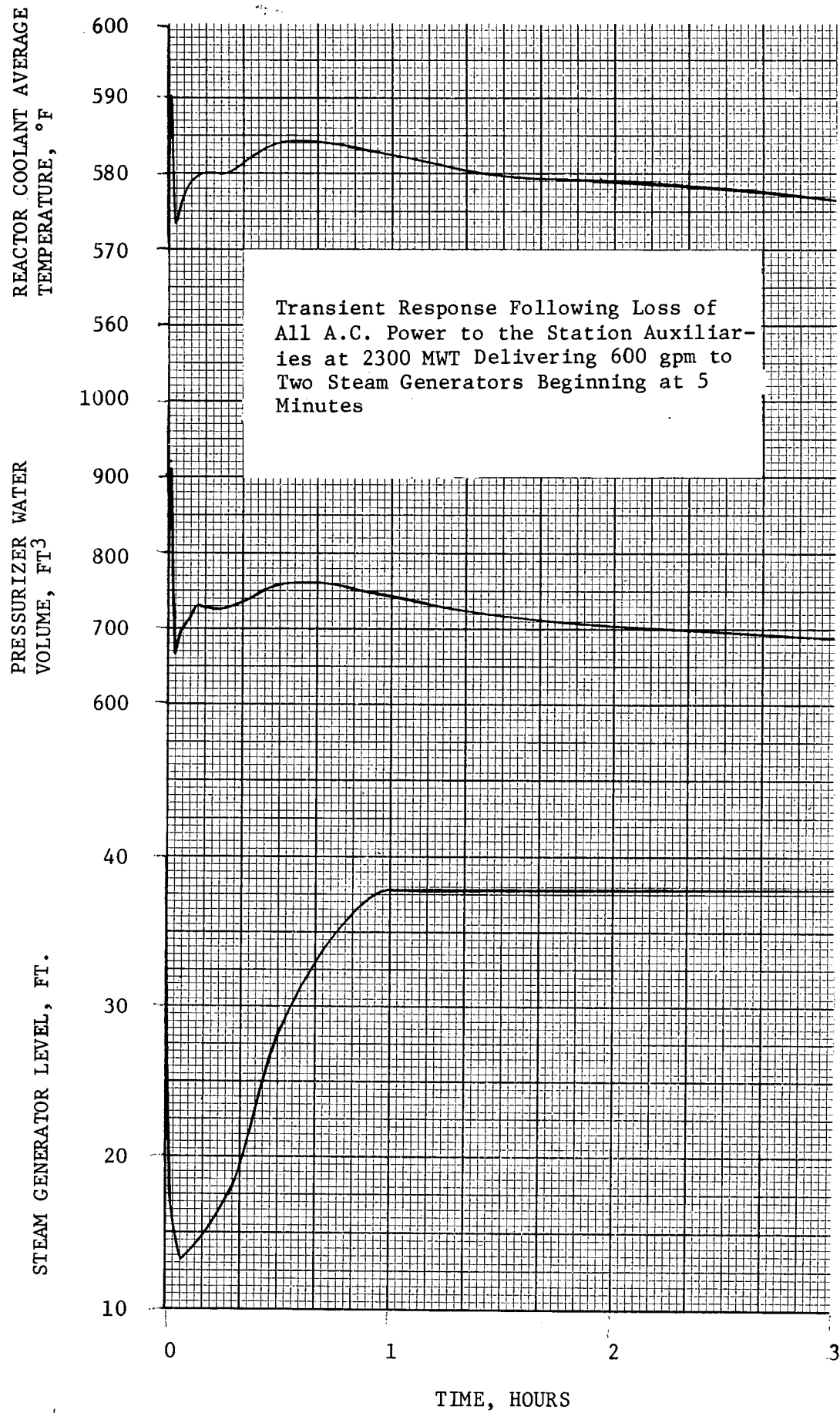


FIGURE 14.1.12-5

14.1.13 LIKELIHOOD OF TURBINE-GENERATOR UNIT OVERSPEED

The present advanced status of the art of rotor forging and inspection techniques guarantees practically defect-free turbine rotors. Further, Westinghouse conservative design eliminates any harmful stress-concentration point, as the no-failure record of Westinghouse turbine-generator confirms.

Due to the redundancy and reliability of the turbine control protection system and of the steam system, the probability occurrence of a unit overspeeding above the design value, i.e., 120%, is very remote.

A description and operation of the electro-hydraulic governing system is located in Section 10.2.

Due to conservative design, very careful rotor forging procurement and rigid inspection, Westinghouse turbine-generator units have never experienced a massive failure.

A survey of the available literature on turbine-generator unit failure shows that the last massive failure of a turbine generator unit occurred about eight years ago. The causes of failure were identified at that time, and provisions were adopted to prevent the recurrence of massive failures. The record since that time demonstrates the soundness of these provisions and correct design.

The no-failure record of Westinghouse turbine generator units, plus the experience gained from the referenced incidents, together with the improvement in the design and inspection techniques in the past nine years indicates that the likelihood of massive turbine-generator failure is extremely remote.

With regard to design and inspection techniques, it is worthwhile to mention that a technical committee of forging suppliers and equipment manufacturers was formed about ten years ago under ASTM to study turbine and generator rotor failures. This group developed the high-toughness NiCrMoV material, now used in all turbine rotors and disks. This Task Force⁽¹⁾ has been very active in making additional improvements in quality and soundness of large forgings and is still in force.

The survey of the literature on massive turbine failures in the last 20 years indicates that all of them occurred between 1953 and 1958.

This survey has pointed out that the rare events of a catastrophic failure of turbines fell into one of two categories:

- 1) Failure by overstressing arising from accidental and excessive overspeed; and
- 2) Failure, due to defects in the material, occurring at about normal speed.

No failure falling in the first category occurred in the USA. The only two documented examples occurred in the United Kingdom. Both accidents were caused by the main steam admission valves sticking in the open position after full load rejection, because of impurities in the turbine control and lubrication oil. The probability of this occurrence in this plant is very remote as previously pointed out.

Besides the provisions in the design of the turbine control and protection system during plant operation, valves will be exercised on a periodic basis, to further preclude the possibility of a valve stem sticking. Analysis of oil samples will be performed as required.

The turbine is periodically overspeeded to check the tripping speed. The remaining tripping devices are periodically checked.

Westinghouse specifies the quality and method of manufacturing of the purchased forgings. Written specifications cover the manufacturing process, the chemical and mechanical properties, the test to be performed, etc. Specifically, the tests performed are both destructive and non-destructive in nature. The destructive tests include tension tests, impact tests, and transition temperature measurement tests. The tension specimens are taken in a radial and/or longitudinal direction. The tensile properties are determined in accordance with ASTM A-370 on a Standard Round 1/2 inch Diameter 2 Inch Gage Length Test specimen. The yield strength is taken as the load per unit of original cross section at which the material exhibits an offset of 0.2 per cent of the original length. The Charpy impact specimens are taken in a radial direction, and the minimum impact strength at room temperature measured. The transition temperature is determined from 6 specimens tested at different temperatures in accordance with ASTM A-443. The specimens are taken in a radial direction and machined in such a manner that the V-notch is parallel to the forging axis. Two specimens are machined from each test bar. All specimens are taken following all heat treatment. Curves of impact strength and per cent brittle failure versus test temperature are drawn.

The non-destructive tests include bore inspection, sulfur printing, magnetic particle test, thermal stability test, and ultrasonic tests.

The bores are visually inspected and the walls of the finished bores shall be free from cracks, pipe shrinkage, gas cavities, non-metallic inclusions, injurious scratches, tool marks and similar defects.

A magnetic particle test is made on each forging to demonstrate the freedom from surface discontinuities. The end faces of the main body and down over and beyond the fillets joining the main body to the shaft portions are magnetic particle tested. The bore is also magnetic particle tested at a high sensitivity level in accordance with ASTM A-275. These inspections are done by Westinghouse inspectors prior to Westinghouse accepting these forgings. After final machining by Westinghouse, rotors are again magnetic particle inspected on the external surfaces by Westinghouse.

The face of the test prolongations at each end of the rotor body or an area on the end faces of the rotor body equivalent to the test prolongations is sulfur printed to determine the freedom from undue ingot corner segregation and excessive sulfide inclusions.

A thermal stability test is performed on the forging at the place of manufacture after all heat treatment has been completed.

The forgings are ultrasonically inspected at the place of manufacture by Westinghouse inspectors.

Based on conservative design, reliable turbine control system, careful rotor forging procurement and rigid inspection, the probability of a combination of excessive overspeed, new-born large forging defects, and operating temperature below the transition temperature is considered practically zero.

14.1.13.1 General Description of the Turbine Units

High Pressure Turbine

The high pressure turbine element, shown in Figure 14.1.13-1 is of a double flow design; therefore, it is inherently thrust balanced. Steam from the four control valves enters at the center of the turbine element through four inlet pipes, two in the base and two in the cover. These pipes feed four double flow nozzle chambers flexibly connected to the turbine casing. Each nozzle chamber is free to expand and contract relative the adjacent chambers.

Steam leaving the nozzle chambers passes through the rateau control stages and then flows through the reaction blading. The reaction blading is mounted in blade rings shown in Figure 14.1.13-2, which in turn are mounted in the turbine casing. The blade rings are centerline supported to insure center alignment while allowing for differential expansion between the blade ring and the casing. The design reduces casing thermal distortion and thus, seal clearances are more readily maintained.

Steam exhausts from the high pressure turbine base, through cross-under piping, to the two combined moisture separator live steam reheater assemblies.

The high-pressure rotor is made of NiCrMoV alloy steel. The specified minimum mechanical properties are given in Table 14.1.13-1.

The main body of the rotor weight is approximately 100,000 lb. The approximate values of the transverse centerline diameter, the maximum diameter, and the main body length are 36", 66" and 138" respectively.

The blade rings and the casing cover and base are made of carbon steel casings. The specified mechanical properties are given in Table 14.1.13-2.

The bend test specimen shall be capable of being bent cold through an angle of 90 degrees and around a pin one inch in diameter without cracking on the outside of the bent portion.

The approximate weight of the four blade rings, the casing cover, and the casing base is 80,000 lb., 140,000 lb., and 160,000 lb., respectively.

The casing cover and base are tied together by means of more than 100 studs. The stud material is an alloy steel having the mechanical properties given in Table 14.1.13-3.

The studs have length ranging from 18 to 66 inches and diameter ranging from 2.75" to 4.5". About 90% of them have diameter ranging between 2.5 and 4 inches. The total stud cross-sectional area is about 900 in² and the total stud free-length volume is about 36,000 in³.

Low Pressure Turbine

The double flow low pressure turbine, shown in Figure 14.1.13-3, incorporates high efficiency blading diffuser type exhaust and liberal exhaust hood design. The low pressure turbine cylinders are fabricated from steel plate to provide uniform wall thickness, thus reducing thermal distortion to a minimum. The entire outer casing is subjected to low temperature exhaust steam.

The temperature drop from the cross-under steam temperature to the exhaust steam temperature is taken across three walls; an inner cylinder number 1,

a thermal shield, and an inner cylinder number 2. This precludes a large temperature drop across any one wall except the thermal shield which is not a structural element, thereby virtually eliminating thermal distortion. The fabricated inner cylinder number 2 is supported by the outer casing at the horizontal centerline and is fixed transversely at the top and bottom and axially at the centerline of the steam inlet, thus allowing freedom of expansion independent of the outer casing. Inner cylinder number 1 is, in turn, supported by inner cylinder number 2 at the horizontal centerline and fixed transversely at the top and bottom and axially at the centerline of the steam inlets, thus allowing freedom of expansion independent of inner cylinder number 2. Inner cylinder number 1 is surrounded by the thermal shield.

The steam leaving the last row of blades flows into the diffuser where the velocity energy is converted to pressure energy, thus improving efficiency and reducing the excitation forces on the last rotating row of blades.

The low pressure rotors are made of NiCrMoV alloy steel. The specified minimum mechanical properties are given in Table 14.1.13-4.

The shrunk-on disks are made of NiCrMoV alloy steel. There are twelve disks shrunk on the shaft with six per flow. These disks experience different degrees of stress when in operation. The present design shows that disk No. 3, starting from the transverse centerline, experiences the highest stress, while disk No. 6 experiences the lowest. The minimum specified mechanical properties for the disks are given in Table 14.1.13-5.

The outer cylinder and the two inner cylinders are mainly made of ASTM A-285 Grade C material. The minimum specified properties are given in Table 14.1.13-6.

14.1.13.2 Consequences of Turbine-Generator Unit Overspeeding

Low Pressure Turbine

Experience and test have shown that the mode of failure of a disk, should it occur, is mainly rupture in two or four parts. The broken parts would then be ejected normally to the rotation axis. Hence, the potential missiles considered for purposes of analysis are:

- a) Half disk
- b) A quarter of disk

There are twelve disks shunk on each low-pressure turbine rotor, with six disks per flow. Numbering the disks from the steam admission, disks No. 1, 2 and 3 are contained within the inner cylinder No. 1, the inner cylinder No. 2, and the outer cylinder (reference is made to Figures 14.1.13-3 and -4). Therefore, if one of these disks breaks, it has to go through the corresponding stationary blade ring, the inner cylinder No. 1, the inner cylinder No. 2, and the outer cylinder. Disks No. 4 and 5 are contained within the inner cylinder No. 2 and the outer cylinder. Hence, if one of these fails, it has to pass through the directly opposite blade ring, the inner cylinder No. 2 and partially within the diffuser and within the outer cylinder. If parts of this disk come loose, they have to go through the directly opposite blade ring and the outer cylinder.

The thickness of the back plate of the three cylinders is given in Table 14.1.13-7.

The bursting speed of each disk has been calculated with a stress analysis based on a tensile strength 20 per cent higher than the minimum specified tensile strength. The 20 per cent increase conservatively accounts for the actual value of the tensile strength, usually observed to be higher than the minimum specified. The values of the minimum and maximum bursting speeds of each disk are listed in the Table 14.1.13-8.

As Table 14.1.13-8 shows, the maximum speed at which the unit might run with no disk failure is 175% of nominal. At this speed, disk No. 3 will burst. As one of the first disks ruptures, the steam flow between the blades of the remaining disks is significantly reduced, the turbine-generator is slowed down, and further disk failures are not anticipated. Since the actual value of the bursting speed of each disk will be between the maximum and minimum previously mentioned, the potentiality of bursting each one of the first five disks exists. The probability of disk No. 6 bursting is more remote. The consequences of rupture of any one of these disks at the maximum speed that the unit might approach in case of turbine runaway have been evaluated and the results are summarized in the following pages.

Table 14.1.13-9 lists the values of the rim radius, the weight, the ejection velocity and ejection translational energy of each disk quarter, at 175% of nominal speed. Table 14.1.13-10 lists the same parameters for half disks.

Disk No. 1, No. 2, and No. 3

Rupture of disk No. 3 has been assumed for purpose of analysis because the four quarters of this disk have more translational kinetic energy than disk No. 1 and No. 2. As the four quarters come loose, they strike and deeply deform the inner cylinder No. 1 and cause some deformation of the inner cylinder No. 2 and of the outer cylinder of less extent.

The rupture is expected to be contained within the unit and no outside missile is anticipated to be generated.

The deformation energy per unit volume of the cylinder material has been evaluated under "static" and "dynamic" loading, based on both minimum specified and actual averaged mechanical properties. Table 14.1.13-11 summarizes the values of the deformation energy per unit volume up to 100%, 75% and 50% of the total elongation, respectively.

It is expected that in order to penetrate through the inner cylinder No. 1, the ruptured disk quarters shall have the kinetic energy necessary to deform about 1/3 of the inner cylinder No. 1 volume to between 50% and 75% of the actual total elongation, i.e., between 100×10^6 ft lb and 150×10^6 ft lb. The anticipated kinetic energy of 4 quarters of disk No. 3 is at the lower limit of the above range, i.e., 100×10^6 ft lb.

For disk fragments to become missiles, they would have to violate not only the integrity of the inner cylinder No. 1, but also that of the inner cylinder No. 2 and of the outer cylinder. As mentioned earlier, quarters of disk No. 3 are not expected to violate the integrity of inner cylinder No. 1. Should violation occur for some unknown reasons, the kinetic energy of the quarters would be small. Therefore, for these fragments to leave the unit, they shall have enough kinetic energy to deform a significant amount of inner cylinder No. 2 and outer cylinder, rather than just the energy necessary to perforate the back plates of these cylinders.

For these reasons, we do not expect external missiles to be generated because of failure of one of the first three disks.

Disk No. 4 and No. 5

Rupture of disk No. 5 has been conservatively assumed for purpose of analysis because the four quarters of this disk have more translational kinetic energy than disk No. 4. As the four quarters come loose, they strike and deeply deform the inner cylinder No. 2, and cause some deformation of the outer cylinder.

The rupture is expected to be contained within the unit and no outside missile is anticipated to be generated.

It is expected that, in order to penetrate through the inner cylinder No. 2, the ruptured disk quarters shall have the kinetic energy necessary to deform about 25% of the inner cylinder No. 2 volume to between 50% and 75% of the actual total elongation, i.e., between 136×10^6 and 200×10^6 ft lb. The anticipated kinetic energy of 4 quarters of disk No. 5 is less than 120×10^6 ft lb.

For disk fragments to become missiles, they do not have to violate only the integrity of the inner cylinder no. 2, but also that of the outer cylinder. Therefore, ejection of quarters of disk No. 4 and 5 outside the unit is not expected.

Disk No. 6

This disk is the least stressed disk, and the disk that has the highest bursting speed range, i.e., 171% - 187% of nominal. The probability of reaching this speed range is quite remote, because one of the other disks is anticipated to fail at lower speed, preventing the unit from reaching the bursting speed range of disk No. 6. For purpose of analysis it has been postulated the occurrence of bursting this disk at the maximum running speed of 175% of nominal.

The damage caused by this failure is expected to be contained within the unit.

Upon bursting, the ejected quarters will strike the coupling flanges of the outer cylinder center and the outer cylinder side. It is expected that, in order to penetrate through the outer cylinder, the ejected quarters shall have the kinetic energy required to deform the directly opposite blade ring, the above mentioned flanges and a two-disk-hub wide portions of the outer cylinder, for a total of $150,000 \text{ in}^3$, to between 50% and 75% of the actual total elongation, i.e., between 112×10^6 ft lb.

and 168×10^6 ft lb. Since the anticipated kinetic energy of 4 disk No. 6 quarters, i.e., 100×10^6 ft lb, is below the lower limit of the required energy range, no external missile is anticipated.

High Pressure Turbine

Due to the very large margin between the high pressure spindle bursting speed and the maximum speed at which the steam can drive the unit with all the admission valves fully open, the probability of spindle failure is practically zero. Therefore, no harmful missile is anticipated in case of turbine runaway.

Based on the admission steam thermodynamic properties and blade geometry, the maximum theoretical speed at which the unit may run is 208% of nominal.

Based on the stress analysis of the low-pressure disks, the maximum actual speed at which the unit may run is 175% of nominal.

The minimum bursting speed of the spindle, based on the minimum specified mechanical properties of the spindle material, is 270% of nominal. The actual bursting speed is closer to 300% of nominal than 270%.

Hence, the actual margin between the bursting speed and the maximum running speed is of the order of 125% of nominal, i.e., $300\% - 175\%$.

No failure of the H. P. is anticipated as a consequence of a unit runaway; and therefore, no missiles are expected to be generated.

REFERENCES

1. Curran, R. M., "History of the Special ASTM Task Force on Large Turbine and Generator Rotors," ASTM Meeting, Purdue University, 1965.

TABLE 14.1.13-1

MINIMUM MECHANICAL PROPERTIES - HIGH PRESSURE ROTOR

Tensile Strength, psi, min.	100,000
Yield Strength, psi, min. (0.2% offset)	80,000
Elongation in 2 inches, per cent, min.	18
Reduction of Area, per cent, min.	45
Impact Strength, Charpy V-Notch, ft-lb (min. at room temperature)	60
50% Fracture Appearance Transition Temperature, °F, Max.	50

TABLE 14.1.13-2
MINIMUM MECHANICAL PROPERTIES - CASINGS

Tensile Strength, psi, min.	70,000
Yield Strength, psi, min.	36,000
Elongation in 2", per cent, min.	22
Reduction of Area, per cent, min.	35

TABLE 14.1.13-3
MECHANICAL PROPERTIES - STUD MATERIAL

	Size, Inches		
	2-1/2 and less	Over 2-1/2 to 4 inch	Over 4 to 7 inch
Tensile Strength, psi, min.	125,000	115,000	110,000
Yield Strength, psi, min (0.2% offset)	105,000	95,000	85,000
Elongation in 2 inches, per cent, min.	16	16	16
Reduction of Area, per cent, min.	50	50	50

TABLE 14.1.13-4

MINIMUM MECHANICAL PROPERTIES - LOW PRESSURE ROTORS

Tensile Strength, psi, min.	115,000
Yield Strength, psi, min. (0.2% offset)	100,000
Elongation in 2 inches, per cent, min.	16
Reduction of Area, per cent, min.	40
Impact Strength, Charpy V-Notch, ft-lb. min. at room temp.	40
50% Fracture Appearance Transition Temperature, °F, max.	80

TABLE 14.1.13-5
MINIMUM MECHANICAL PROPERTIES - DISKS

	<u>Disk No. 3</u>	<u>Disk No. 1,2,4,5 and 6</u>
Tensile Strength, psi, min.	130,000	120,000
Yield Strength, (Hub) psi, (0.2% offset)	120,000-135,000	110,000-125,000
Yield Strength, psi (Rim)	100,000	
Elongation in 2" (Disk Hub), per cent, min.	14	15
Elongation in 2" (Disk Rim), per cent, min.	18	17
Reduction of Area (Disk Hub), per cent, min.	35	38
Reduction of Area (Disk Rim), per cent, min.	45	43
Impact Strength, (Hub and Rim), Charpy V-Notch, ft-lb, min, at room temp.	50	50
50% Fracture Appearance Transi- tion Temperature (Disk Hub and Rim) °F, max.	0	0

TABLE 14.1.13-6
MINIMUM MECHANICAL PROPERTIES - CYLINDERS

Tensile Strength, psi, min.	55,000
Yield Strength, psi, min.	30,000
Elongation in 8", per cent, min.	24
Elongation in 2", per cent, min.	28

Whenever plates of thickness >2 " are employed, they are made of ASTM
A-212 Grade A.

TABLE 14.1.13-7
THICKNESS - BACK PLATE OF CYLINDERS

Inner cylinder No. 1	2 inches
Inner cylinder No. 2	1.25 inches
Outer cylinder	1.25 inches

TABLE 14.1.13-8
DISK BURSTING SPEED

<u>Type of Disk</u>	Bursting Speed (per cent of <u>nominal</u>)	
	<u>Maximum</u>	<u>Minimum</u>
Disk No. 1	179	163
Disk No. 2	181	165
Disk No. 3	175	153
Disk No. 4	179	163
Disk No. 5	178	162
Disk No. 6	187	171

TABLE 14.1.13-9
RUPTURE IN FOUR QUARTERS AT 175% OF NOMINAL SPEED

<u>Type of Disk</u>	<u>Rim Radius (inches)</u>	<u>Weight (lb)</u>	<u>Ejection Velocity (ft/sec)</u>	<u>Ejection Translation Kinetic Energy (ft lb)</u>
Quarter of Disk No. 1	51.875	2050	855	23.2×10^6
Quarter of Disk No. 2	51.875	1912.5	855	21.7×10^6
Quarter of Disk No. 3	51.875	2455	855	25.0×10^6
Quarter of Disk No. 4	51.234	2575	845	28.6×10^6
Quarter of Disk No. 5	49.162	2900	810	29.6×10^6
Quarter of Disk No. 6	43.800	3100	722	25.1×10^6

TABLE 14.1.13-10

RUPTURE IN TWO HALVES AT 175% OF NOMINAL SPEED

<u>Type of Disk</u>	<u>Rim Radius (inches)</u>	<u>Weight (lb)</u>	<u>Ejection Velocity (ft/sec)</u>	<u>Ejection Translational Kinetic Energy (ft lb)</u>
Half of Disk No. 1	51.875	4100	605	23.3×10^6
Half of Disk No. 2	51.875	3825	605	21.7×10^6
Half of Disk No. 3	51.875	4910	605	25.0×10^6
Half of Disk No. 4	51.234	5150	598	28.6×10^6
Half of Disk No. 5	49.162	5800	573	29.6×10^6
Half of Disk No. 6	43.800	6200	510	25.1×10^6

TABLE 14.1.13-11
DEFORMATION ENERGY PER UNIT VOLUME

A. BASED ON THE MINIMUM SPECIFIED MECHANICAL PROPERTIES

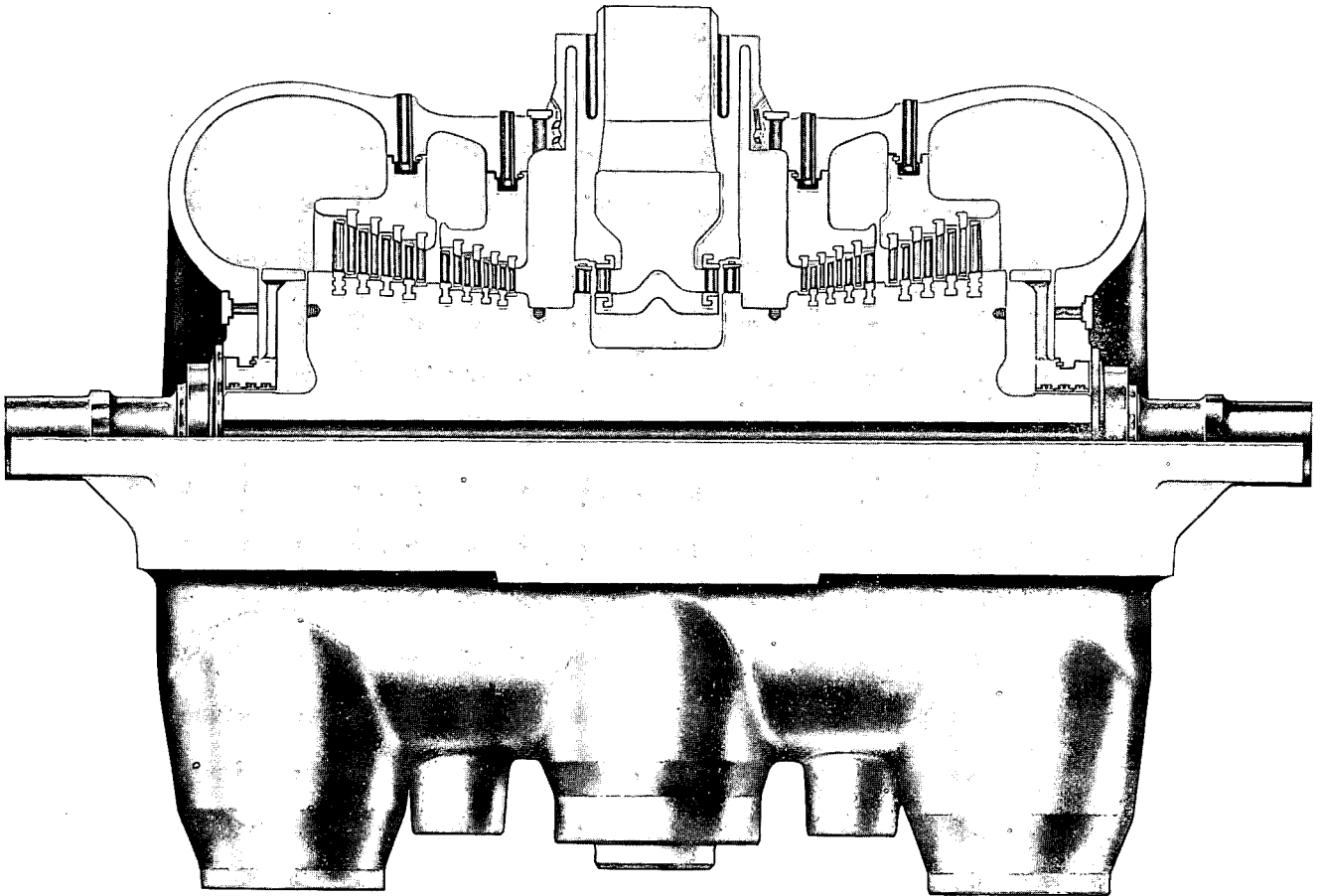
	up to 50% ϵ_{μ}	up to 75% ϵ_{μ}	up to 100% ϵ_{μ}
Under "static" loading	4,400 $\frac{\text{in lb}}{\text{in}^3}$	7,000 $\frac{\text{in lb}}{\text{in}^3}$	10,200 $\frac{\text{in lb}}{\text{in}^3}$
Under "dynamic" loading	7,900 $\frac{\text{in lb}}{\text{in}^3}$	11,900 $\frac{\text{in lb}}{\text{in}^3}$	15,800 $\frac{\text{in lb}}{\text{in}^3}$

B. BASED ON THE ACTUAL AVERAGED MECHANICAL PROPERTIES

	up to 50% ϵ_{μ}	up to 75% ϵ_{μ}	up to 100% ϵ_{μ}
Under "static" loading	6,000 $\frac{\text{in lb}}{\text{in}^3}$	9,900 $\frac{\text{in lb}}{\text{in}^3}$	14,300 $\frac{\text{in lb}}{\text{in}^3}$
Under "dynamic" loading	9,000 $\frac{\text{in lb}}{\text{in}^3}$	13,500 $\frac{\text{in lb}}{\text{in}^3}$	18,000 $\frac{\text{in lb}}{\text{in}^3}$

HIGH PRESSURE CYLINDER

1800 RPM DOUBLE-FLOW DESIGN

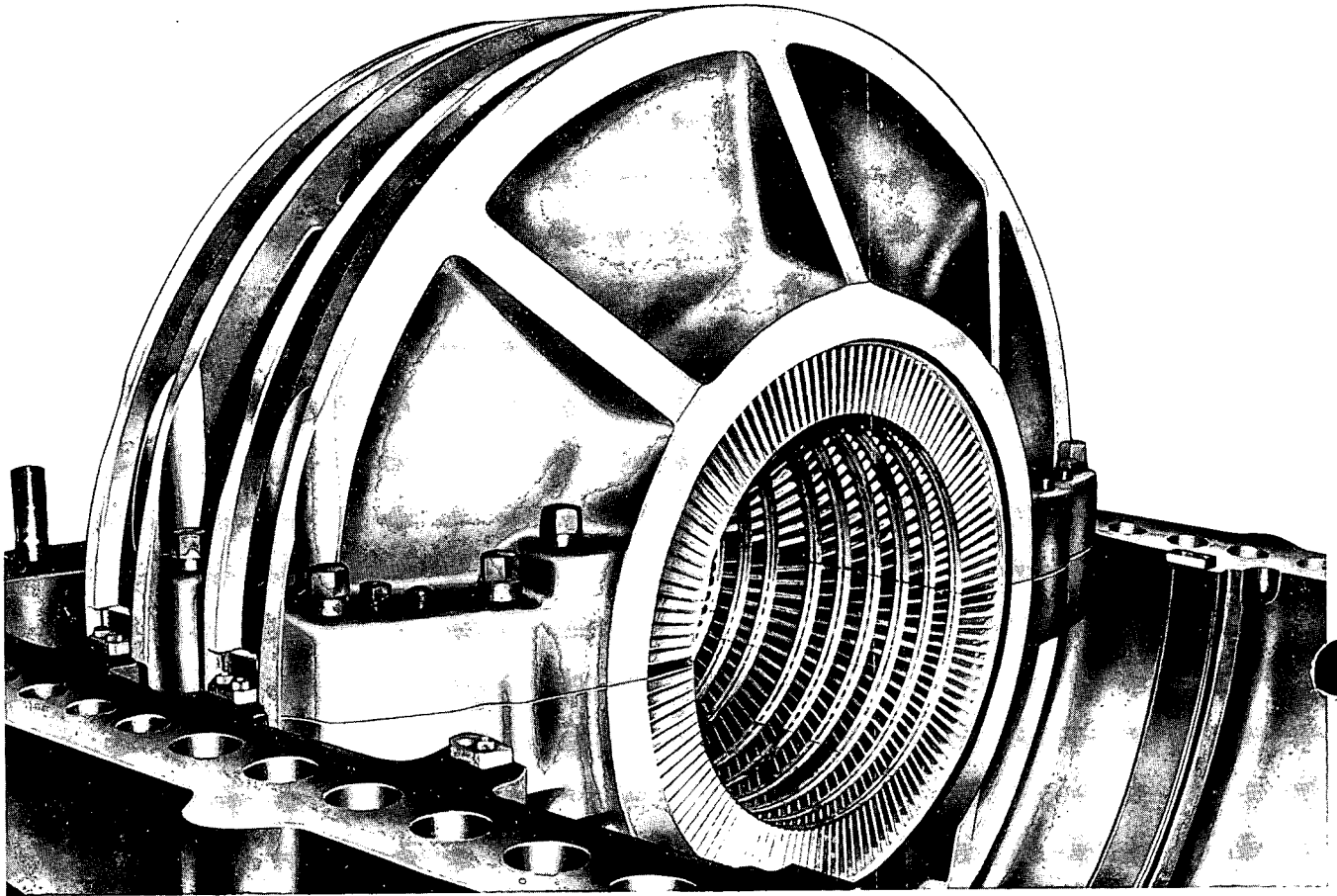


FEATURES

1. Four separate nozzle chambers permit freedom of expansion and contraction during starting and load changes.
2. Double flow design insures thrust balance.
3. Rotor checked in heater box for dynamic balance prior to shipment.
4. Ultrasonic test of rotor performed at steel mill and at the Westinghouse factory.

FIGURE 14.1.13-1

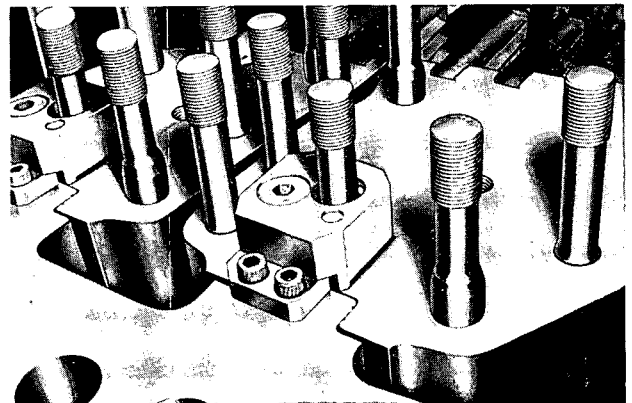
BLADE RINGS



Blade rings of large high-pressure, high temperature turbine, with stationary blades in place.

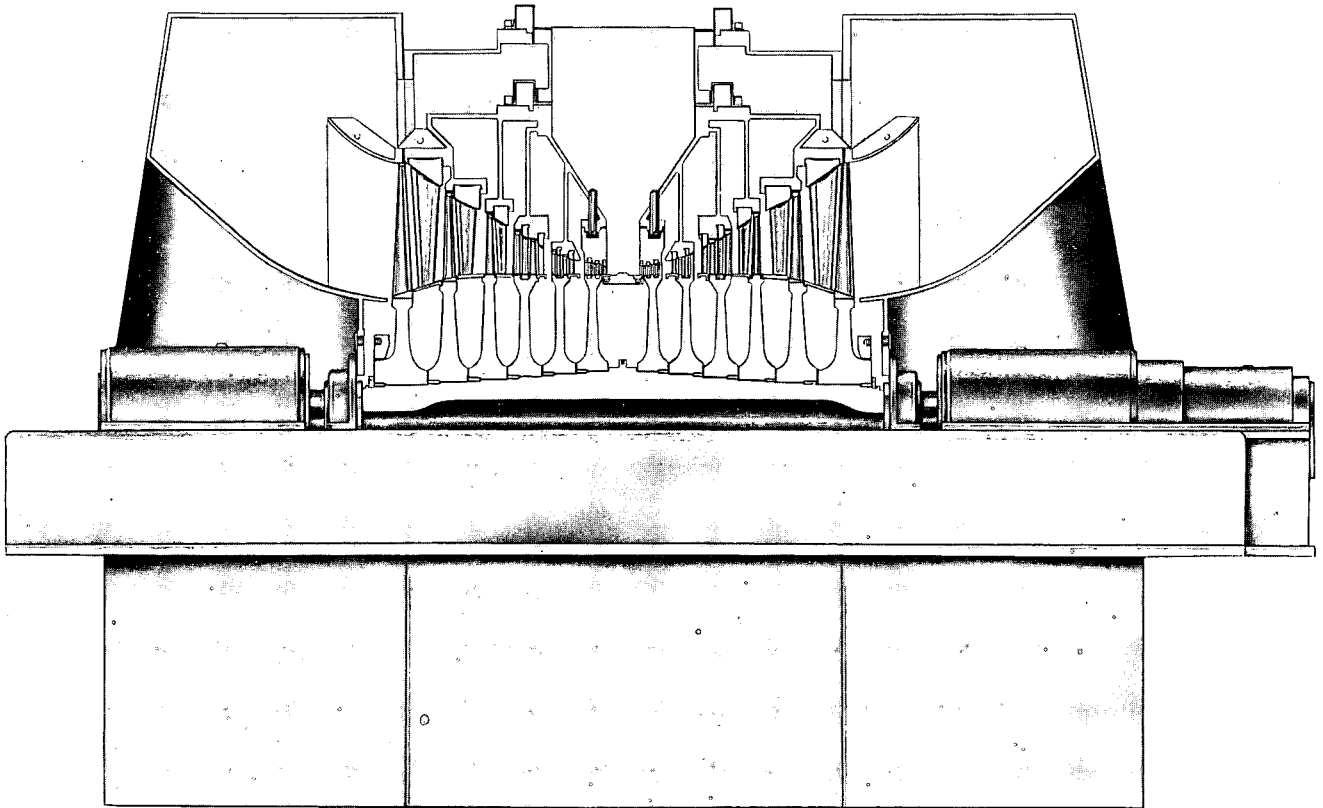
FEATURES

1. Centerline supporting block insures center alignment while allowing differential expansion between blade ring and cylinder.
2. Blades are inserted in blade ring halves.
3. Tongue and groove holds blade ring in position.
4. Metallic seals between blade rings and cylinder prevent leakage of steam in support grooves.
5. Upper plate, in cylinder cover, prevents any "riding-up" of the blade ring.



View of turbine cylinder and blade ring, showing method of supporting and locking lower blade ring in position.

LOW-PRESSURE ELEMENT 1800-RPM DOUBLE-FLOW DESIGN

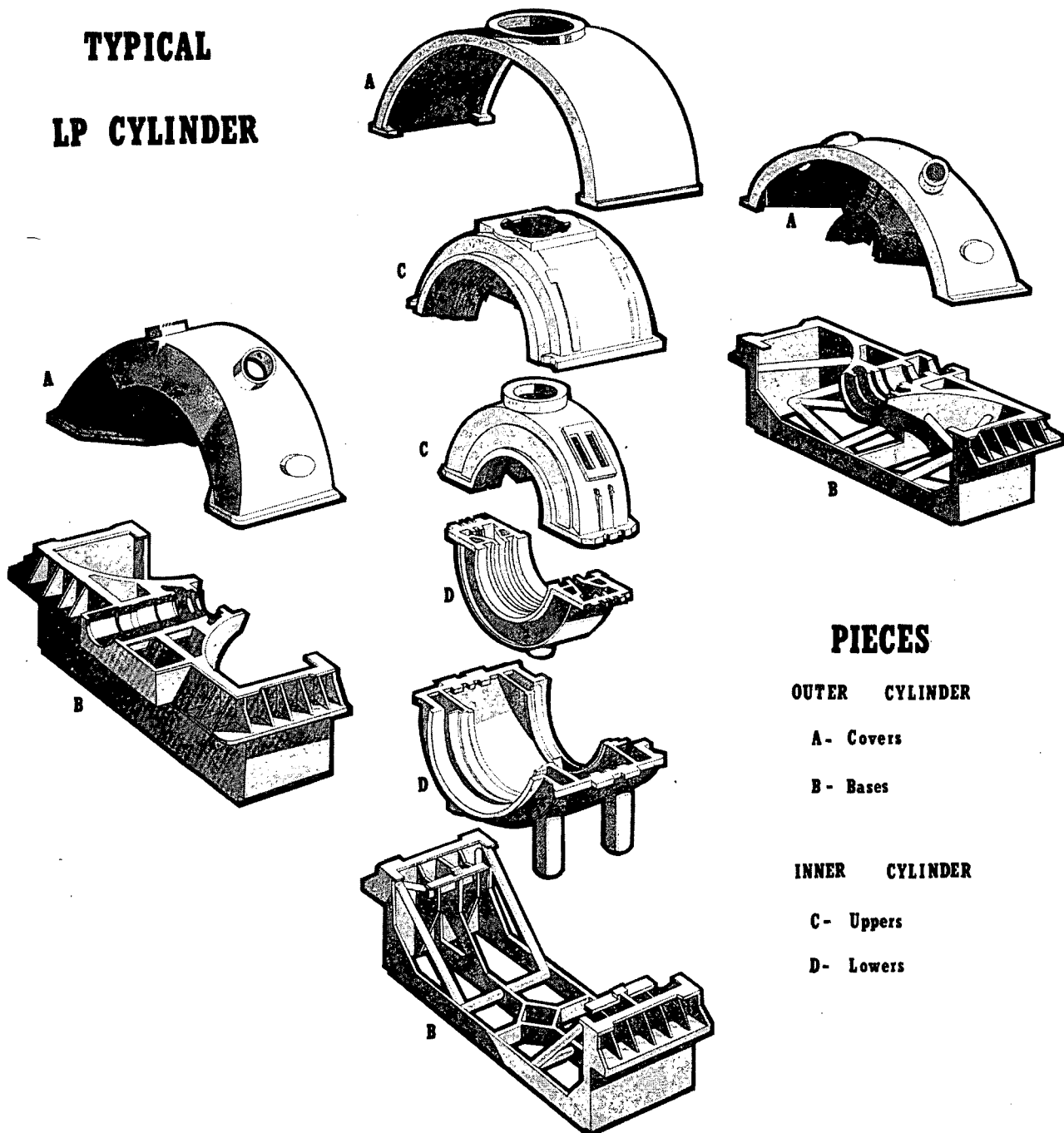


FEATURES

1. Blade ring, supported at the horizontal centerline and fixed transversely at the top and bottom by dowel pins, allows freedom of expansion independent of the casing.
2. Entire exhaust casing is at exhaust steam temperature.
3. Exhaust hood of laboratory-proved design minimizes hood loss.
4. Provision for extraction zones with moisture removal.
5. Casing and blade ring of fabricated steel construction.

FIGURE 14.1.13-3

TYPICAL LP CYLINDER



PIECES

OUTER CYLINDER

A - Covers

B - Bases

INNER CYLINDER

C - Uppers

D - Lowers

FIGURE 14.1.13-4

14.2

STANDBY SAFETY FEATURES ANALYSIS

Adequate provisions have been included in the design of the unit and its standby engineered safety features to limit potential exposure of the public to well below the limits of 10 CFR 100 for situations which have a very low probability of occurrence, but which could conceivably involve uncontrolled releases of radioactive materials to the environment. The situations which have been considered are:

- a) Fuel Handling Accidents
- b) Accidental Release of Waste Liquid
- c) Accidental Release of Waste Gases
- d) Rupture of a Steam Generator Tube
- e) Rupture of a Steam Pipe
- f) Rupture of a Control Rod Drive Mechanism Housing - Rod Cluster Control Assembly (RCCA) Ejection

14.2.1 FUEL HANDLING ACCIDENTS

The following fuel handling accidents are evaluated to ensure that no hazards are created:

- a) A fuel assembly becomes stuck inside reactor vessel.
- b) A fuel assembly or control rod cluster is dropped onto the floor of the reactor cavity or spent fuel pit.
- c) A fuel assembly becomes stuck in the penetration valve.
- d) A fuel assembly becomes stuck in the transfer carriage or the carriage stuck.

Causes and Assumptions

The possibility of a fuel handling incident is remote because of the administrative controls and physical limitations imposed on fuel handling operations. All refueling operations are conducted in accordance with prescribed procedures under direct surveillance of a supervisor technically trained in nuclear safety. Also, before any refueling operations begin, verification of complete rod cluster control assembly insertion is obtained by tripping each rod individually to obtain indication of rod drop and disengagement from the control rod drive mechanisms. Boron concentration in the coolant is raised to the refueling concentration and verified by sampling. Refueling boron concentration is sufficient to maintain the clean, cold, fully loaded core subcritical with all rod cluster assemblies withdrawn. The refueling cavity is filled with water meeting the same boric acid specifications. As the vessel head is raised, a visual check is made to verify that the drive shafts are free in the mechanism housing.

After the vessel head is removed, the rod cluster control drive shafts are removed from their respective assemblies using the containment crane and the drive shaft unlatching tool. A spring scale is used to indicate that the drive shaft is free of the control cluster as the lifting force is applied.

The fuel handling manipulators and hoists are designed so that fuel cannot be raised above a position which provides adequate shield water depth for the safety of operating personnel. This safety feature applies to handling facilities in both the containment and in the spent fuel pit area. In the spent fuel pit, the design of storage racks and manipulation facilities is such that:

Fuel at rest is positioned by positive restraints in a safe, subcritical, geometrical array, with no credit for boric acid in the water.

• Fuel can be manipulated only one assembly at a time.

Violation of procedures by placing one fuel assembly in juxtaposition with any group of assemblies in racks will not result in criticality.

Crane facilities do not permit the handling of heavy objects, such as a spent fuel shipping container, above the fuel racks. ✓

Adequate cooling of fuel during underwater handling is provided by convective heat transfer to the surrounding water. The fuel assembly is immersed continuously while in the refueling cavity or spent fuel pit.

Should a spent fuel assembly become stuck in the transfer tube, natural convection will maintain adequate cooling. The fuel handling equipment is described in detail in Section 9.4.

Two Nuclear Instrumentation System source range channels are continuously in operation and provide warning of any approach to criticality during refueling operations. This instrumentation provides a continuous audible signal in the containment, and would annunciate a local horn and a horn and light in the plant control room if the count rate increased above a preset low level.

Refueling boron concentration is sufficient to maintain the clean, cold, fully loaded core subcritical by at least 10 per cent with all rod cluster control assemblies inserted. At this boron concentration the core would also be more than 2 per cent subcritical with all control rods withdrawn. The refueling cavity is filled with water meeting the same boric acid specification.

All these safety features make the probability of a fuel handling incident very low. Nevertheless, it is possible that a fuel assembly could be dropped during the handling operations. Therefore, this incident is analyzed both from the standpoint of radiation exposure and accidental criticality.

Special precautions are taken in all fuel handling operations to minimize the possibility of damage to fuel assemblies during transport to and from the spent fuel pit and during installation in the reactor. All irradiated fuel handling operations are conducted under water. The handling tools used in the fuel handling operations are conservatively designed and the associated devices are of a fail-safe design.

In the fuel storage area, the fuel assemblies are spaced in a pattern which prevents any possibility of a criticality accident. Also, the design of the facility is such that it is not possible to carry heavy objects, such as a spent fuel transfer cask, over the fuel assemblies in the storage racks. In addition, the design is such that only one fuel assembly can be handled at a given time.

The motions of the cranes which move the fuel assemblies are limited to a low maximum speed. Caution is exercised during fuel handling to prevent the fuel assembly from striking another fuel assembly or structures in the containment or fuel storage building.

The fuel handling equipment suspends the fuel assembly in the vertical position during fuel movements, except when the fuel is moved through the transport tube.

The design of the fuel assembly is such that the fuel rods are restrained by grid clips which provide a total restraining force of approximately 60 pounds on each fuel rod. If the fuel rods are in contact with the bottom plate of the fuel assembly, any force transmitted to the fuel rods is limited due to the restraining force of the grid clips. The force transmitted to the fuel rods during fuel handling is not of a magnitude great enough to breach the fuel rod cladding. If the fuel rods are not in contact with the bottom plate of the assembly, the rods would have to slide against the 60 pound friction force. This would have the effect of absorbing a shock and thus limit the force on the individual fuel rods.

After the reactor is shut down, the fuel rods contract during the subsequent cooldown and would not be in contact with the bottom plate of the assembly.

Considerable deformation would have to occur before the rod would make contact with the top plate and apply any appreciable load on the fuel rod. Based on the above, it is felt that it is unlikely that any damage would occur to the individual fuel rods during handling. If one assembly is lowered on top of another, no damage to the fuel rods would occur that would breach the integrity of the cladding.

If during handling the fuel assembly strikes against a flat surface, the loads would be distributed across the fuel assemblies and grid clips and essentially no damage would be expected in any fuel rods.

If the fuel assembly were to strike a sharp object, it is possible that the sharp object might damage the fuel rods with which it comes in contact but breaching of the cladding is not expected. It is on this basis that the assumption of the failure of an entire row of fuel rods (15) is a very conservative upper limit.

Analyses have been made assuming the extremely remote situation where a fuel assembly is dropped and strikes a flat surface, where one assembly is dropped on another, and where one assembly strikes a sharp object. The analysis of a fuel assembly assumed to be dropped and strikes a flat surface considered the stresses the fuel cladding was subjected to and any possible buckling of the fuel rods between the grip clip supports. The results showed that the buckling load at the bottom section of the fuel rod, which would receive the highest loading, was below the critical buckling load and the stresses were relatively low and below the yield stress. For the case where one assembly is dropped on top of another fuel assembly, the loads will be transmitted through the end plates and the RCC guide tubes of the stuck assembly before any of the loads reach the fuel rods.

The end plates and guide thimbles absorb a large portion of the kinetic energy as a result of bending in the lower plate of the falling assembly. Also, energy is absorbed in the struck assembly top end plate before any load can be transmitted to the fuel rods. The results of this analysis indicated that the buckling load on the fuel rods was below the critical buckling loads and the stresses in the cladding were relatively low and below yield.

The refueling operation experience that has been obtained with Westinghouse reactors has verified the fact that no fuel cladding integrity failures are expected to occur during any fuel handling operations.

Rupture of one complete out row of fuel rods in a withdrawn assembly is assumed as a conservative limit for evaluating the environmental consequences of a fuel handling incident. The remaining fuel assemblies are so protected by the storage rack structure that no lateral bending loads would be produced. No damage has resulted from an experimentally axial applied load of 2200 lb. to a fuel assembly. The maximum column load expected to be experienced in service is approximately 1000 lb. This information was used in the fuel handling equipment design to establish the limits for inadvertent axial loads.

Activity Release Characteristics

For the assumed accident there would be a sudden release of the gaseous fission products held in the voids between the pellets and cladding of fifteen fuel rods. The low temperature of the fuel during handling operations precludes further significant release of gases from the pellets themselves after the cladding is breached. Halogen release is also greatly minimized due to their low volatility at these temperatures. The strong tendency for iodine in vapor and particulate form to be scrubbed out of gas bubbles during their ascent to the water surface further alleviates the inhalation hazard.

Decontamination factors of $10^{-3(1)}$ have been measured with much shallower water depths and much higher gas-to-water ratios. In a Westinghouse laboratory apparatus, elemental iodine (I_2) was passed in an air stream through a solution of 2000 ppm boron as boric acid. This solution is chemically similar to that in the spent fuel storage pit. The contact time in this apparatus corresponded to a bubble rise of 1.6 cm. Initially, the iodine decontamination factor (D.F.) in this apparatus was about 90%. The value decreased with time as the concentration of iodine in solution approached saturation, as expected. The D.F. at zero aqueous iodine concentration agreed with that obtained with an iodine fixing reagent (sodium thiosulfate) in solution, indicating that gas phase diffusion to the bubble wall was controlling when the laden bubbles contacted fresh solution. This condition can be assumed to represent the scrubbing of gas bubbles released from an accidental cladding failure as they rise through a vast reservoir of iodine free solution in the spent fuel pit. The calculated contact time in the accident can be related to the experiment by the ratio of the submergence, which is 24 feet, in the case of the plant, compared with 1.6 cm in the experiment. Assuming the same mass transfer rate in the bubble the D.F. of 10^{-3} would be obtained in a rise of only 9.9 cm. While this extrapolation is undoubtedly optimistic, it indicates that a large margin is available in the height of bubble rise in the pool to compensate for differences in bubble size and the decay of eddy motion inside the bubble with time. Conservatively assuming all of the iodine in the gap of the 15 rods (390 curies I-131) is present in the gaseous phase and taking credit for the 10^{-3} decontamination factor, the estimated I-131 release from the water surface is 0.39 curie.

The noble gas activity calculated present in the gas gap of the 15 rods is given in Table 14.2.1-1. These activities are based on a 90 hour decay period following operation at 2300 MWt for a full core cycle. This is the minimum delay before a fuel assembly can be moved following shutdown.

Method of Analysis

The activity could be released either in the containment or in the auxiliary (fuel storage) building. Both areas ventilation systems are in operation under administrative control during refueling hence in calculating doses inside the structures uniform dilution is assumed within the structure. Radioactivity monitors would immediately indicate and alarm the increased activity level. Activity in the containment would automatically close the purge ducts. In evaluating dose to refueling personnel inside the containment 15 minutes is assumed a reasonable time for evacuation. In the fuel storage building the integrated dose is evaluated based on the 8,000 cfm ventilation rate and the 50,000 ft³ free volume. In the containment, the dose is based on the 35,000 cfm purge rate and the 1.55×10^6 ft³ free volume.

In calculating offsite exposure it is assumed that the incident occurs in the spent fuel pit or the containment and that the activity is discharged to the atmosphere at the ground level through doors in either building. This results in maximum ground level doses. This assumption is very conservative for two reasons: the ventilation systems exhaust to atmosphere at an elevated point and the containment and fuel handling building doors are closed. The whole body doses are based on the model described in Section 14.3.

Dispersion of this activity is computed using the Gaussian plume dispersion formula and taking credit for building wake dilution as included in the two hour dispersion factor developed in Section 14.3.5.

Summary of Calculated Doses and Criticality

The calculated doses are summarized in Table 14.2.1-2 and are less than 10CFR100 limits. The permissible containment re-entry time after reduction to Xe-133 occupational MPC is eight hours, and the fuel storage area re-entry time is one half hour.

Thus, it is concluded that a dropped fuel assembly would present no criticality hazard and would generate an insignificant radiation exposure at the site boundary (425 meters).

REFERENCE

- (1) Diffey, H. R. et. al., "Iodine Clean-up in a Steam Suppression System," International Symposium on Fission Product Release and Transport Under Accident Conditions, Oak Ridge, Tennessee, CONF-65047, Vol. 2, Pg. 776-804 (1965).

TABLE 14.2.1-1
NOBLE GAS ACTIVITY RELEASE FROM FUEL HANDLING INCIDENT

<u>Isotope</u>	<u>Activity (Curies, equivalent Xe-133)</u>
Kr-85	67
Xe-133(m)	65
Xe-133	700
Xe-135	0.02

TABLE 14.2.1-2
SUMMARY OF FUEL HANDLING INCIDENT DOSE

	<u>Whole Body Dose (rem)</u>	<u>Thyroid Dose (rem)</u>
Dose for 15 min. exposure inside Containment (No purging)	1	4
Dose in Spent Fuel Building for Duration of Accident with ventilation	12	54
Dose at Site Boundary	<0.1	0.2

14.2.2 ACCIDENTAL RELEASE-RECYCLE OR WASTE LIQUID

Accidents in the auxiliary building which would result in the release of radioactive liquids are those which may involve the rupture or leaking of system pipe lines or storage tanks. The largest vessels are the three liquid holdup tanks, each sized to hold two-thirds ($2/3$) of the reactor coolant liquid volume, which are used to process the normal recycle or waste fluids produced. The contents of one tank will be passed through the liquid processing train while another tank is being filled.

All liquid waste components are located in the auxiliary building except the reactor coolant drain and the pressurizer relief tanks and any leakage from the tanks or piping will be collected in the building sump to be pumped back into the liquid waste system. The liquid holdup tank vault volumes are sufficient to hold the full volume of a liquid holdup tank without overflowing to areas outside the vault.

The holdup tanks are also equipped with safety pressure relief and designed to accept without loss of function the maximum potential seismic forces at the site. Liquids in the Chemical and Volume Control System flowing into and out of these tanks are controlled by manual valve operation and governed by prescribed administrative procedures.

The volume control tank design philosophy is similar in many respects to that applied for the holdup tanks. Level alarms, pressure relief valves and automatic tank isolation and valve control assure that a safe condition is maintained during system operation. Excess letdown flow is directed to the holdup tanks via the reactor coolant drain tank.

Piping external to the containment running between the containment and the auxiliary building area will be in concrete pipe chases.

The incipient hazard from these process or waste liquid releases is derived only from the volatilized components. The releases are described and their effects summarized in Section 14.2.3.

The evaluation of the credibility of the accidental release of radioactive fluids above maximum normal concentration (4×10^{-5} $\mu\text{c/cc}$) from the Waste Disposal System discharge is based upon the following review of waste discharge operating procedure, monitoring function description, monitor failure mode and the consequences of a monitor failure.

The procedure for discharging liquid wastes is as follows:

- a) A batch of waste is collected in one waste condensate tank (capacity 1000 gal).
- b) The tank is isolated
- c) The tank contents are recirculated to mix the liquid
- d) A sample is taken for radiochemical analysis
- e) If analysis indicates that release can be made within permissible limits, the quantity of activity to be released is recorded on the basis of the liquid volume in the tank and its activity concentration. If release can not be made within permissible limits, the waste is returned to the waste holdup tank.
- f) To release the liquid, the last stop valve in the discharge line (which is normally locked shut) must be unlocked and opened; a second valve, which trips shut automatically on high radiation signal from the monitor, must be opened manually; a waste condensate pump must be started manually and the normal 20 gpm flow rate established on the flow indicator provided; and finally the recirculation valve must be closed. Liquid is now being pumped overboard.

As the operating procedure indicates, the release of liquid waste is under administrative control. The monitor is provided to maintain surveillance over the release.

The monitor is provided with the following features:

- a) A calibration source is provided to permit the operator to check the monitor before discharge by pressing a button in the control room to activate the circuitry.
- b) If the monitor falls off scale at any time, an indicator visible to the operation in the control room lights.
- c) If the power supply to the monitor fails, a high radiation alarm is annunciated. The trip valve also closes.
- d) The radiation trip valve is failed closed, normally closed.

It is concluded that the administrative controls imposed on the operator combined with the safety features built into the equipment provide a high degree of assurance against accidental release of waste liquids.

No credible mechanism exists for accidental release of waste liquids to Lake Robinson. A diffusion analysis was performed, however, to determine the concentrations which would result in the lake if a release was assumed. Details of the analysis are presented in section 2.6.4, under Diffusion of Short Term Releases. Maximum instantaneous activity release to the lake which would not result in peak concentrations in excess of 10 CFR 20 MPC limits is listed in Table 2.6-5.

14.2.3 ACCIDENTAL RELEASE - WASTE GAS

The leakage of fission products through cladding defects can result in a buildup of radioactive gases in the reactor coolant. Based on experience with other operational, closed cycle, pressurized water reactors, the number of defective fuel elements and the gaseous coolant activity is expected to be low. The shielding and sizing of components such as demineralizers and the waste handling system are based on activity corresponding to 1% defective fuel which is at least an order of magnitude greater than expected. Tanks accumulating significant quantities of radioactive gases during operation are the gas decay tanks, the volume control tank, and the liquid holdup tanks.

The volume control tank accumulates gases over a core cycle by stripping action of the entering spray. Equilibrium gaseous activity for the tank based on operation with 1% defective fuel is tabulated in Table 14.2.3-1. During a refueling shutdown this activity is vented to the waste gas system and stored for decay. Rupture of this tank is assumed to release all of the contained noble gases plus that small amount contained in the 60 gpm flow from the demineralizers which would continue for up to five minutes before isolation would occur. The released activity would be 14,000 curies equivalent Xe-133.

The liquid holdup tanks receive reactor coolant, after passing through demineralizers, during the process of coolant deboration. The liquid is stored and then processed through the boric acid evaporators for recycle. Each of the three liquid holdup tanks is sized to hold two-thirds of the reactor coolant liquid volume. The contents of one tank are passed through the liquid processing train while another tank is being filled. In analyzing the consequence of rupture of a holdup tank it is assumed that 100% of the contained noble gas activity is released. This activity is much less than that available for possible release from a waste gas decay tank due to approximately six hours holdup tank filling time during which activity decay occurs and due to the reactor coolant dilution during the letdown operation.

The waste gas decay tanks receive the radioactive gases from the liquids processed by the waste disposal system. The maximum storage of waste gases occurs after a refueling shutdown at which time the gas decay tanks store the radioactive gases stripped from the reactor coolant. The maximum noble gas activities calculated in the reactor coolant based on 1% fuel defects are approximately 90,000 equivalent curies of Xe-133. The maximum activity that can be stored in one tank is approximately 55,000 equivalent curies of Xe-133. The reduction occurs on account of the decay of short lived isotopes during the stripping operation.

Dose Evaluation

Offsite exposure is evaluated for noble gases release based on the model described in Section 14.3 including the effect of dilution in the wake of the containment building, a one m/sec wind velocity and the short term dispersion factor at the site boundary, i.e., $X/Q = 7.1 \times 10^{-4} \text{ sec/m}^3$. Assuming that the incident occurred immediately after a refueling shutdown following operation with 1% defective fuel, the off-site whole body dose would be less than 2 rem.

The iodine present in the vapors of the above tanks would be minimal. Based on an iodine removal factor of 10 in the mixed bed demineralizers the maximum iodine concentration in the liquid of the volume control tank or the liquid holdup tank would be less than 0.2 $\mu\text{c/cc}$ I-131 when operating with 1% defective fuel. An iodine partition factor on the order of 10^{-4} is expected between the liquid and vapor. The corresponding gaseous iodine release from a holdup tank, which is the largest of the above tanks, would be 2.5 millicuries I-131 which would result in a negligible thyroid dose. It is therefore concluded that an accidental waste gas release would present no hazard to the health and safety of the public.

TABLE 14.2.3-1
VOLUME CONTROL TANK NOBLE GAS ACTIVITY

<u>Isotope</u>	<u>Activity (curies)</u>
Kr-85	3
Kr-85m	60
Kr-87	24
Kr-88	107
Xe-133	12,200
Xe-135	280

The above activities are computed for the maximum possible vapor space (5.7 m^3) when operating with 1% fuel defects. The activity present in the liquid is negligible by comparison.

14.2.4 STEAM GENERATOR TUBE RUPTURE

The event examined is a complete tube break adjacent to the tube sheet, since a minor leak may not necessitate immediate action depending on the particular circumstances. If a tube breaks, reactor coolant would discharge into the secondary system. Since the reactor coolant is radioactive, methods of operation to limit uncontrolled condensate release have to be considered.

Once the reactor coolant system pressure is below the steam generator design pressure the faulty steam generator will be isolated by and the possibility of uncontrolled leakage removed.

The following sequence of events is initiated by a tube rupture:

1. Rapidly falling pressure and level in the pressurizer will initiate a safety injection signal, tripping the unit. The safety injection signal automatically terminates normal feedwater and initiates auxiliary feedwater. While not necessary for protection, there is sufficient capacity in the secondary system to contain in a controlled manner any leakage that might pass from the primary system to the secondary system, should no action be taken to isolate the leaks.
2. The steam generator liquid monitor and the air vacuum pump radiation monitor will alarm, indicating the passage of primary fluid into the secondary system. The air vacuum pump discharge is automatically diverted back to the plant vent within a few seconds.
3. The unit trip will automatically shut off steam flow through the turbine and will open steam bypass valves and bypass steam to the condenser.
4. In the unlikely event of concurrent loss of power, the loss of circulating water through the condenser would eventually result in loss of condenser vacuum and valves in the condenser bypass lines would automatically close to protect the condenser, thereby causing steam relief to be to atmosphere.

5. Cooldown procedures are followed which entail:
 - a) boration by the high head safety injection pumps.
 - b) regulating pressurizer level with spray or relief valves.
 - c) reducing safety injection flow in order to reduce reactor coolant pressure to several hundred psi subcooling.
 - d) condenser relief (if available) or atmospheric relief in order to reduce the reactor coolant temperature.
6. Isolation of the faulty steam generator is achieved by:
 - a) further reducing safety injection flow so as to drop the RCS pressure below 1100 psi (steam generator design pressure)
 - b) closing the steam line stop valve connected to the affected steam generator (determined by steam generator liquid sample activity monitor) and blocking the atmospheric relief
 - c) turning off the auxiliary feedwater flow to that steam generator
7. Ordinarily this would end the leakage during the interval while cooldown is continuing by steam bypass from the intact steam generators. Should the faulty steam generator's outlet valve not close, then the main steamline bypass valves would be closed and atmospheric relief from the intact steam generators would be used for plant cooldown.
8. After the residual heat removal system is in operation, the condensate accumulated in the secondary system can be examined. If the radioactivity level is in excess of that allowed, the condensate can be processed through the waste disposal system.

The faulty unit will be isolated by a steam line isolation valve once the reactor coolant pressure is reduced below 1100 psia. This can be accomplished in approximately 30 minutes and will terminate the mass flow into the secondary system and steam relief from the faulty steam generator.

With power available to the circulating water pumps the steam is bypassed to the condenser.

With concurrent loss of power a portion of the reactor coolant system activity is released to atmosphere in steam relief during the 30 minutes to isolate the faulty steam generator.

All of the noble gas activity contained in the portion of reactor coolant discharged into the steam generator during the 30 minutes to isolate is assumed released to atmosphere.

The iodine transferred into the steam generator is assumed to partition between the liquid and vapor phases of the steam generator and the portion contained in the steam relief is assumed released to atmosphere. A distribution factor of 4×10^{-3} curies/cm³ steam / curies/cm³ water (1) has been selected as being representative of the pH and pressure conditions within the steam generator.

During the 30 minute period to isolate the faulty steam generator 70,000 lbs of reactor coolant are discharged into the steam generator and 57,000 lbs of steam are relieved to atmosphere. Based on a reactor coolant system activity concentration corresponding to 1% defective fuel the noble gas activity release to atmosphere is 9,500 equivalent curies Xe-133. The corresponding iodine activity discharge into the steam generator is 78 curies equivalent I-131 of which 3.9 curies are released to atmosphere.

The resultant site boundary dose is less than 0.3 rem whole body and less than 2 rem to the thyroid using the two hour meteorological dispersion factor discussed in Section 14.3.5.

For reasons to be discussed later in this section, the multiple spontaneous occurrence of gross tube failures in a single incident is not considered credible. In order to perform a rigorous analysis of the flow dynamics of blowdown through multiple tube ruptures one must understand and define mathematically the physical configuration of the ruptures. Because no reasonable mechanism exists for the multiple ruptures, it is instead just as meaningful to analyze the consequences of a pipe rupture, equivalent in terms of discharge rate to various multiples of the single tube rupture discharge rate.

Such an analysis reveals that the core cooling system will prevent clad damage for break discharge rates equal to or smaller than that resulting from a broken pipe between 4 inches and 6 inches in diameter. The discharge rates which bracket the onset of clad damage correspond to 18 and 40 times the discharge from a single severed steam generator tube. Actually the ratio would be much larger owing to the fact that the discharge from a tube failure will be limited by the back pressure in the steam generator. Ultimately the tube discharge would terminate when the reactor coolant system and the steam generator reached pressure equilibrium. The operator can initiate cooldown through the unaffected steam generators.

The discharge rate required to lift a secondary safety valve is about 15 times the rate from a single severed tube.

These conclusions are based on single-failure mode performance of the core cooling system. Clad damage is prevented in those cases where the top of the core does not become uncovered.

The discharge rate required to cause the top of the core to become uncovered is 18 to 40 times the rate from a single severed tube.

The incredibility of multiple simultaneous tube failures is supported by the following reasoning:

1. At the maximum operating internal pressure the tube wall sees only about 1530 psi, compared with a calculated bursting pressure in excess of 11,100 psi based on ultimate strength at design temperature (factor of 7.3); and compared with a prefabrication test pressure of 7,000 psi (factor of 4.5).
2. The above margin applies to the longitudinal failure mode, induced by hoop stress. This failure mode is the least likely to cause propagation of failure tube-to-tube. An additional factor of two applies to ultimate pressure strength in the axial direction tending to resist double-ended failure (total factor of 14.6).
3. Failures induced by fretting, corrosion, erosion or fatigue, in addition to being rendered extremely improbable by design, are of such a nature as to produce tell-tale leakage in substantial quantity while ample metal remains to prevent severance of the tube (a small fraction of the original tube wall section, as indicated by the margin derived in 2). Thus it is virtually certain that any incipient failures that would develop to the point of severe leakage requiring a shutdown for repair would happen long before the large safety margin in pressure strength is lost.

REFERENCE

1. M. A. Styrikovich, O. I. Martynova, K. Ya. Katkovskaya, I. Ya. Dubrovskii, And I. N. Smirnova, "Transfer of Iodine from Aqueous Solutions to Saturated Vapor," Atomnaya Energiya, Vol. 17, No. 1, pp. 45-49, July 1964.

14.2.5 RUPTURE OF A STEAM PIPE

A rupture of a steam pipe is assumed to include any accident which results in an uncontrolled steam release from a steam generator. The release can occur due to a break in a pipe line or due to a valve malfunction. The steam release results in an initial increase in steam flow which decreases during the accident as the steam pressure falls. The energy removal from the Reactor Coolant System causes a reduction of coolant temperature and pressure. With a negative moderator temperature coefficient, the cooldown results in a reduction of core shutdown margin. If the most reactive control rod is assumed stuck in its fully withdrawn position, there is a possibility that the core will become critical and return to power even with the remaining control rods inserted. A return to power following a steam pipe rupture is a potential problem only because of the high hot channel factors which may exist when the most reactive rod is assumed stuck in its fully withdrawn position. Assuming the most pessimistic combination of circumstances which could lead to power generation following a steam line break, the core is ultimately shut down by the boric acid in the Safety Injection System.

The analysis of a steam pipe rupture is performed to demonstrate that:

- 1) With a stuck rod and minimum engineered safety features the core remains in place and essentially intact so as not to impair effective cooling of the core.
- 2) With no stuck rod and all equipment operating at design capacity, insignificant cladding rupture occurs.

Although DNB and possible clad perforation (no clad melting or zirconium - water reaction) following a steam pipe rupture are not necessarily unacceptable, the following analysis, in fact, shows that no DNB occurs for any rupture assuming the most reactive rod stuck in its fully withdrawn position.

The following systems provide the necessary protection against a steam pipe rupture:

- 1) Safety Injection System Actuation from any of the following*:
 - a. One out of three pressurizer coincident low pressure and low level signals.
 - b. Two out of three differential pressure signals between any steam line and the main steam header.
 - c. High steam flow in two out of three lines (one out of two per line) in coincidence with either low reactor coolant system average temperature (two out of three) or low steam line pressure (two out of three).
 - d. Two out of three high containment pressure signals.
- 2) The overpower reactor trips (nuclear flux and ΔT) and the reactor trip occurring upon actuation of the Safety Injection System.
- 3) Redundant isolation of the main feedwater lines. Sustained high feedwater flow would cause additional cooldown, thus, in addition to the normal control action which will close the main feedwater valves, any safety injection signal will rapidly close all feedwater control valves, trip the main feedwater pumps, and close the feedwater pump discharge valves.
- 4) Trip of the fast acting steam line stop valves (designed to close in less than 5 seconds with no flow) on:
 - a. High steam flow in two out of three lines (one out of two per line) in coincidence with either low reactor coolant system average temperature (two out of three) or low steam line pressure (two out of three).

* The details of the logic used to actuate Safety Injection are discussed in Section 7.

- b. Two out of three differential pressure signals between any steam line and the main steam header.
- c. Two out of three high containment pressure signals.

Each steam line has a fast closing stop valve and a check valve. These six valves prevent blowdown of more than one steam generator for any break location even if one valve fails to close. For example, for a break upstream of the stop valve in one line, closure of either the check valve in that line or the stop valves in the other lines will prevent blowdown of the other steam generators.

Steam flow is measured by monitoring dynamic head in nozzles inside the steam pipes. The nozzles (16.5" I.D. vs a pipe diameter of 23.8" I.D.) are located inside the containment near the steam generators and also serve to limit the maximum steam flow for any break further downstream. In particular, the nozzles limit the flow for all breaks outside the containment.

Method of Analysis

The analysis of the steam pipe rupture has been performed to determine:

- 1) The core heat flux and reactor coolant system temperature and pressure resulting from the cooldown following the steam line break. A full plant digital computer simulation has been used.
- 2) The thermal and hydraulic behavior of the core following a steam line break. A detailed thermal and hydraulic digital computer calculation has been used to determine if DNB occurs for the core conditions computed in (1) above. This calculation solves the continuity, momentum, and energy equations of fluid flow in the core and with the Macbeth critical heat flux correlation (see reference in paragraph 7 below) determines the margin to DNB.

The following assumptions were made:

- 1) A .0177 shutdown reactivity from the rods at no load conditions. This is the end of life design value including design margins with the most reactive rod stuck in its fully withdrawn position. The actual shutdown capability is expected to be significantly greater.
- 2) The negative moderator coefficient corresponding to the end of life core with all but the most reactive rod inserted. The variation of the coefficient with temperature and pressure has been included. The k versus temperature at 1000 psia corresponding to the negative moderator coefficient used is shown in Figure 14.2.5.1. In computing the power generation following a steam line break, the local reactivity feedback from the high neutron flux in the region of the core near the stuck control rod has been included in the overall reactivity balance. The local reactivity feedback is composed of doppler reactivity from the high fuel temperatures near the stuck control rod and moderator feedback from the high water enthalpy near the stuck rod. For the cases analyzed where steam generation occurs in the high flux regions of the core, the effect of void formation on the reactivity has also been included. The effect of power generation in the core on overall reactivity is shown in Figure 14.2.5-2. The curve assumes end of life core conditions with all rods in except the most reactive rod which is assumed stuck in its fully withdrawn position (completely removed from core).
- 3) Minimum safety injection capability corresponding to two out of three safety injection pumps in operation (only one pump is conservatively assumed to ~~assumed to~~ operate following a loss of outside power). 20,000 ppm boron is assumed in the Safety Injection System. The time delays required to sweep the low concentration boric acid from the safety injection piping prior to the delivery of the 20,000 ppm boron have been included in the analysis.

- 4) A steam generator heat transfer coefficient of 13100 BTU/sec°F. This is considered conservative since no allowance for reduction of the heat transfer UA as the water level falls into the tube region has been made. Furthermore, higher steam generator UA values will result in lower reactor coolant temperature at full power which in turn will result in an increase in the available shutdown margin at zero load.
- 5) Hot channel factors corresponding to one stuck rod -- the rod giving the highest factor at end of life. The hot channel factors account for the void existing local to the stuck rod at the pressure that occurs during the return to power phase following the steam break. This void in conjunction with the large negative moderator coefficient partially offsets the effect of the stuck rod. The hot channel factors depend upon the core temperature, pressure, and flow and, thus, are different for each case studied. The values used for each case are given in Table 14.2.5-1. The calculations used to obtain the hot channel factors again assume end of life core conditions with all rods in except the most reactive rod.
- 6) Five combinations of break sizes and initial plant conditions have been considered in determining the core power and Reactor Coolant System transient.
 - a) Complete severence of a pipe outside the containment, downstream of the steam flow measuring nozzle, initially at no load conditions with outside power available.
 - b) Complete severence of a pipe inside the containment at the outlet of the steam generator initially at no load conditions with outside power available.
 - c) Case (a) above with loss of outside power simultaneous with the steam break.

- d) Case (b) above with the loss of outside power simultaneous with the steam break.
- e) A break equivalent to a steam flow of 430 lbs/sec at 1000 psia from one steam generator with outside power available.

All the cases above assume initial hot shutdown conditions with the rods inserted (except for one stuck rod) at time zero. Should the reactor be just critical or operating at power at the time of a steam line break the reactor will be tripped by the normal overpower protection system when the power level reaches a trip point. Following a trip at power the reactor coolant system contains more stored energy than at no load, the average coolant temperature is higher than at no load and there is appreciable energy stored in the fuel. Thus, the additional stored energy is removed via the cooldown caused by the steam line break before the no load conditions of reactor coolant system temperature and shutdown margin assumed in the analyses are reached. After the additional stored energy has been removed, the cooldown and reactivity insertions proceed in the same manner as in the analysis which assume no load condition at time zero. However, since the initial steam generator mass is greatest at no load, the magnitude and duration of the reactor coolant system cooldown are less for steam line breaks occurring at power.

- 7) In determination of the critical flux at which burnout could occur for conditions, not covered by the W-3 correlation, the Macbeth correlation is used. This correlation is discussed in AEEW-R-267, dated August, 1963, "Burnout Analyses Part 4: Application of a Local Conditions Hypothesis to World Data for Uniformly Heated Round Tubes and Rectangular Channels", by R. V. Macbeth.
- 8) In computing the steam flow during a steam line break, the Moody Curve (Figure 3 of the article by F. S. Moody in Transaction of the ASME Journal of Heat Transfer, February 1965, page 134) for $\frac{SL}{D} = 0$ were used.

Results

The results presented are a conservative indication of the events which would occur assuming a steam line rupture. The worst case assumes that all of the following occur simultaneously.

- 1) Minimum shutdown reactivity margin of 1.77%.
- 2) The most negative moderator temperature coefficient for the rodged core at end of life.
- 3) The rod having the most reactivity stuck in its fully withdrawn position.
- 4) One safety injection pump or one safety injection valve fails to function as designed.

Core Power and Reactor Coolant System Transient

Figure 14.2.5-3 shows the Reactor Coolant System transient and core heat flux following a steam pipe rupture (complete severance of a pipe) outside the containment, downstream of the flow measuring nozzle at initial no load conditions. The break assumed is the largest break which can occur anywhere outside the containment either upstream or downstream of the isolation valves. Outside power is assumed available such that full reactor coolant flow exists. The transient shown assumes the rods inserted at time 0 (with one rod stuck in its fully withdrawn position) and steam release from only one steam generator. Should the core be critical at near zero power when the rupture occurs the initiation of safety injection by high differential pressure between any steam generator and the main steam header or by high steam flow signals in coincidence with either low reactor coolant system temperature or low steam line pressure will trip the reactor. Steam release from at least two steam generators will be prevented by either the check valves or by automatic trip of the fast acting stop valves in the steam lines by the high steam flow signals in coincidence with either low reactor coolant system temperature or low steam line pressure. Even with the failure of one valve,

release is limited to no more than 5 seconds for two steam generators while the third generator blows down. (The steam line stop valves are designed to be fully closed in less than 5 seconds with no flow through them. With the high flow existing during a steam line rupture, the valves will close considerably faster).

As shown in Figure 14.2.5-3, the core becomes critical with the rods inserted (with the design shutdown assuming one stuck rod) at 24 seconds. Boron solution at 20,000 ppm enters the Reactor Coolant System from the Safety Injection System at 60 seconds with a delay of 14 seconds required to clear the Safety Injection System lines of low concentration boric acid. The 14 seconds delay is taken from the time at which the system pressure has fallen to 1250 psia and in the delay for sweeping the Safety Injection System of low concentration boric acid if the system pressure were constant at 1000 psia. Since the pressure is less than 1000 psia during most of the 14 seconds and since the shutoff head of the safety injection pumps is 1500 psia, the 14 seconds is somewhat conservative.

The computer calculation used assumes the boric acid is mixed with and diluted by the water flowing in the reactor coolant system prior to entering the reactor core. The concentration after mixing depends upon the relative flow rates in the Reactor Coolant System and in the Safety Injection System. The variation of mass flow rate in the Reactor Coolant System due to water density changes is included in the calculation as is the variation of flow rate in the Safety Injection System due to changes in the Reactor Coolant System pressure. The Safety Injection System flow calculation includes the line losses in the system as well as the pump head curve.

No credit has been taken for the 2,000 ppm boron which enters the Reactor Coolant System prior to the 20,000 ppm boric acid. The peak core average heat flux for this case is 11% of the value at 2200 MWt.

Figure 14.2.5-4 shows the case of a steam line rupture at the exit of a steam generator at no load. The sequence of events is similar to that described above for the rupture outside the containment except power generation occurs. The peak core average heat flux is 38% of the value at 2200 MWt.

Figures 14.2.5-5 and 14.2.5-6 show the responses for the previous breaks except a loss of outside power is assumed at time 0, which then results in a Reactor Coolant System flow coastdown. The safety injection system delay time includes the time required to start safety injection pumps on the diesels. Only one safety injection pump is assumed in Figures 14.2.5-5 and 14.2.5-6. In both these two cases there is a return to power and the peak powers are 15% and 24% respectively.

Figure 14.2.5-7 shows the transient following a break equivalent to a steam flow of 430 lbs/sec. at 1000 psia with steam release from one steam generator. The assumed steam release is larger than or equal to the capacity of any single dump or safety valve. In this case safety injection is initiated automatically by low pressurizer pressure and level at 121 seconds. Boron solution at 20,000 ppm enters the Reactor Coolant System at 161 seconds. For the transient, there is no return to criticality. After 161 seconds the 20,000 ppm boron provides sufficient negative reactivity to keep the reactor shut down and well below criticality while the steam generator empties and causes further cooldown. The cooldown for the case shown in Figure 14.2.5-7 is more rapid than the case of steam release from all steam generators through one dump or safety valve. The transient is quite conservative with respect to cooldown, since no credit is taken for the energy stored in the system metal or the energy stored in the other steam generators. Since the transient occurs over a period of ~ two minutes, the neglected stored energy is likely to have a significant effect in slowing the cooldown.

It should be noted that following a steam line break only one steam generator blows down completely. Thus, two steam generators are still available for dissipation of decay heat at times after the steam break transient is over and the steam relief valves have been sized to cover this condition.

Margin to Critical Heat Flux

Using the transients of Figures 14.2.5-4 and 14.2.5-6 with breaks assumed inside the containment for reference plant parameters, the Macbeth critical heat flux correlation was used to determine the margin to burn-out. The power and flow conditions were used with various core pressures and core inlet temperatures bracketing the values shown in Figures 14.2.5-4, and 14.2.5-6. The hot channel factors for each case are listed in Table 14.2.5-1. The analyses showed that the heat flux remains below the critical value in all cases. The minimum DNBR was greater than 1.9 in all the analyses. The lowest value occurred for the break inside the containment with outside power available assuming an inlet temperature of 420°F and a reactor coolant pressure of 1000 psia. The breaks outside the containment result in lower core heat fluxes than those inside the containment and, thus, also do not cause DNB anywhere in the core.

Containment Integrity Evaluation

For the break inside the containment at the exit of a steam generator, the total mass and energy release to the containment have been conservatively computed as 187,500 lbs, and 166.5×10^6 Btu, respectively. Assuming an instantaneous release to the containment and no credit for containment safeguards, the containment pressure has been calculated to be 30 psig compared to the containment design value of 42 psig.

Conclusions

Although DNB and possible clad perforation (no clad melting or zirconium - water reaction) following a steam pipe rupture are not necessarily unacceptable, the above analysis, in fact, shows that no DNB occurs for any rupture assuming the most reactive rod stuck in its full withdrawn position.

TABLE 14.2.5-1

Nuclear Hot Channel Factors Used in Steam Break Analyses. Values assume the End of Life Rodded with One Stuck Rod

Case	Nuclear	
	$F_{\Delta h}$	F_z
Figure 14.2.5-3, Outside Containment Break, Outside Power Available	8.1	2.45
Figure 14.2.5-4, Inside Containment Break, Outside Power Available	5.2	1.91
Figure 14.2.5-5, Outside Containment Break, Loss of Outside Power	Not computed since average power is considerably less than the case of Figure 14.2.5-6	
Figure 14.2.5-6, Inside Containment Break, Loss of Outside Power	2.85	2.22

VARIATION OF REACTIVITY WITH CORE TEMPERATURE
AT 1000 PSIA FOR THE END OF LIFE RODDED CORE
WITH ONE ROD STUCK
(ASSUMES 0 POWER)

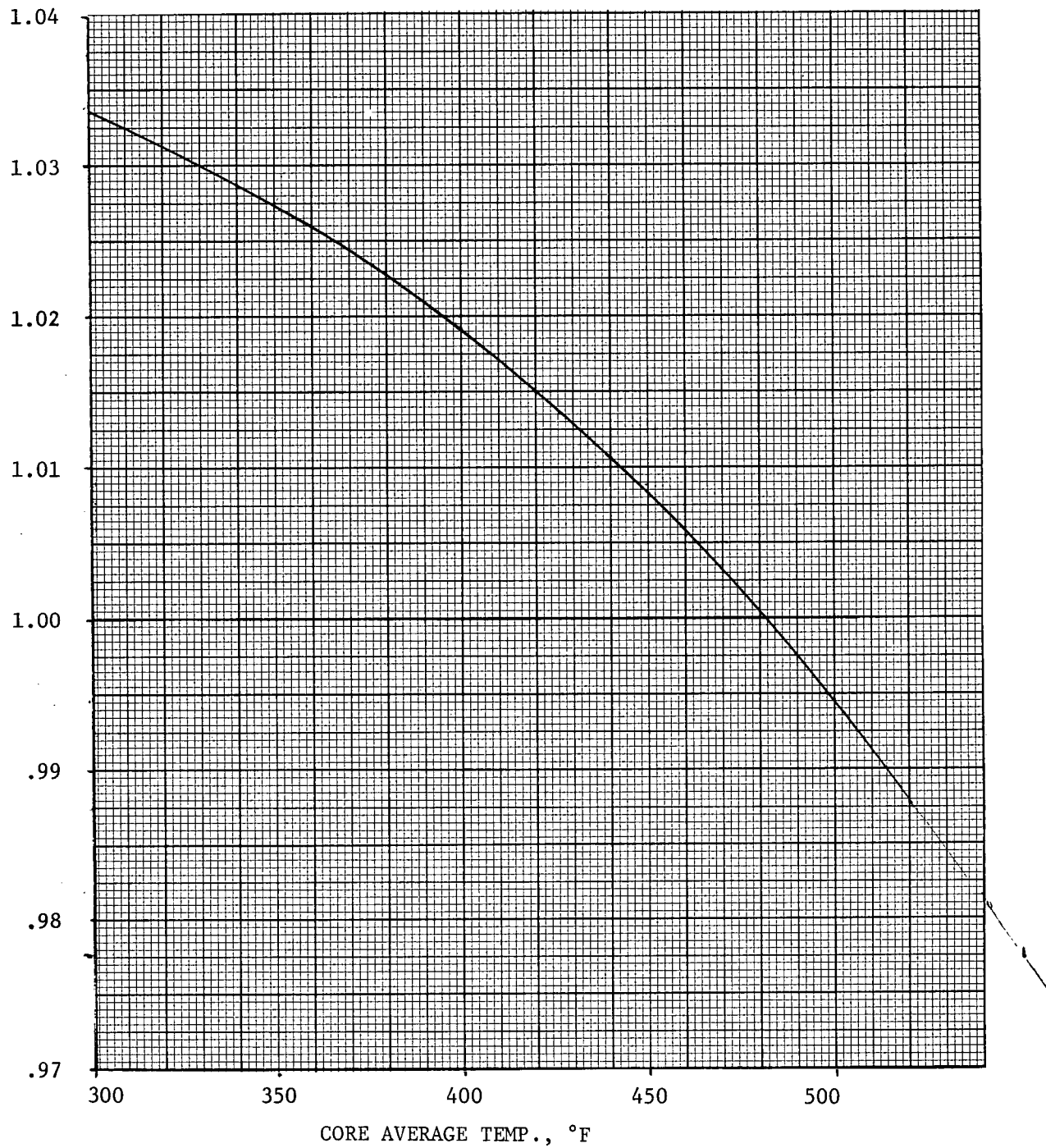


Figure 14.2.5-1

VARIATION OF REACTIVITY WITH POWER AT CONSTANT
CORE AVERAGE TEMPERATURE. VALUES INDICATED
WERE USED IN STEAM PIPE RUPTURE ANALYSES
FOR THE END OF LIFE RODDED CORE WITH ONE
ROD STUCK

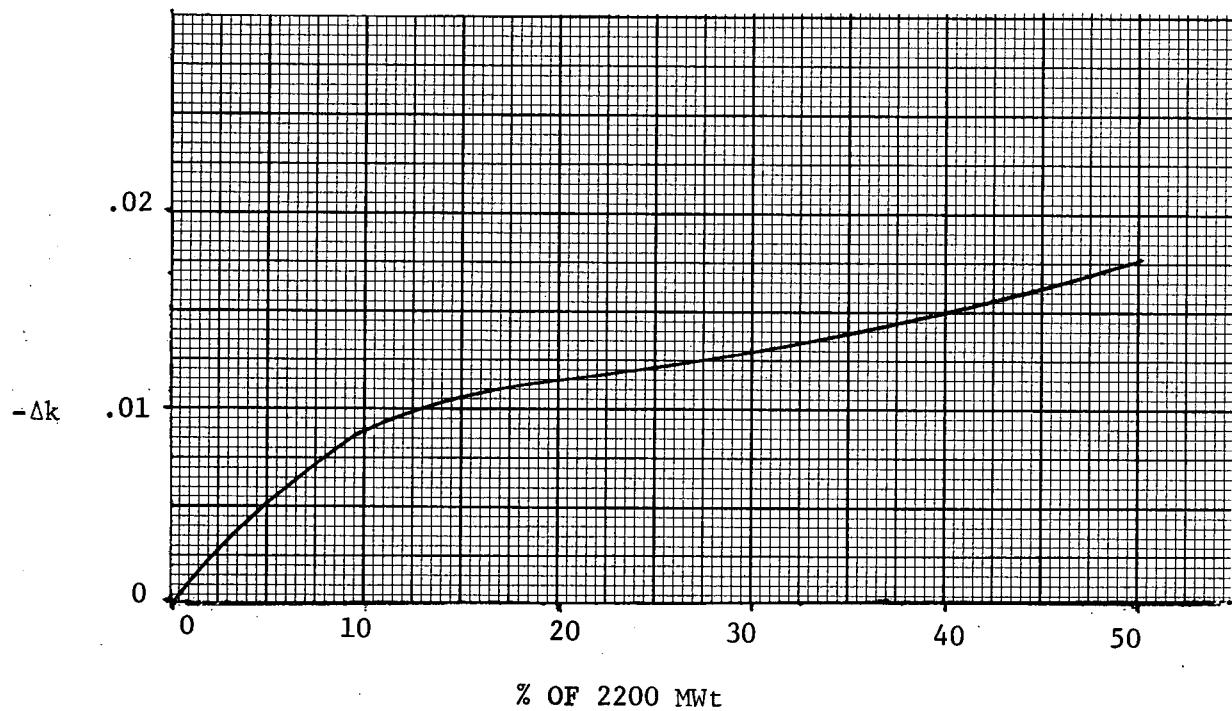


Figure 14.2.5-2

STEAM LINE BREAK DOWNSTREAM OF FLOW MEASURING
NOZZLE WITH SAFETY INJECTION, OUTSIDE POWER AVAILABLE

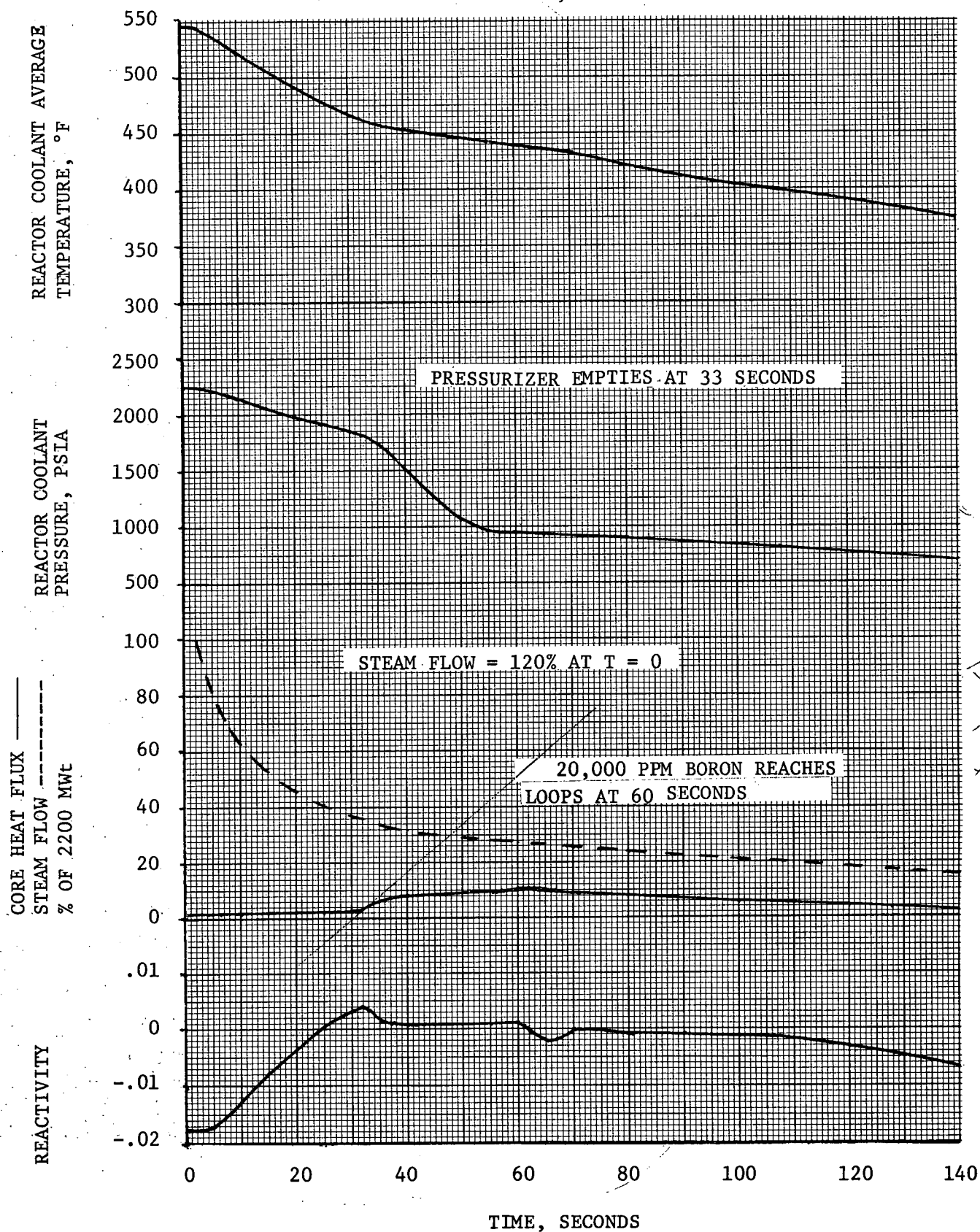


FIGURE 14.2.5-3

STEAM LINE BREAK AT EXIT OF STEAM
GENERATOR WITH SAFETY INJECTION, OUTSIDE POWER
AVAILABLE

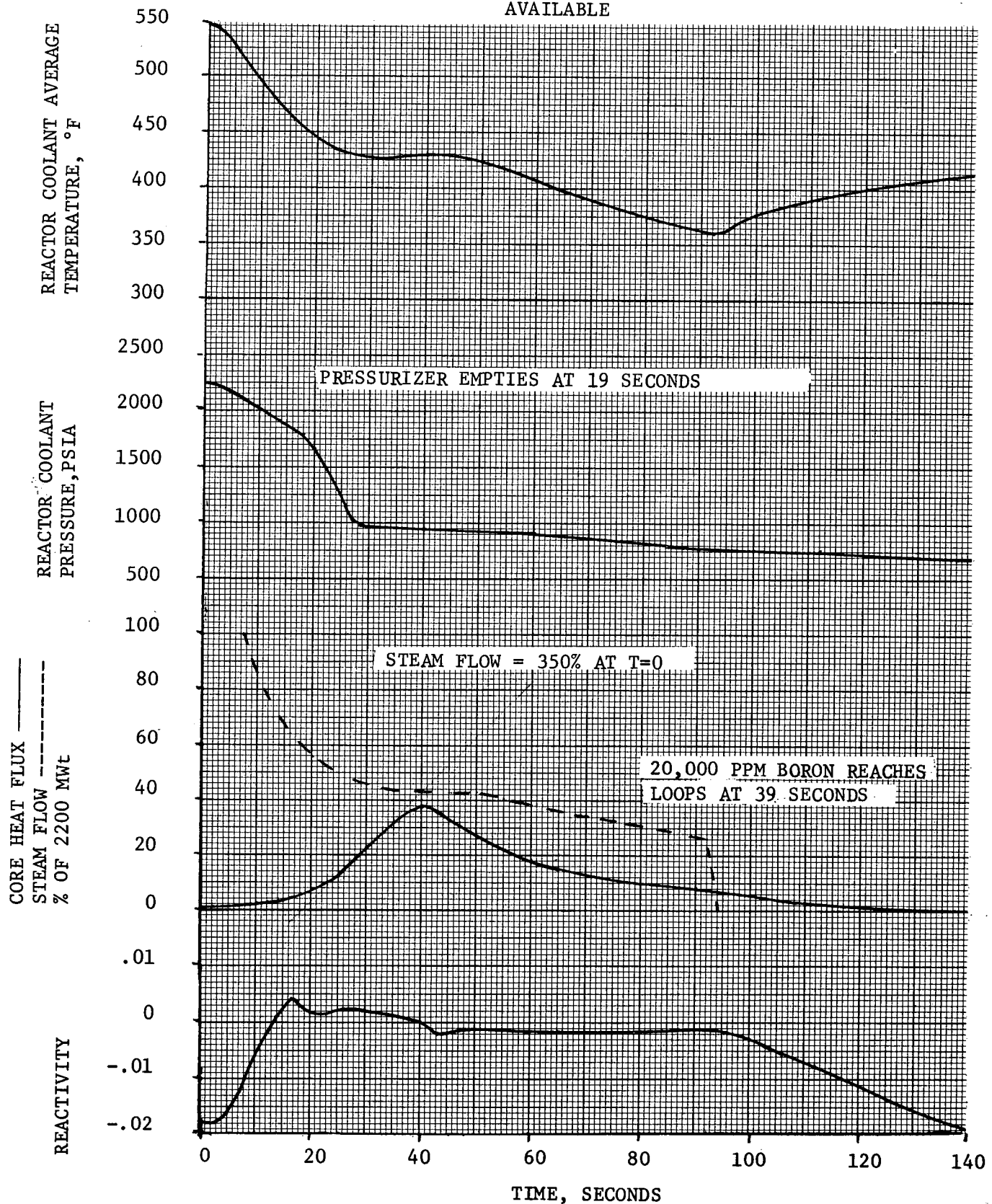


FIGURE 14.2.5-4

STEAM LINE BREAK DOWNSTREAM OF FLOW
MEASURING NOZZLE WITH SAFETY INJECTION, LOSS OF OUTSIDE POWER

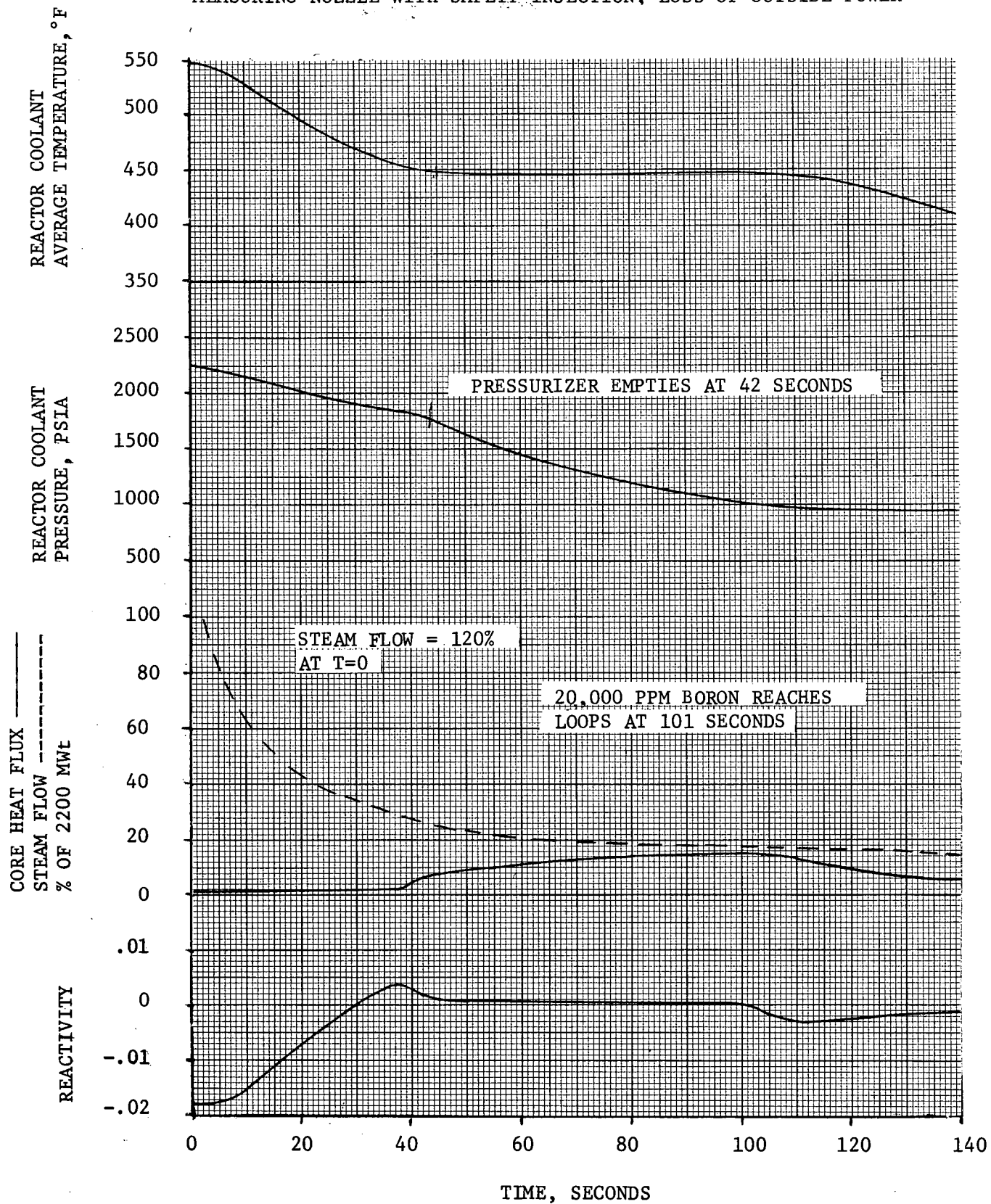


FIGURE 14.2.5-5

STEAM LINE BREAK AT EXIT OF STEAM GENERATOR
WITH SAFETY INJECTION, LOSS OF OUTSIDE POWER

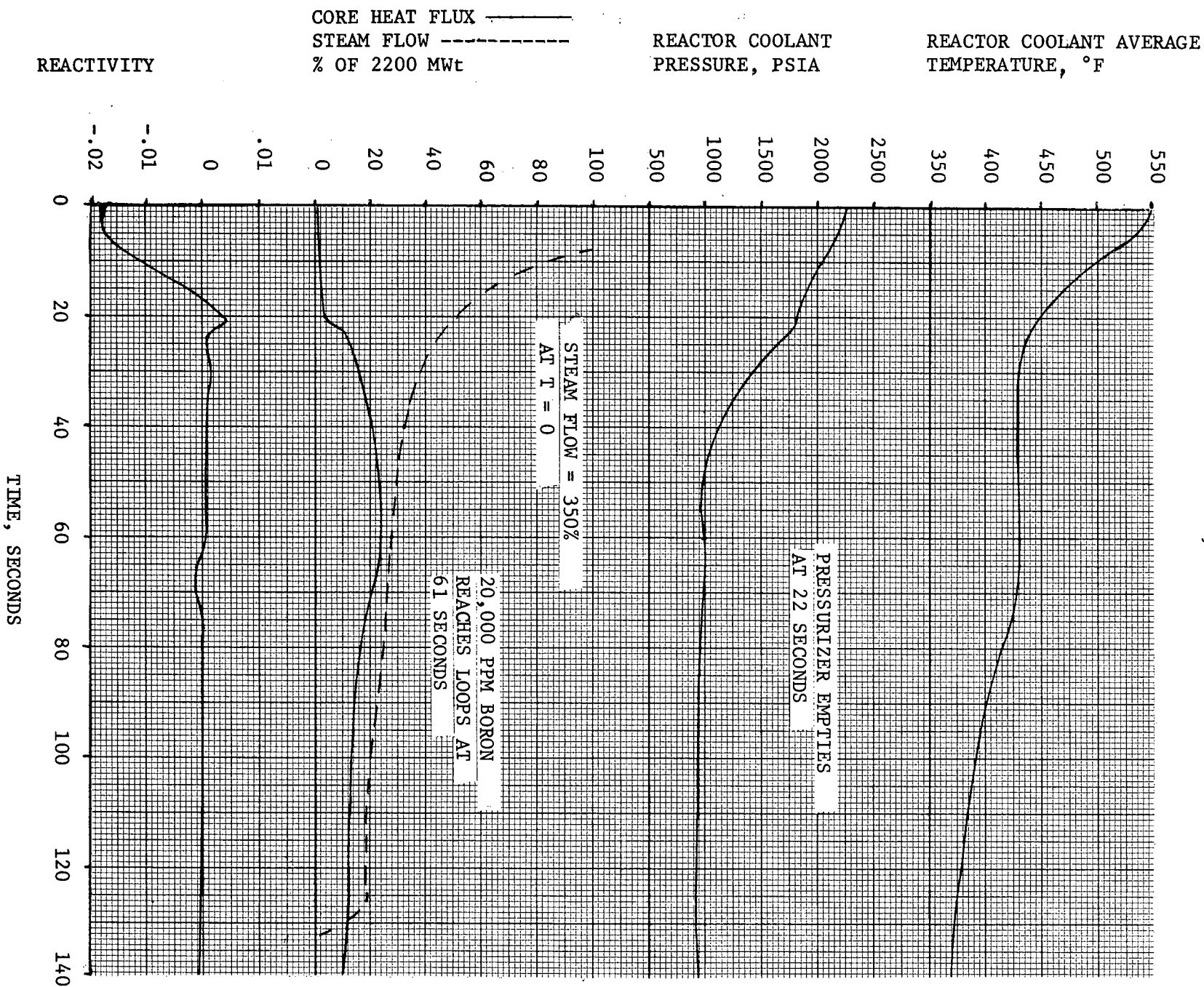


FIGURE 14.2.5-6

STEAM LINE BREAK EQUIVALENT TO 430 LBS/SEC
AT 1000 PSIA, OUTSIDE POWER AVAILABLE

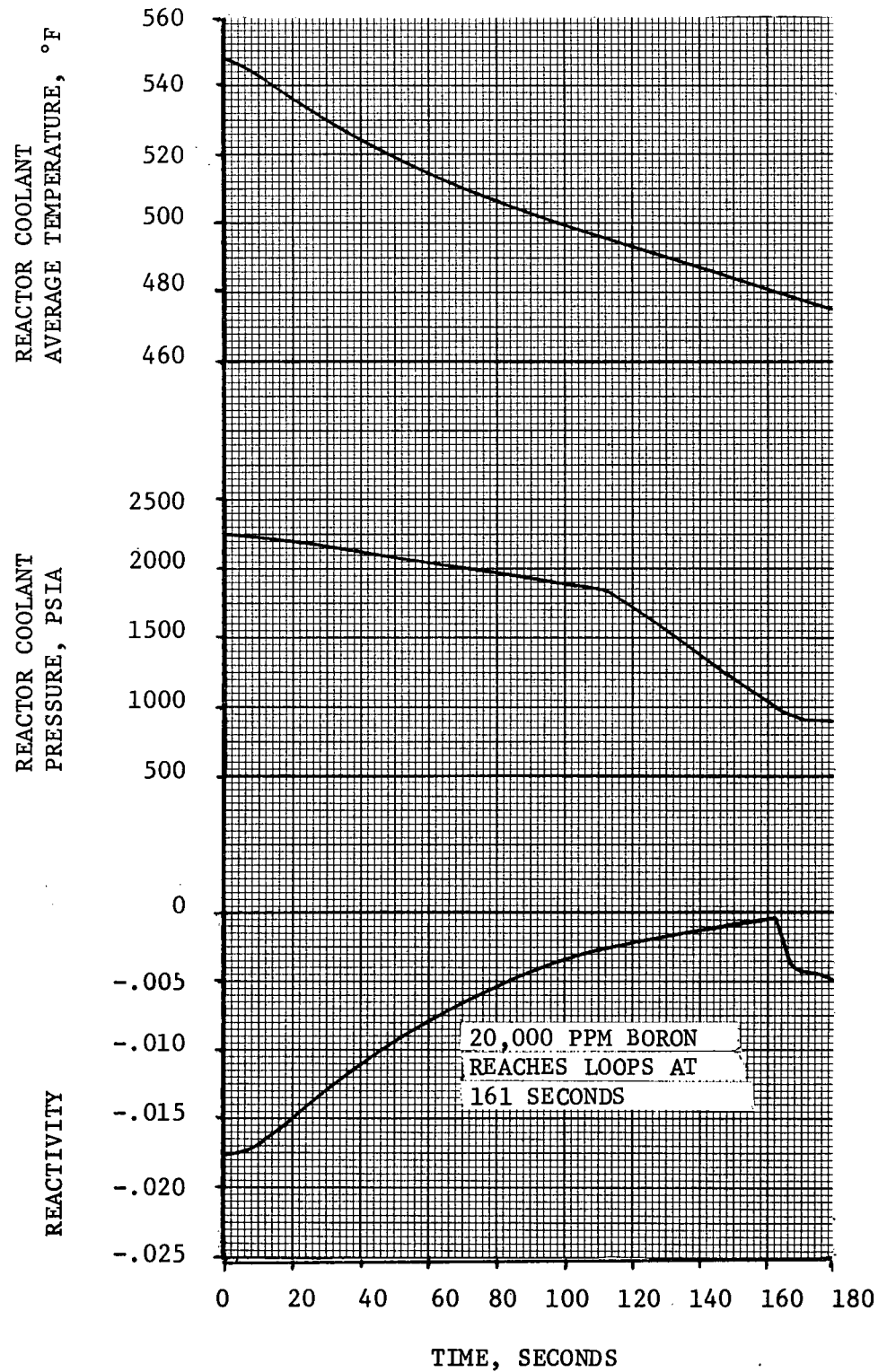


FIGURE 14.2.5-7

SCHEMATIC SHOWING THE LOCATION OF THE STEAM LINE STOP VALVES, CHECK VALVES, AND FLOW MEASURING NOZZLES

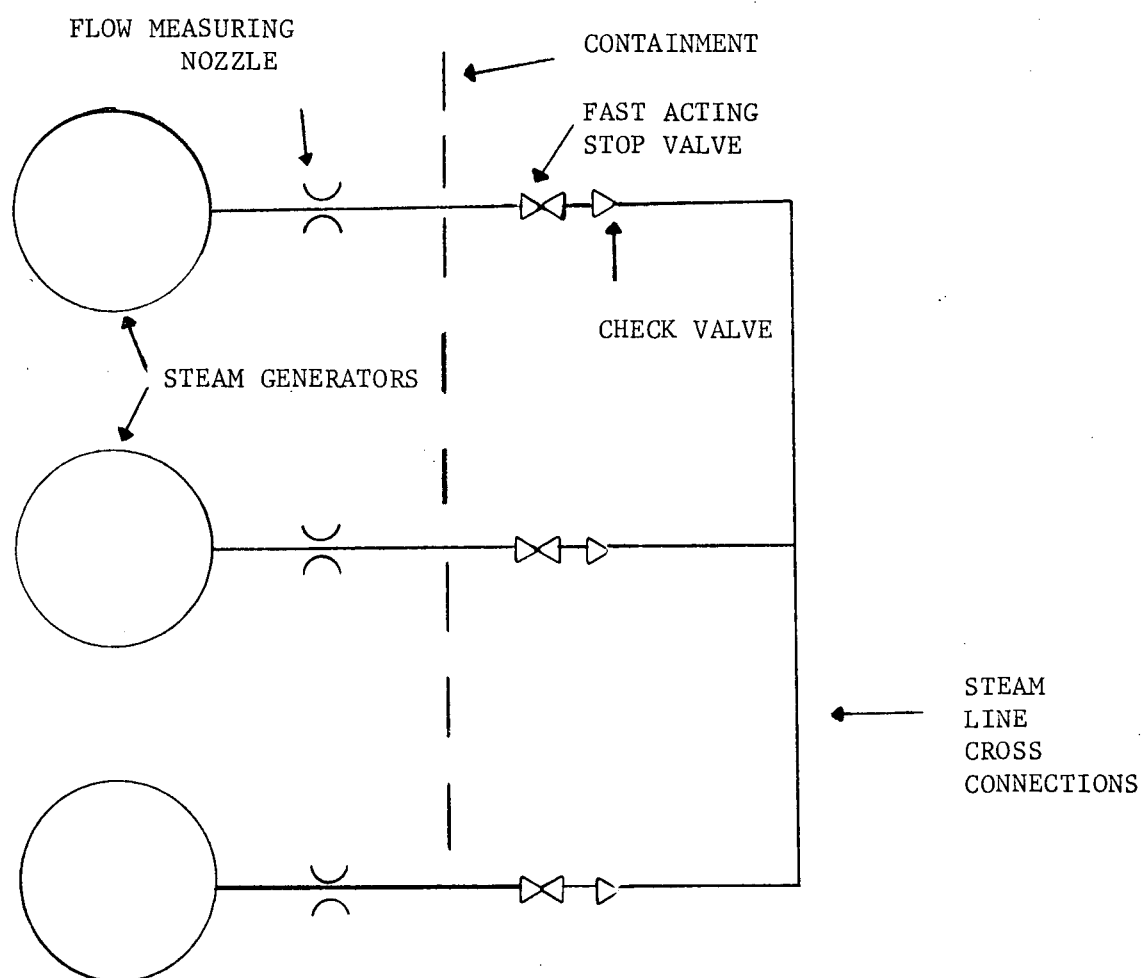


FIGURE 14.2.5-8

14.2.6 RUPTURE OF A CONTROL ROD MECHANISM HOUSING-RCCA EJECTION

In order for this accident to occur, a rupture of the control rod mechanism housing must be postulated creating a full system pressure differential acting on the drive shaft. The resultant core thermal power excursion is limited by the Doppler reactivity effect of the increased fuel temperature and terminated by reactor trip actuated by high nuclear power signals.

A failure of a control rod mechanism housing sufficient to allow a control rod to be rapidly ejected from the core is not considered credible for the following reasons:

- a) Each control rod drive mechanism housing is completely assembled and shop-tested at 4100 psi.
- b) The mechanism housings will be individually hydrotested to 3105 psig as they are installed on the reactor vessel head to the head adapters, and checked during the hydrotest of the completed Reactor Coolant System.
- c) Stress levels in the mechanism are not affected by system transients at power, or by thermal movement of the coolant loops. Moments induced by the design earthquake can be accepted within the allowable primary working stress range specified by the ASME code, Section III, for Class A components.
- d) The latch mechanism housing and rod travel housing are each a single length of forged type-304 stainless steel. This material exhibits excellent notch toughness at all temperatures that will be encountered.

The joints between the latch mechanism and the head adapter and between the latch mechanism and the rod travel housing are threaded joints, reinforced using canopy type seal welds.

The operation of a chemical shim plant is such that the severity of an ejection accident is inherently limited. Since control rod clusters are used to control load variations only and core depletion is followed with boron dilution, there are only a few rods in the core at full power. Proper positioning of these rods is monitored by a control room alarm system. There are low and low low level insertion monitors with visual and audio signals. Operating instructions require boration at the low level alarm and emergency boration at the low low alarm. The control rod position monitoring and alarm systems are described in detail in Section 7.3 and in Reference 1. For all cases, utilizing the flexibility in being able to select the control rod cluster groupings, radial locations and positions as a function of load, the design minimized the peak fuel and clad temperatures. It is shown that in no case does clad melting occur.

This section describes the models used and the results obtained. Only the initial few seconds of the power transient are discussed, since the long term considerations are the same as for a loss of coolant accident.

Method of Analysis

The calculation of the transient is performed in two stages, first an average core calculation and then a hot region calculation. The average core is analyzed to determine the average power generation with time including the various total core feedback effects, i.e., Doppler reactivity and moderator density reactivity. Enthalpy and temperature transients in the hot spot are

determined by adding a multiple of the average core energy generation to the hotter rods and performing a transient heat-transfer calculation. The asymptotic power distribution calculated without feedback is pessimistically assumed to persist throughout the transient.

Average Core

The nuclear power transients are calculated using the CHIC-KIN code developed by the Bettis Atomic Power Laboratory for similar analyses.⁽²⁾ This code solves the point kinetics equations, with feedback from an axially and radially segmented fuel element. CHIC-KIN results have been compared with SPERT results for two dissimilar cores over a wide range of periods with good agreement.

The largest temperature rises, and hence the largest reactivity feedbacks occur in channels where the power is higher than average. Since the weight of a region is dependent on flux, these regions also have high weights. This means that the reactor feedback is larger than that indicated by a simple single channel analysis. Physics calculations have been carried out for temperature changes with a flat temperature distribution, and with a large number of axial and radial temperature distributions. Reactivity changes were compared and effective weighting factors determined. These weighting factors take the form of multipliers which when applied to single channel feedbacks correct them to effective whole core feedbacks for the appropriate flux shape. The values used in the analyses are listed in Table 14.2.6-2. For this study, six delayed neutron groups were used and the fuel rod was divided into eight radial increments, with a ninth increment for the clad. Five axial segments were employed. The calculation is essentially a single analysis representing the core average conditions.

Prompt heat generation directly in the coolant is assumed to be 2.6 percent of the nuclear power generation. This number is based on LEOPARD calculations.⁽³⁾ Heat generation in the fuel pellet is assumed to occur non-uniformly radially with a slight reduction in the center due to self-shielding effects.

Hot Region

The average core energy addition calculated as described above is multiplied by the appropriate hot channel factors and the worst cases analyzed using a detailed heat transfer code. The zirconium water reaction is explicitly represented and all material properties are represented as functions of temperature. The Tong, Sandberg and Bishop correlation (as described in Section 3.2.2) is used to determine the film boiling heat transfer coefficient after DNB. The resulting coefficient is reduced by 30% to allow for scatter in the basic data used to derive the correlation. (This corresponds to three standard deviations.)

The energy levels assumed for fuel melting are given in Table 14.2.6-1.

Selection of Input Parameters

Input parameters for the analyses were conservatively selected on the basis of calculated values and a parameter study.⁽⁴⁾ The more important parameters are discussed below, and the values used given in Table 14.2.6-2.

Ejected rod worth

Basic values for the ejected rod worths were calculated using PDQ 7. Since this is a two dimensional code it was not possible to take account of the part length rods directly. For a given ejected rod, the worth was calculated first assuming part length rods and then with no part length rods.

The overall ejected rod worth was then assumed to be the linear average of the two values. This introduces pessimism into the analysis since the part length rod region is only one fourth of the core length and does not hold 50% of the axial reactivity weight. Also the worst ejected rod is not always fully inserted, and may not even overlap the part length bank. A 20% margin is added to the ejected rod worth in order to account for possible azimuthal flux tilts.

Delayed neutron fraction β

No margin was subtracted from the calculated value of β , since margin had already been inserted into the reactivity calculation via the ejected rod worth. The values used are 0.69% ΔK at the beginning of life, and 0.52% ΔK at the end of first cycle operation.

Hot Channel Factor

In all cases the radial hot channel factor was higher in the part length region. The value used in the analyses was determined using PDQ 7, and taking no credit for the flux flattening effects of reactivity feedback.

The axial hot channel factor is highest when the part length rods are moved far away from the flux peak. However, this in general results in the minimum ejected rod worth. Also, the axial and radial peaks are not coincident under these conditions. Analyses indicate that the worst hot spot transient occurs when the part length rods are located in the peak. Axial hot channel factors were calculated with the part length rods in the middle of the core. This results in a conservatively high flux peaking, since to be consistent with the assumed ejected rod worth, the rods should be located in the flux peak.

The total transient hot channel factor F_q was obtained by multiplying the axial and radial hot channel factors. A further margin of 20% was added to account for possible aximuthal flux tilts.

Reactivity Weighting Factor

The reactivity weighting factor was reduced by 10% to allow for errors in the weighting calculation and a further 10% to allow for errors in the basic reactivity temperature coefficient calculations. This factor was applied to both the Doppler and moderator density feedbacks.

Moderator Temperature Coefficient

For conservatism, the core reactivity was assumed to be independent of moderator temperature, at the beginning of core life, even though the coefficient is always negative. At the end of life, the calculated reactivity versus density curves were reduced by 10% of the value at operating density. This was in addition to the two 10% margins in the weighting factor.

Heat Transfer Data

For the average core it is conservative to assume a high gap conductance and fuel thermal conductivity at the beginning of core life, when the moderator coefficient is assumed to be zero. A value of 2.65 Btu/hr ft °f was assumed for the fuel conductivity and 10,000 Btu/hr ft² °F for the gap conductance. At the end of life a given quantity of heat produces more feedback in the moderator than in the fuel, and it is therefore conservative to assume a low gap conductance and fuel thermal conductivity. Values of 750 Btu/hr ft² °F and 2.2 Btu/hr ft °F respectively were assumed.

The code used to determine the hot spot transient contains standard curves of thermal conductivity versus fuel temperature. This facility was used in the analyses. In order to obtain pessimistically high initial fuel temperatures, a low initial gap conductance of 750 Btu/hr ft² °F was used in most cases. For the high power cases, the value was adjusted to yield the same center fuel temperature as that derived in the detailed thermal hydraulics calculations. During a transient the gap conductance can be expected to rise. For the possible range of gap conductances, the peak center fuel temperature is independent of the gap conductance during the transient. The cladding temperature is however strongly dependent on the gap conductance and is highest for high gap conductances. For conservatism a high value of 10,000 Btu/hr ft² °F has been used during transients. This value corresponds to a negligible gap resistance and a further increase would have essentially no effect on the rate of heat transfer.

Coolant Mass Flow Rates

When the core is operating at full power, all three coolant pumps will always be operating. However, for zero power conditions, the system may be operating with one pump. The principal effect of operating at reduced flow is to reduce the film boiling heat transfer coefficient. This results in higher peak cladding temperatures, but does not affect the peak center fuel temperature. Reduced flow also lowers the critical heat flux. However, since DNB is always assumed at the hot spot, and since the heat flux rises very rapidly during the transient, this produces only second order changes in the cladding and center fuel temperatures. All zero power analyses for both average core and the hot spot have been conducted assuming single loop operation.

Trip Reactivity Insertion

The rods were assumed to be released 0.5 seconds after the initiation of ejection. The delay is constituted of 0.2 seconds for the instrumentation to produce a signal, 0.15 seconds for the trip breaker to open and 0.15 seconds for coil release. In calculating the shape of the insertion versus time curve all the rods are assumed to be dropping as a single bank from the fully withdrawn position. This means that the initial movement is through the low worth region at the extreme top of the core, and produces a pessimistically slow reactivity insertion versus time curve.

The scram reactivity insertion is based on calculated rod worths with a 10% margin. The stuck and ejected rods together are assumed to reduce the final rod holding by twice the calculated stuck rod worth.

Lattice Deformations

Reactivity insertion as a result of lattice deformation was considered. In the region of the hot spot there will be a large power gradient. Since the fuel rods are free to move in a vertical direction, differential expansion between separate rods cannot produce distortion. However, the temperature gradients across individual rods may produce a force tending to bow the midpoint of the rods toward the hot spot. Physics calculations indicate that the net result of this would be a negative reactivity insertion. In practice, no significant bowing is anticipated, since the structural rigidity of the core is more than sufficient to withstand the forces produced.

Boiling in the hot spot region will produce a net fluid flow away from that region. However, the fuel heat is released to the water relatively slowly, and it is considered inconceivable that cross flow will be sufficient to produce significant lattice forces. Even if massive and rapid boiling, sufficient to distort the lattice, is hypothetically postulated, the large void fraction in the hot spot region would produce a reduction in the total core moderator to fuel ratio, and a large reduction in this ratio at the hot spot. The net effect would therefore be a negative feedback. It is concluded that no conceivable mechanism exists for a net positive feedback resulting from lattice deformation. In fact, a small negative feedback may result. The effect is pessimistically ignored in the following analyses.

Cases Considered

In all cases the worst ejected rod in terms of both rod worth and hot channel factors is a control bank rod, and so no separate analyses are presented for the ejection of shim or part length rods.

Results

Beginning of Life; Full Power

The rod program limits the control bank holding to 0.5% ΔK for this condition. The reactor is sub-prompt critical with the worst ejected rod worth of 0.22% ΔK . The peak power reached is 1.42 times full power and the peak hot spot clad and center fuel temperatures are respectively 2220°F and 4850°F. The results are shown in Figures 14.2.6-1 through 14.2.6-3.

Beginning of Life; Zero Power

For this condition there will be one control bank fully inserted and a second bank almost fully inserted. Only one pump has been assumed to be operating. The worst ejected rod worth of 0.71% ΔK results in the core becoming prompt critical. The peak hot spot cladding and center fuel temperatures are respectively 1360°F and 1710°F. The results are shown in Figures 14.2.6-4 through 14.2.6-6.

End of Life; Full Power

The rod program limits the control bank holding to 0.3% ΔK . The worst ejected rod worth is 0.092% ΔK . The peak power reached is 1.20 times normal full power. Peak cladding and center fuel temperatures are respectively 1930°F and 4620°F. The results are shown in Figures 14.2.6-3, 14.2.6-7, and 14.2.6-8.

End of Life; Zero Power

For this condition two control banks are fully inserted, and a third bank partially inserted. Assuming that only one main coolant pump is running, the worst ejected rod worth of 0.84% ΔK will result in hot spot peak cladding and fuel temperatures of respectively 2120°F and 2900°F. The results are shown in Figures 14.2.6-6 and 14.2.6-9, and 14.2.6-10.

Fission Product Release

It is assumed that fission products are released from the gaps of all rods entering DNB. In all cases considered less than 15% of the rods entered DNB. (This corresponds to 2% of the core volume.) The position with regard to fission product release is therefore much better than for the double ended coolant pipe break, the maximum hypothetical accident, for which over 70% of the rods are assumed to release fission products.

Pressure Surge

It is shown that there is no danger of fuel dispersal into the coolant. The pressure surge may therefore be calculated on the basis of conventional heat transfer from the fuel and prompt heat generation in the coolant. The most severe excess addition of energy to the coolant occurs for the high power end of life case. In order to estimate the magnitude of this pressure transient, average channel and hot spot heat transfer calculations were performed using a high gap conductance and without assuming DNB. The power curves used for these calculations represented a limiting case which initiated center melting at the hot spot. Using these heat flux data, a THINC 3 run was conducted to determine the volume surge without the benefit of pressure feedback. This volume surge was subsequently used as the basis for a pressure calculation. The results indicated that starting at 2250 psi a peak pressure of about 2340 psi occurs some 1.5 seconds after rod ejection.

Conclusions

Even on the most pessimistic basis, the analyses indicated no clad melting. It was concluded that there was no danger of sudden fuel dispersal into the coolant. The pressure surge was shown to be insufficient even to lift relief valves and it was concluded that there was no danger of consequential damage to the primary circuit. The amount of fission products released as a result of clad rupture during DNB is considerably less than in the case of the double ended main coolant pipe break.

REFERENCES

1. "Power Distribution Control of Westinghouse PWR's," WCAP-7208 (1968).
2. Redfield, J. A., "CHIC-KIN -- A Fortran Program for Intermediate and Fast Transients in a Water Moderated Reactor," WAPD-TM-479, January, 1965.
3. Barry, R. F., "The Revised LEOPARD Code - A Spectrum Dependent Non-Spatial Depletion Program," WCAP-2759 (1965).
4. Rod Ejection Section of Rochester Gas and Electric Final Safety Report.
5. Conway and Hein, Journal of Nuclear Materials (15.1), 1965.
6. Ogard & Leary, "High Temperature Heat Content and Heat Capacity of Uranium Dioxide - Plutonium Dioxide Solid Solutions," LA-DC-8620.

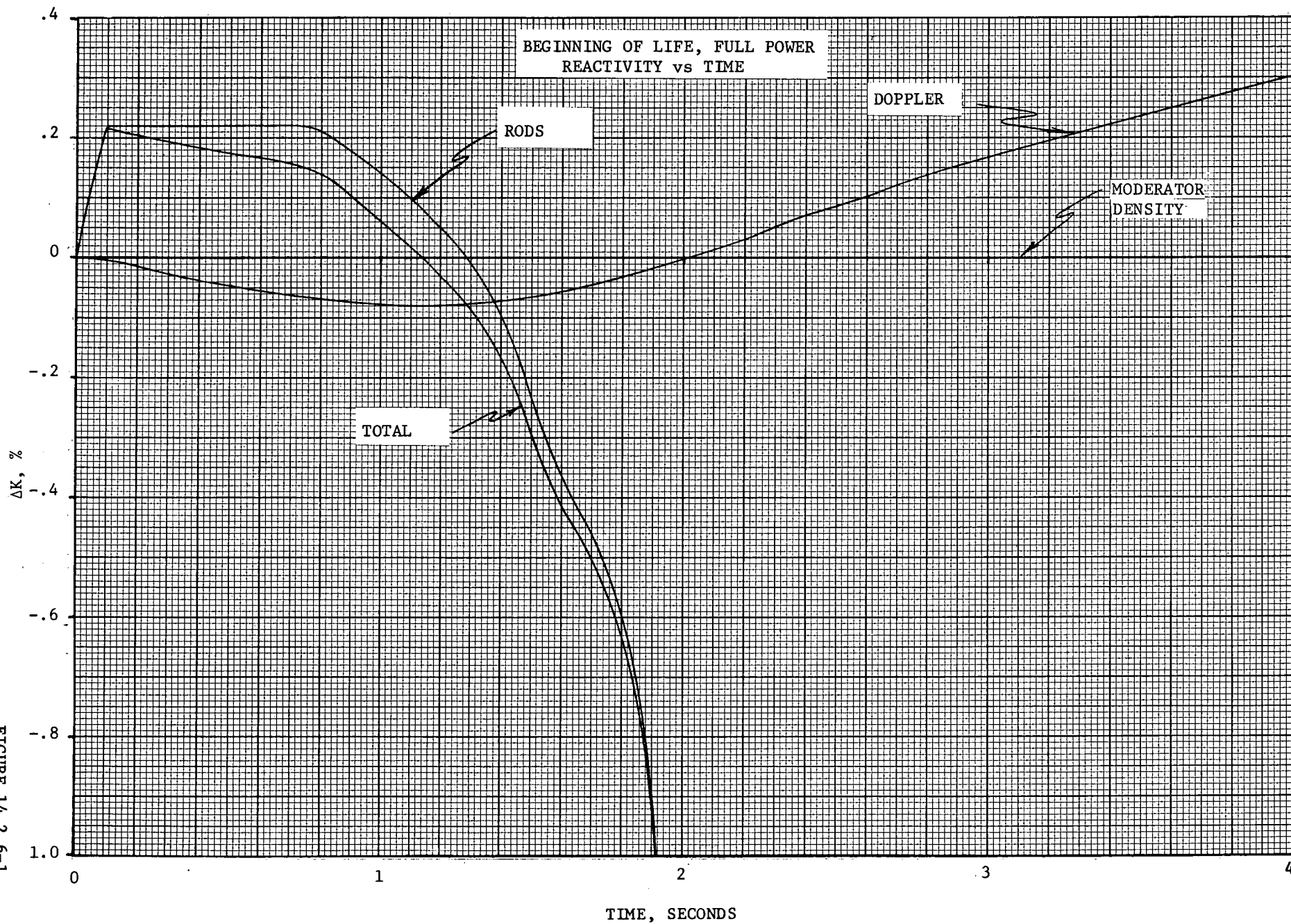
TABLE 14.2.6-1

 UO_2 PROPERTIES^(5,6)

	Beginning of Life Enthalpy <u>Btu/lb</u>	End of Life Enthalpy <u>Btu/lb</u>
Solid at Room Temperature	0	0
Solid at Melting Temperature	414	391
Liquid at Melting Temperature	533	510

TABLE 14.2.6-2

Time in Life		Beginning	Beginning	End	End
Power Level		0	2346 Mw	0	2346 Mw
Ejected rod worth % ΔK		0.71	0.22	0.84	0.092
Delayed neutron fraction % ΔK		0.69	0.69	0.52	0.52
Feedback reactivity weighting		1.65	1.65	3.53	1.42
Trip rod worth	% ΔK	2.98	4.83	0.76	4.85
Average core gap heat transfer coefficient	Btu/hr ft ² °F	10,000	10,000	750	750
Average core fuel thermal conductivity	Btu/hr ft °F	2.65	2.65	2.2	2.2
Initial hot spot gap heat transfer coefficient	Btu/hr ft ² °F	750	2,000	750	2,000
Transient hot spot gap heat transfer coefficient	Btu/hr ft ² °F	10,000	10,000	10,000	10,000
Initial moderator density coefficient	$\Delta K/\text{gm}/\text{cm}^3$	0	0	0.208	0.161
Prompt neutron lifetime	Micro seconds	15	15	15	15
F_q after rod ejection		6.30	6.23	18.85	4.85
F_q before rod ejection		-	3.23	-	3.23
Number of operating pumps		1	3	1	3
Max. fuel pellet average temperature	°F	1550	3629	2560	3280
Max. fuel center temperature	°F	1710	4850	2900	4620
Max. Clad temperature	°F	1360	2220	2120	1930



(°F)

BEGINNING OF LIFE, FULL POWER
3 LOOP OPERATION

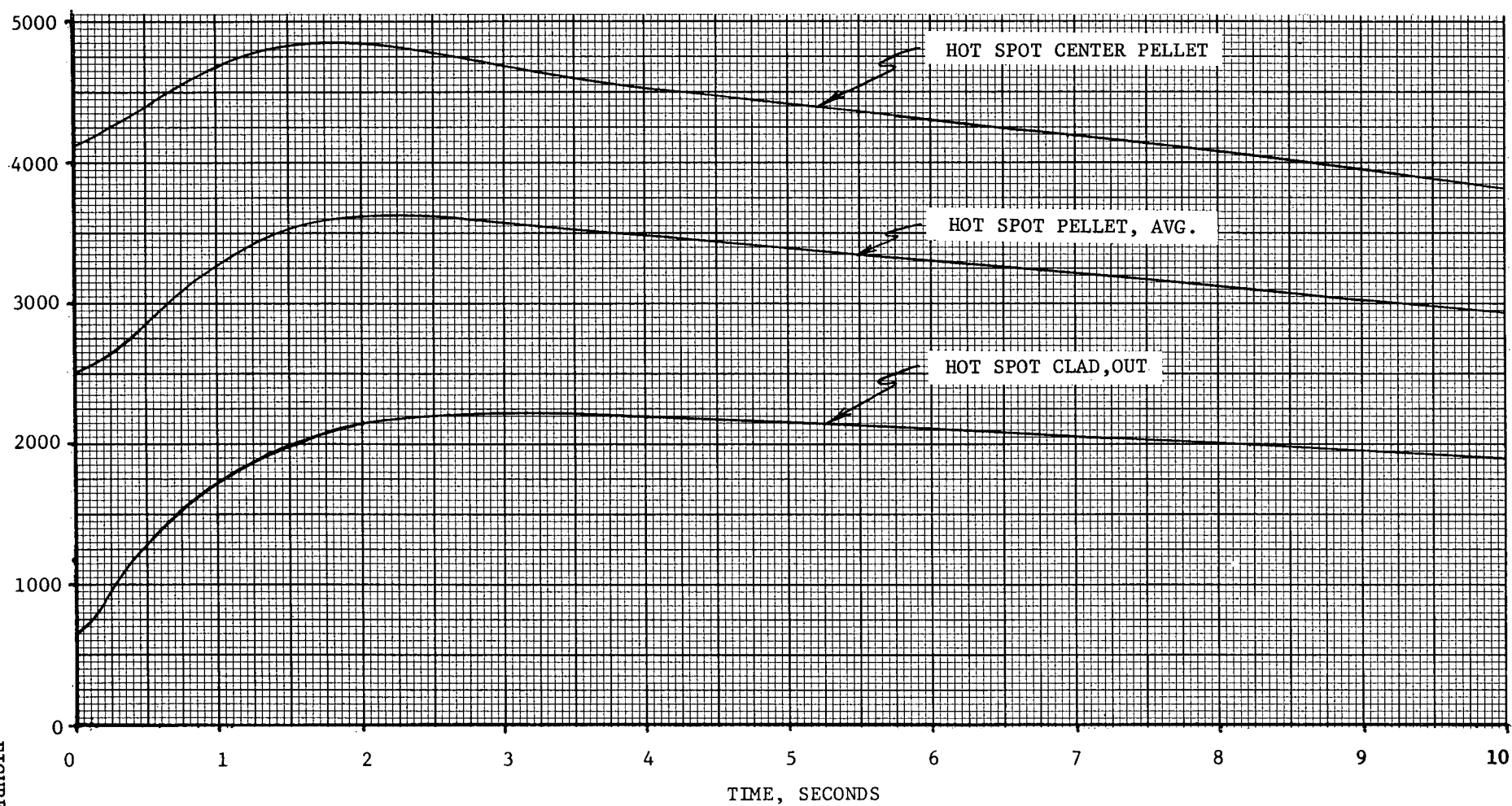


FIGURE 14.2.6-2

POWER vs TIME

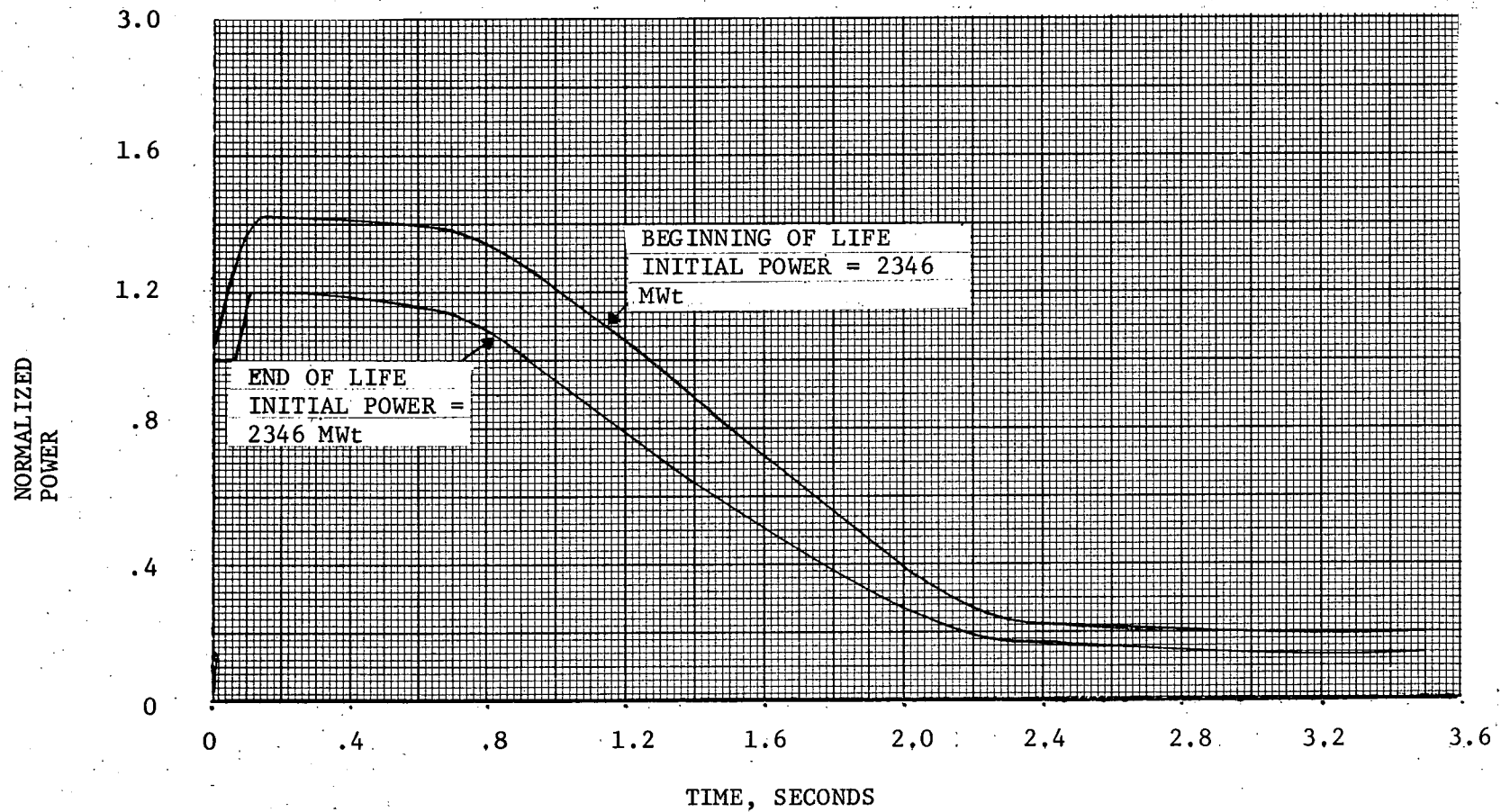
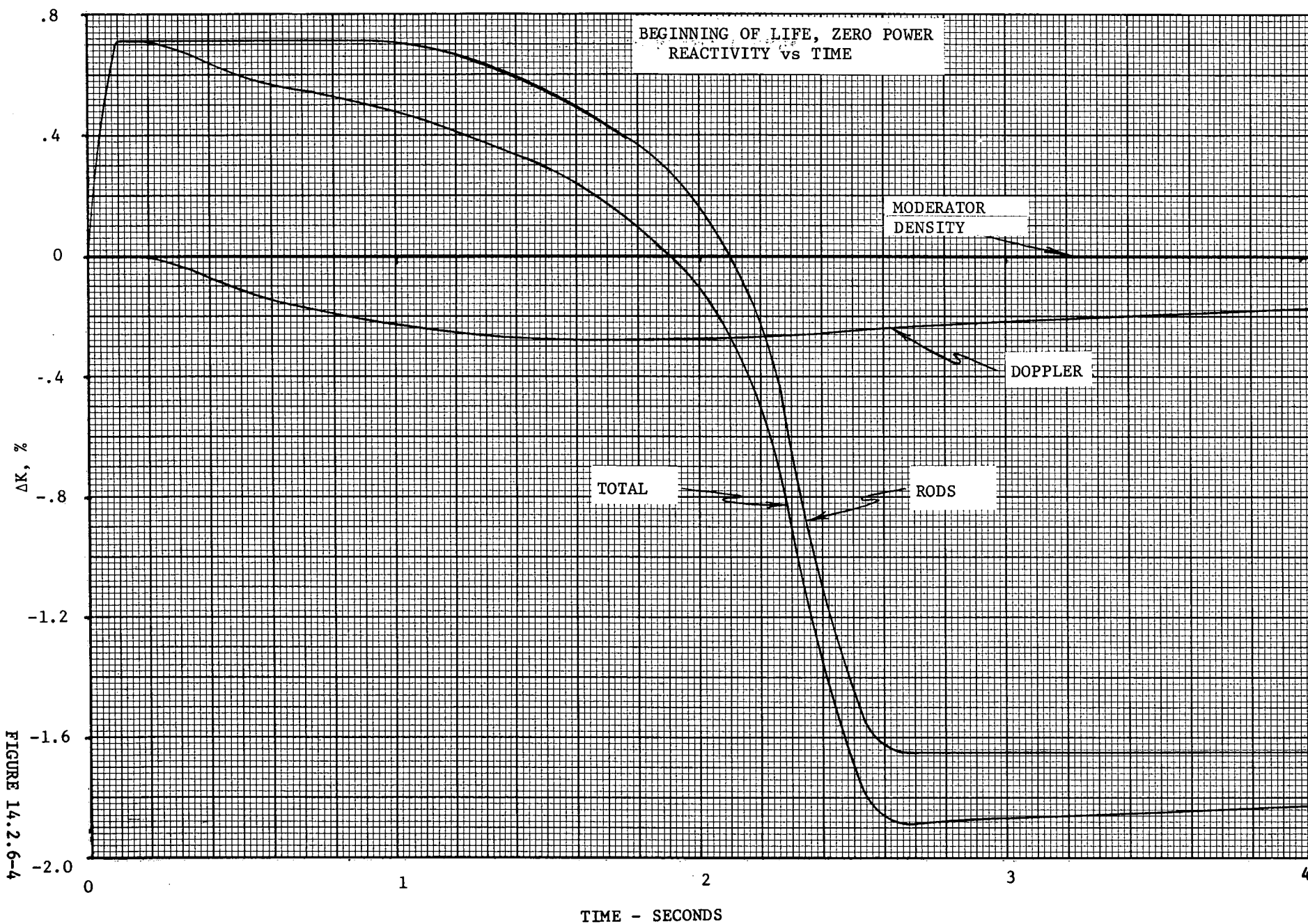


FIGURE 14.2.6-3



(°F)

BEGINNING OF LIFE, ZERO POWER
1 LOOP OPERATION

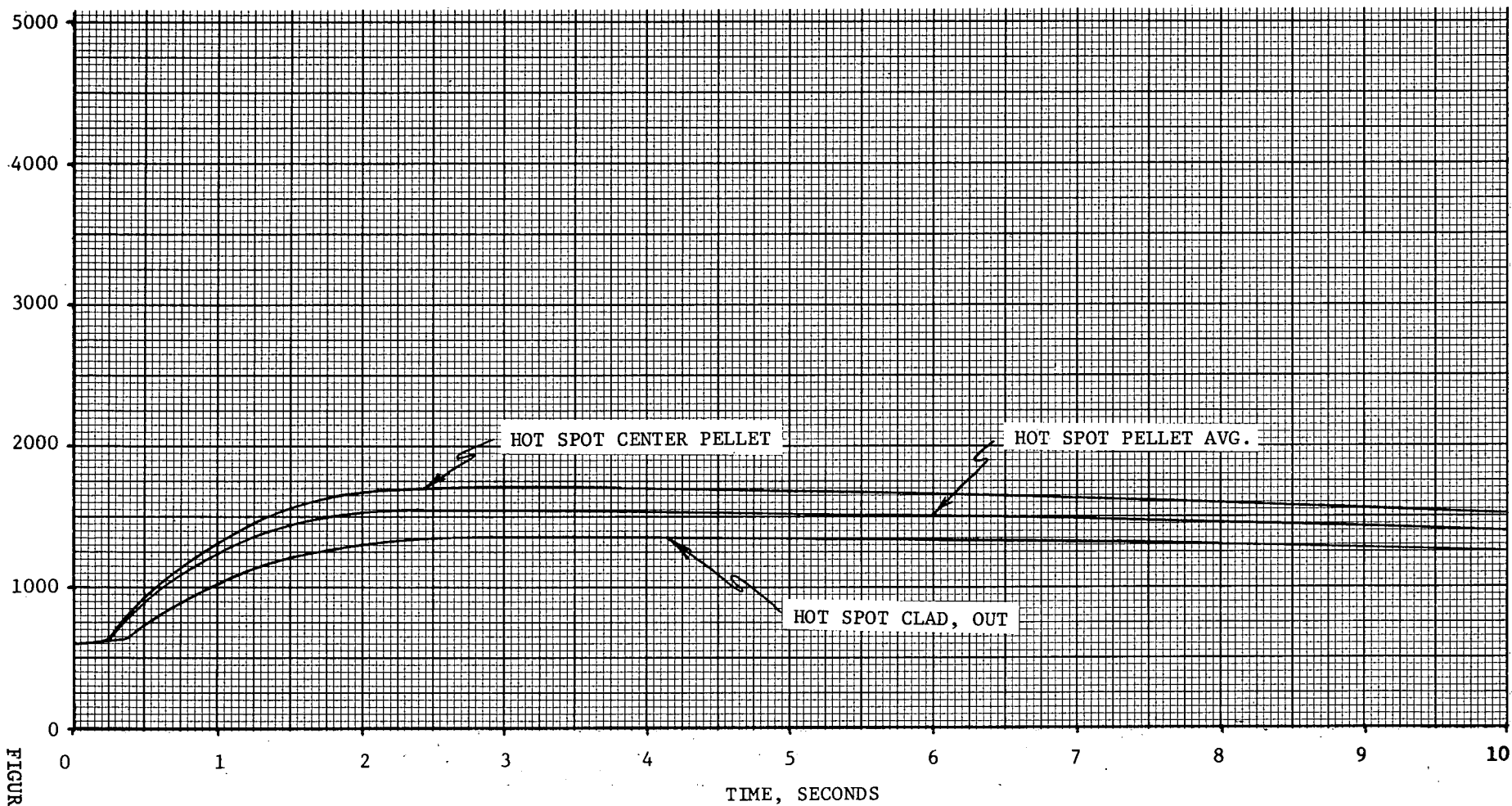


FIGURE 14.2.6-5

POWER vs TIME

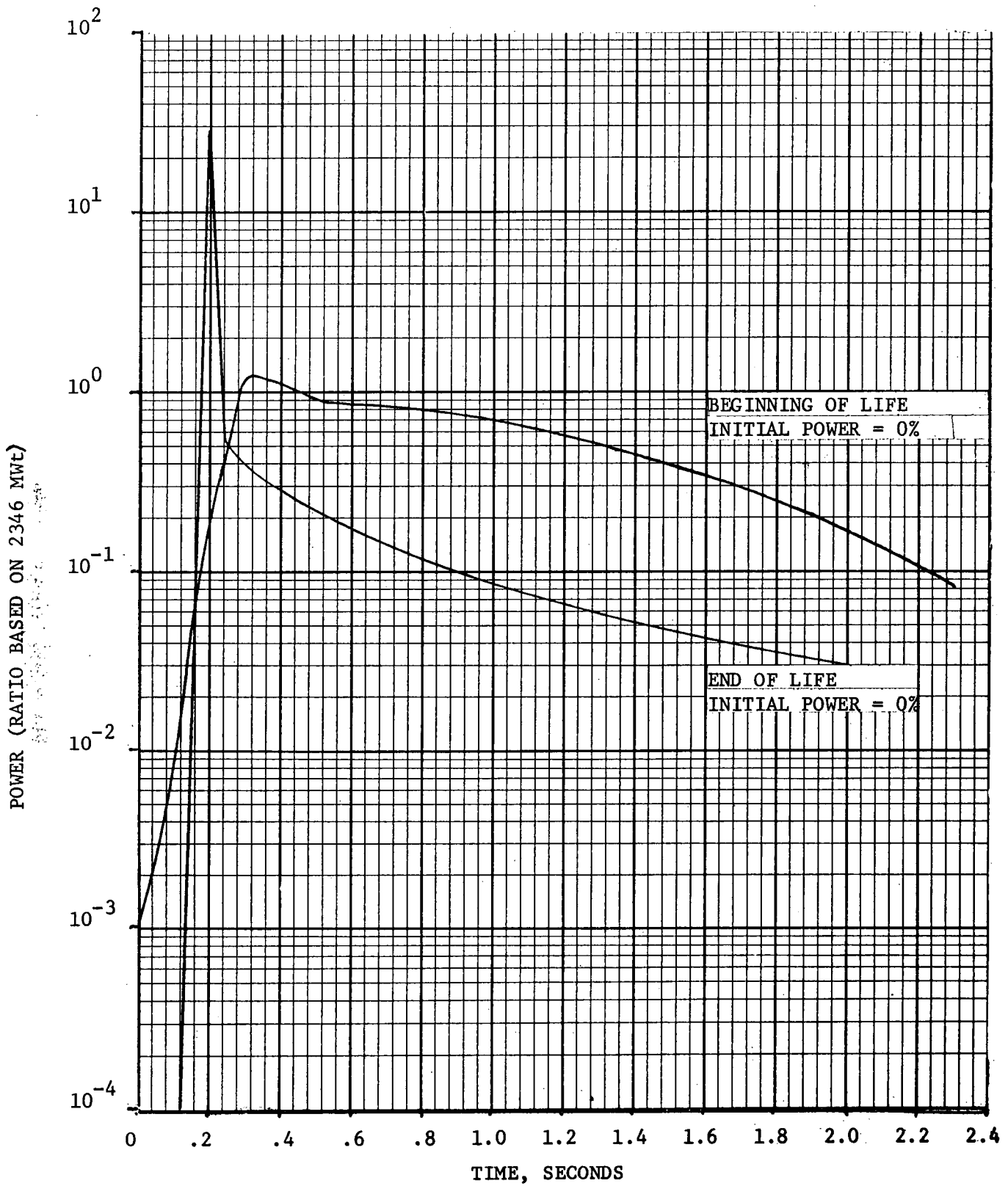


FIGURE 14.2.6-6

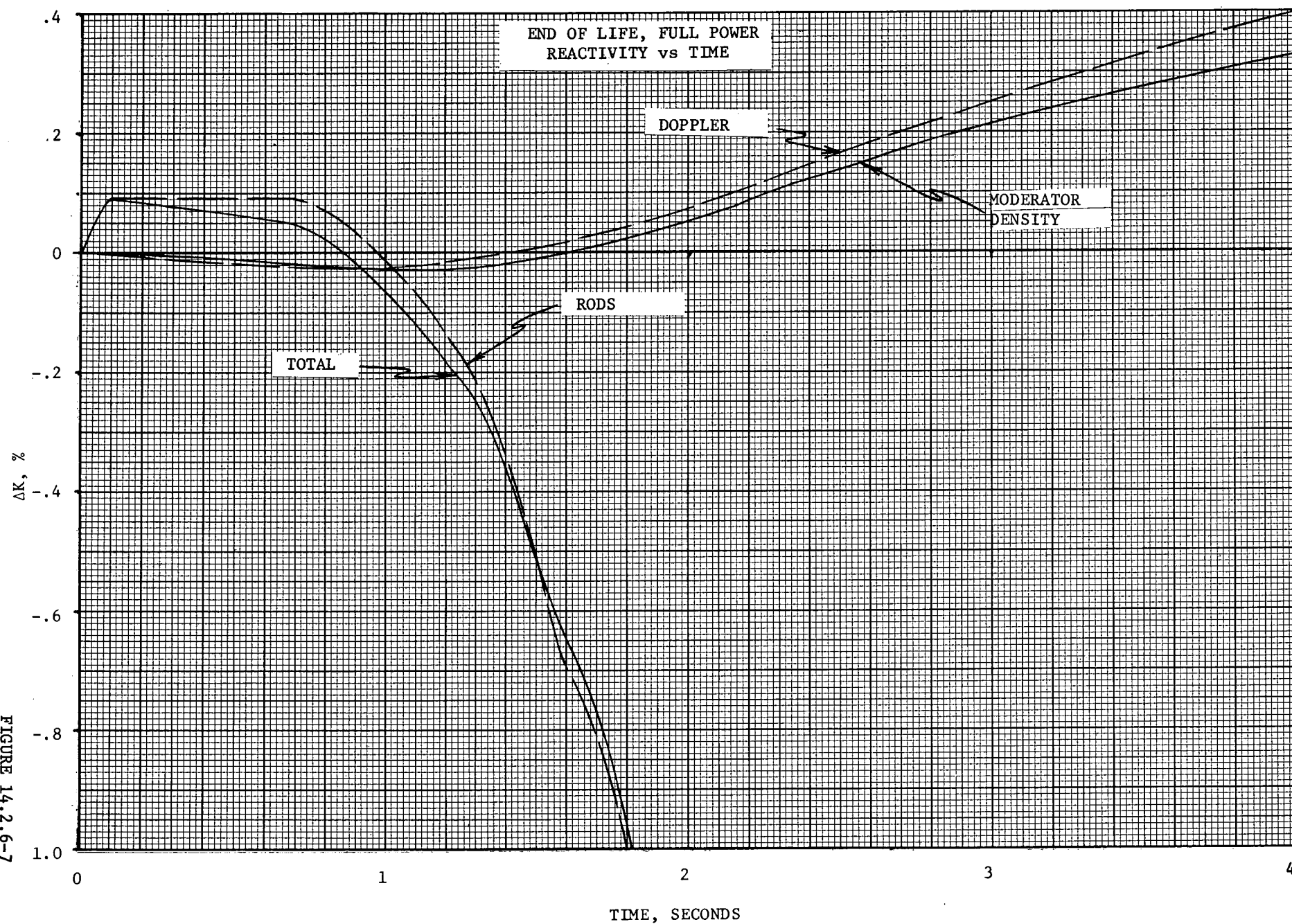


FIGURE 14.2.2.6-7

(°F)

END OF LIFE, FULL POWER
3 LOOP OPERATION

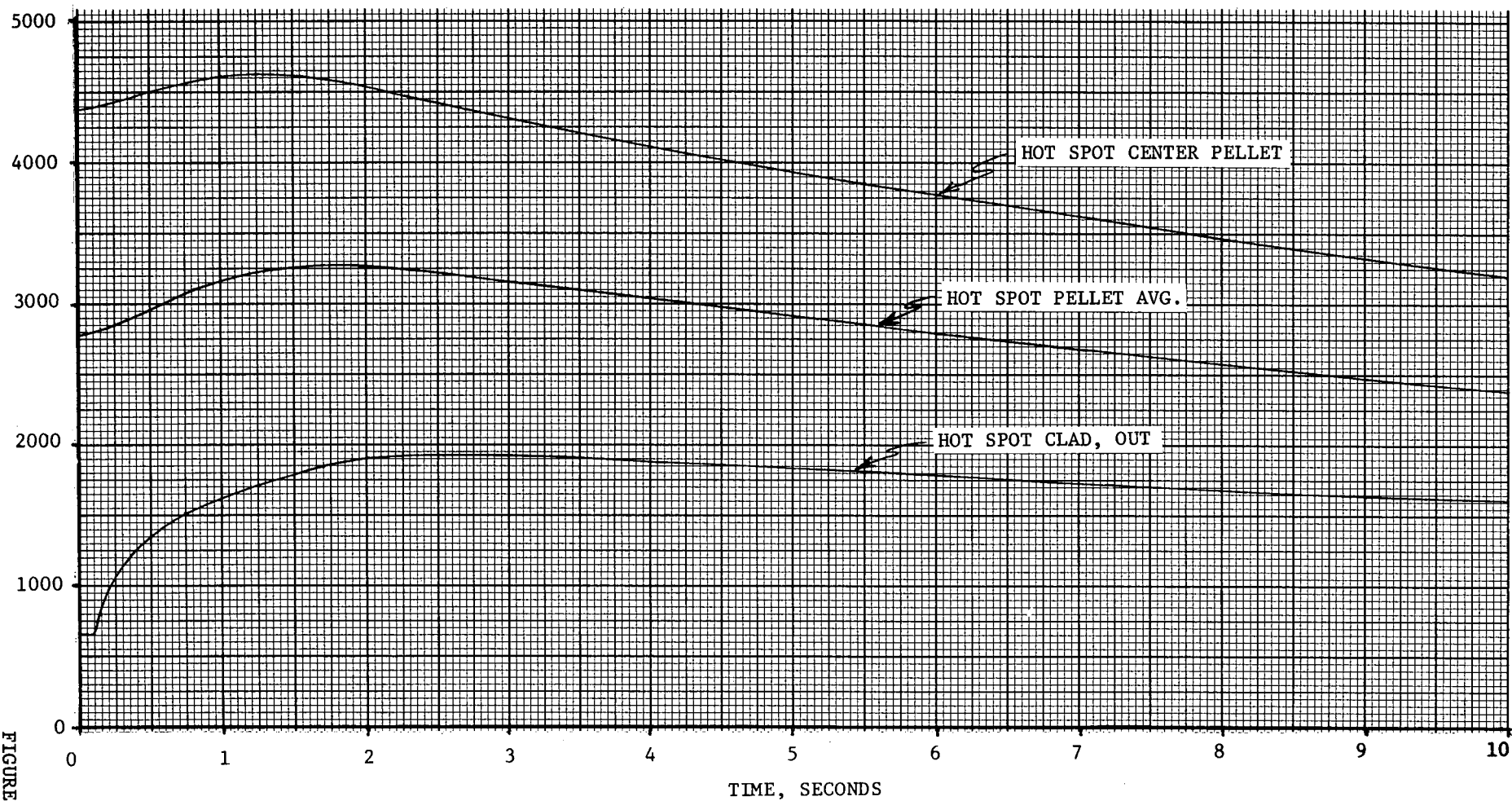


FIGURE 14.2.6-8

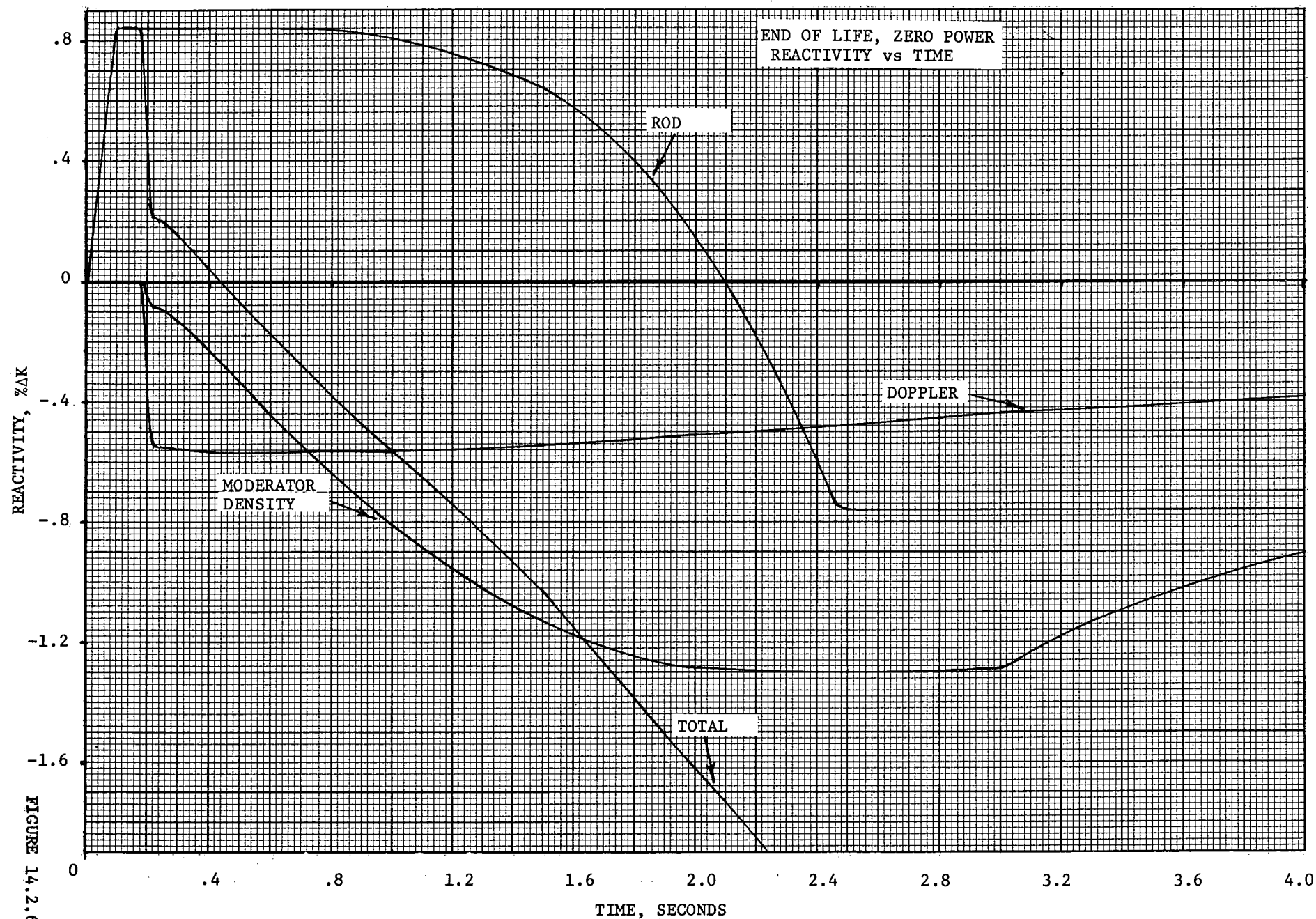


FIGURE 14.2.6-9

(°F)

END OF LIFE, ZERO POWER
1 LOOP OPERATION

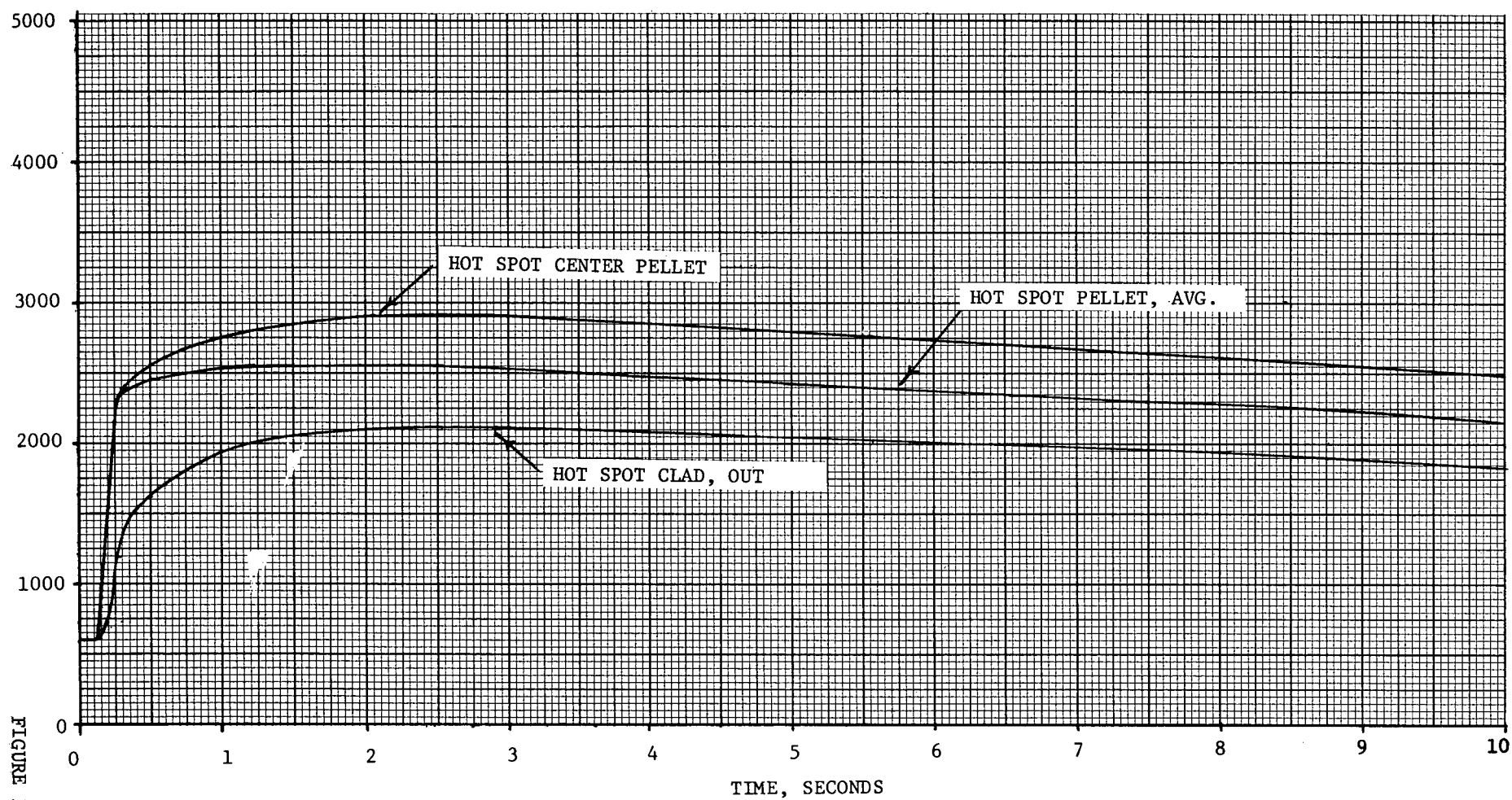


FIGURE 14.2.6-10

14.3 PRIMARY SYSTEM PIPE RUPTURE

14.3.1 GENERAL

A loss-of-coolant accident may result from a rupture of the Reactor Coolant System or of any line connected to that system up to the first closed valve. Ruptures of very small cross section will cause expulsion of coolant at a rate which can be accommodated by the charging pumps. Should such a small rupture occur, these pumps would maintain an operational level of water in the pressurizer, permitting the operator to execute an orderly shutdown. A moderate quantity of coolant containing such radioactive impurities as would normally be present in the coolant, would be released to the containment.

Should a larger break occur, resultant loss of pressure and pressurizer liquid level will cause reactor trip and initiation of safety injection. These countermeasures will limit the consequences of the accident in two ways:

- a) Reactor trip and borated water injection will supplement void formation in causing rapid reduction of the nuclear power to a residual level corresponding to delayed fissions and fission product decay.
- b) Injection of borated water ensures sufficient flooding of the core to prevent excessive temperatures.

The safety injection system, even when operating on emergency power, limits the cladding temperature to below the melting temperature of Zircaloy - 4 and below the temperature at which gross core geometry distortion, including clad fragmentation, may be expected. In addition the total core metal-water reaction is limited to less than 1%. This is valid for reactor coolant piping ruptures up to and including the double ended rupture of a reactor coolant loop. Consequences of these ruptures are well within those described later in this section for the hypothetical accident and are therefore well within the limit of 10 CFR 100.

The following paragraphs will describe the method of analysis used and results of the calculations to demonstrate that the Safety Injection System meets the core cooling requirements for the full range of break sizes.

14.3.2 CORE THERMAL TRANSIENT

Method of Analysis

The analysis of the loss-of-coolant accident is divided into three major phases:

- 1) Blowdown. This calculation provides a description of the thermal and hydraulic response of the Reactor Coolant System to a rupture, through depressurization and the operation of the emergency cooling systems. The basic information concerning the dynamic environment of the reactor core is thus provided for use in reactor kinetics and core cooling analysis.
- 2) Reactor Kinetics. The nuclear transient is forced by the blowdown dynamics and in turn affects the blowdown. The kinetics calculation determines the energy added to the core, an essential input to the core cooling analysis.
- 3) Core cooling. Based on the above information, a detailed analysis of reactor core cooling is performed to determine the core clad temperature.

The division of the study into these three phases permits a careful evaluation of the importance of various assumptions on each significant aspect of the overall problem. These three phases are described in detail in the following paragraphs.

Blowdown Analysis - FLASH Code

The blowdown analysis is performed using FLASH-R⁽¹⁾, a digital computer code developed at Bettis and WAPD to better conform with commercial PWR systems. This code uses three regions, each at a different pressure, to simulate the Reactor Coolant System. Two regions are the upper and lower volumes, corresponding to the hot and cold volumes in the coolant loop, and these are connected by flow paths through the reactor core and through the intact loop piping and steam generators. The third region is the pressurizer, connected to the upper region by the surge line. Inertia and pressure losses are calculated in each connecting line, including the main coolant pump coastdown and cavitation.

The above simulation of the Reactor Coolant System permits a lumping into control volumes of relatively uniform pressure and temperature regions. In normal system operation, all of the pressure rise occurs across the reactor coolant pumps and most of the pressure drop occurs across the core. Similarly the temperature rise occurs across the core, while the temperature drop occurs across the steam generators. During blowdown, the core and the reactor coolant pumps offer most of the resistance to flow.

Heat is removed from the main coolant system by the steam generators until the coolant temperature drops below the steam-side temperature. Heat addition in the core for the current study was input in the form of heat flux as function of time, based on more detailed core studies, described in the next section.

Flow through a leak is calculated, in subcooled conditions, using Fauske's⁽²⁾ model for metastable flow for short pipes, or Moody's⁽³⁾ model for homogeneous equilibrium flow for long pipes. Once the leaking region reaches saturation, Moody's correlation is used for both cases. A double-ended break is represented as a "short-pipe" leak from the near region and a "long-pipe" leak from the farther region, while smaller breaks are treated as "short-pipe" leaks from the near region only.

The code contains a bubble-separation model assuming an upward velocity of two feet/second of bubbles through water. This determines the quality of flow through breaks and through the core and piping during blowdown. The actual times of uncovering of the core, however, are calculated using FLASH R code results, with the assumption of complete separation of steam from water. This is a conservative measure to avoid taking credit for froth height in determining core water level. The use of the above flow correlations and bubble separation model conservatively overpredicts the mass loss through the break.

Modifications were made to the original FLASH program to account for the specific system configurations of the system: these included the singlepass rod-type core, and the location of the reactor coolant pump, the accumulator and injection pumps characteristics. A calculation was added to the FLASH program which determines the flow rate into the lower volume of the Reactor Coolant System from the accumulator. The flow rate calculation is based on the pressure difference between the Reactor Coolant System and accumulator gas pressure and the resistance of the accumulator lines. The accumulator tank gas pressure is assumed to expand isentropically to replace the injected accumulator water. The accumulator pressure, and liquid and gas inventories are continually calculated. Accumulator injection continues until the tanks are emptied. In addition, applicability of the FLASH Code was extended by the incorporation of a detailed core flooding calculation. This calculation considers the steam bubble in the core formed by steam generation when the core is reflooded. The water in the downcomer rises at a faster rate than the core water level. Thus, a static driving head is developed to drive the generated steam through the resistance of the loop piping and Reactor Coolant System components.

In summary, this phase of the analysis requires as input the reactor coolant system description and initial conditions, break size and location, energy addition in the core, and emergency core cooling system characteristics. The analysis produces as output the blowdown pressure, enthalpy, uncover and recovery times, core flow, core pressure drop, and the conditions required to determine reactor trip.

The FLASH-R Code has been used to predict the blowdown and refill transient presented for this plant. Several investigators⁽¹³⁾ have compared this analysis to experiments and found the code conservative in two principal areas: rate of depressurization and mass of water left after blowdown.

This conservatism is generally attributed to the critical flow boundary condition. The correlation, as used in this analysis, overpredicts the mass flow through the break and thus the analysis overstates the severity of the transient. A better comparison between analysis and experiment is obtained when the break area used in the analysis is reduced to about 80% of the experimental value.

Thus the transient which is ascribed to the double ended rupture would, in fact, occur for a larger break and conversely the analysis done for a smaller rupture represents the true double-ended break.

Since the whole spectrum of break sizes less than or equal to the double-ended rupture has been analyzed, adequate protection has therefore been demonstrated even when the break flow takes on the smaller, more realistic, values.

Essentially the same critical flow correlations are used in the SLAP analysis and hence this discrepancy would be expected again. This has been confirmed by some unpublished comparisons with W APD blowdown experiments.

Core Power Transient CHIC-KIN

The basic tool used for the reactor kinetics calculation is the CHIC-KIN⁽⁴⁾ code, which has a point kinetics model and a single channel fuel and coolant description. In this study the channel was divided axially into five sections, with density in each section a function of pressure and enthalpy, plus nucleate boiling void. A nucleate boiling model for highly subcooled conditions was used, even though a large part of the coolant is saturated throughout the transient.

That is, when the clad surface is hotter than saturation temperature, 10% of the heat flux goes into local boiling void, which has a mean lifetime of 0.1 second. This was done to minimize apparent void formation in order to retard reactor shutdown and yield a conservatively high energy input. Since the hot channels of the core have greater than average void fraction the use of an average channel model reduces the apparent void. This yields a conservatively high energy input. In addition, coolant bypass around the core was neglected, reducing the calculated void.

Each axial fuel rod section was divided into nine radial regions for the heat transfer calculation. Conservatively high values of fuel conductivity and gap conductance were assumed for the Kinetics calculation. These give a reasonable minimum initial average fuel temperature, thus reducing heat transfer rate during shutdown, and thereby again minimizing void formation.

For moderator density reactivity feedback the calculated density coefficient as a function of density for beginning of life with no control rods was uniformly reduced to correspond to zero coefficient at the initial average density at the nominal conditions. The curve yields a 1% negative reactivity with a density reduction of 25%; whereas the calculated curve would show approximately twice this feedback for the same density change. The density coefficient at beginning of life corresponds to a temperature coefficient of $-0.5 \times 10^{-4} \delta k / ^\circ F$ at nominal temperature.

Doppler reactivity feedback was simulated as a function of the average fuel temperature, with a weighting factor of 1.6 used as an upper limit for the initially unrodded core to reduce the rate of power decrease during shutdown.

Six groups of delayed neutrons were used. For the total effective fraction, a conservative maximum of 0.0072 was used to slow down power decay. Average core pressure was input as a function of time from the FLASH-R output. For the $1/2 \text{ ft}^2$ break the core inlet flow as shown by the FLASH-R code calculations was used as input to CHIC-KIN. For all other breaks with violent flow reversal and then near-stagnation, the core pressure drop as indicated by FLASH-R was assumed to be a reasonable representation of the forcing action between the two large liquid regions of the system.

This pressure drop was used as input to CHIC-KIN, which calculated flow response taking into account inertia and, losses at inlet and outlet, across the grids and friction along the fuel rod. The resulting flow transients were very close to those obtained by FLASH-R.

Trip would be activated in all cases by low pressurizer pressure. For the $1/2 \text{ ft}^2$ break case this would occur in approximately 1.25 seconds. Significant trip rod reactivity effect was calculated to start in 2.25 seconds after the break, and $-0.025 \delta k$ is inserted over the following 2.2 seconds.

For the larger breaks, trip would be similarly actuated, but because void formation is adequate for shutdown, trip was not simulated in these studies.

Core Cooling Analysis - LOCTA Code

The LOCTA-R2 transient digital computer program was developed for evaluating fuel pellet and cladding temperatures during a loss-of-coolant accident. It determines the extent of the Zircaloy-steam reaction and the magnitude of the resulting energy release in Zircaloy clad cores.

The transient heat conduction equation is solved by means of finite differences, considering only heat flow in the radial direction. A lumped parameter method is used; the fuel containing three radial nodes and the cladding one radial node.

Internal heat generation can be specified as a function of time. The decay heat from any initial power level can be calculated by the code. The decay heat is based on the heat generated from

- a) fission products,
- b) capture products, and
- c) delayed neutrons

It is assumed that the core has been irradiated for an infinite period of time.

In addition to decay heat, the code calculates the heat generated due to the Zircaloy-steam reaction. The $\text{Zr-H}_2\text{O}$ reaction is governed by the parabolic rate equation unless there is an insufficient supply of steam available, then a "steam limited" evaluation is made. However, for the cases considered, the parabolic rate equation was used. The buildup of the Zircaloy-oxide film is calculated as a function of time, and its effect on heat transfer is considered. An isothermal clad melt is considered based on the heat of fusion of Zircaloy. Once the Zircaloy metal melts, it is retained by Zirc-oxide, and slumps against the fuel. The Zircaloy-steam reaction may continue until the oxide melts. If the oxide melts the remaining Zircaloy is assumed to fall, and 10% of this metal is assumed to react with additional water which is available in the vessel.

The code has been developed to stack axial sections and thereby describe the behavior of a full length region as a function of time. A mass and energy balance is used in evaluating the temperature rise in the steam as it flows through the core.

The initial conditions of the fuel rod are specified as a function of power. The following core conditions are also introduced as a function of time, as determined by the FLASH-R Code:

1. Mass flow rate through the core
2. Coolant quality
3. Pressure

Heat transfer coefficients during the various phases of the accident are evaluated in the following manner:

1. Nucleate boiling film coefficients on the order of $20,000 \text{ Btu/hr-ft}^2\text{-}^\circ\text{F}$ are used until DNB. The correlation applied during this period is: ⁽⁵⁾

$$\Delta T_{\text{Sat}} = 1.9e^{-P/900} (q'')^{1/4}$$

2. When DNB occurs, it is assumed that the fuel rods can immediately develop a condition of stable film boiling. No credit is taken for higher transition boiling coefficients that exist prior to the establishing of a stable film on the fuel rods. The correlation used during this period is:⁽⁶⁾

$$h = 0.023 \frac{k_v}{D_e} \left[\frac{\rho_v D_e}{\mu_v} \left(\frac{Q_1 + Q_v}{A_c} \right) \right]^{0.8} \left(\frac{C_{\rho} \mu}{k} \right)_v^{0.4}$$

3. During the time the core is uncovered (period of steam flow through the core), laminar or turbulent forced convective coefficients and radiative coefficients are evaluated.

For laminar forced convection to steam:^(7,8)

$$\left(\frac{hD}{k} \right)_{iso} = 3.66$$

$$h/h_{iso} = \left(\frac{T_b}{T_w} \right)^{0.25}$$

For turbulent forced convection to steam:^(9,10)

$$\frac{hD}{k} = 0.020 \left(Re_b \right)^{0.8} \left(Pr_b \right)^{0.4} \left(\frac{T_w}{T_b} \right)^{-0.5}$$

Where

- h - Heat transfer coefficient on outer surface of fuel rod (Btu/hr-ft²-°F)
D_e - Equivalent diameter of flow channel - (ft)
ρ - Density (lbs/ft³)
μ - Viscosity (lbs/ft-hr)
Q - Volumetric flow rate (ft³/hr)
A_c - Area of flow channel (ft²)

- C_p - Specific heat (Btu/lb-°F)
 k - Thermal conductivity (Btu/hr-ft-°F)
 T - Temperature (°F)

Subscripts:

- v - Evaluation of the property at the saturated vapor condition
 l - Evaluation of the property at the saturated liquid condition
 b - Evaluation of the property at the bulk fluid condition
 w - Evaluation of the property at the clad surface temperature
4. The rising clad temperature transient is turned around after the lower portion of the core has been reflooded. Conservative heat transfer coefficients of the order of 25 Btu/hr-ft² are calculated for this initial reflooding period using the dispersed flow theory heat transfer correlation⁽⁶⁾ and result from the two-phase flow which is present due to entrainment. This entrainment process is initiated when a steam velocity of approximately 7 ft/sec based on work of R.F. Davis⁽¹¹⁾ is evaluated leaving the flooded region of the core.

The analytical model used during the core reflooding phase of the accident has been compared to experimental data obtained from the FHUST⁽¹²⁾ experimental tests in conjunction with the LOFT program. With the same geometric configuration, flow conditions, etc. as that used in the experimental studies, the Westinghouse design model predicts clad temperature turn around times to be greater than those obtained from the FHUST data, indicating the Westinghouse model is conservative.

Information generated by LOCTA R-2 as a function of time includes:

1. Fuel temperature,
2. Clad temperature,
3. Steam temperature,
4. Amount of metal-water reaction,
5. Volume of core metal, and
6. Total heat released to coolant

Small Break Analysis - SLAP Code

For small breaks up to about a 6 inch diameter hole the digital computer code, SLAP, is employed to calculate the transient depressurization of the reactor coolant system as well as to describe the mass and enthalpy flow through the break. The code considers three volumes.

1. The reactor coolant system
2. The pressurizer, and
3. The steam generators (shell side).

Fluid can flow between the pressurizer and the reactor coolant system, while heat can be transferred between the reactor coolant system and the secondary. The code uses the equations of state, continuity and energy conservation to define the condition in each volume as a function of time. Fluid flow between the pressurizer and the reactor coolant system is defined by the momentum equation. Heat is transferred between the steam generators and the reactor coolant system unless the liquid level falls below the level of the tubes. The heat transfer rate is assumed to be zero for that portion of the tubes not covered by shell-side water. Heat transfer to the steam generator decreases as the temperature difference between the primary and secondary is reduced.

Thermodynamic conditions are initialized by designating the size of each volume as well as

1. the reactor coolant system pressure and temperature
2. the pressurizer level, and
3. the secondary pressure and level.

The initial fluid flow between the pressurizer and the reactor coolant system is zero since the pressure in these volumes is essentially equal. The initial heat transfer rate to the steam generator is equal to the operating power.

When a break occurs in the reactor coolant system, subcooled water is assumed to initially flow out the opening. The flow is defined by the correlation of Fauske⁽²⁾. He concluded that for sharp-edged orifices test data can be accurately evaluated using the incompressible flow equations for a nozzle.

Once the reactor coolant system fluid becomes a two phase mixture, a different break flow correlation is used. The new flow scheme is defined by the correlation of Moody,⁽³⁾ which specifies the two phase critical discharge out the break.

The pressure decrease in the reactor coolant system causes fluid to flow from the pressurizer, resulting in a pressure decrease in the pressurizer. Reactor trip occurs when the pressurizer low pressure set point is reached. Safety injection is actuated when the pressurizer low pressure and low level set point are reached.

Injection water flow into the reactor coolant system is defined by an input table of injection flow rate as a function of system pressure. A start up delay time is also included. Injection water is allowed to flow once the safety injection signal is generated and the delay time is exceeded. The accumulators automatically discharge their fluid when the reactor coolant system pressure drops below the accumulator set point.

Before the reactor trip signal occurs, it is assumed that the heat being generated in the core is removed via the secondary. The mass and energy entering and leaving the secondary are assumed to be equal. When reactor trip occurs, isolation valves are assumed to close, preventing secondary flow to or from the steam generator. Heat from decay, hot internals, and the vessel enters the reactor coolant system fluid. The pressure in the secondary increases and heat enters from the hotter reactor coolant system. Secondary steam discharges from the steam generators when safety valve set pressure is reached. Emergency feedwater flow as a function of time is specified by input tables. Steam flow as a function of dump valve flow area is specified to simulate the operation of the power operated dump valves.

The code follows the pressure and mass in each volume as a function of time.

Conservatism in the Core Cooling Analysis

Some conservatisms which are inherent in the analytical models just presented are:

- a) DNB is assumed to occur at 0.5 seconds for all breaks. This assumption is felt to be especially conservative for the smaller breaks where the flows remain high during the initial blowdown period.
- b) When DNB occurs, it is assumed that the fuel rods can develop a condition of stable film boiling. No credit is taken for higher transition boiling coefficients that exist prior to the establishing of a stable film in the fuel rods. Conditions could exist by using a transition boiling model where a return to the nucleate boiling region would occur rather than entering stable film boiling.
- c) The times the core becomes uncovered and recovered are calculated by the FLASH R code. Tests have verified that FLASH R underpredicts the amount of water remaining in the vessel during blowdown. A more realistic blowdown model would show that the core is uncovered for a shorter time period than that calculated in the above mentioned transients.
- d) For the small breaks when long periods of blowdown exist the present analyses do not consider natural circulation in the core, which may result in significantly lower cladding temperatures.

Results

The capability of the Emergency Core Cooling System to meet the design criterion is analyzed for the following range of break sizes and location:

1. Large breaks, cold leg
 - a) Double ended severance of the Reactor Coolant Pipe
 - b) 6 ft²
 - c) 3 ft², and
 - d) .5 ft²
2. Small breaks, cold leg (SLAP)
 - a) 6 inch
 - b) 4 inch
 - c) 3 inch
 - d) 2 inch

For all of the above breaks the clad temperature transient is presented for the case where the contents of one accumulator tank was assumed spilled through the break. For hot leg breaks all of the accumulators empty into the reactor vessel. The above list of cold leg breaks result in more severe core temperature transients than the equivalent hot leg breaks. Thus the detailed analysis of hot leg breaks is not presented. Full flow from the safety injection pumps was assumed at 25 seconds.

Results - Large Area Ruptures

The power level used in the loss of coolant evaluations performed for the reactor includes a 2% increase above the maximum calculated core thermal rating of 2292 MWt to account for errors in the steam cycle calorimetric measurements.

Blowdown and Refill

Figures 14.3.2-1 to 14.3.2-4 are plots of the water volume in the reactor vessel for the large area ruptures. During blowdown, the volumes plotted represent an equivalent liquid volume which would result if the liquid and gas phases were completely separated. No credit is taken for an increased froth height due to voids created by boiling in the core. The volume of

liquid remaining in the vessel after blowdown is used as a starting point to predict the liquid lead during the refilling phase. It should be noted here that the FLASH code conservatively underpredicts this quantity of water remaining in the vessel at the end of blowdown, when compared to experimental data (LOFT semiscale tests, etc.), so that this conservatism is carried throughout the refill phase of the predicted water levels.

Several factors have been considered in the analysis that could adversely affect the flow of emergency cooling water to the core. These are:

- a. Accumulator water carried out of the break, or to other parts of the system during blowdown.
- b. Steam bubble formation when accumulator water refloods the core.
- c. The affect of the nitrogen gas entering the vessel.

The method of determining the affect of these factors is discussed in the following paragraphs.

Accumulator By Pass

The flow from each accumulator enters the cold leg pipe between the outlet of the reactor coolant pumps and the cold leg nozzles. The maximum flow rate from two accumulators is 4485 lbs/sec. This occurs for the double-ended cold leg break shortly after the beginning of injection. This flow rate is approximately 16.6% of the steady state flow rate of 27,000 lbs/sec for normal plant operation, and therefore, there is no possibility of choking the downcomer and backing the flow to other parts of the system.

Flow into the inlet of the vessel is also enhanced by the reactor coolant pump, which would be coasting down during the transient and would tend to force coolant in the direction of the reactor. Further, a characteristic of

the reactor coolant pumps prevent back-flow through the pumps under the injection condition. Each pump has a diffuser which effectively serves as a weir to impede back-flow through the pump. The weir effect of the suction/diffuser section of the pump can be seen in the schematic Figure 14.3.2-5. The discharge pipe has to be full of water before the weir can be over-topped. The water required to fill the discharge piping between the reactor coolant pipe and the vessel is accounted for in the calculations.

The possibility of accumulator water being carried out with the blowdown was also considered.

The FLASH R computer code is used to predict the rate of mass discharge through the break in the loss-of-coolant accident analysis evaluation. A very conservative bubble rise correlation is used to predict the bubble entrainment and corresponding froth level in the annulus of the reactor vessel. This results in an extension in the duration of two phase blowdown. Comparison with LOFT tests has indicated that FLASH R overpredicts the amount of water lost through the break. No attempt has been made to modify the bubble rise correlation or to perform a momentum analysis to predict a more realistic blowdown. Such a modification would predict more water remaining in the vessel after blowdown, and a faster reflooding of the core.

In the FLASH R analysis of the transient, the accumulators are injecting during blowdown and loss of accumulator water because of the upward velocity and resulting entrainment in the annulus is considered. When the accumulators begin to inject (600 psi) the quiet water level has dropped below the bottom of the core. In the FLASH R calculation a conservative froth level remains at the level of the nozzles, more than 17 feet above the quiet level, and a two phase entrained blowdown is continuing. Note that no credit is taken for the froth level in the core cooling analysis.

Only a portion of the accumulator injection takes place during blowdown. For the double-ended break, accumulator injection begins at 6.2 seconds and blowdown is completed at 11 seconds. The entire contents of the accumulator are not injected until 35 seconds. During blowdown only 17,400, lbs. of the total accumulator mass of 95,790 lbs. is injected (2 of 4 accumulators considered). Therefore, only about 20% of the accumulator injection is subject to loss through the break during blowdown, and this is accounted for in the analysis of the transient.

In summary the correlations used in the FLASH code to predict the mass loss through the break, from both the mass initially in the reactor coolant system and the mass added to the system by the accumulators, conservatively account for the water being carried to the break.

Steam Bubble

When the core is reflooded by the accumulators special consideration is given to steam generation in the core which could retard the reflooding process. Steam will be generated around the hot fuel rods, causing a pressure build-up in the core region. This steam must be vented from the system through the break. The flow paths are illustrated in Figure 14.3.2-5. The worst break location for this is a cold leg break, where the steam must flow through the reactor coolant pipes, steam generator, and reactor coolant pump to escape.

There are two paths available for the steam to flow to the break. The first path is directly to the break through the broken loop. The other path is through the two intact loops, back into the inlet annulus, and finally to the break through the inlet nozzle in the broken leg. Because of the pressure drop due to steam flow between the core and inlet annulus, the liquid level in the downcomer annulus will rise at a faster rate than the core level. This will continue until the water head between the downcomer and core level equals the pressure drop of steam flowing through the loops to the break.

The relationship between this downcomer head and corresponding steam flow rate through the loops is shown in Figure 14.3.2-6. The resistance to steam flow used for this curve is based on the resistance of the loop piping, steam generators and pumps (assuming the expected condition of empty loop seals) and a saturation pressure of 57 psia at the completion of blowdown, which corresponds to the containment pressure.

The model used for the refill calculation allows for this resistance to the steam flow, and the core liquid level predicted by the revised FLASH code is consistent with the necessary pressure differential between downcomer and core.

The height of downcomer above the calculated liquid level is available as an additional head of water to cause steam flow through the core. This available head would permit steam flow in excess of the calculated flow, or an additional back-pressure build-up due to water filled loop seals (as discussed below) without any loss of safety injection water.

The available downcomer head during the refilling of the core for the double-ended cold leg break is shown in Figure 14.3.2-7. Comparison of this available head to the head needed for a steam flow sufficient to cool the core shows the considerable margin in potential steam driving head. Only 0.9 feet of head is required to drive the steam to the cold leg break location, while 16.4 feet is available. This allows considerable margins for variations in the pressure drop calculation such as the effect of entrainment and decreases in the system saturation pressure during containment cooldown.

In the unlikely event that all recirculation loop seals (pipe between steam generator and reactor coolant pump) were filled at the end of blowdown, the escape paths for the steam from the core would be temporarily blocked causing a rapid pressure buildup in the core. However, the available downcomer head far exceeds the head needed to blow the liquid out of the loop seals (8.5 ft) as shown in Figure 14.3.2-7. Filled loop seals would, therefore, result in the rapid filling of the downcomer until the head in the downcomer has reached 8.5 feet. This would be followed by a back

flow of the water from the downcomer into the core until downcomer head and steam pressure are equalized. No accumulator water would be lost and the delay in covering the first 2 feet of the core would be insignificant.

It is concluded, therefore, that the downcomer head accounted for in the calculation of liquid level in the core is sufficient to drive the calculated steam flow to the cold leg break. In the event of a steam flow lower than that calculated, the liquid level in the core would rise at a faster rate, thereby recovering the core with liquid sooner than predicted, while a steam flow higher than the calculated flow is possible with the available head in the downcomer. In this event the liquid level in the core would rise at a slower rate than that predicted, however, the higher steam flow would increase the margin in the core cooling capacity.

Nitrogen Interference

Nitrogen gas enters the system after the accumulator injection is complete and the core maximum temperatures have already been greatly reduced. For a cold leg break the accumulator gas actually helps prevent the steam binding situation, i.e., the gas pressure at the reactor vessel inlet nozzle would tend to retard the rise of injection water in the downcomer annulus. No credit is taken for this in the steam bubble calculations.

The gas entering the system will, in part, escape through the break by venting around the downcomer annulus to the break location and, in part, occupy the high dead spaces in the reactor coolant system. The latter gas volumes, however, cannot impede the flow of core cooling water.

For the hot leg break some of the gas could bubble into the coolant around the bottom of the core barrel, but the majority of the gas would vent in the reverse flow direction to the break. The nitrogen thus dissolved in the coolant has little effect on the cooling in the core.

Core Power Transient During Blowdown

The core power transients calculated are shown in Figure 14.3.2-8. For the 0.5 ft² break, the initial subcooled decompression does not form enough void to shutdown the core. As pressure continues to drop, however, the power drops until it is near 50% power when trip becomes effective.

For the larger breaks the faster subcooled blowdown and subsequent rapid continued depressurization introduce voids much more rapidly and extensively than in the case of a small break. Backflow through the core also forces a saturated steam-water mixture from the reactor outlet plenum down into the core, adding to the voiding. The result is that for the 3 ft², 6 ft² and double-ended breaks studied, the reactor shuts down immediately.

For these cases, a "standardized" decay heat plus delayed neutron curve was used as a minimum power level as indicated in Figure 14.3.2-8 in the thermal analysis, even though this power is significantly higher than the power actually calculated with the conservative assumptions listed.

Core Thermal Analysis Results

The core thermal analysis was determined using the blowdown and recovery data and the core power transients which were described in the previous sections.

Figures 14.3.2-9 through 14.3.2-12 present a plot of core pressure and core flow and the calculated heat transfer coefficient used for all breaks. The zirconium-metal water reaction was computed to be less than 1% in all cases and is an insignificant factor in the containment transient. A summary of the important results is as follows:

Break Size, Cold Leg	Maximum Clad Temperature, °F	Total % Clad Burst
Double-ended	2450	75
6 ft ²	2190	73
3 ft ²	1780	65
0.5 ft ²	2050	77

Figures 14.3.2-13 through 14.3.2-16 present the maximum clad temperature transients for the design case and the case where adiabatic conditions exist after blowdown for the double-ended, 6 sq ft and 3 sq ft cold leg break sizes. For the 0.5 sq ft break, blowdown is not complete until after reflooding has resulting in effective cooling of the core and a continuously decreasing cladding temperature. This occurs at approximately 104 seconds. The case with adiabatic conditions after this time is presented in Figure 14.3.2-16.

Experimental Program For Fuel Rod Evaluation

The performance of the fuel rods during a simulated loss of coolant accident has been evaluated in a test program which is described in WCAP-7379-L volume I and volume II.

Volume I (Westinghouse proprietary) describes burst, quench and eutectic formation tests with unirradiated tubes and an evaluation of the data from both volumes. An interpretation with regard to the postulated sequence during the loss-of-coolant accident is given.

Volume II (non-proprietary) reports the results of work under AEC Contract At (30-1) 3017 and describes burst and quench tests on irradiated tubes.

Results: Fragmentation of Clad as a Result of Quenching

No rod shattering or any observable change in the geometric appearance of the rod occurred for any temperature of Zr-oxide combination that would be expected following a loss of coolant accident for this plant. Failure of the samples occurred only for Zr-oxide conditions which far exceed the maximum postulated Zr-H₂O reaction for this plant.

Results: Eutectic Formations

Tests results from the eutectic formation series indicated that operation in excess of postulated peak fuel cladding temperatures for a period of several minutes did not disturb the coolant flow area although evidence of reaction and some local melting at the point of contact did occur. In no case did the tube fuse to the spring nor were droplets or sputtering detected to block the coolant flow area. These tests were run under more severe conditions than those expected in this reactor during a loss of coolant accident.

Results: Clad Perforation and Deformation

During a loss-of-coolant accident, the clad temperature may get sufficiently higher, so that bursting or swelling of the clad would occur by virtue of the internal gas pressure and the significant reduction of clad strength. Clad bursting or swelling is of concern due to the possibility of releasing large quantities of fuel and/or blocking the flow channel sufficiently so that core cooling would be insufficient to prevent fuel rod melting.

3 Early flow blockage analyses⁽¹⁴⁾ took the very conservative and unsubstantiated position that four rods would fail into the same flow channel at the same elevation. This geometry arrangement would result in the most pessimistic flow blockage that could occur. Based upon the previously reported expansion data of 10 to 15 percent per rod, an equivalent single-channel blockage of about 50 percent could be projected. This amount of blockage would result in a negligible increase in the clad temperature and in the extent of metal-water reaction.

More recent burst tests⁽¹⁵⁾ have invalidated the earlier assumption of uniform flow blockage of 10-15% for a single rod: expansions considerably greater than 10-15% have been obtained.

The single rod bursts were random both aximuthally and axially although the length of the uniformly heated zone was short. It is expected that uniform axial heating over a longer length will also demonstrate randomness. It is important to note that satisfactory ECCS performance requires only a small fraction of the flow channel to be unblocked at a given location, and only a minimal amount of axial stagger between bursts is needed to ensure this even with all other factors in their most adverse combination.

The single rod tests have indicated that rod to rod interference may occur following rod burst and must be considered. The quantitative evaluation of the influence of adjacent rods in a fuel assembly would be difficult, if not impossible, to determine analytically. Therefore, the rod burst program was extended to include multi-rod burst tests. Westinghouse has performed multi-rod burst tests (MRBT) to demonstrate that the rods in a PWR rod bundle burst randomly so that a minimal flow channel area, for core cooling purposes, is maintained.

An 8 x 8 array of 3 ft long rods, surrounded by a heated shield, forms the basic test configuration. The center 4 x 4 rods are pressurized. Actual grid sections were used to note their affect, if any. Radial power variations, including the presence of thimble tubes, were simulated in the 4 x 4 array. Twelve tests on the 4 x 4 rod bundles were conducted for the following range of variables: 200 and 2250 psia nominal initial pressure (at 725°F), and 5, 20 and 50°F/sec nominal heatup rate from the initial temperature using unirradiated, unhydrided Zircaloy. Duplicate tests were run at each set of conditions. The MRBT results are applicable for both initially internal pressurized and non-pressurized fuel rods. Fuel rods for H. B. Robinson Unit No. 2 are designed such that the end of life internal gas pressure does not exceed the external primary system pressure of 2250 psia. This criteria is satisfied for both pressurized and non-pressurized fuel rods. As stated above, the range of variables considered in the MRBT cover both low (200 pisa) as well as high (2250 psia) internal gas pressures and slow (5°F/sec) as well as fast (50°F/sec) heating rates.

Amendment 7

Preliminary analysis of the test data indicates that the burst locations do occur in a staggered manner axially along the fuel rods, thus making impossible the occurrence of an extensive flow area blockage capable of preventing adequate core cooling. The maximum average (assembly-wise) flow area blockage measured inside the pressurized and heated 4 x 4 array was less than 50% of the nominal flow area at any elevation. This value was obtained by averaging the results of all duplicate runs. The corresponding local assembly flow redistribution would result in less than a 25% reduction in the local assembly mass flow rate when compared to the no flow blockage case.

A preliminary analysis was made to determine the effect of geometry distortion, as seen in the MRBT, on the peak clad temperature experienced in a double-ended cold leg break loss-of-coolant accident. The analysis assumed for the hottest assembly a worst case geometry similar to that shown in Figures 14.3.2-29 and 14.3.2-30 which represents a cross section of the internal 4 x 4 array. In evaluating the effect of geometry distortion, the flow redistribution between assemblies was first determined. This assembly-wise flow redistribution was then superimposed on a subchannel analysis considering both subchannel local flow area reduction and rod to rod contact. The effect of the rod to rod contact was determined by analyzing the three dimensional transient temperature distribution in the hottest fuel rod. No convective heat transfer was considered for the portion of the fuel rod in contact with the adjacent rods. Heat transfer coefficients, adjusted for the reduction in flow area, were used for the remaining clad surface. This is a more realistic manner for determining the effects of geometry distortion than just considering a local subchannel blockage. The heat generated by the metal-water reaction was conservatively evaluated using Baker's parabolic rate law even where no flow, and therefore, no convective heat removal was assumed.

A double-ended cold leg break LOCA analysis for the H. B. Robinson Unit No. 2 reactor, utilizing the preliminary results of the MRBT just described, yielded a peak clad temperature increase of less than 100°F over the no blockage analyses previously presented.

Clad Perforation Model

Calculations are performed to determine the number of fuel rods that might fail during the thermal transient following a rupture in the primary cooling systems. In this analysis, fuel rods are considered to fail when the differences between the internal and external pressure exceeds the rod burst pressure.

The calculations are performed in the following manner:

- A. The maximum clad temperature vs. time transients on the rods in the core are calculated assuming no change in the core geometry.
- B. For each radial region of the core, a burst pressure vs. time curve is obtained by combining the temperature transient curve and the burst pressure vs. temperature curve.
- C. The hot fuel volumes and the hot clad volumes obtained in the fuel rod transient study are used to determine the hot void volume in the fuel rod as a function of time. The internal gas pressure distribution as a function of time is calculated considering the actual fuel rod power histories at the end of the equilibrium cycle when the maximum internal pressures are expected to exist.
- D. All rods are assumed to fail if at any time during the transient the difference between internal gas pressure and external system pressure exceeds the burst pressure of the clad.
- E. An evaluation is then performed to determine the rod with the lowest power rating (kw/ft) which fails. All rods above this power level then are considered as exhibiting rod bursting.

Results of the rod burst evaluation is presented in the table on page 14.3.2-19.

Results - Small Breaks

The analysis carried out and presented in the previous section demonstrated the adequacy of the accumulators to terminate core exposure and limit the temperature rise of the core for large area ruptures. For smaller breaks the discharge of fluid through the hole is less severe and for small enough breaks the high head safety injection pump is capable of maintaining flooding of the core hot spot for the entire blowdown. Where the hot spot remains covered no clad damage is expected.

Rupture of very small cross sections (up to about the equivalent of a 3/4" connecting pipe) will cause expulsion of coolant at a rate which can be accommodated by two of the three charging pumps well before the core is uncovered. Since instrument taps and sample connections are less than 3/4" diameter protection from rupture of this line is afforded by the charging pumps.

For smaller leaks, (up to about 1/2 inch) these pumps would maintain an operational level of water in the pressurizer, permitting the operator to execute an orderly shutdown. It should be noted that the safety injection pump also provide protection for these small ruptures.

Should a larger break occur, resultant loss of pressure and pressurizer liquid level will cause reactor trip and initiation of safety injection supplementing the charging flow.

Using the SLAP code, break sizes of 2, 3, 4, and 6 inch equivalent diameters were analyzed. The analysis shows that for breaks smaller than 2", the core is not uncovered, and thus they are not presented. Three combinations of safety injection pump availability were considered. These were:

1. Full system; three pumps, all lines delivering.
2. Single Failure; two pumps delivering through all lines.

3. Single failure; two pumps delivering, one line spills.

The delivery curves for these cases are presented in Figure 14.3.2-17. For cases two and three the pumps are operated on diesel power.

The Reactor Coolant System pressure and volume for these cases are presented in Figure 14.3.2-18 through 14.3.2-21 and 14.3.2-22 through 14.3.2-25, respectively.

As indicated on the curves the hot spot remains flooded for all breaks up to and including a 4" diameter hole. It should be noted that the volumes presented are the quiet levels. No credit is taken for the actual froth level that would occur due to void formation in the core.

The existence of a water filled loop seal was considered in the transient. That is, the plot of the water level in the core takes into account the depression of the core water level necessary to maintain a full downcomer and loop seal. This depicts a break for the worst break location, i.e., a cold leg break between the pump outlet and the reactor vessel inlet.

Therefore, from the results of analyses it is concluded that a break size of about 4 inches defines the upper limit of protection afforded by two high head safety injection pumps.

For a 6 inch break the hot spot is uncovered for a short period of time for the minimum injection case, but remains covered for the full injection case.

All breaks up to and including a 4" diameter hole were analyzed with the safety injection pumps delivering through five lines since hot leg injection is available in five minutes. All 6" breaks were analyzed with three lines delivering.

A core thermal analysis was performed for the 6 inch break with peak clad temperatures being evaluated for the following cases:

1. DNB occurring at 0.5 seconds after the break.
2. No DNB occurs.

The analysis utilized the benefit of the froth level core volume transient shown in Figure 14.3.2-26 for the minimum safety injection case. Assuming DNB occurs (Case 1) the peak clad temperature of 1585°F occurs at the hot spot (core mid-plane). For Case 2, since no DNB occurs and the hot spot of the core never becomes uncovered, the hot spot clad temperature gradually decreases from its initial steady state value of approximately 720°F. However, the upper portion of the hot rod obtains a slightly higher maximum clad temperature of approximately 1000°F due to the portion of the rod being uncovered for approximately 70 seconds. During this uncover period, the upper part of the hot rod is cooled by the steam generated in the covered portion of that core.

In the previous cases no credit was taken for operator action. Since time is available in a small break accident, it is expected that the operator will take control of the accident. By dumping steam through the steam generator relief valves the Reactor Coolant System can be depressurized. This depressurization of the Reactor Coolant System would result in less discharge through the break and greater addition from the Safety Injection System. The net result is a greater capability to maintain core flooding.

The action the operator would perform for this accident would be very similar to a normal cooldown. In a blackout situation the atmospheric dump valves are used, and when power is available the condenser dump would be used.

Figure 14.3.2-27 presents the volume transient for the several breaks considering only atmospheric steam dump and the minimum safety injection pump case. The pressure transients for these cases is presented in Figure 14.3.2-28.

Conclusion

For breaks up to and including the double-ended severance of a reactor coolant pipe, the Safety Injection System with partial effectiveness will prevent clad melting and assure that the core will remain in place and substantially intact with its essential heat transfer geometry preserved. The final core cooling systems design meets the core cooling criteria with substantial margin for all cases. It was also concluded from this study that the high head pumps are capable of maintaining hot spot core flooding for all break sizes up to approximately a 4-inch connecting pipe. For larger breaks the needed protection is supplied by the accumulators.

REFERENCES

1. "Flash; a Program for Digital Simulation of the Loss of Coolant Accident" S. F. Margolis, and J. A. Redfield, Bettis Atomic Power Laboratory, Report WAPD-TM-534.
2. "The Discharge of Saturated Water Through Tubes", By H. K. Fauske, AICHE, Reprint 30, Seventh National Heat Transfer Conference, AICHE and ASMR, Cleveland, Ohio, August 9 to 12, 1964.
3. "Maximum Flow Rate of Single Component, Two-Phase Mixture" by F. H. Moody Paper No. 64-HT-35, and ASME publication.
4. "CHIC-KIN ... A Fortran Program for Intermediate and Fast Transients in a Water Moderated Reactor", V. A. Redfield, WAPD-TM-479, January 1, 1965.
5. W. H. Jens, and P. A. Lottes, "Analyses of Heat Transfer, Burnout, Pressure Drop, and Density Data for High Pressure Water," USAEC Report ANL-4627, 1951.
6. R. S. Dougall, and W. M. Rohsenow, "Film Boiling on the Inside of Vertical Tubes with Upward Flow of the Fluid at Low Qualities," MIT Report No. 9079, September, 1963.
7. H. Hausen, "Darstellung des Wärmeüberganges in Rohren durch verallgemeinerte Potenzbeziehungen," VDI Zeit., No. 4, p. 91, 1943.
8. W. M. Kays, "Numerical Solutions for Laminar-Flow Heat Transfer in Circular Tubes," Trans ASME, vol. 77, 1955, pp. 1265-2374.
9. D. M. McEligot, P. M. Magee, and G. Leppert, "Effect of Large Temperature Gradients on Convective Heat Transfer: The Downstream Region," J. of Heat Transfer, vol. 87, 1965, pp. 67-76.
10. D. M. McEligot, L. W. Ormand, and H. C. Perkins, "Internal Low Reynolds - Number Turbulent and Transitional Gas Flow with Heat Transfer," J. of Heat Transfer, vol. 88, 1966, pp. 239-245.
11. Davis, R. F., "The Physical Aspect of Steam Generation at High Pressure and the Problem of Steam Contamination," I. Mech. E., (1940).
12. "Fuel Heatup Simulation Tests", K. A. Dietz (ed.) Quarterly Technical Report, Engineering and Test Branch, October 1967 - December 1967, IDO-17242 (May 1968).
13. K. V. Moore, R. P. Rose, Transaction of ANS, Volume 9, No. 2, pg. 559 1966.

REFERENCES (Continued)

14. WCAP 7304-L "Safety Related Research and Development for Westinghouse Pressurized Water Reactors", April 1969, Page 28.
15. WCAP 7379-L "Performance of Zircaloy Clad Fuel Rods during a Loca-Single Rod Test", October 3, 1969.

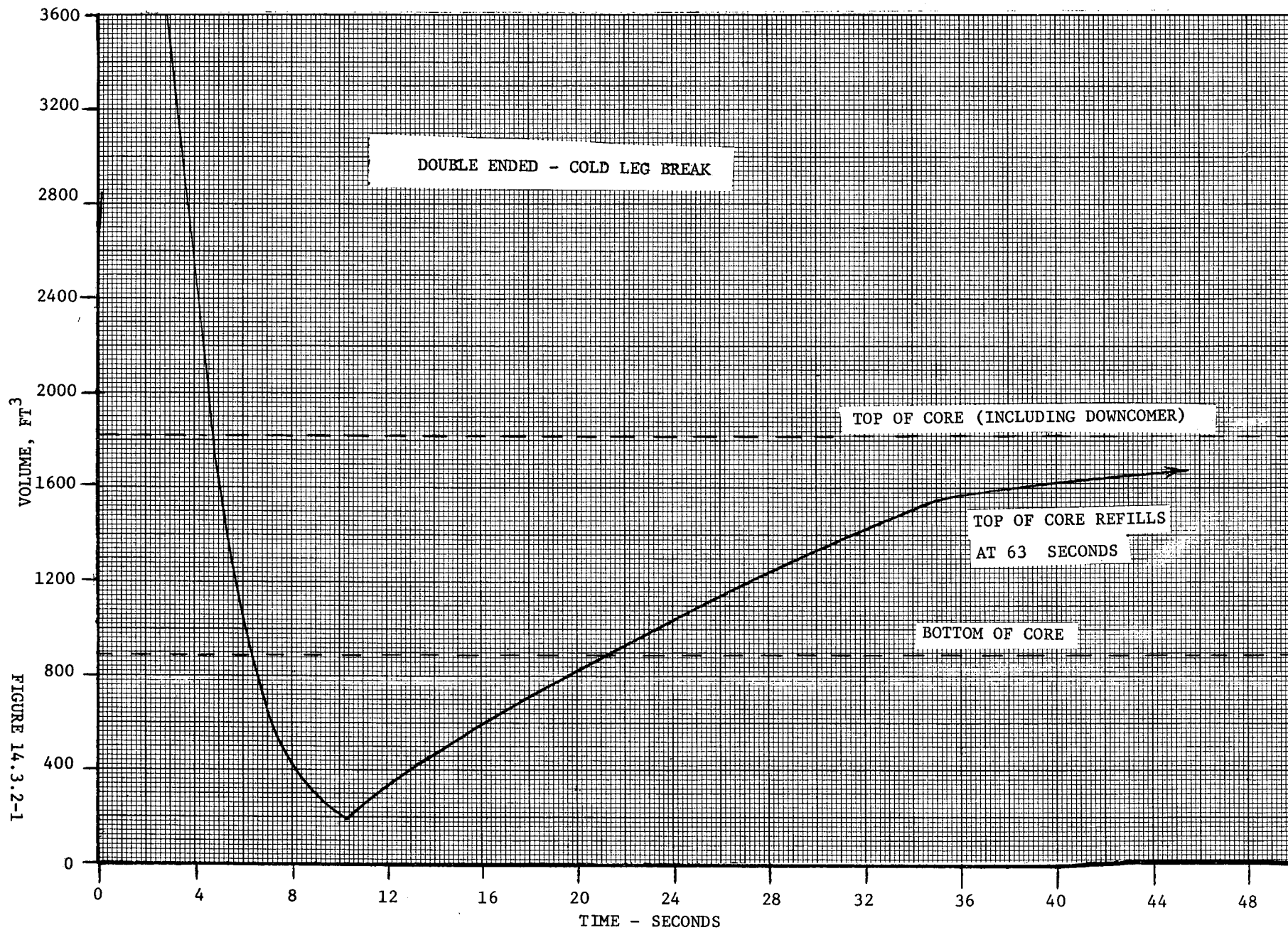


FIGURE 14.3.2-1

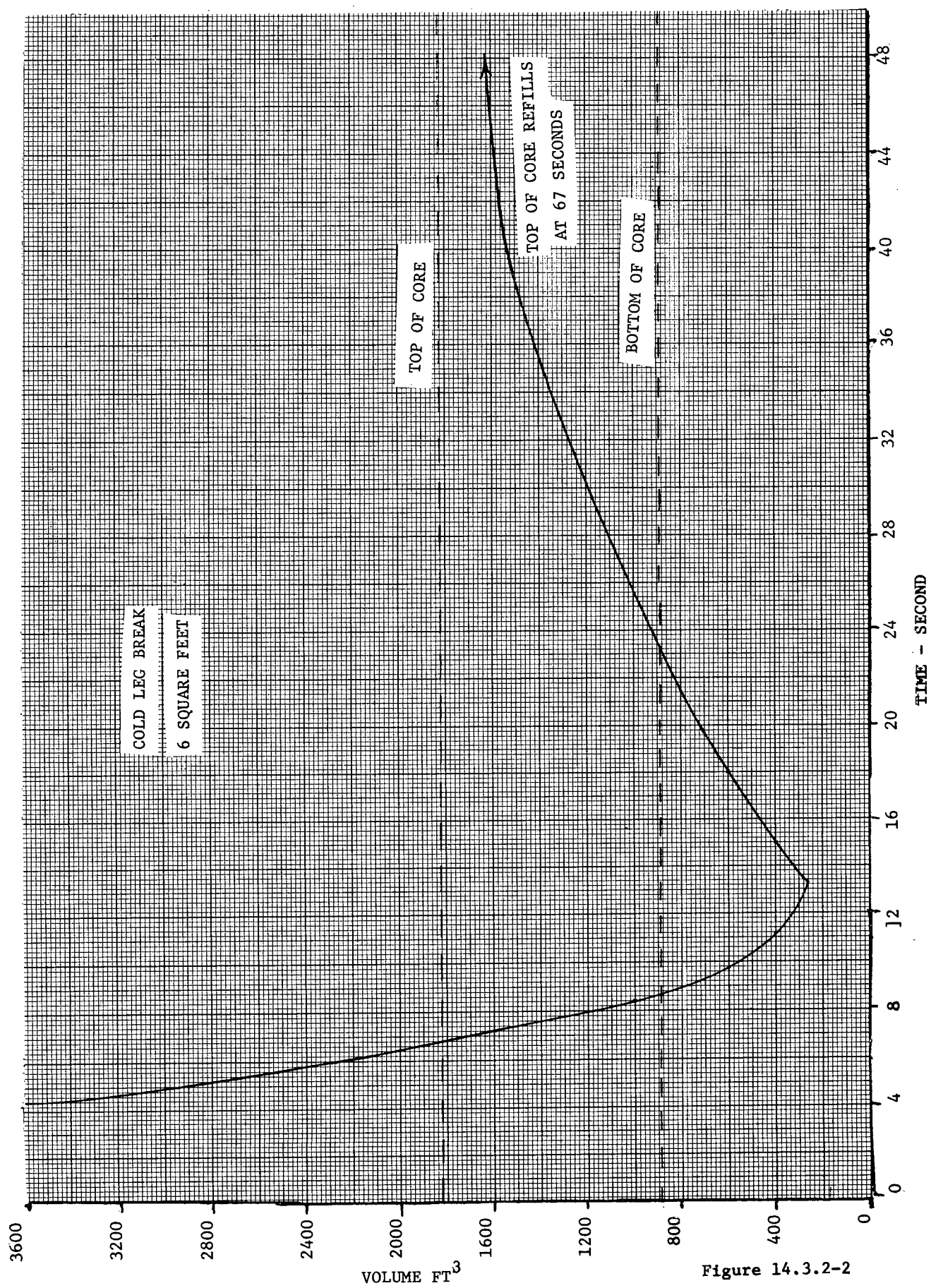
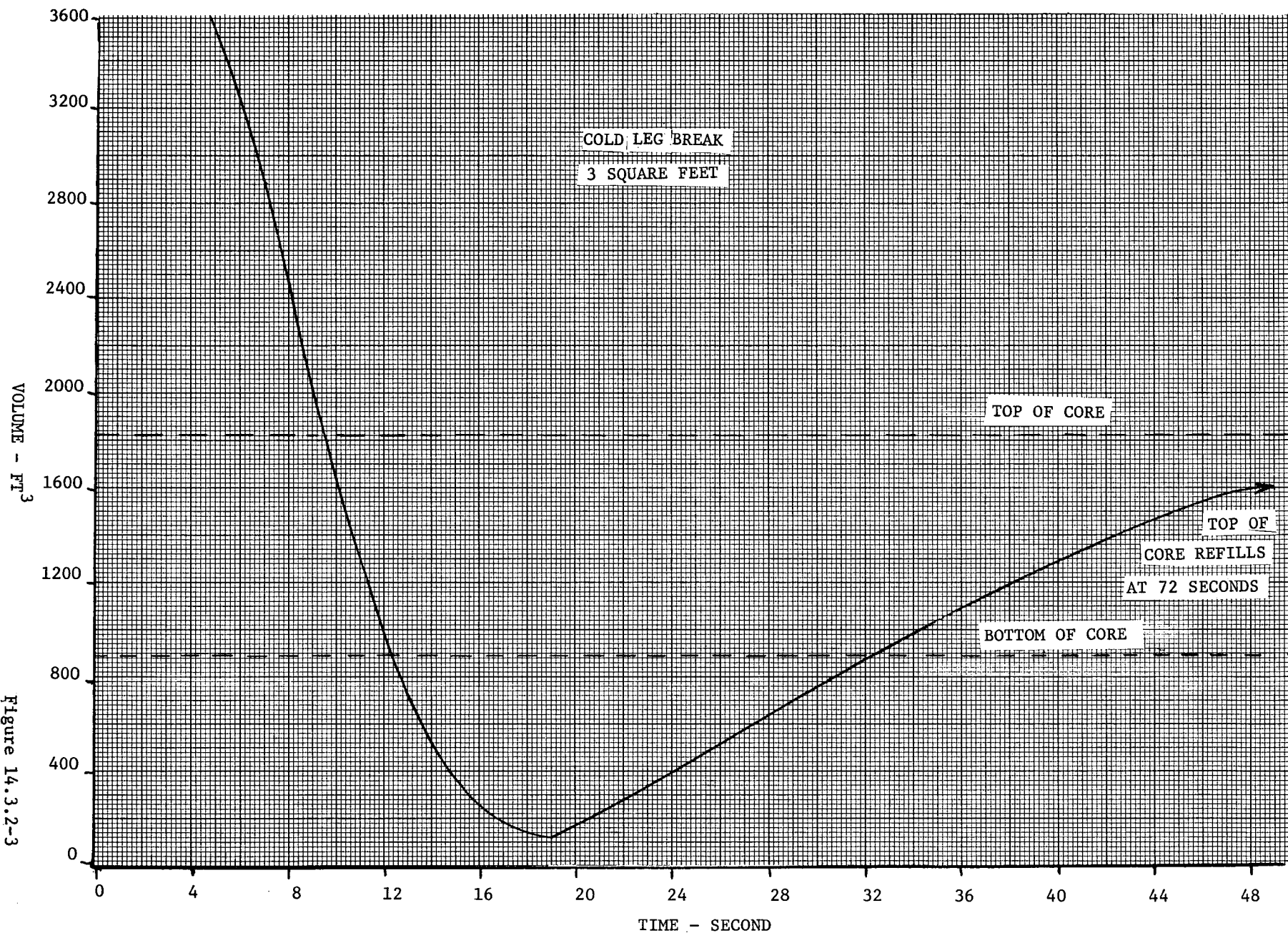


Figure 14.3.2-2

Figure 14.3.2-3



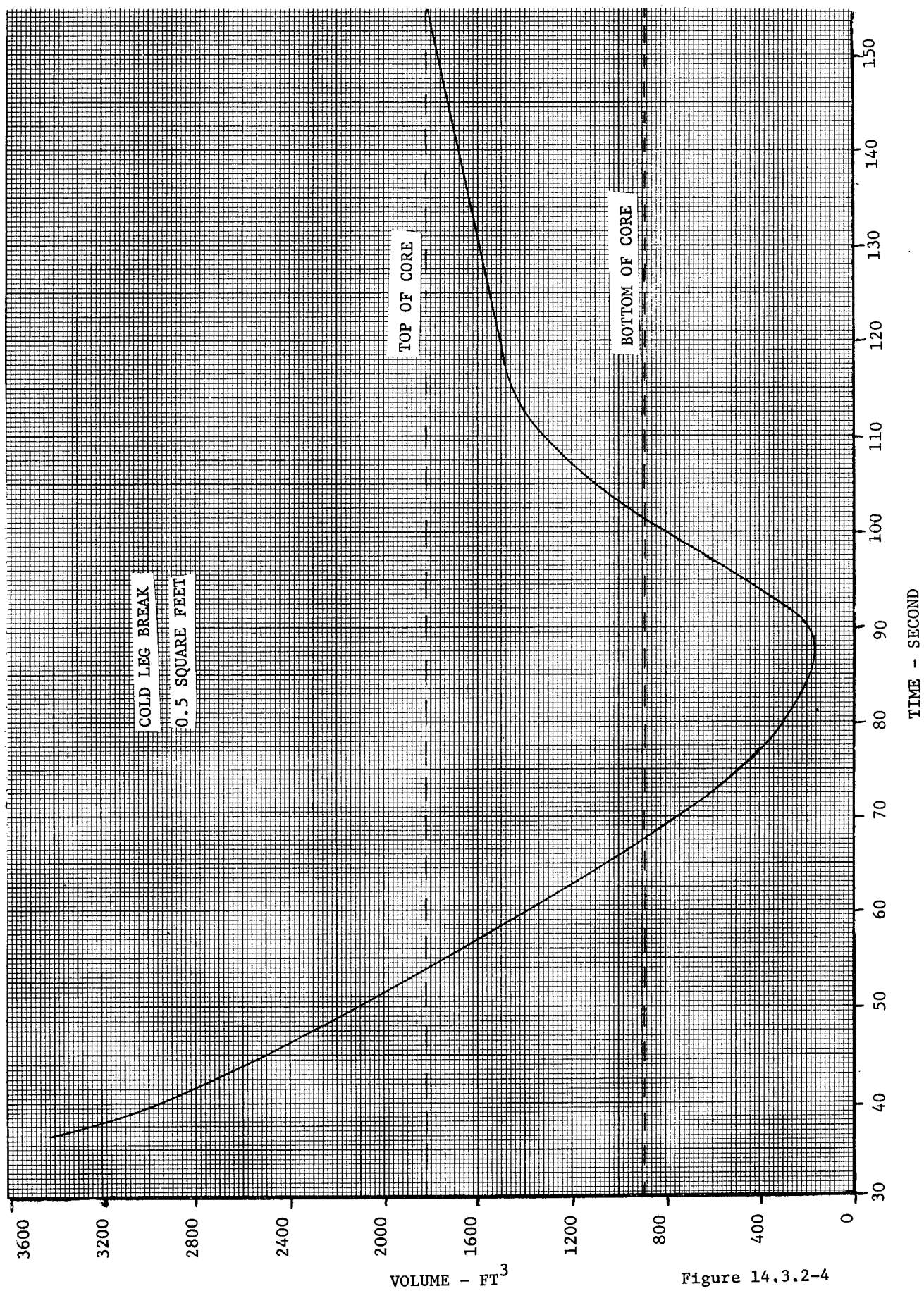
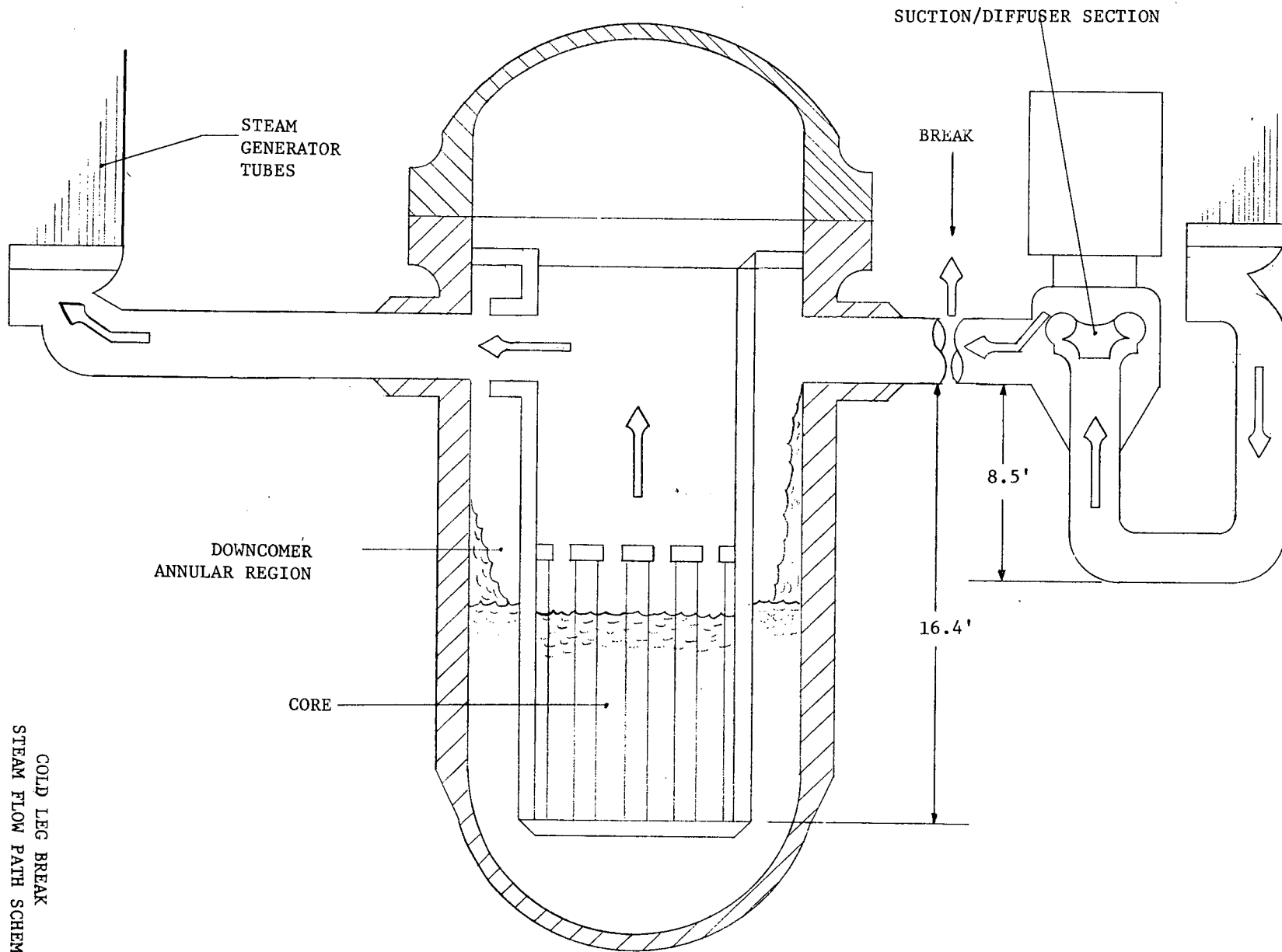


Figure 14.3.2-4



COLD LEG BREAK
STEAM FLOW PATH SCHEMATIC
FIGURE 14.3.2-5

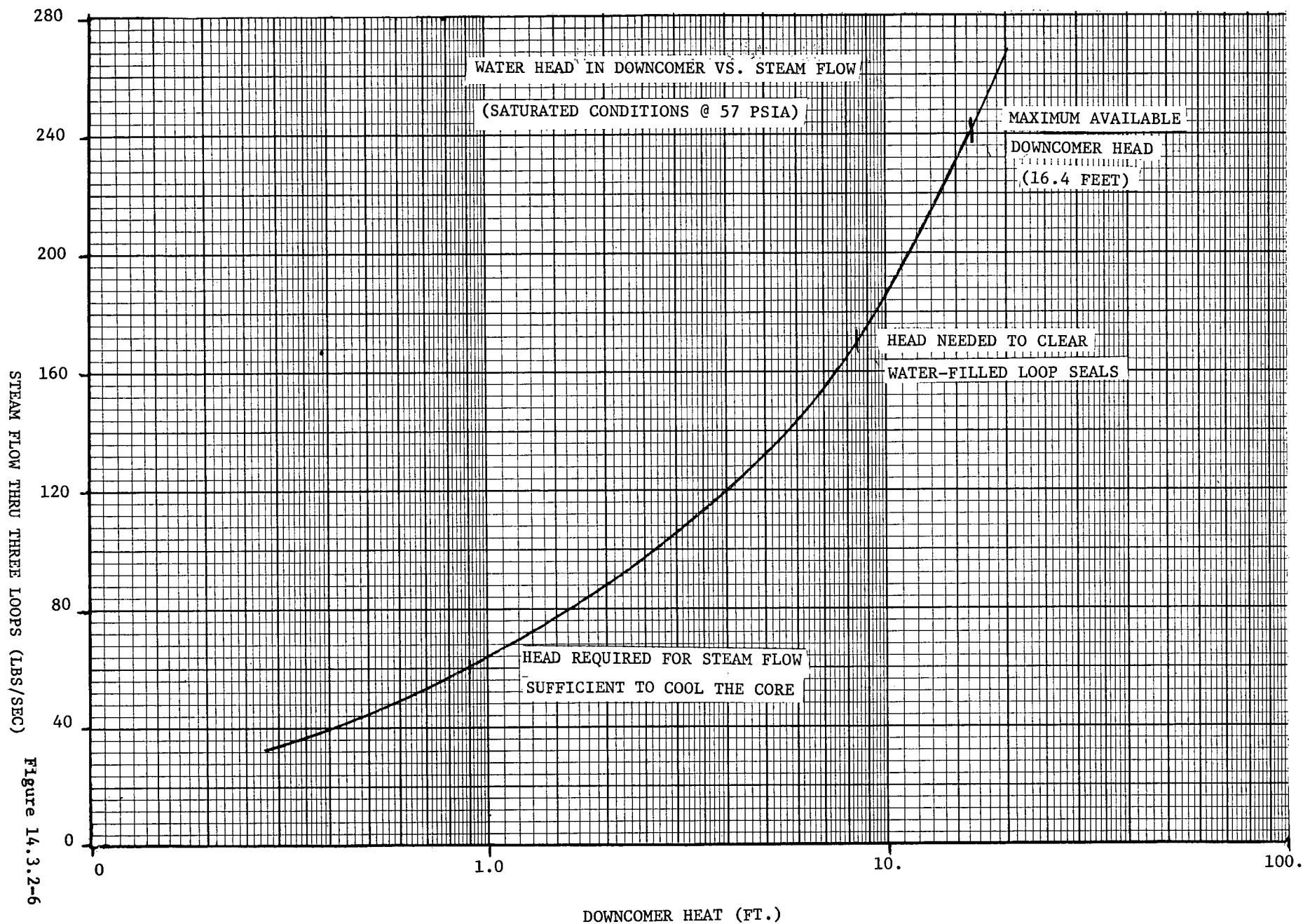


Figure 14.3.2-6

AVAILABLE DOWNCOMER HEAD VS. TIME
DOUBLE-ENDED COLD LEG BREAK

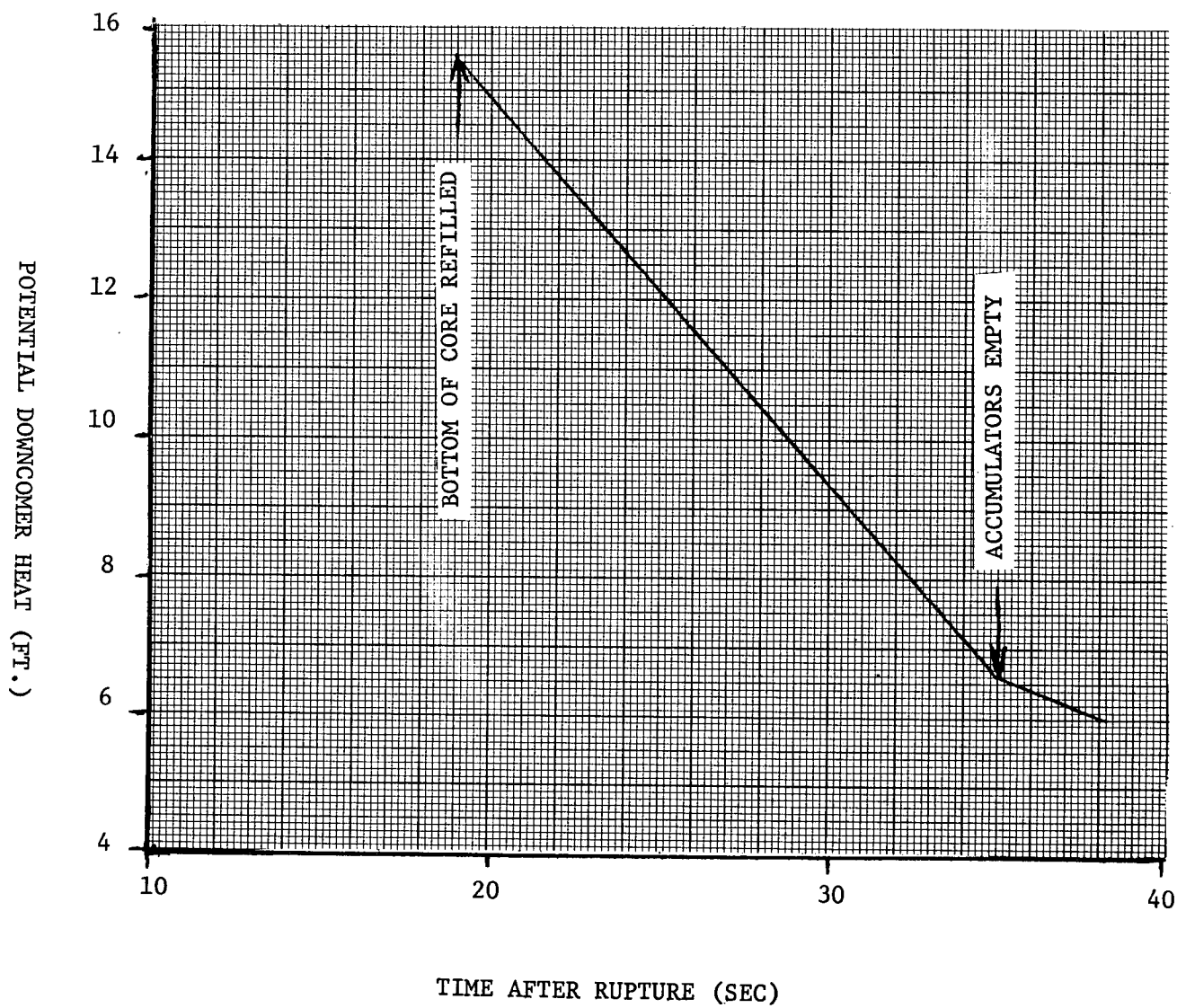


Figure 14.3.2-7

POWER TRANSIENT DURING BLOWDOWN

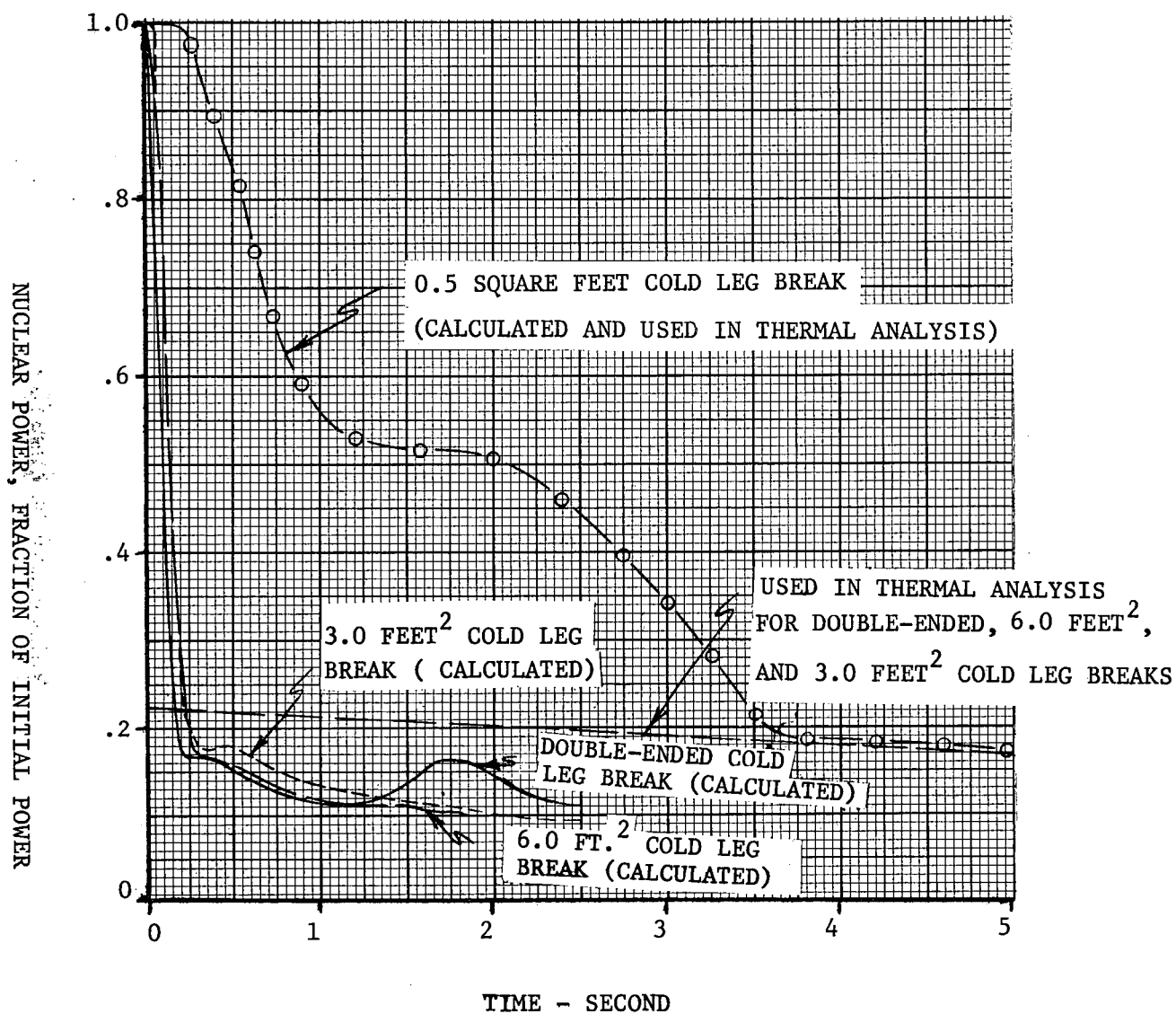


Figure 14.3.2-8

DOUBLE-ENDED COLD LEG BREAK

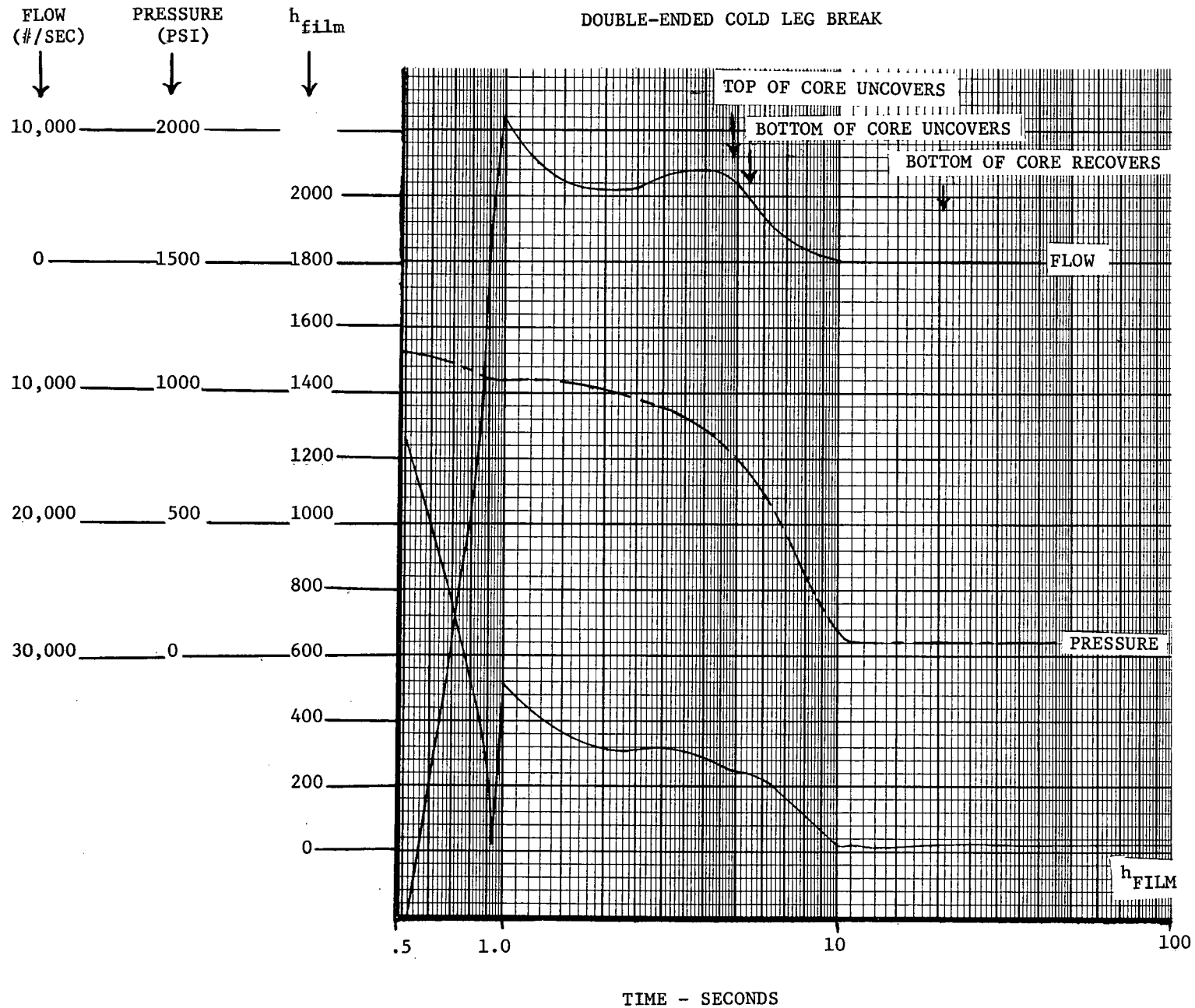


Figure 14.3.2-9

COLD LEG BREAK
6 SQUARE FEET

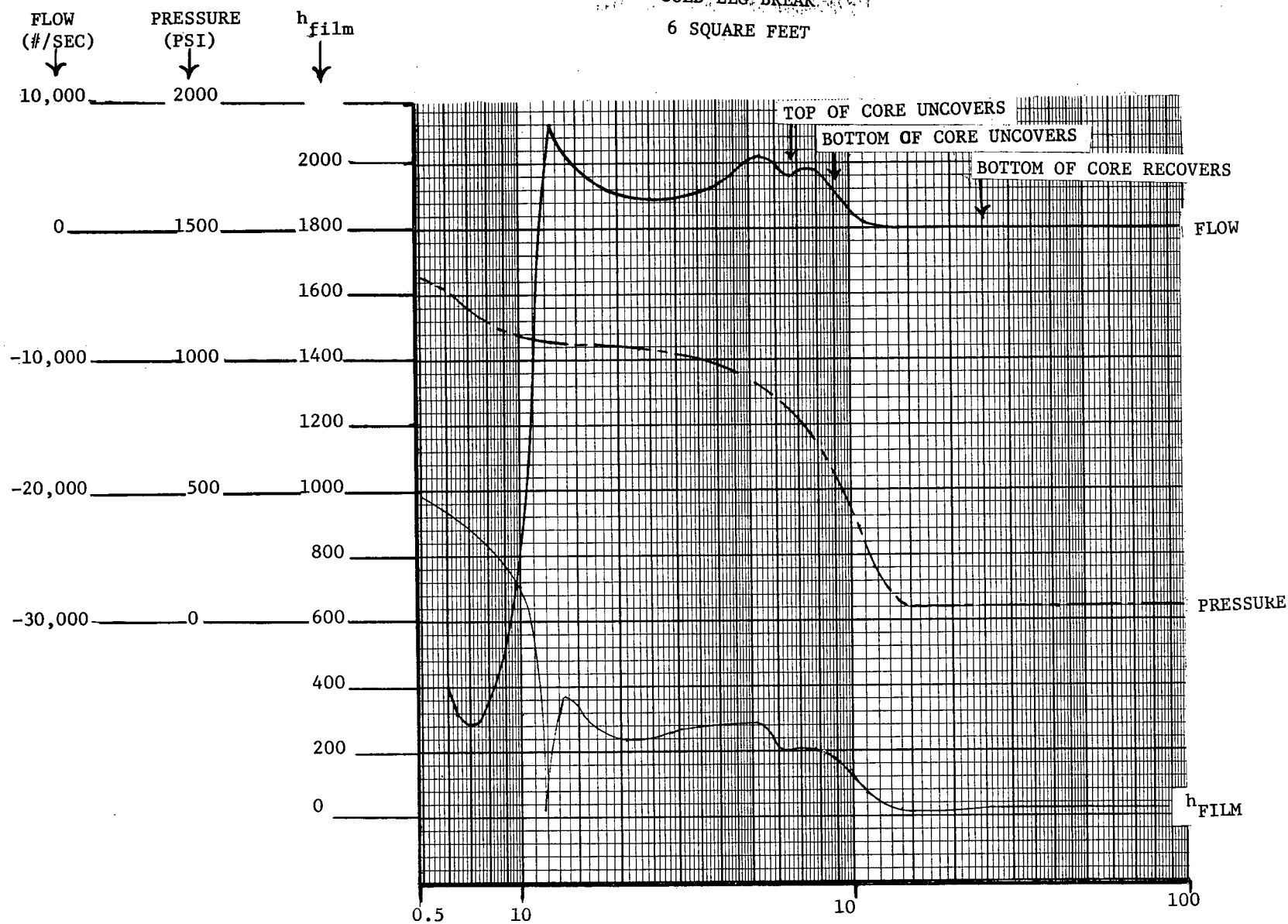


Figure 14.3.2-10

COLD LEG BREAK
3 SQUARE FEET

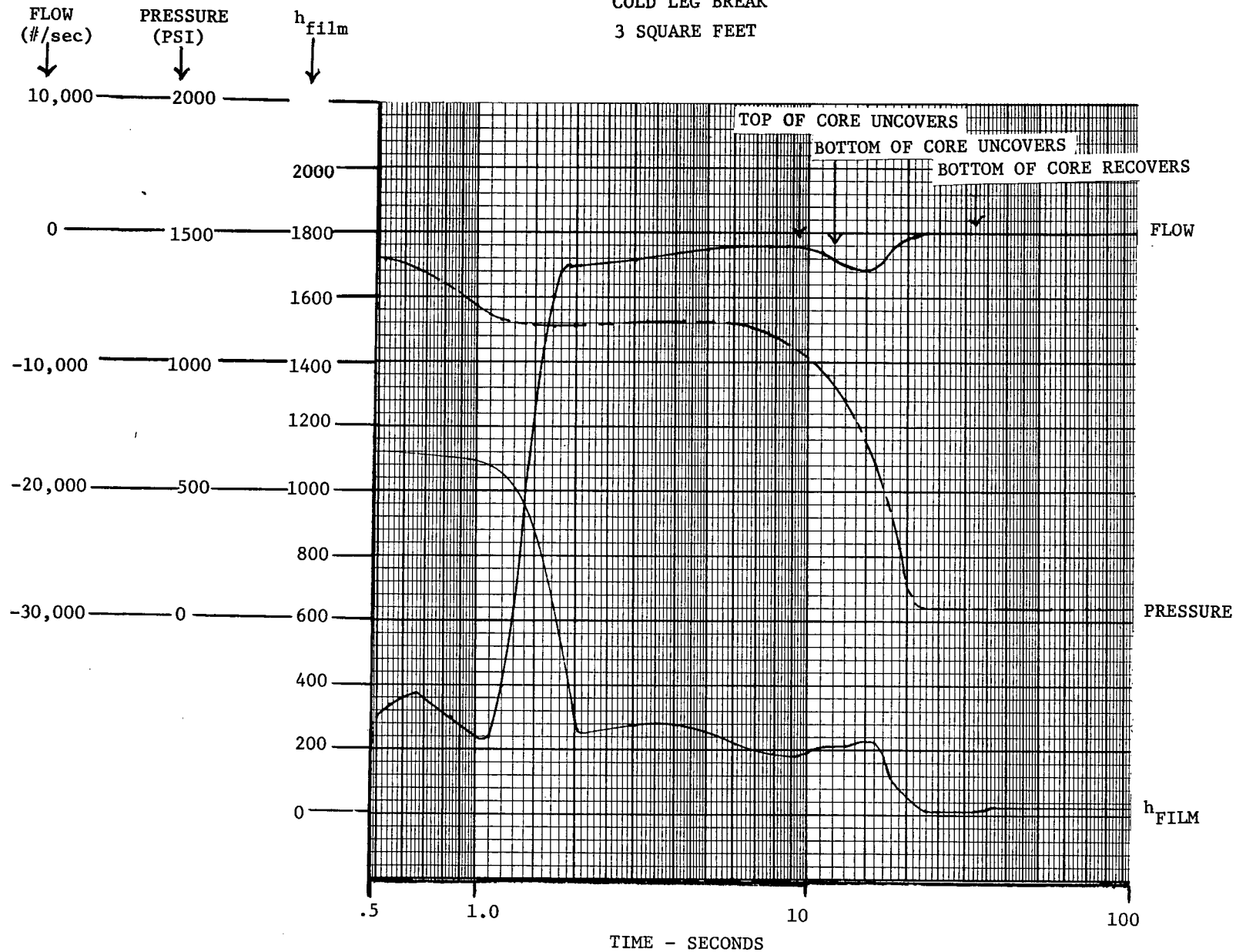


Figure 14.3.2-11

COLD LEG BREAK
.5 SQUARE FEET

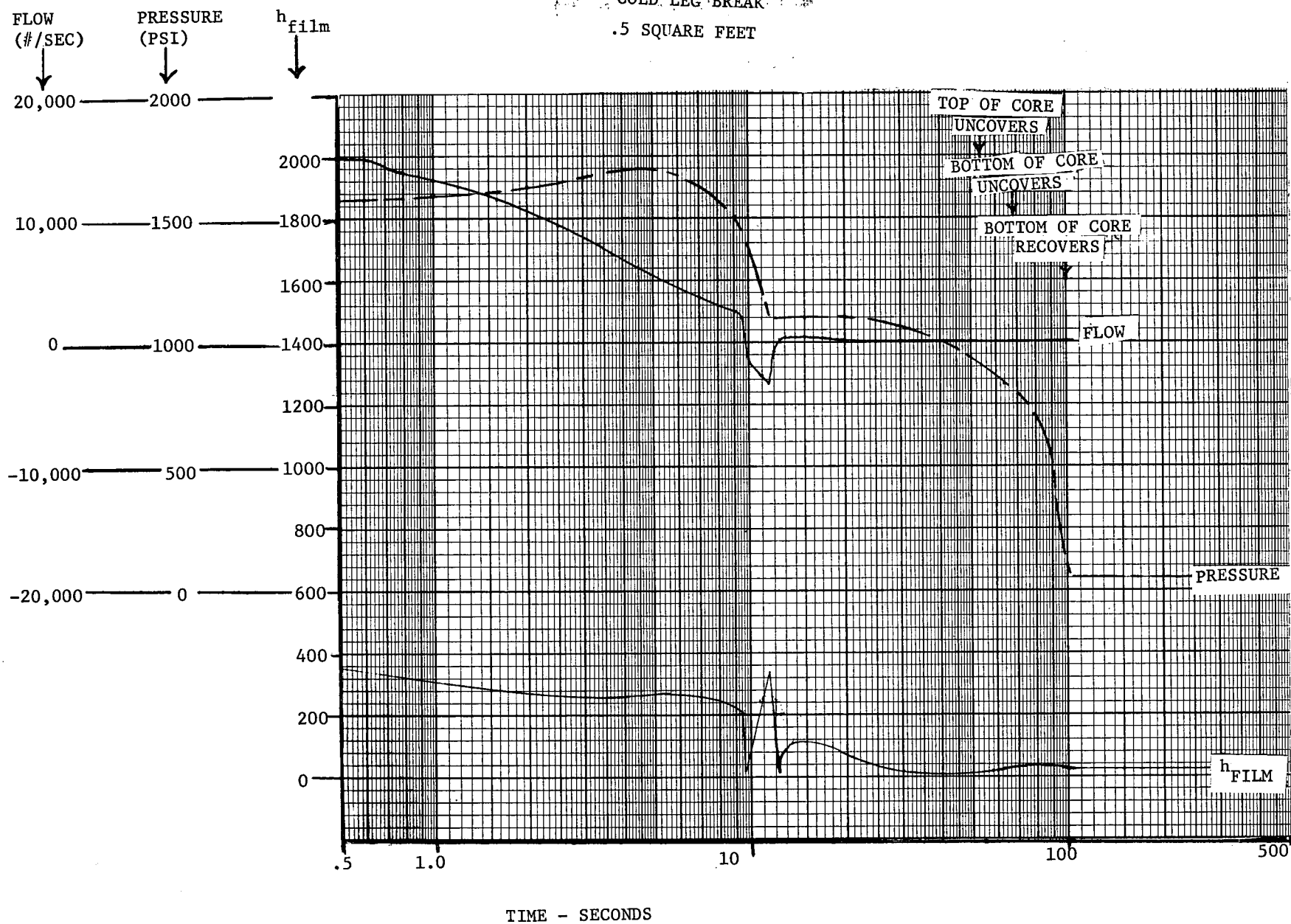


Figure 14.3.2-12

DOUBLE-ENDED COLD LEG BREAK
HOT SPOT CLAD TEMPERATURE VS. TIME

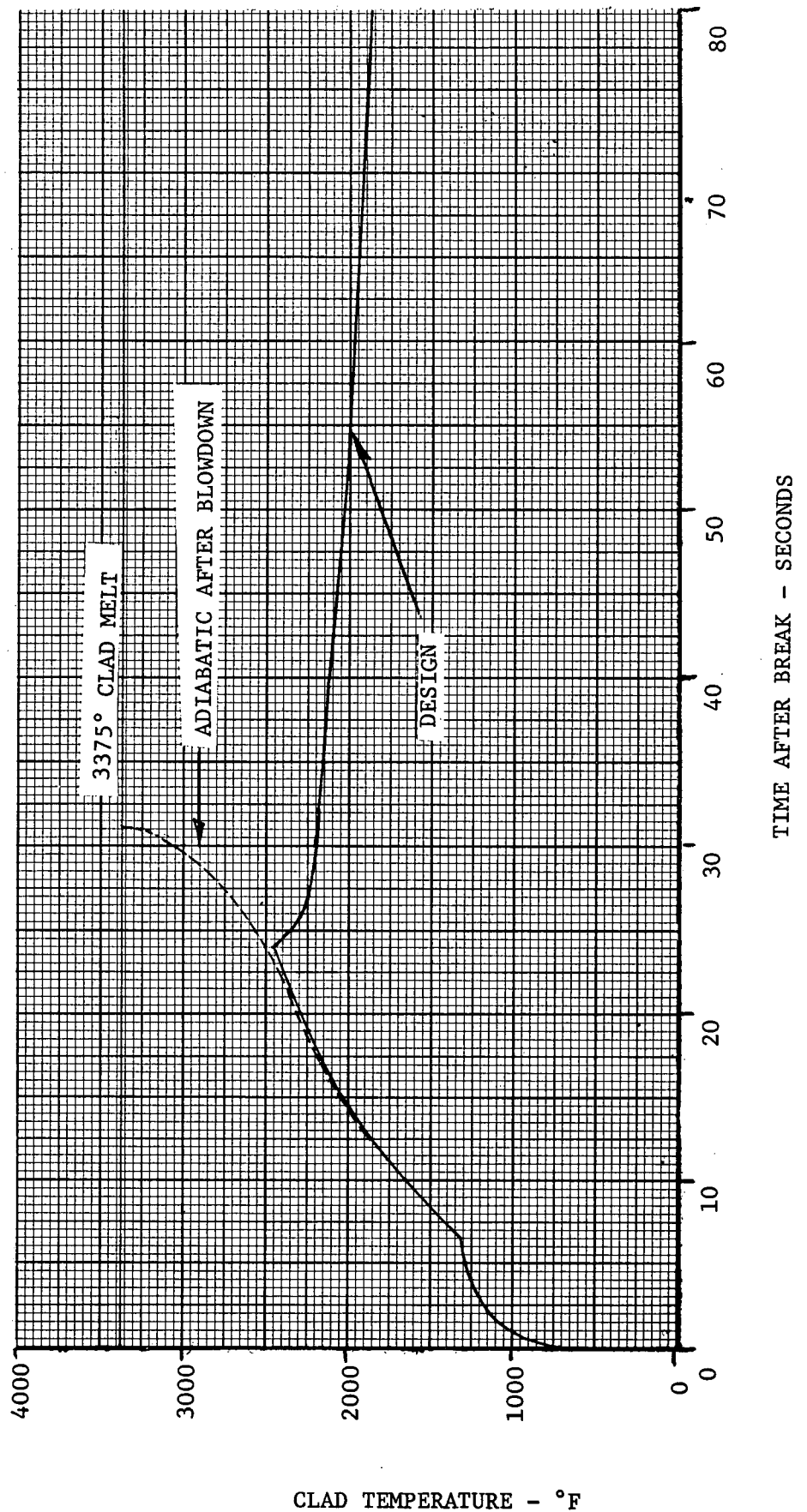


Figure 14.3.2-13

COLD LEG BREAK

6 FEET²

HOT SPOT CLAD TEMPERATURE VS TIME

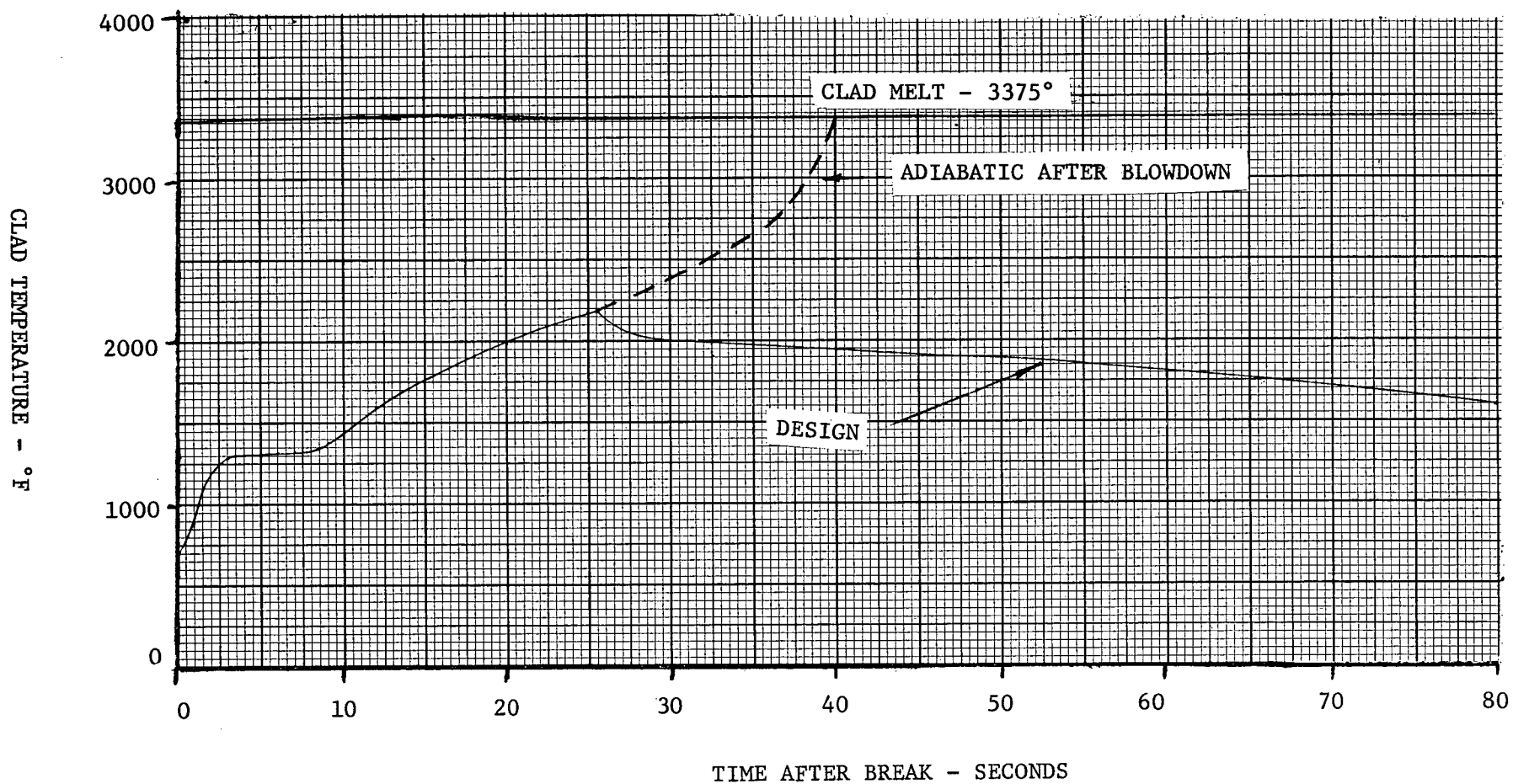


Figure 14.3.2-14

COLD LEG BREAK
3.0 FEET²
HOT SPOT CLAD TEMPERATURE VS. TIME

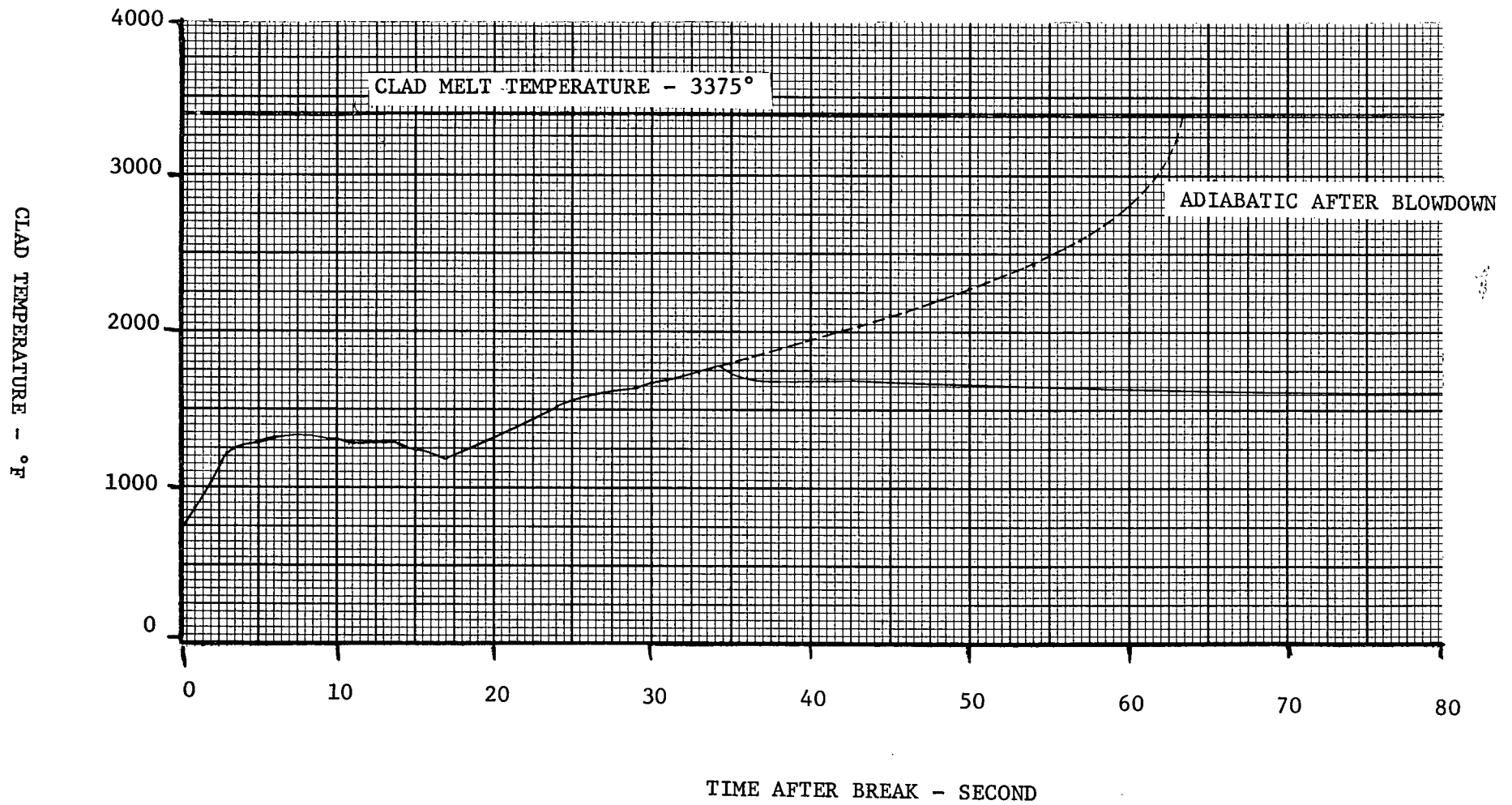


Figure 14.3.2-15

COLD LEG BREAK
0.5 FEET²
HOT SPOT CLAD TEMPERATURE VS. TIME

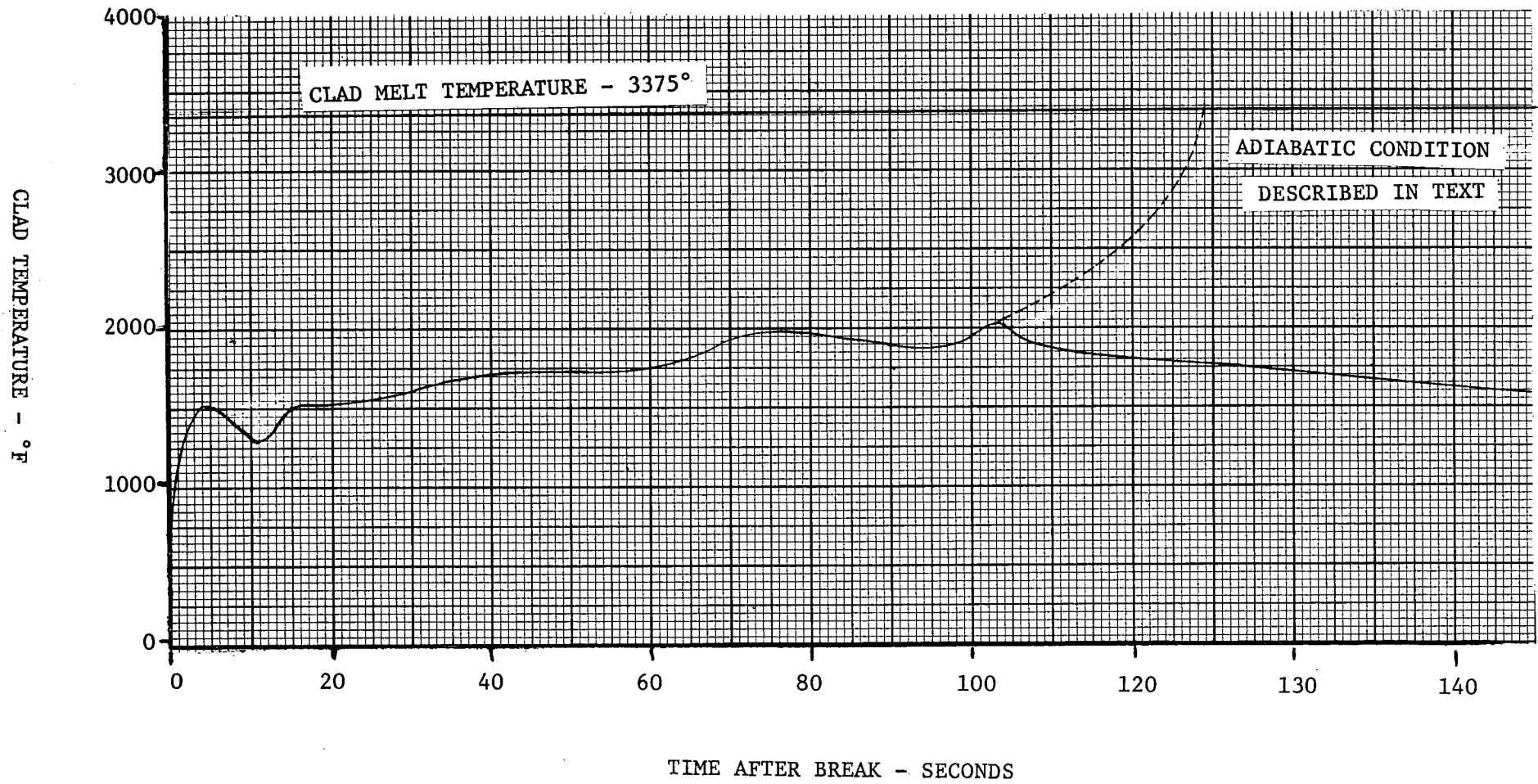


Figure 14.3.2-16

SAFETY INJECTION CURVE

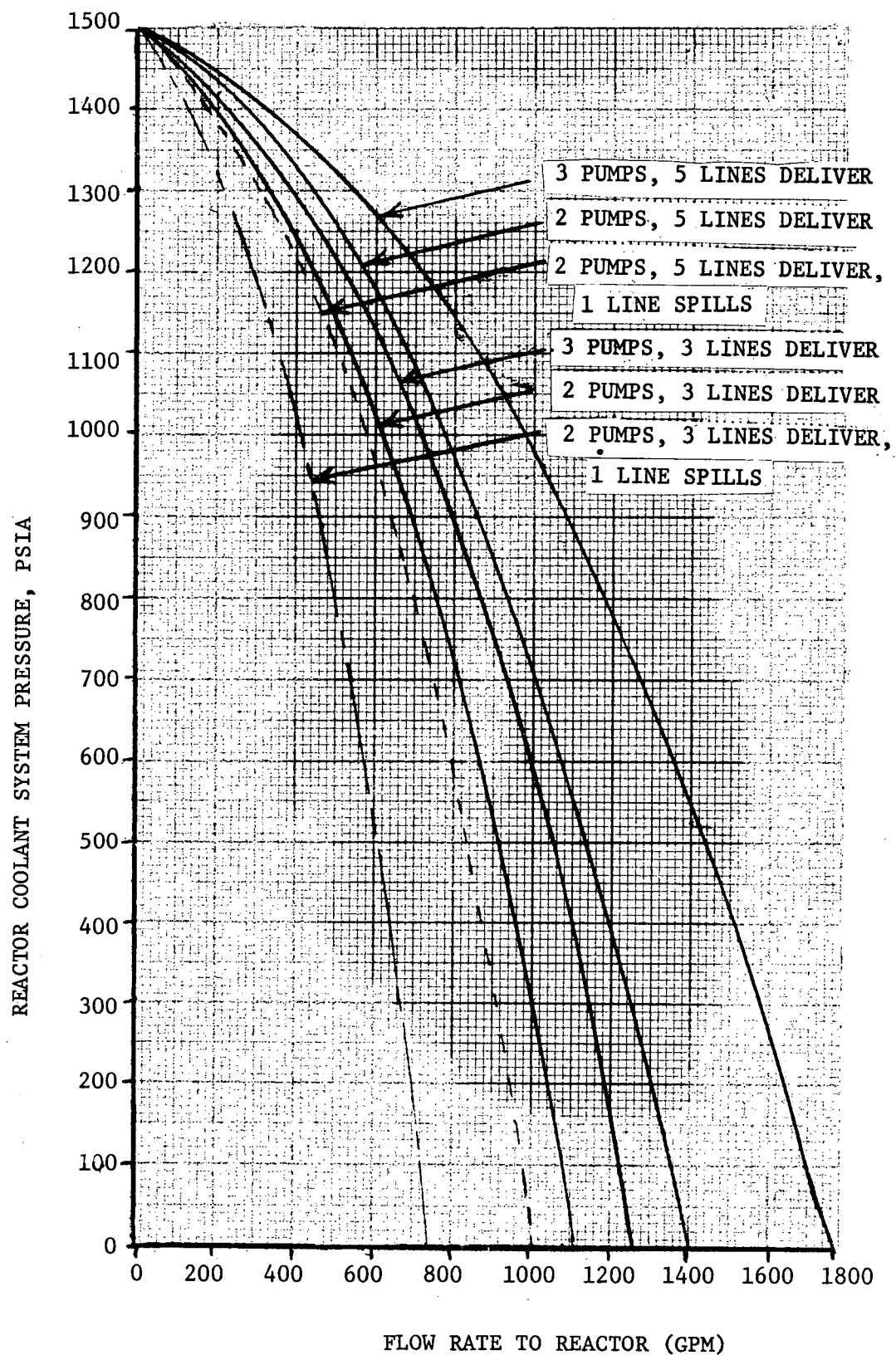


Figure 14.3.2-17

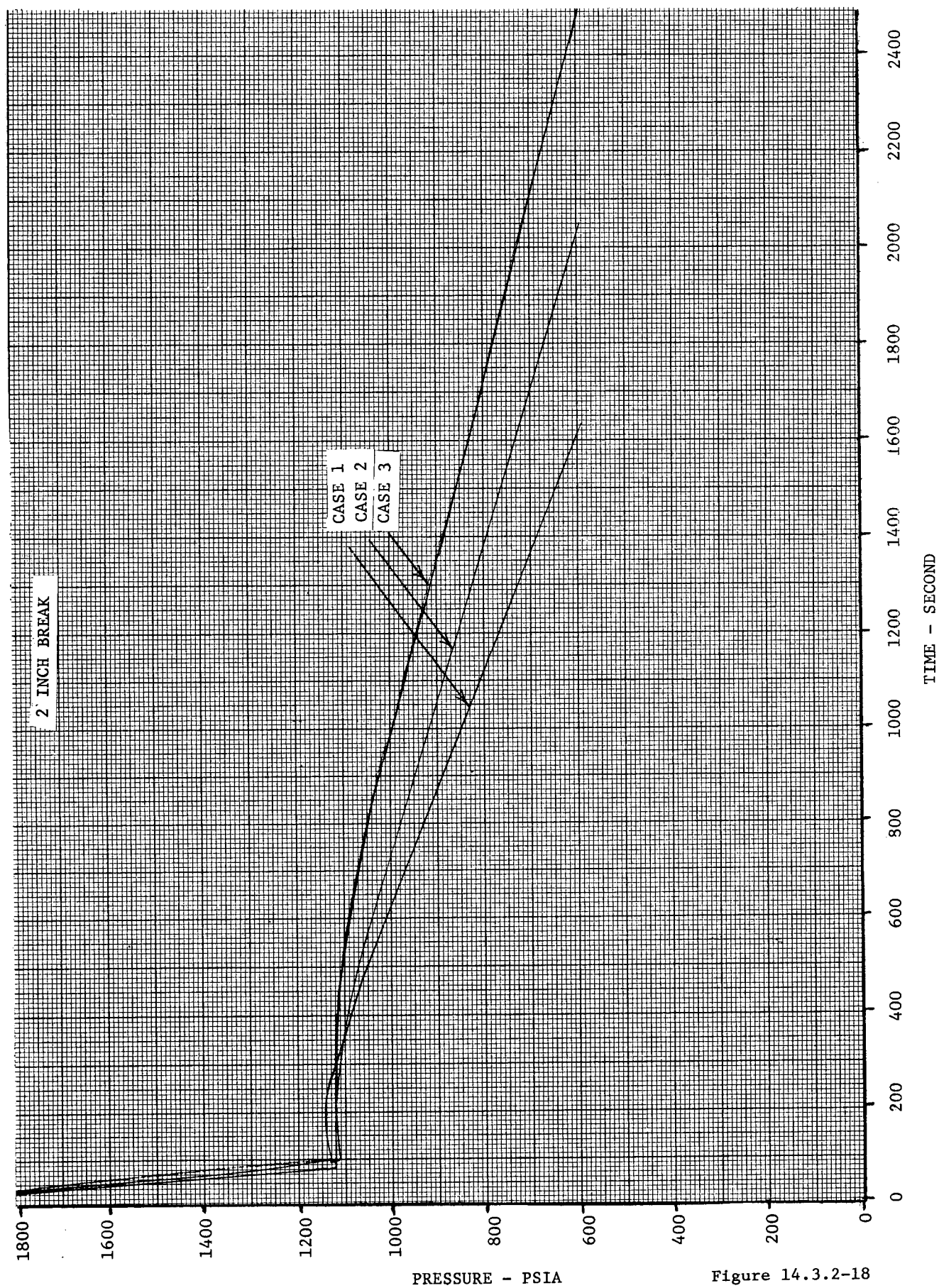


Figure 14.3.2-18

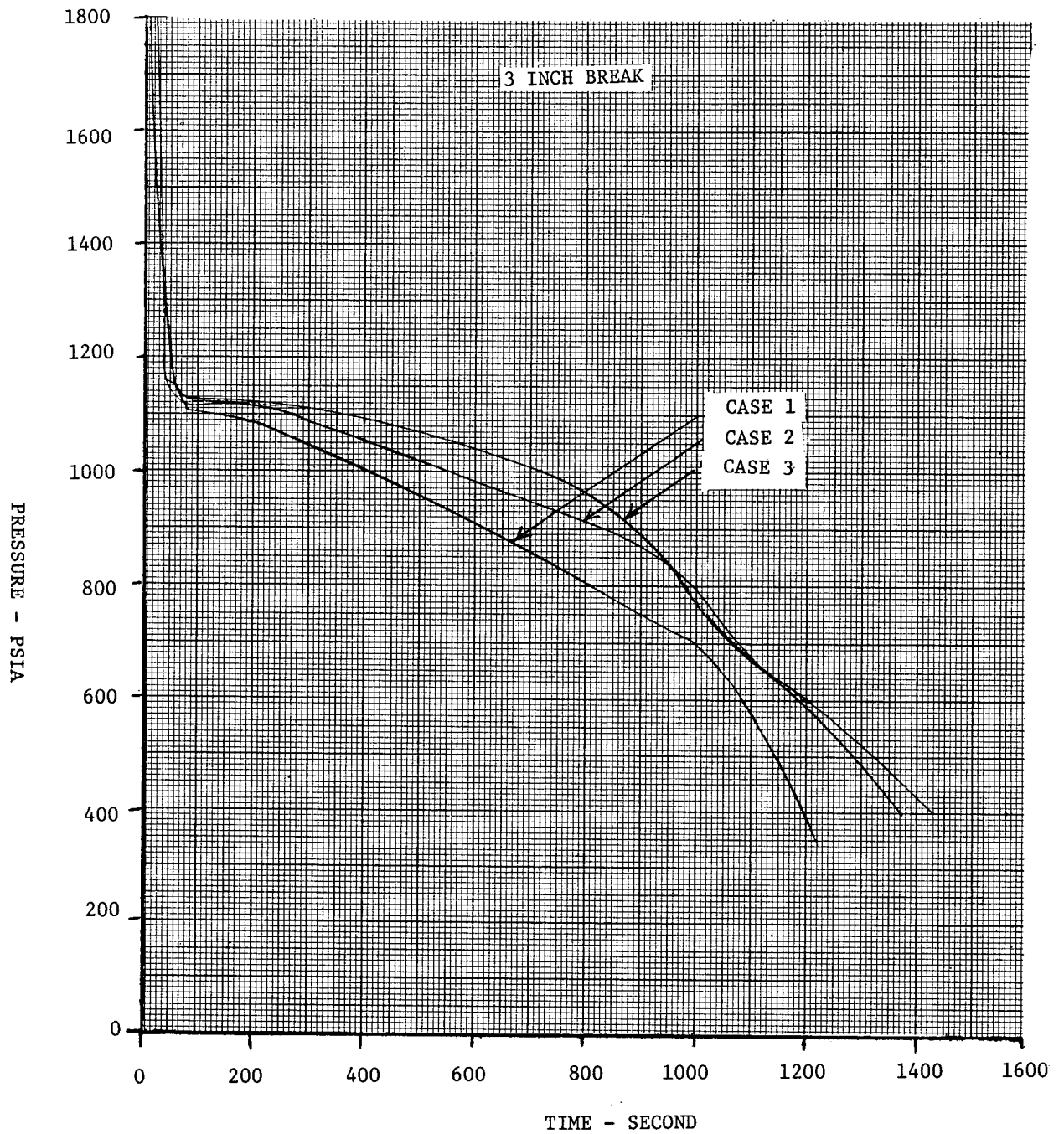


Figure 14.3.2-19

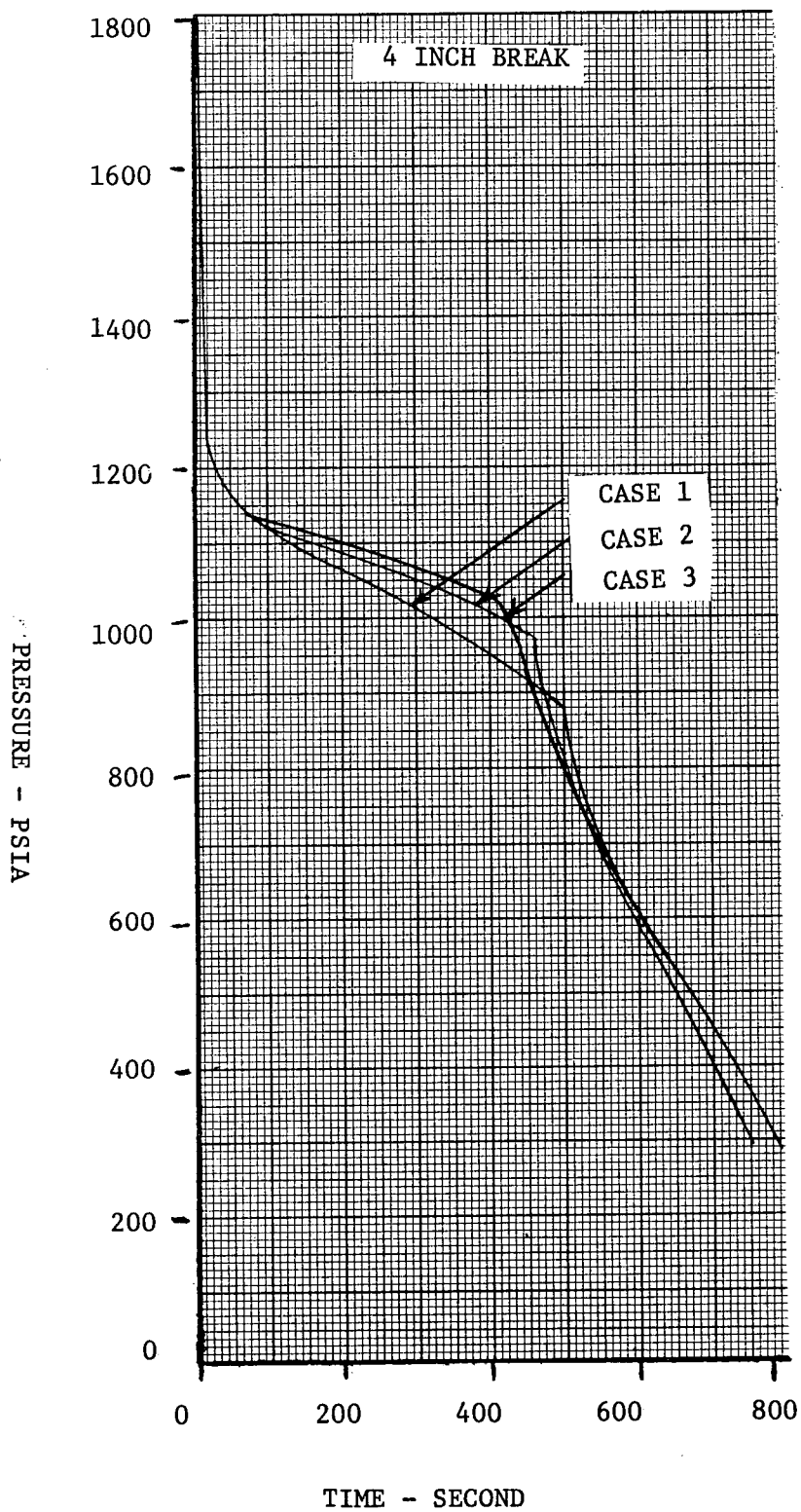


Figure 14.3.2-20

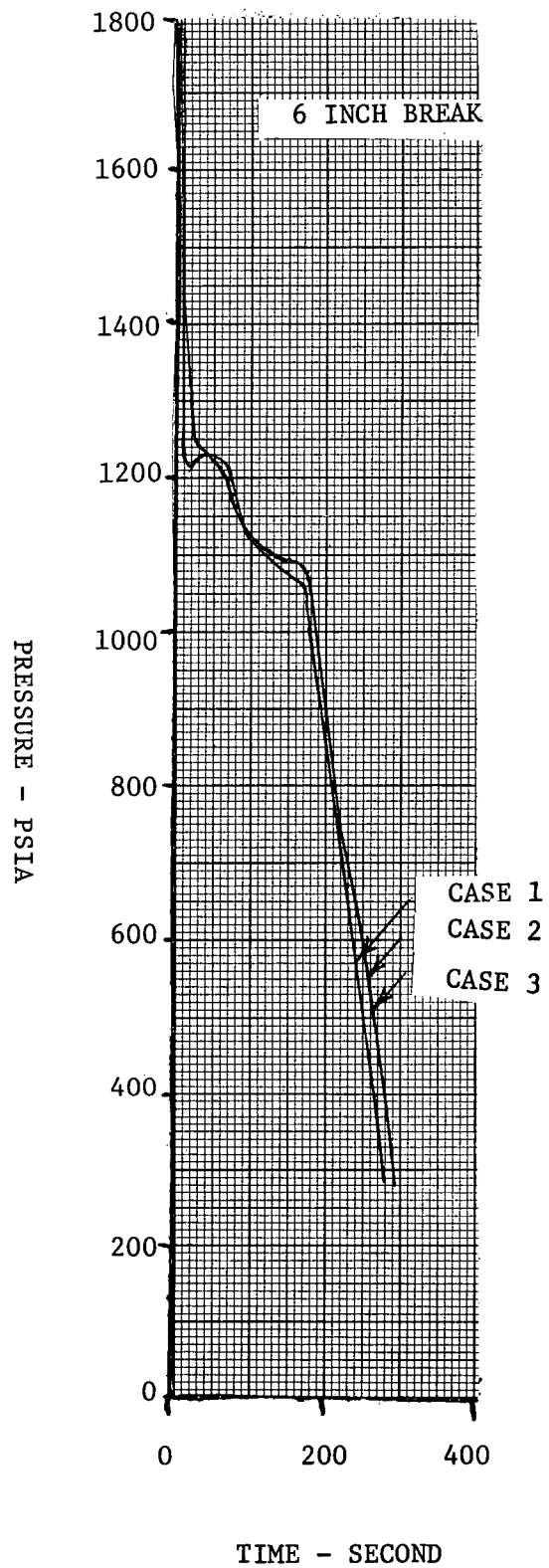


Figure 14.3.2-21

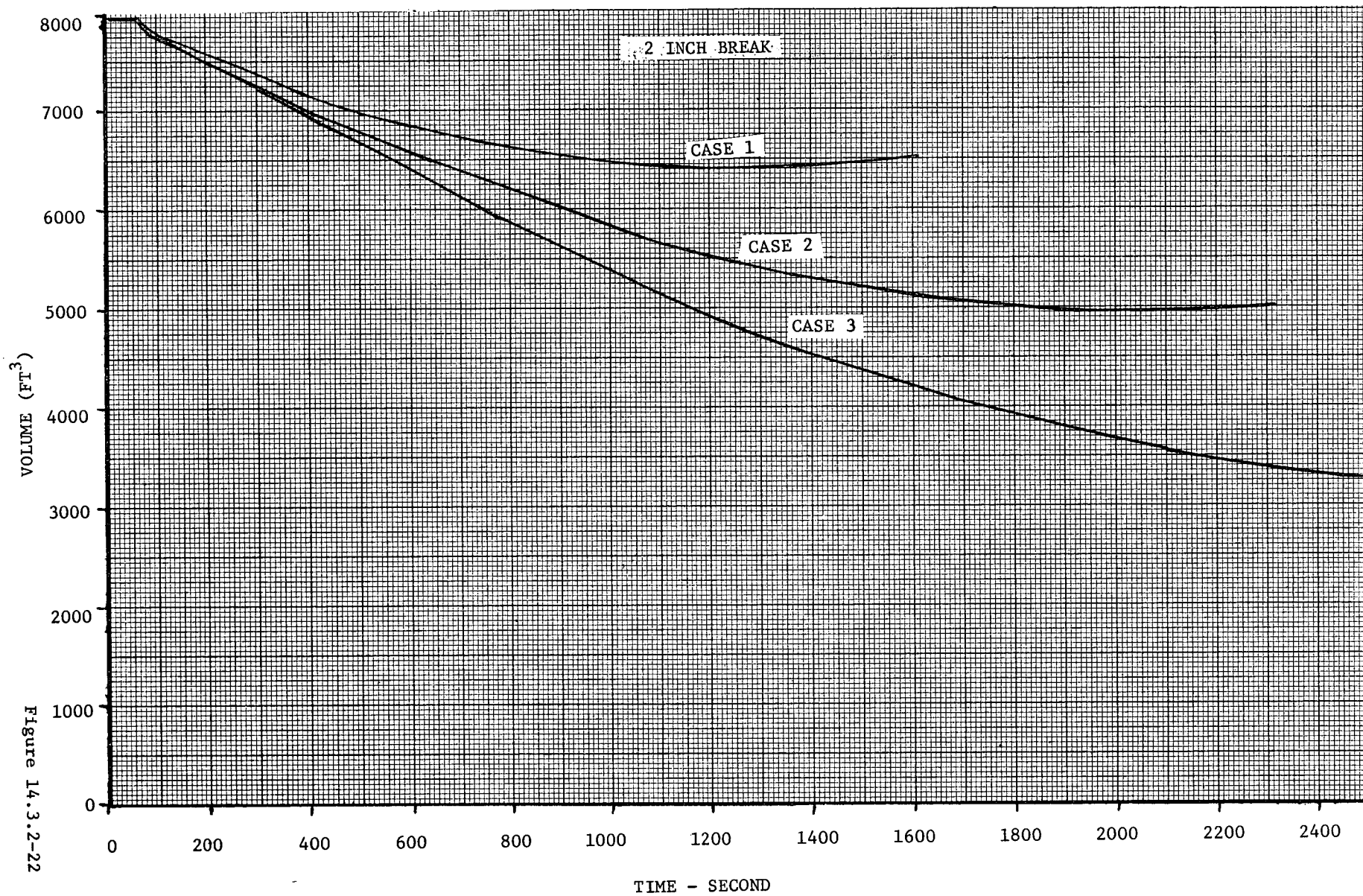


Figure 14.3.2-22

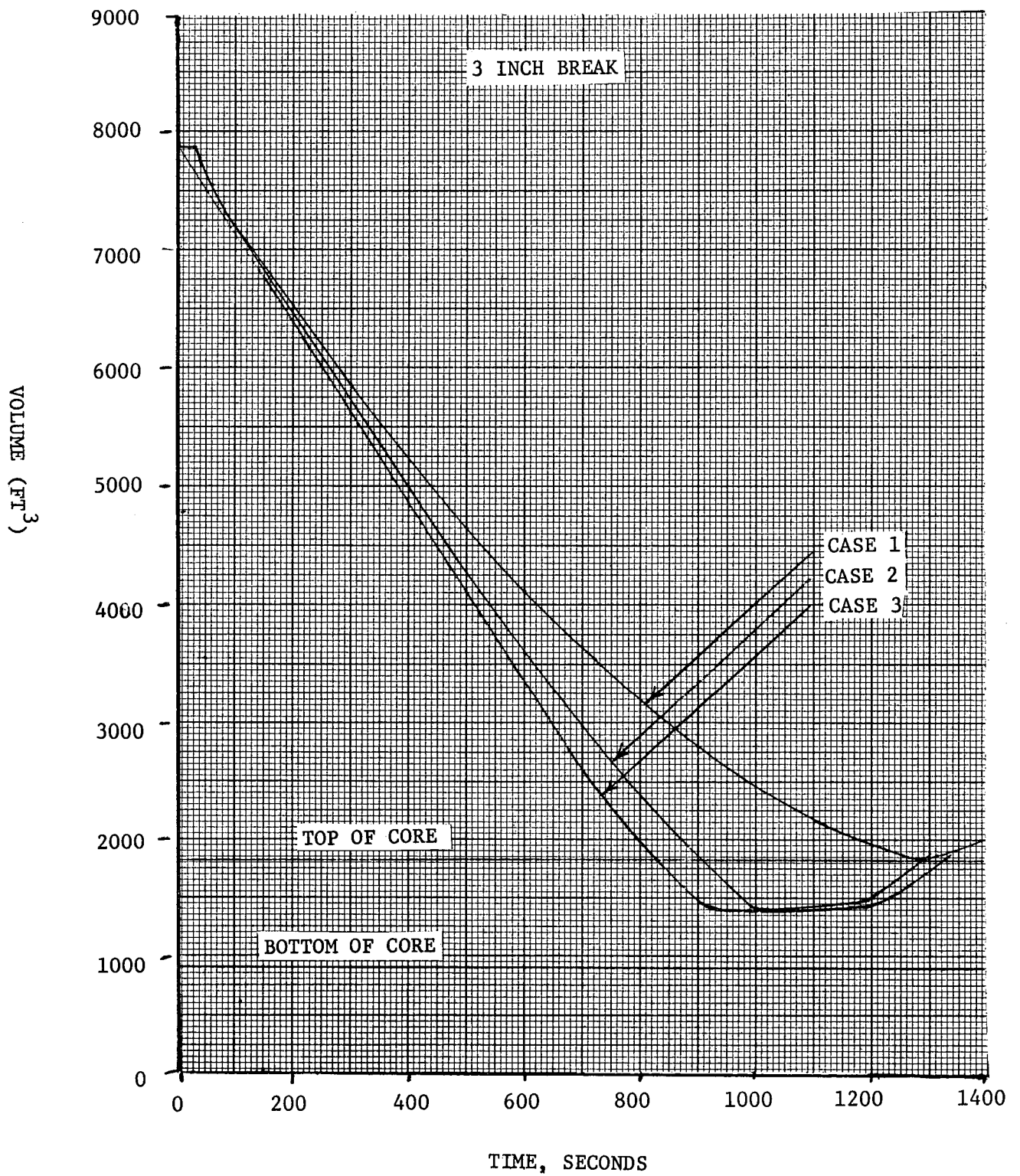


Figure 14.3.2-23

4 INCH BREAK

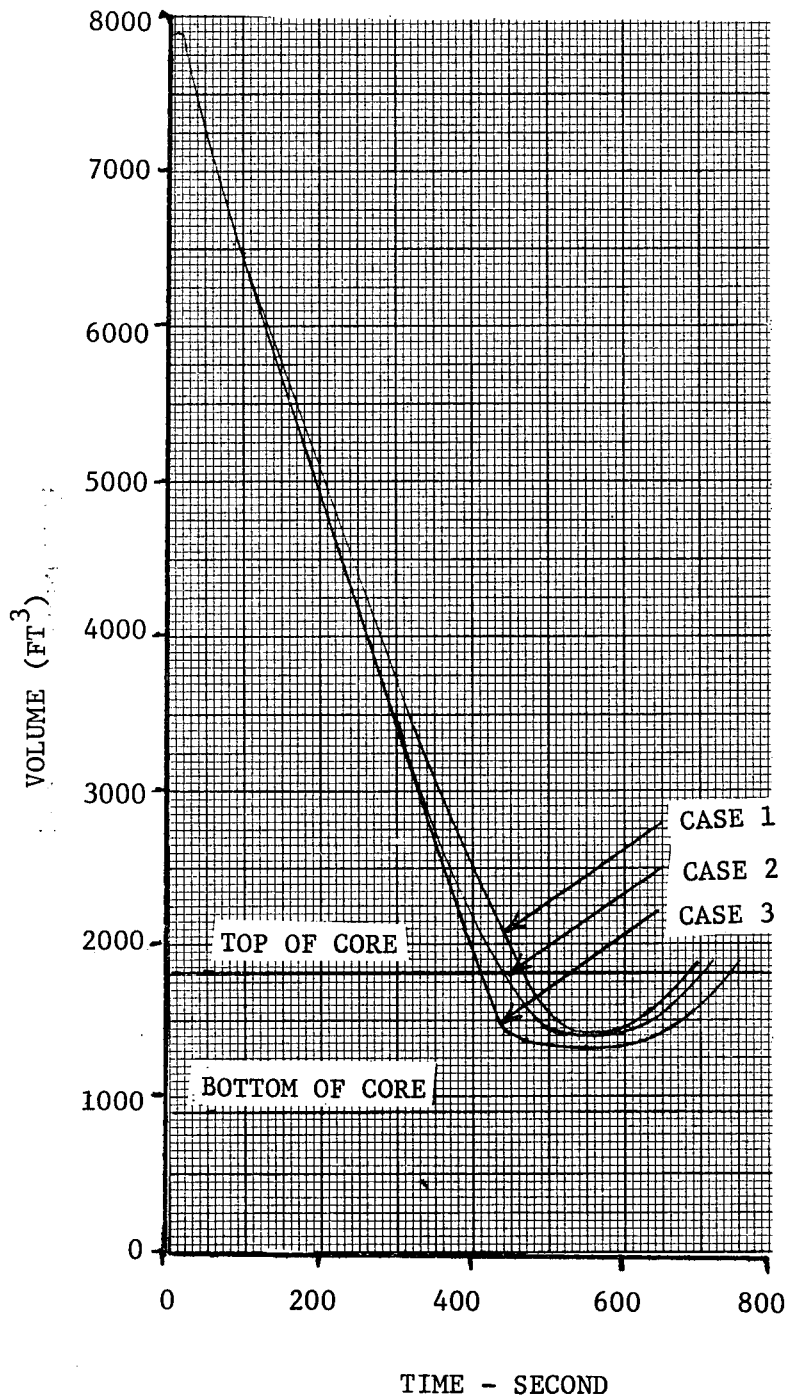


Figure 14.3.2-24

6 INCH BREAK

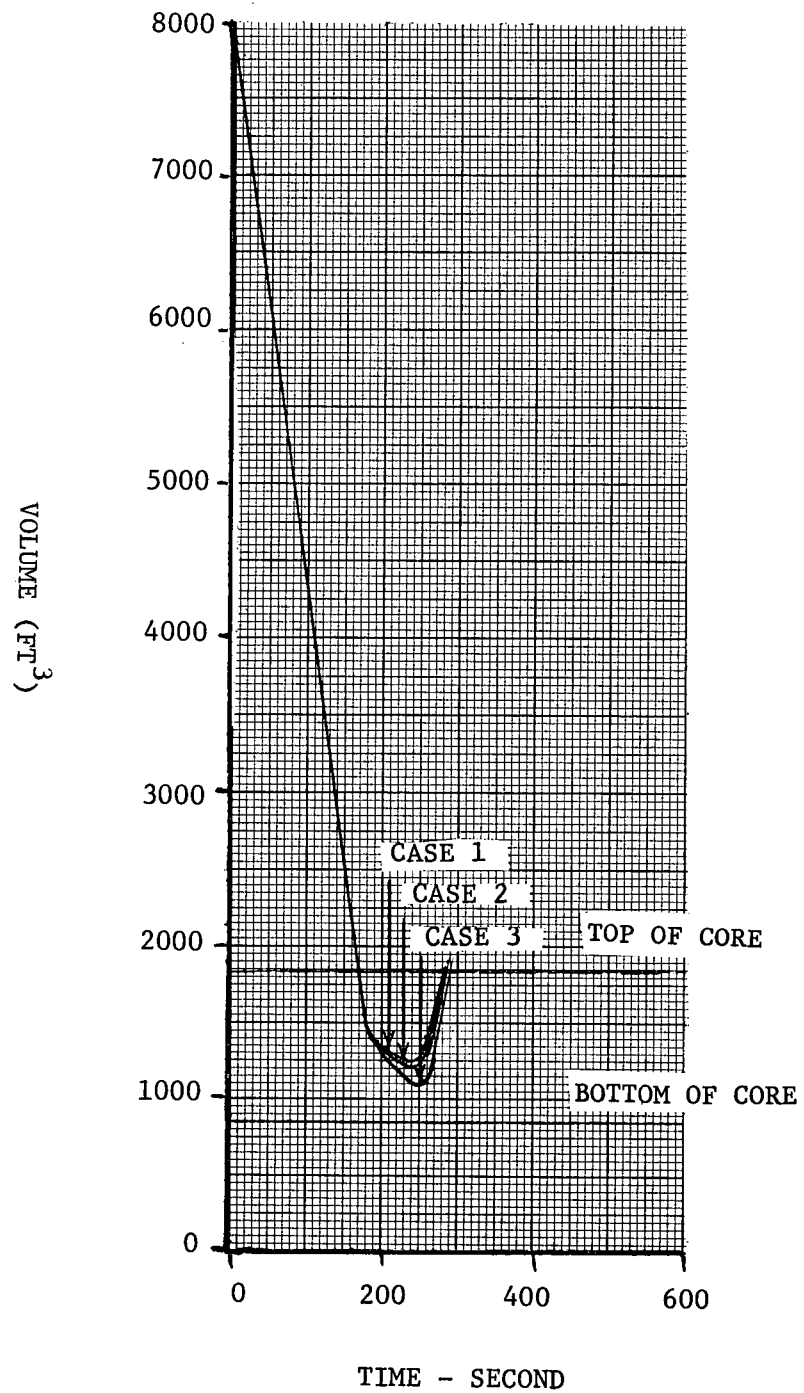


Figure 14.3.2-25

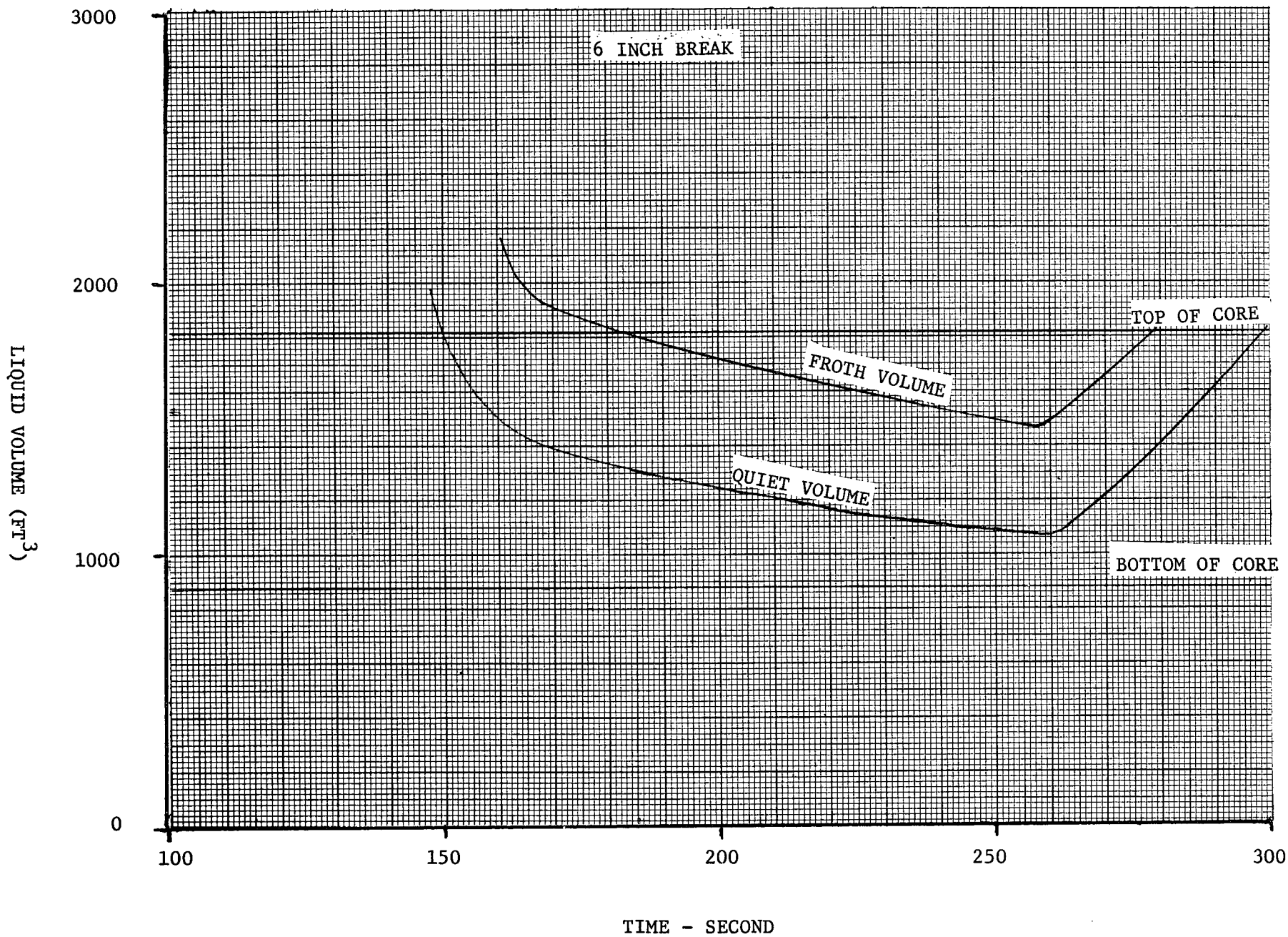


Figure 14.3.2-26

CASE 3
WITH STEAM GENERATOR DUMP

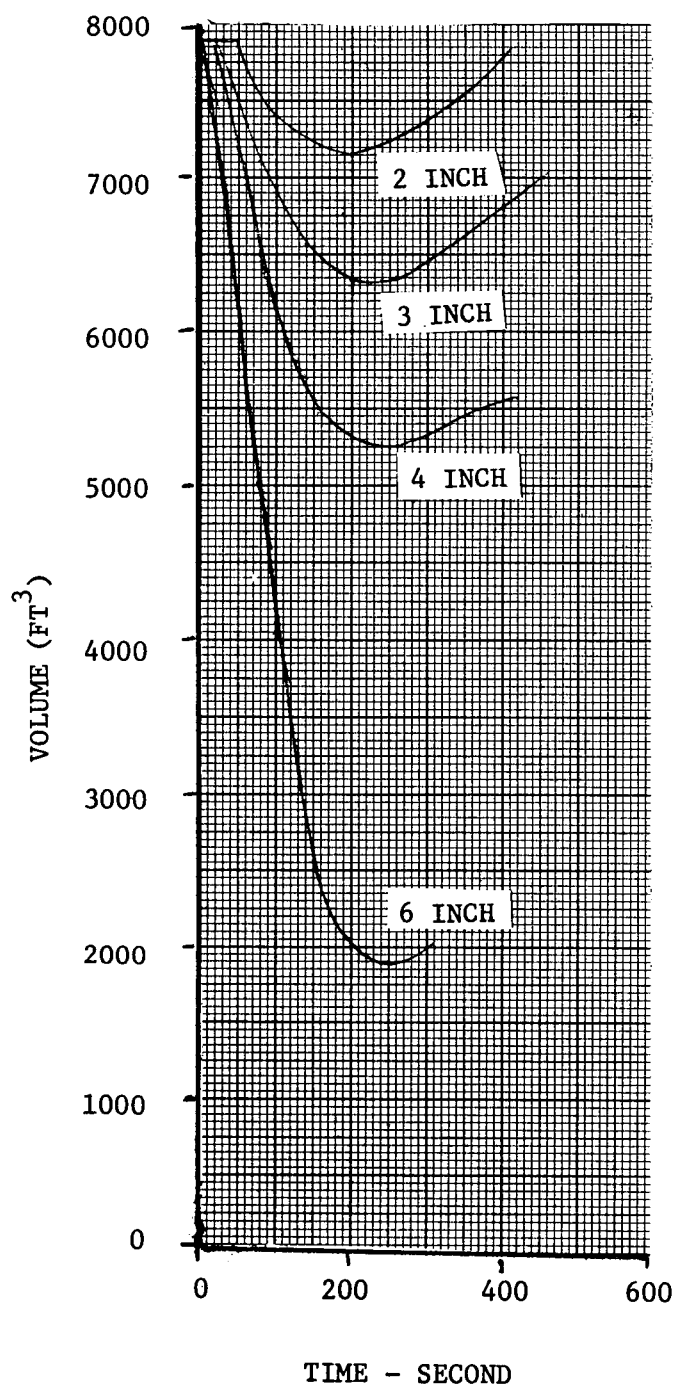


Figure 14.3.2-27

CASE 3
WITH STEAM GENERATOR DUMP

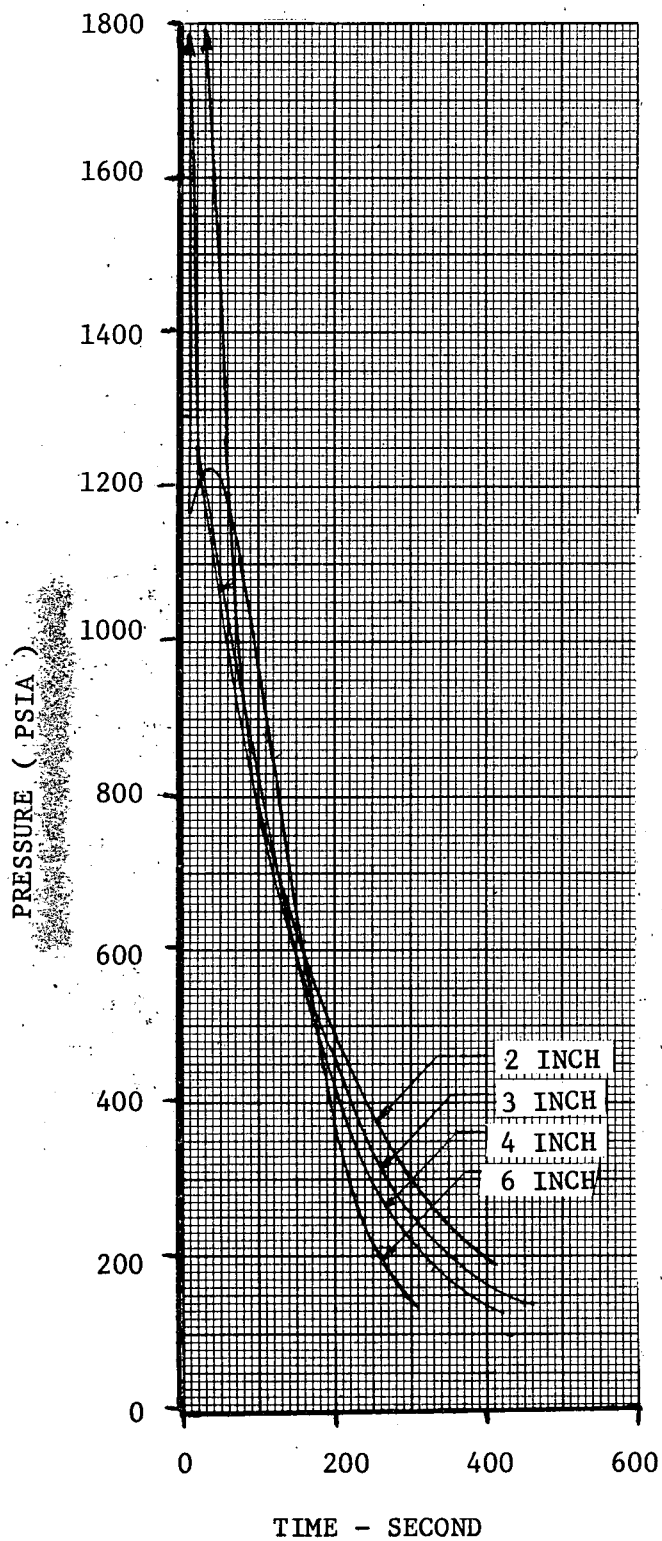


Figure 14.3.2-28

I-3-4

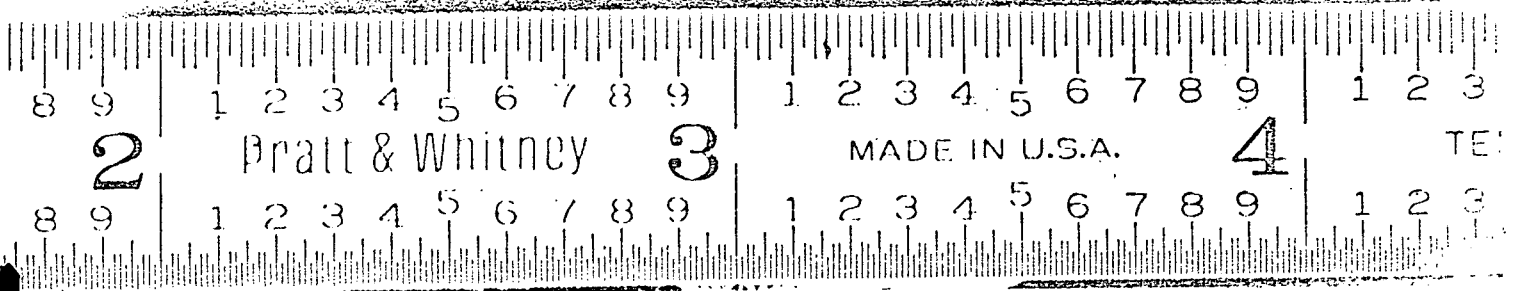
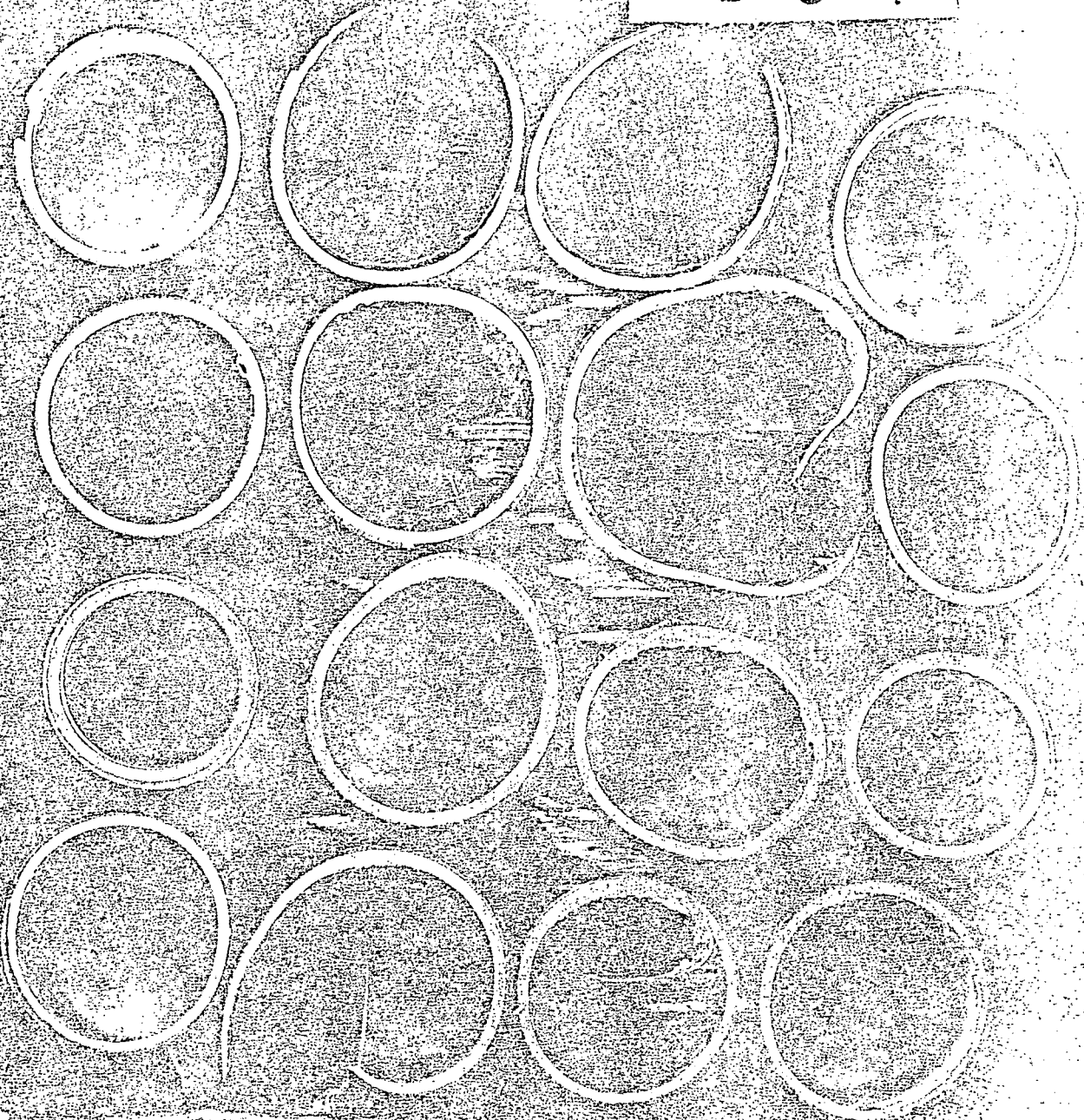


FIG. 14.3.2-29 MULTI-ROD BURST TEST -
BUNDLE CROSS SECTION

K-3-4

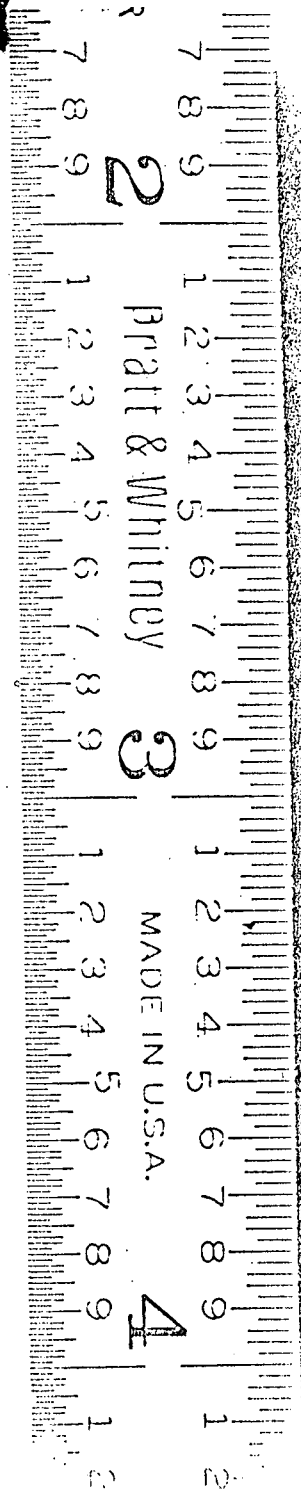
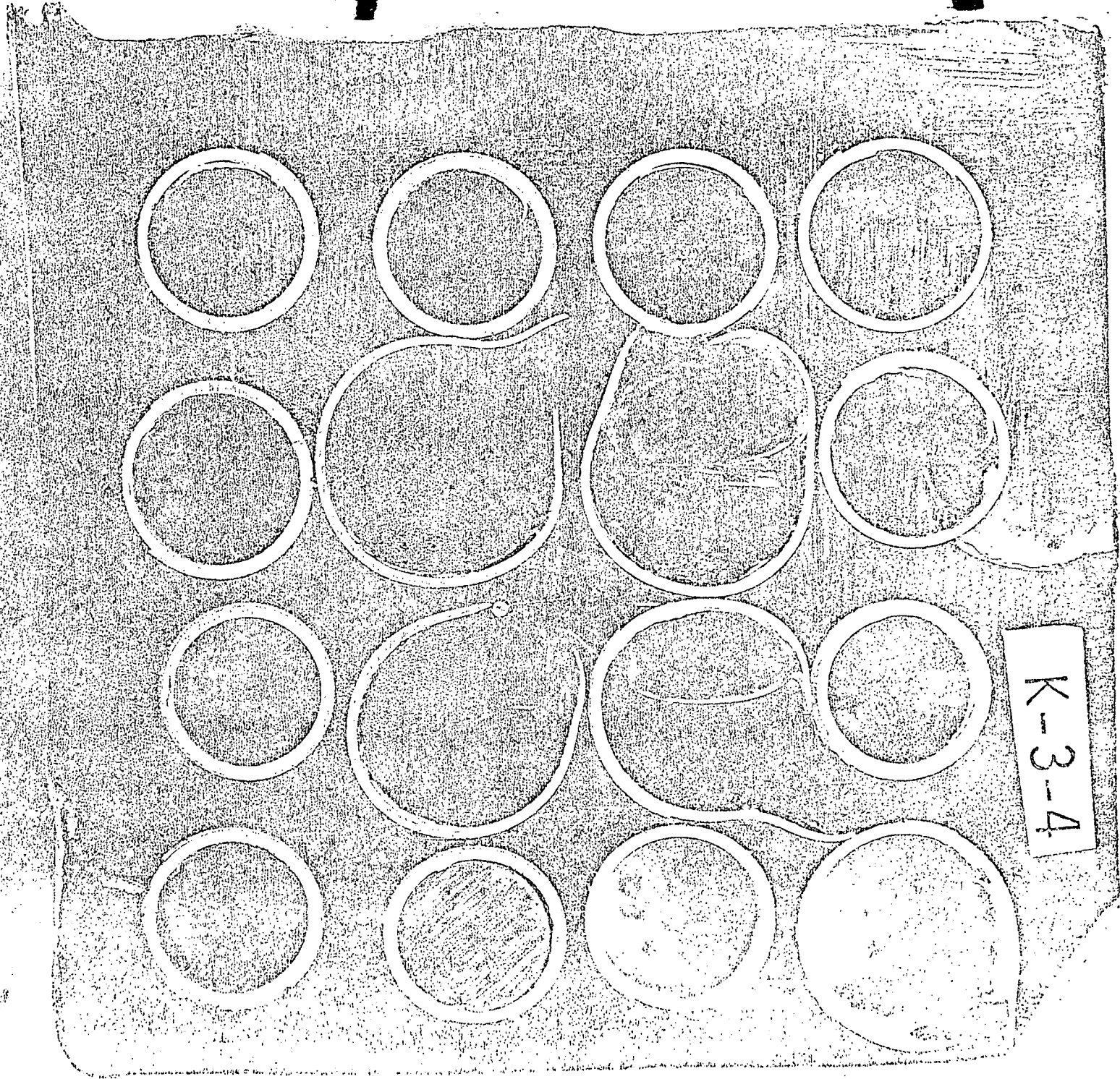


Fig. 14.3.2-30 MULTI-ROD BURST TEST -
BUNDLE CROSS SECTION

14.3.3 CORE AND INTERNALS INTEGRITY ANALYSIS

Internals Evaluation

The forces exerted on reactor internals and core, following a loss-of-coolant accident, are computed by employing the BLOWDN-1 digital computer program developed for the space-time-dependent analysis of multi-loop PWR plants.

Design Criteria

The basic requirement of any loss-of-coolant accident, including the double-ended severance of a reactor coolant pipe, is that sufficient integrity be maintained to permit the safe and orderly shutdown of the reactor. This implies that the core must remain essentially intact and deformation of internals must be sufficiently small so that primary loop flow, and particularly, adequate safety injection flow is not impeded.

The ability to insert control rods to the extent necessary to provide shutdown following the accident must be maintained. Maximum allowable deflection limitations are established for those regions of the internals that are critical for plant shutdown.

The allowable and no loss of function deflection limits under dead loads plus the maximum earthquake and/or blowdown excitation loads are presented in Table 14.3.3-1. These limits have been established by correlating experimental and analytical results.

Blowdown and Force Analysis

BLOWDN-1 is a digital computer program for calculation of pressure, velocity, and force transients in reactor primary coolant systems during the subcooled portion of blowdown caused by a loss-of-coolant accident.

During this phase of the accident, large amplitude rarefaction waves are propagated through the system with the velocity of sound causing large differences in local pressures. As local pressures drop below saturation, causing formation of steam, the amplitudes and velocities of these waves drastically decrease. Therefore, the largest forces across the reactor internals due to wave propagation occur during the subcooled portion of blowdown.

Blowdown Model

The analytical model used in BLOWDN-1 is the same as that of the WHAM computer program developed by Kaiser Engineers for the LOFT program.⁽⁵⁾

The program utilizes the exact solutions to the time dependent, one dimensional, compressible fluid flow equations in which the velocity of propagation of acoustic waves greatly exceeds the fluid velocity. Analytic solutions for the interior points of conduits of uniform flow-passage area are well known.^(1,2) They predict the existence of compression and rarefaction waves which travel through the fluid with the velocity of sound. Fluid pressures and velocities at any given point in space are proportional to the local sums and differences, respectively, of the magnitude of the waves which travel in opposite directions.

Solutions at the boundaries of these uniform flow area conduits (which for convenience will be referred to as "legs") are obtained through application of the mass and energy conservation laws. The latter, in the case of orifices, bends, and sudden changes of flow area, accounts for hydraulic losses. Hydraulic losses due to friction are represented by equivalent orifices.

The boundary condition at the location of the system's rupture is in the form of a discharge flow equation. The discharge flow equation incorporates the best available fit to known data^(3,4) on metastable flow of that fluid through short pipes and/or orifices, depending on the postulated rupture type.

A time-dependent rupture flow area is specified and approximated by a sequence of stepwise changes. Each step increase in the exit flow area generates a rarefaction wave as the compressed fluid escapes through the rupture. A train of waves is thus sequentially generated and sent upstream. When the waves encounter abrupt changes of flow passage area or branches to other "legs", they are both transmitted through and reflected from, such junctions with modified amplitudes. When reflected compression waves reach the rupture location they affect the discharge flow and generate new waves because of the change in the local pressure just upstream of the rupture.

Apart from calculations involving boundary conditions, BLODWN-1 assigns exact solutions to local fluid pressures and velocities throughout the system. Therefore, it does not suffer from the propagation of truncation errors and from numerical instabilities associated with the methods of analysis in which the time dependent differential equations representing the conservation laws are solved simultaneously by finite difference approximations.

BLODWN-1 utilizes the technique of branching on a one-dimensional flow system to approximate the actual three-dimensional conditions. This is accomplished by using fictitious tees at all junctions of the one-dimensional network of legs. For example, if local histories of fluid pressure on both sides of the thermal shield and the core barrel, as functions of distance from the inlet nozzle in both the axial and the circumferential direction are desired, a hydraulic network of circumferential and vertical legs is used to represent this annular flow region.

Comparison With Experimental Data

BLODWN-1 is an evolution of the program WHAM.⁽⁵⁾ The only changes made were to provide graphical output and storage of results and incorporate a detailed treatment of a double-ended pipe rupture. The comparison of WHAM results with tests obtained by Phillips Petroleum Company during their semi-scale blowdown experiments is shown in Figure 14.3.3-1 and 14.3.3-2 which are reproduced from Reference 6. Since no changes have been made in the analysis, this comparison is equally valid for BLODWN-1.

Force Model

BLODWN-1 evaluates the pressure and velocity transients for a maximum of 4000 locations throughout the system. These pressure and velocity transients are stored as a permanent tape file and are made available to the program FORCE which utilizes a detailed geometric description in evaluating the loadings on the reactor internals.

Each reactor component for which force calculations are required is designated as an element and assigned an element number. Forces acting upon each of the elements are calculated summing the effects of:

1. The pressure differential across the element
2. Flow stagnation on, and unrecovered orifice losses across the element
3. Friction losses along the element

Input to the code, in addition to the BLODWN-1 pressure and velocity transients, includes the effective area of each element on which acts the force due to the pressure differential across the element, a coefficient to account for flow stagnation and unrecovered orifice losses, and the total area of the element along which the shear forces act.

RESPONSES OF REACTOR INTERNALS TO BLOWDOWN FORCES

Vertical Excitation

Structural Model and Method of Analysis

The response of reactor internals components due to an excitation produced by complete severance of a primary loop pipe is analyzed. Assuming a double-end pipe break occurs in a very short period of time, the rapid drop of pressure at the break produces a disturbance which propagates along the primary loop and excites the internal structure. The characteristics of the hydraulic excitation, combined with those of the structures affected, presents a unique dynamic problem.

The internal structure is simulated by a multi-mass system connected with springs and dashpots representing the viscous damping due to structural and impact losses. The gaps between various components, as well as Coulomb type of friction, is also incorporated into the overall model. Since the fuel elements in the fuel assemblies are kept in position by friction forces originating from the preloaded fuel assembly grid fingers, any sliding that occurs between the fuel rods and assembly is considered as Coulomb type of friction. A series of mechanical modes of local structures were developed and analyzed so that certain basic nonlinear phenomena previously mentioned could be understood. Using the results of these models, a final eleven-mass model is adopted to represent the internal structure under vertical excitation. Figure 14.3.3-3 is a schematic representation of the internal structures. The eleven-mass model is shown in Figure 14.3.3-4. A comparison between Figure 14.3.3-3 and 14.3.3-4 shows the parallel between the plant and the model. The modeling is conducted in such a way that uniform masses are lumped into easily identifiable discrete masses while elastic elements are represented by springs. A legend for the different masses is given in Table 14.3.3-2. The masses are readily recognized as Items W1 through W11. The core barrel and the lower package are easily discernable. The fuel assemblies have been segregated into two groups. The majority of the fuel mass, W4, is indirectly connected to the deep beam structure represented by mass W8. There is also a portion of the fuel mass, W6, which connects through the long columns to the top plate. The stiffness of the top plate panels is represented by K10 and the stiffness of the upper core plate panels is represented by K8. The hold down spring, K1, is bolted-up between the flange of the deep beam structure and the core barrel flange with the preload, P1. After preloading the hold down spring, a clearance, G1, exists between the core barrel flange and the solid height of the hold down spring. Within the fuel assemblies, the fuel elements W4 and W6 are held in place by frictional contact with the grid spring fingers. Coulomb damping is provided in the analysis to represent this frictional restraint.

The analytical model is also provided with viscous terms to represent the structural damping of the elastic elements. The viscous dampers are represented by C1 through C11.

Restrictions are placed on the displacement amplitudes by specifying the free travel available to the dynamic masses. Available displacements are designated by symbols G1 through G8.

The displacements are tested during the solution of the problem to see if the available travel has been achieved. When the limit of travel has been attained, stops are engaged to arrest further motion of the dynamic masses. The stops or snubbers are designated by the symbols S1 through S11.

Contact with the snubbers results in some damping of the motion of the model. The impact damping of the snubbers is represented by the devices D1 through D11.

During the assembly of the reactor, bolt-up of the closure head presets the spring loading of the core barrel and the spring loading on the fuel assemblies. Since the fuel assemblies in the model have been segregated into two groups, two preload values are provided in the analysis. Preload values P1, P3, and P5 represent the hold down spring preload on the core barrel and the top nozzle springs preload values on the fuel assemblies.

The formulation of the transient motion response problem and digital computer programming were performed. The effects of an earthquake vertical excitation are also incorporated into the program.

In order to program the multi-mass system, the appropriate spring rates, weights, and forcing function for the various masses were determined. The spring rates and weights of the reactor components are calculated separately for each plant. The forcing functions for the masses are obtained from the FORCE program described in the previous section. It calculates the transient forces on reactor internals during blowdown using transient pressures and fluid velocities.

For the blowdown analysis the forcing functions are applied directly to the various internal masses.

For the earthquake analysis of the reactor internals, the forcing function, which is simulated earthquake response, is applied to the multi-mass system at the ground connections (the reactor vessel). Therefore, the external excitation is transmitted to the internals through the springs at the ground connections.

Results

Analysis is performed for 1 msec, 5 msec, and 20 msec hot leg and cold leg breaks. The response of the structure to this type of excitation indicates that the vertical motion is irregular with peaks of very short duration. The deflections and motion of some of the reactor components are limited by the solid height of springs as is the case of the hold down spring located above the barrel flange.

The internals behave as a highly nonlinear system during the vertical oscillations produced by the blowdown forces. The nonlinearities are due to the Coulomb frictional forces between grids and rods, and to gaps between components causing discontinuities in force transmission. The frequency response is consequently a function not only of the exciting frequencies in the system, but also of the amplitude. Different break conditions excite different frequencies in the system. This situation can be seen clearly when the response under blowdown forces is compared with the one due to vertical seismic acceleration. Under seismic excitation, the system behaves practically linearly because the component's motion is not sufficient to cause closing of the various gaps in the structure or slippage in the fuel rods.

Under certain blowdown excitation conditions, the core moves upward, touches the core plate, and falls down on the lower structure causing oscillations in all the components. During the time that the oscillations occur and depending on its initial position, the fuel rods slide on the fuel assembly. The response shows that the case could be represented as two large vibrating masses (the core and the barrel) and the rest of the system

oscillating at an average frequency of 100-110 cps with respect to the barrel and the core. The lower structure is oscillating at an average frequency of 100-110 cps with respect to the barrel and the core. The upper flange, with respect to the barrel, oscillates at a frequency of 50-80 cps. The same structure under seismic excitation shows a "natural" frequency of approximately 20-30 cps; in this case, the difference can be explained because after a hot leg break the upper plenum of the reactor compresses the flange downward increasing the stiffness of the structure. The lower structure shows "natural" frequencies of approximately 90-100 cps when the core is in contact and approximately 100-120 cps when the core is lifted. From the several cases analyzed, a frequency of 200-300 cps has been seen present very frequently in the upper package after the fuel assembly touches the upper core plate. The same structure shows a "natural" frequency of 20-25 cps when the structure is excited by the seismic accelerations.

The effect of damping has also been considered and its effect is to cause the higher frequencies to disappear rapidly after each impact or slippage.

The results of the computer program give not only the frequency response of the components, but also the maximum impact force and deflections. From these results, the stresses are computed using the standard "Strength of Material" formulas. The impact stresses are obtained in an analogous manner using the maximum forces seen by the various structures during impact.

Analyses of multi loop PWR plants are continuing and results for the three loop plant design will be obtained.

Analysis of Effects of Loss of Coolant and Safety Injection on the Reactor Vessel

The analysis of the effects of injecting safety injection water into the reactor coolant system following a postulated loss of coolant accident are being incorporated into a WCAP report to be submitted to the AEC.

For the reactor vessel, three modes of failure are considered including the ductile mode, brittle mode and fatigue mode.

- a) Ductile Mode - the failure criterion used for this evaluation is that there shall be no gross yielding across the vessel wall using the material yield stress specified in Section III of the ASME Boiler and Pressure Vessel Code. The combined pressure and thermal stresses during injection through the vessel thickness as a function of time have been calculated and compared to the material yield stress at the times during the safety injection transient.

The results of the analyses showed that local yielding may occur in approximately the inner 12 per cent of the base metal and in the cladding.

- b) Brittle Mode - the possibility of a brittle fracture of the irradiated core region has been considered from both a transition temperature approach and a fracture mechanics approach.

The failure criteria used for the transition temperature evaluation is that a local flaw cannot propagate beyond any given point where the applied stress will remain below the critical propagation stress at the applicable temperature at that point.

The results of the transition temperature analysis showed that the stress-temperature condition in the outer 65 per cent of the base metal wall thickness remains in the crack arrest region at all times during the safety injection transient. Therefore, if a defect were present in the most detrimental location and orientation (i.e., a crack on the inside surface and circumferentially directed), it could not propagate any further than approximately 35 per cent of the wall thickness, even considering the worst case assumptions used in this analysis.

The results of the fracture mechanics analysis, considering the effects of water temperature, heat transfer coefficients and fracture toughness of the material as a function of time, temperature and irradiation will be included in the report. Both a local crack effect and a continuous crack effect have been considered with the latter requiring the use of a rigorous finite element axisymmetric code.

- c) Fatigue Mode - the failure criterion used for the failure analysis was the one presented in Section III of the ASME Boiler and Pressure Vessel Code. In this method the piece is assumed to fail once the combined usage factor at the most critical location for all transients applied to the vessel exceeds the code allowable usage factor of one.

The results of this analysis showed that the combined usage factor never exceeded 0.2, even after assuming that the safety injection transient occurred at the end of plant life.

In order to promote a fatigue failure during the safety injection transient at the end of plant life, it has been estimated that a wall temperature of approximately 1100°F is needed at the most critical area of the vessel (instrumentation tube welds in the bottom head).

The design basis of the Safety Injection System ensures that the maximum Zircaloy cladding temperature does not exceed the Zircaloy-4 melt temperature. This is achieved by prompt recovery of the core through flooding, with the passive accumulator and the injection systems. Under these conditions a vessel temperature of 1100°F is not considered a credible possibility and the evaluation of the vessel under such elevated temperatures is for a hypothetical case.

For the ductile failure mode, such hypothetical rise in the wall temperature would increase the depth of local yielding in the vessel wall.

The results of these analyses show that the integrity of the reactor vessel is never violated.

The safety injection nozzles have been designed to withstand ten postulated safety injection transients without failure. This design and associated analytical evaluation was made in accordance with the requirements of Section III of the ASME Boiler and Pressure Vessel Code.

The maximum calculated pressure plus thermal stress in the safety injection nozzle during the safety injection transient was calculated to be approximately 50,900 psi. This value compares favorably with the code allowable stress of 80,000 psi.

These ten safety injection transients are considered along with all the other design transients for the vessel in the fatigue analysis of the nozzles. This analysis showed the usage factor for the safety injection nozzles was 0.47 which is well below the code allowable value of 1.0.

The safety injection nozzles are not in the highly irradiated region of the vessel and thus they are considered ductile during the safety injection transient.

The effect of the safety injection water on the fuel assembly grid springs has been evaluated and due to the fact that the springs have a large surface area to volume ratio, being in the form of thin strips, and are expected to follow the coolant temperature transient with very little lag hence, no thermal shock is expected and the core cooling is not compromised.

Evaluations of the core barrel and thermal shield have also shown that core cooling is not jeopardized under the postulated accident conditions.

REFERENCES

1. J. Parmakian: "Water-Hammer Analysis", Prentiss Hall (1955).
2. V. L. Streeter and E. B. Wylie: "Hydraulic Transients", McGraw-Hill, Page 19, (1967).
3. F. R. Zaloudek: "The Critical Flow of Hot Water Through Short Tubes", HW-77594, May 1968.
4. H. K. Fauske: "The Discharge of Saturated Water Through Tubes", Chem. Eng. Progress Symp. Series Heat Transfer-Cleveland, No. 59, Vol. 61, (1965).
5. S. Fabric: "Computer Program WHAM for Calculation of Pressure Velocity, and Force Transients in Liquid Filled Piping Networks," Kaiser Engineers Report No. 67-49-R (November 1967).
6. S. Fabric: "Early Blowdown (Water Hammer) Analysis for Loss of Fluid Test Facility", Kaiser Engineers Report No. 65-28-RA (April, 1967).

TABLE 14.3.3-1

INTERNALS DEFLECTIONS UNDER ABNORMAL OPERATION
(Inches)

	Allowable Limit	No Loss-of- Function Limit
<u>Upper Barrel</u> , expansion/compression (to assure sufficient inlet flow area/and to prevent the barrel from touching any guide tube to avoid disturbing the RCC guide structure).	3	6
<u>Upper Package</u> , axial deflection (to maintain the control rod guide structure geometry).	1	2
<u>RCC Guide Tube</u> , cross section dis- tortion (to avoid interference between the RCC elements and the guides).	0.035	0.072
<u>RCC Guide Tube</u> , deflection as a beam (to be consistent with conditions under which ability to trip has been tested).	1.0	1.5
<u>Fuel Assembly Thimbles</u> , cross section distortion (to avoid interference between the control rods and the guides).	0.035	0.072

The allowable limit deflection values given above correspond to stress levels for the internals structure well below the limiting criteria given by the collapse curves in WCAP-5890, Rev. 1. Consequently, for the internals the geometric limitations established to assure safe shutdown capability are more restrictive than those given by the failure stress criteria.

TABLE 14.3.3-2

MULTI-MASS VIBRATIONAL MODEL-DEFINITION OF SYMBOLS

W1 - Core Barrel
 W2 - Lower Package
 W3 - Fuel Assemblies Major
 W4 - Fuel Rods Major
 W5 - Fuel Assemblies Minor
 W6 - Fuel Rods Minor
 W7 - Core Plate & Short Column
 W8 - Deep Beam
 W9 - Core Plate & Long Columns
 W10 - Top Plate (Ctr.)
 W11 - Core Barrel

K1 - Hold Down Spring
 K2 - Lower Package Major
 K3 - Top Nozzle Springs Major
 K5 - Top Nozzle Springs Minor
 K7 - Short Columns
 K8 - Upper Core Plate
 K9 - Long Columns
 K10 - Top Plate
 K11 - Core Barrel

Snubbers

S1 - Core Barrel Flange
 S2 - Hold Down Spring
 S3 - Top Nozzles Bars, Major
 S4 - Pedestal Bars, Major
 S5 - Top Nozzles Bars, Minor
 S6 - Pedestal Bars, Minor
 S7 - Top Nozzle Bumpers, Major
 S8 - Top Nozzle Bumpers, Minor
 S9 - Pedestals, Major
 S10 - Pedestals, Minor
 S11 - Deep Beam Flange

Impact Dampers

D1 - Barrel Flange
 D2 - Hold Down Spring
 D3 - Top Nozzle Bars, Major
 D4 - Pedestal Bars, Major
 D5 - Top Nozzle Bars, Minor
 D6 - Pedestal Bars, Minor
 D7 - Top Nozzles, Major
 D8 - Top Nozzles, Minor
 D9 - Pedestal, Major
 D10 - Pedestal, Minor
 D11 - Deep Beam Flange

Structural Dampers

C1 - Hold Down Springs
 C2 - Lower Package
 C3 - Top Nozzle, Major
 C5 - Top Nozzle, Minor
 C7 - Short Columns
 C8 - Upper Core Plate
 C9 - Long Columns
 C10 - Top Plate
 C11 - Core Barrel

Clearances

G1 - Hold Down Spring
 G3 - Fuel Rod Top, Major
 G4 - Fuel Rod Bottom, Major
 G5 - Fuel Rod Top, Minor
 G6 - Fuel Rod Bottom, Minor
 G7 - Fuel Assembly Major
 G8 - Fuel Assembly Minor

Preloads

P1 - Hold Down Spring
 P3 - Top Nozzle Springs Major
 P5 - Top Nozzle Springs Minor

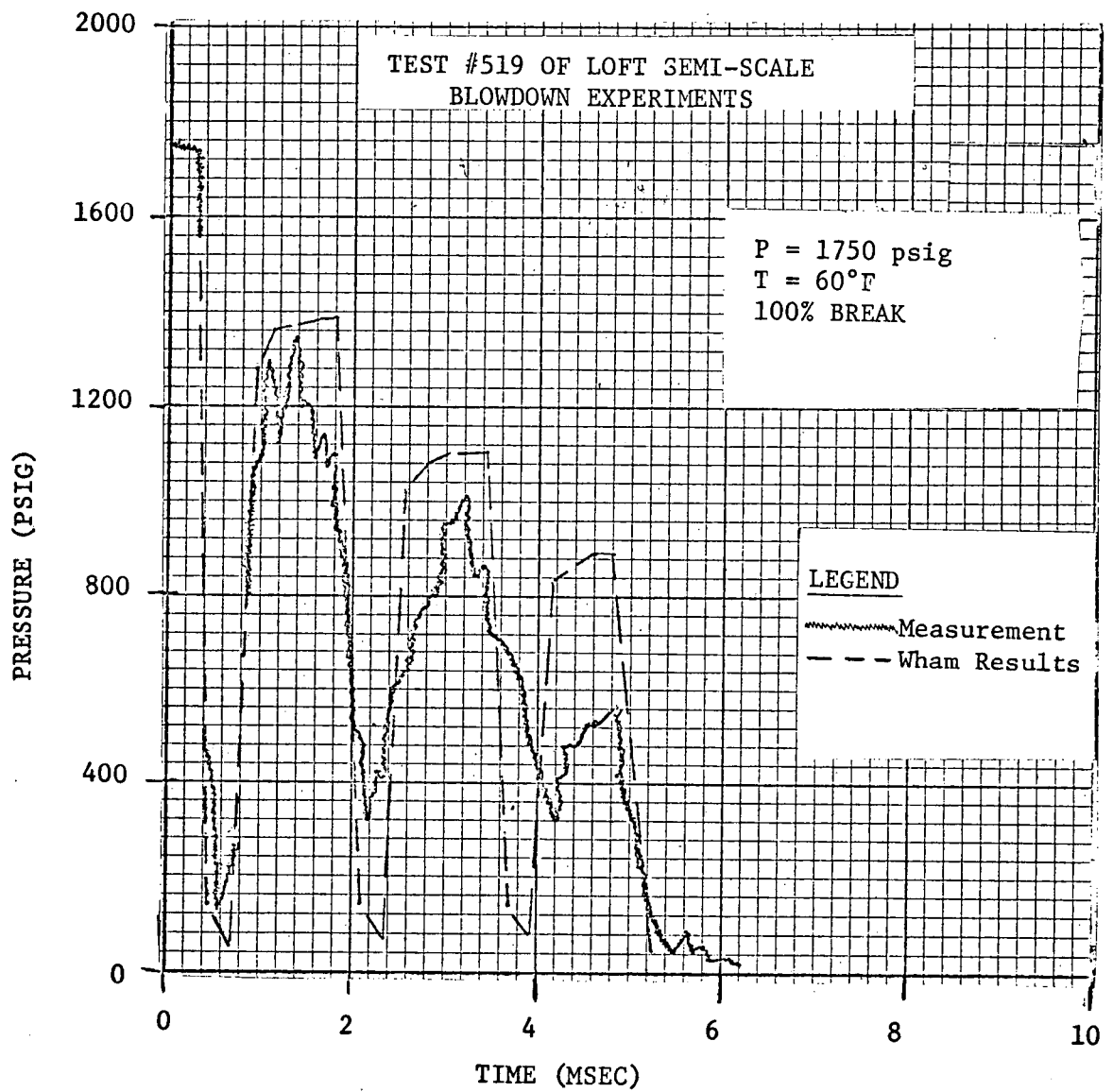
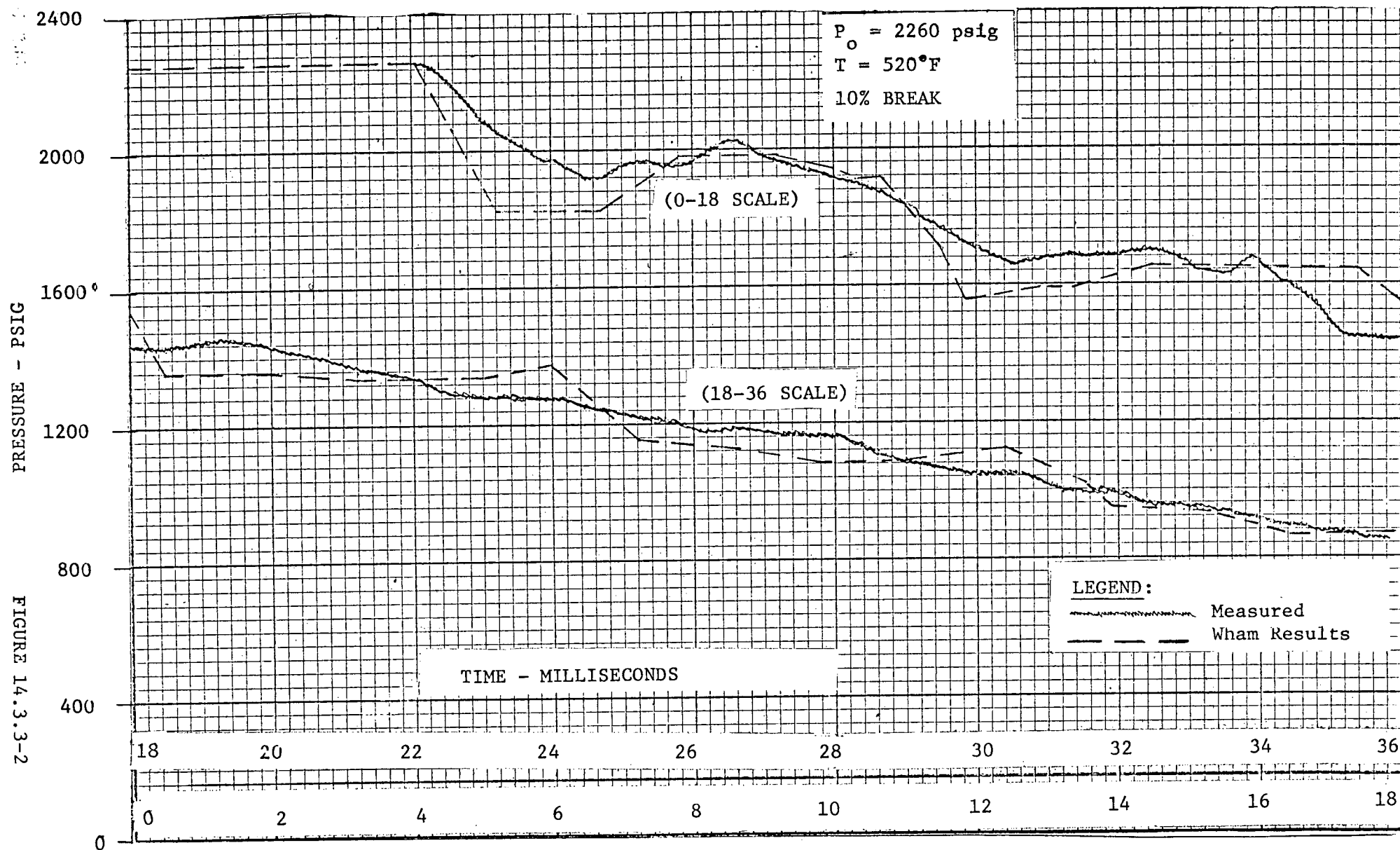
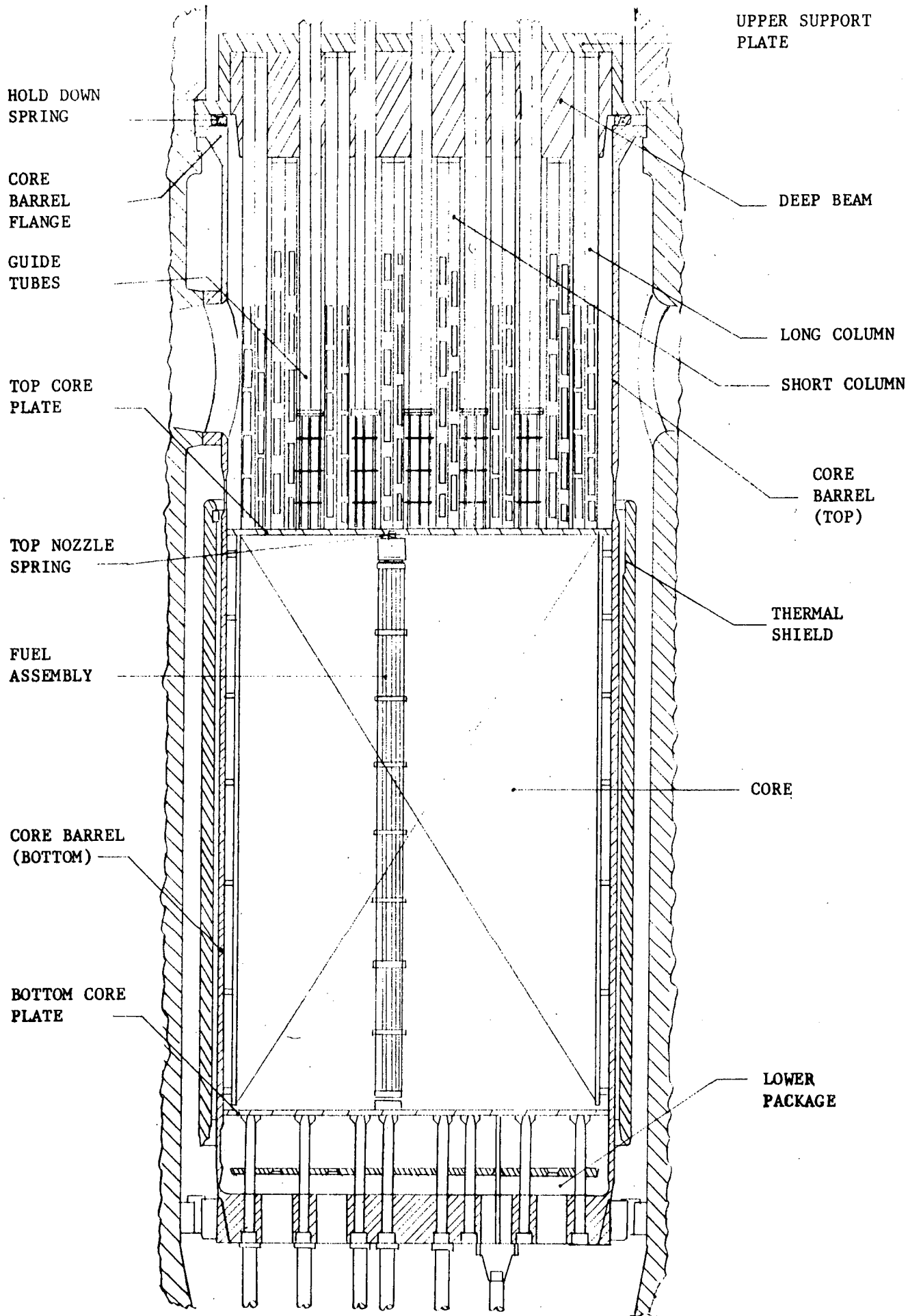


FIGURE 14.3.3-1

TEST #560 OF LOFT SEMI-SCALE BLOWDOWN EXPERIMENTS





REACTOR VESSEL INTERNALS
FIGURE 14.3.3-3

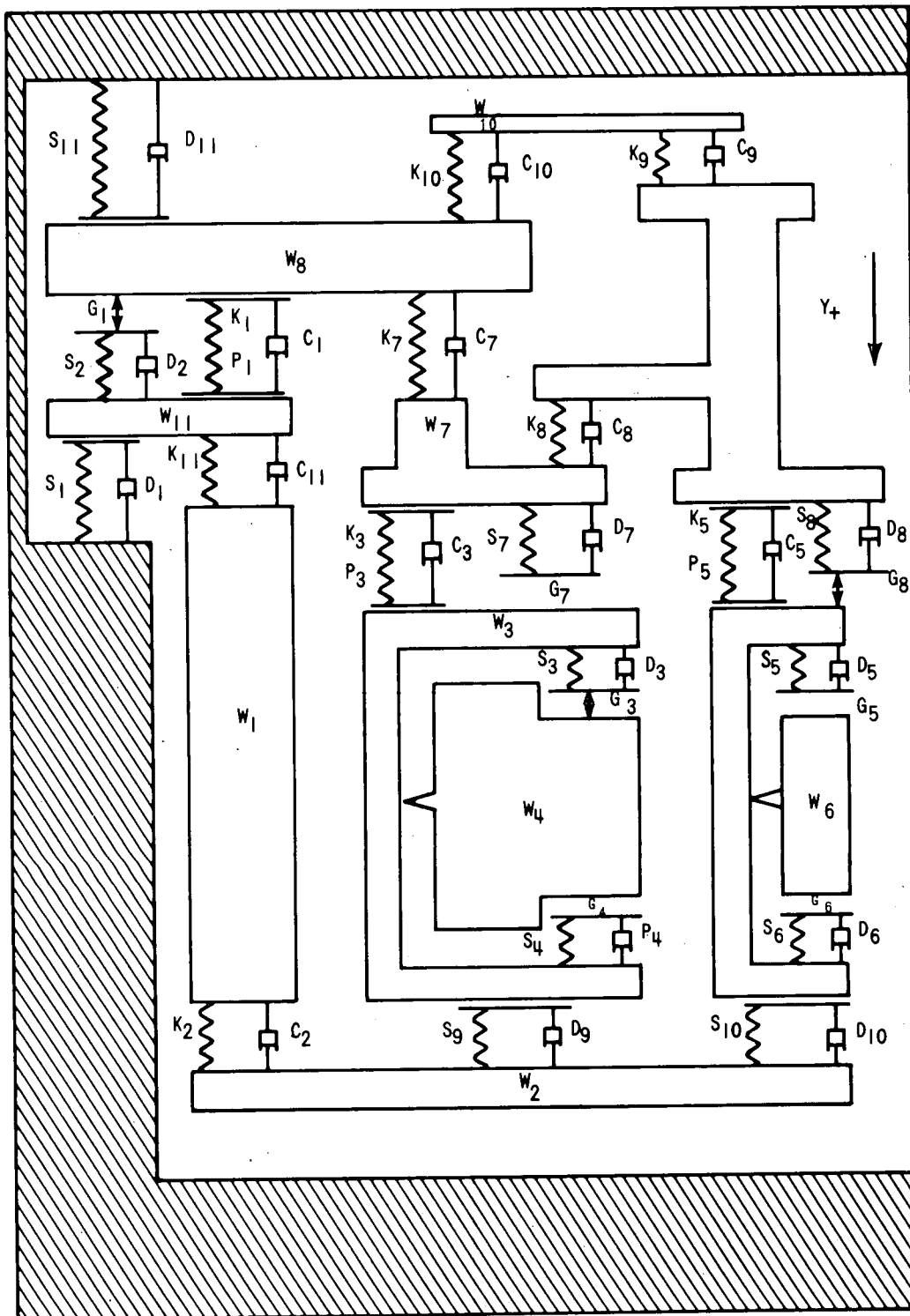


Figure 14.3.3-4. Multi-Mass Vibrational Model

Method of Analysis

Calculation of containment pressure and temperature transients is accomplished by use of the digital computer code, COCO. The analytical model is restricted to the containment volume and structure. Transient phenomena within the Reactor Coolant System affect containment conditions by means of convective mass and energy transport through the pipe break.

For analytical rigor and convenience, the containment air-steam-water mixture is separated into two systems. The first system consists of the air-steam phase, while the second is the water phase. Sufficient relationships to describe the transient are provided by the equations of conservation of mass and energy as applied to each system, together with appropriate boundary conditions. As thermodynamic equations of state and conditions may vary during the transient, the equations have been derived for all possible cases of superheated or saturated steam, and subcooled or saturated water. Switching between states is handled automatically by the code. The following are the major assumptions made in the analysis:

- a) Discharge mass and energy flow rates through the Reactor Coolant System break are established from the coolant blowdown and core thermal transient analysis (described in the preceding paragraphs).
- b) At the break point, the discharge flow separates into steam and water phases. The saturated water phase is at the total containment pressure, while the steam phase is at the partial pressure of the steam in the containment.
- c) Homogeneous mixing is assumed. The steam-air mix and the water phase have uniform properties. More specifically, thermal equilibrium between the air and steam is assumed. This does not imply thermal equilibrium between the steam-air mixture and the water phase.

- d) Air is taken as an ideal gas, while compressed water and steam tables are employed for water and steam thermodynamic properties.

During the transient, there is energy transfer from the steam-air and water systems to the internal structures and equipment within the shell.

Provision is made in the computer analysis for the effects of several engineered safeguards, including internal spray, fan coolers, and recirculation of sump water. The heat removal from containment steam-air phase by internal spray is determined by allowing the spray water temperature to rise to the steam-air temperature.

Energy Sources

The amount mass of energy carried into the containment during blowdown is calculated by the FLASH computer code. The following is a summary of all the energy sources potentially available for transfer to the containment for a loss-of-coolant accident.

- a) Reactor Coolant Energy
- b) Accumulator (Mixes with Reactor Coolant System)
- c) Initial Core Stored Energy
- d) Core Internals Metal Energy
- e) Reactor Vessel Metal (below vessel nozzles)
- f) Core Power Generation (Shut down energy and decay heat)
- g) Zr - H₂O reaction

All the power generated by the core during blowdown is transferred to the coolant, and reaches the containment. The initial core stored and metal sensible energy is transferred to the coolant by a time dependent temperature difference calculation. It should be emphasized that the energy transferred from the core to the coolant for the containment evaluation far exceeds that transferred from the core thermal evaluation. That is to say, a conservatively high core heat transfer coefficient is used for

the containment evaluation, while a conservatively low coefficient is used during the core thermal evaluation. Between the end of blowdown and the beginning of core reflooding there is no energy entering the containment. While the core is being reflooded the remaining stored energy in the core and internals causes a portion of the accumulator water to be boiled, and this energy is transferred to the containment.

Any energy addition resulting from a $\text{Zr-H}_2\text{O}$ reaction is also considered. The reaction energy reaches the containment by transfer to coolant, while the recombination energy of the H_2 generated in the reaction is added directly to the steam-air mixture in the containment. The hydrogen is assumed to burn as it is produced.

Finally, hot metal surfaces not cooled by safety injection water (reactor vessel above nozzles and steam generator tubes) are simulated as hot walls in contact with the containment steam-air mixture. A small heat transfer coefficient is employed to reflect actual conditions since these surfaces are covered by stagnant steam inside the reactor coolant system.

The following are some additional conservative assumptions used in the analysis:

- a) The reactor power is based on operation at the maximum calculated power of 2300 MWt.
- b) The decay heat is based on power operation for an infinite time.
- c) Coolant temperatures are the maximum levels attained in steady state operation, including allowance for instrument error and deadband.
- d) Gross system volumes are calculated from component dimensions, to which is added a 3% margin.

- e) Pressurizer liquid inventory at the nominal full power level plus an appropriate margin for instrument error and deadband.

Energy Sinks

Containment Structures

Provision is made in the containment pressure transient analysis for heat transfer through , and heat storage in, both interior and exterior walls. Every wall is divided into a large number of nodes. For each node, a conservation of energy equation expressed in finite difference form accounts for transient conduction into and out of the node and temperature rise of the node. Table 14.3.4-1 is a summary of the containment structural heat sinks used in the analysis.

The heat transfer coefficient to the containment surface is calculated by the code based primarily on the work of Tagami⁽¹⁾. From this work it was determined that the value of the heat transfer coefficient increases parabolically to peak value at the end of blowdown and then decreased exponentially to a stagnant heat transfer coefficient which is a function of steam to air weight ratio.

It should be noted that this method is different than that presented in the Preliminary Facility Description and Safety Analysis Report. In that report the heat transfer coefficients were based on the work of Kolflat⁽²⁾. The revised method of calculation results in decreased heat transfer to the containment structure during blowdown.

Tagami Presents a plot of the maximum value of h as a function of "coolant energy transfer speed," defined as:

$$\frac{\text{total coolant energy transferred into containment}}{(\text{containment vessel volume}) (\text{time interval to peak pressure})}$$

From this the maximum of h for steel is calculated:

$$h_{\max} = 75 \frac{E}{t_p V} 0.60$$

h_{\max} = maximum value of h (Btu/hr ft² °F)

t_p = time from start of accident to end of blowdown

V = containment volume (Ft³)

E = initial coolant energy (Btu)

The parabolic increase to the peak value is given by:

$$h_s = h_{\max} \sqrt{\frac{t}{t_p}} \quad 0 \leq t \leq t_p \quad (2)$$

h_s = heat transfer coefficient for steel (Btu/hr ft² °F)

t = time from start of accident (sec)

The exponential decrease of the heat transfer coefficient is given by:

$$h_s = h_{\text{stag}} + (h_{\max} - h_{\text{stag}}) e^{-0.05 (t-t_p)} \quad t > t_p \quad (3)$$

where

$$h_{\text{stag}} = 2 + 50x \quad 0 \leq x \leq 1.4 \quad (4)$$

h_{stag} = h for stagnant conditions (Btu/hr ft² °F)

x = steam to air weight ratio in containment

For concrete the heat transfer coefficient is taken as 40% of the value calculated for steel.

Air-Recirculation Fan-Coolers

The ability of the containment air recirculation coolers to function properly in the accident environment is demonstrated by the Westinghouse computer code "HECO". The code determines the plate-fin cooling coil heat removal rate when operating in a saturated steam-air mixture.

In the code a mass flow rate of cooling water is first established.

This determines the tube inside film coefficient. Next the resistance to heat transfer between the cooling water and the outside of the fin collars is computed; including inside film coefficient, fouling factor*, tube radial conduction, fin-collar interface resistance, and conduction across the fin collars. The analysis now becomes iterative. One now assumes an overall heat transfer rate Q_{tot} . The temperature at the outside of the fin collars is determined from Q_{tot} and the sum of the resistances cited above.

A second iterative procedure is now established. The variable whose value is assumed is the effective film coefficient between the fins and the gas stream, which involves the effect of convective heat transfer and mass transfer. With this value of $h_{effective}$, one can determine fin efficiency and the fin temperature distribution. It is assumed that a condensate film exists on the vertical fins. An analysis is performed which relates this film thickness to the rate of removal due to gravity and shear, and the rate of addition of condensate by mass transfer from the bulk gas. In the process, from an energy balance, one determines the temperature of the interface between the bulk gas and the condensate;

* A fouling factor of $.001 \text{ hr-ft}^2\text{-}^\circ\text{F}/\text{BTU}$, under both normal and design basis accident conditions, has been assumed for cooling coil design purposes. This value is conventionally used in sizing heat exchangers cooled by lake water at 125°F or less (Reference 5), and is considered conservative for this application. Computer analysis of the coils selected shows that the required post-accident heat removal rate can be achieved with a fouling factor approaching $.002 \text{ hr-ft}^2\text{-}^\circ\text{F}/\text{BTU}$.

this is necessary for determining the mass transfer rate from the gas. Now that the thickness of the condensate film is known, the value of the assumed $h_{\text{effective}}$ is checked from the relation $h_{\text{eff}} = K_{\text{water}} / \delta_{\text{film}}$. If the assumed and computed values are not the same, a new guess is made and calculations repeated until the assumed and computed values are equal.

When this occurs, the heat transfer rate from the fins and fin collar is computed, using the standard equations for fin and fin collar heat transfer and the values of $h_{\text{effective}}$ and film-bulk gas interface temperature. If this value is not the same as Q_{tot} , initially assumed in order to determine fin collar temperature, the whole analysis is repeated with a new estimate of Q_{tot} . When, finally, the heat transfer rate to the cooling water from the fin collar equals the resulting computed rate to the fin collar and fins from the gas, the effect of this heat transfer rate on the cooling water is computed. The water exit temperature is established and this value is used as the inlet temperature for the next heat exchanger pass. Also, the effect of convective heat transfer and condensate mass transfer are determined relative to the gas composition and thermodynamic state. The updated gas state is used as inlet conditions for the next pass. The process is now repeated for the second, third etc. passes until the gas exits the heat exchanger.

The mass transfer coefficients used in the "HECO" code were derived from analyses and reports of experimental data contained in references 3, 4, and 5. From reference 3 the mass flow rate of condensate is defined by

$$\dot{m} = \bar{h}_D (\rho_{\text{sg}} - \rho_{\text{sw}})$$

From ref. (3), pp. 471-473, experimental data for mass and heat transfer are correlated by the expression.

$$\frac{\bar{h}_D}{u_s} (Sc)^{-2/3} = \bar{St} (Pr)^{-2/3}$$

as shown in Figure 16-10 of ref. (1). Thus

$$\begin{aligned} \bar{h}_D &= u_s \cdot St \left(\frac{Sc}{Pr} \right)^{2/3} \\ \bar{h}_D &= \frac{u_s \cdot h}{\rho C u_s} \left(\frac{Sc}{Pr} \right)^{2/3} \end{aligned} \quad (2)$$

As reference (3) points out, for large partial pressures of the condensing components, equation (2) must be corrected by a factor P_t/P_{am} . Thus h_D is defined by

$$\bar{h}_D = \frac{h}{\rho C} \frac{P_t}{P_{am}} \left(\frac{Sc}{Pr} \right)^{2/3} \quad (3)$$

This is essentially the same result as reported by ref. (4) pg. 343 and reference (6).

Reference 3 states that experiments show equation (1) to be valid when the Schmidt number does not differ greatly from 1.0. Equations (1) and (3) are combined to give the mass transfer rate, which is

$$\dot{m} = \frac{h}{\rho C} \frac{P_t}{P_{am}} \left(\frac{Sc}{Pr} \right)^{2/3} (\rho_{sg} - \rho_{sw})$$

An approximation was made in assuming that $\left(\frac{Sc}{Pr} \right)^{2/3} \approx 1.0$ thus the local mass transfer rate was computed from

$$\dot{m} = \frac{h}{\rho C} \frac{P_t}{P_{am}} (\rho_{sg} - \rho_{sw})$$

The heat transfer rate due to condensation is computed from

$$q_1 = \frac{\dot{m} \lambda h P}{\rho C P_{am} t} (\rho_{sg} - \rho_{sw})$$

where ρ_{sg} is evaluated at the local bulk gas temperature

ρ_{sw} is evaluated at the local gas-condensate interface temp.

λ is evaluated at the local gas-condensate interface temp.

P and C are evaluated at the local bulk gas temperature

The heat transfer coefficient, h, was determined from experiments on W plate-fin coils which are the same geometry as are used in this application.

The heat transfer rate, locally, is computed from

$$q_2 = h (T_g - T_i)$$

The basis for selecting these values is that the authorities cited as references have shown, through analyses and through cited experiments, that the methods used are accurate.

The air ride pressure drop across the cooling coils under design basis accident condition is estimated to be approximately 1.9 in. H₂O, or .07 psi. This will have negligible effect on the heat removal capability of the cooling coils.

The pressure of non-condensable gases are taken into consideration by virtue of the fact that the theory behind the analyses assumed that the condensable vapor must diffuse through a non-condensable gas.

Application of this method results in the fan-cooler heat removal rate per fan presented in Figure 14.3.4-1.

Nomenclature

- \dot{m} mass flow rate of condensate, lbm/hr-ft^2
 \bar{h}_D mass transfer coefficient, ft/hr .
 ρ_{sg} Density of saturated steam at local bulk gas temp., lbm/ft^3
 ρ_{sw} Density of saturated steam at local condensate-gas interface temperature, lbm/ft^3
 u_s Free steam gas velocity, ft/min .
 Sc Schmidt number, M/pD , dimensionless
 μ Viscosity of bulk gas, lbm/ft-hr .
 ρ Bulk gas density, lbm/ft^3
 D Gas-air diffusion coefficient, $\frac{\text{ft}^2}{\text{hr}}$
 St Stanton number, h/pcu_s , dimensionless
 h Convective heat transfer coefficient, $\text{BTU/hr-ft}^2\text{-}^\circ\text{F}$
 C Specific heat of bulk gas, $\text{BTU/lbm-}^\circ\text{F}$
 P_r Prandtl number, $\mu c/k$, dimensionless
 k Thermal conductivity of bulk gas, $\text{BTU/hr-ft-}^\circ\text{F}$
 P_t Total gas pressure, lb/ft^2
 P_{am} Air log-mean $\frac{P_{aw} - P_{ag}}{\ln \frac{P_{aw}}{P_{ag}}}$, lb/ft^2
 P_{aw} Partial pressure of air at the local gas-condensate interface, lb/ft^2
 P_{ag} Partial pressure of air at the local bulk gas temperature, lb/ft^2
 λ Latent heat of vaporization (or condensation) at the local gas-condensate interface temperature, BTU/lbm
 q_1 Local heat transfer rate due to condensation, BTU/hr-ft^2
 q_2 Local heat transfer rate due to convection, BTU/hr-ft^2
 T_g Local bulk gas temperature, $^\circ\text{F}$
 T_i Local gas-condensate interface temperature, $^\circ\text{F}$.

Reactor Containment Fan Cooler Cooling Coil Test Summary

In the event of a loss-of-coolant accident of a pressurized water reactor system, compressed water at thermodynamic conditions of approximately 600°F and 2250 psig would flash into the containment building. This condition causes the containment atmosphere to become a high pressure steam saturated environment, limited to a maximum pressure of 40 to 60 psig in most dry containment buildings. One of the active containment cooling systems employed to remove energy from the atmosphere and reduce the containment pressure is the Reactor Containment Fan Cooler System. An integral part of this system are plate-finned cooling coils. These heat exchangers remove sensible heat during normal operation, but become condensers in the post accident environment. Because there was limited experimental information available concerning the performance of plate-finned cooling coils operating in a condensing environment in the presence of a non-condensable (air), Westinghouse undertook a demonstration test to establish the validity of its selection procedure.*

The test method was to subject a scaled coil to a parametric test. These parameters were: containment pressure (with corresponding steam density and temperature), air flow rate, cooling water flow rate, cooling water temperature, and entrained water content. Each parametric test condition was then used as input to the computer program used in coil selections. The results of the test and the computer program predictions were compared to establish the applicability.

In all cases considered the measured heat transfer rate is greater than that predicted by the computer code predictions. The range of parameters variations was selected to be consistent with the design points of the reactor containment fan cooling coils contained in actual plants. It is apparent that for this specific type of heat exchanger, functioning in the range of environments tested, no moisture separator is needed to protect the coils from excessive waterlogging due to entrained spray droplets.

* Test description and results are presented in the Westinghouse proprietary report, WCAP, 7336-L, "Topical Report - Reactor Containment Fan Cooler Cooling Coil Test"

The extension of the test to full size units is merely an increase in component size and total flow quantities, but not a change in controlling parameters. It is concluded that the test demonstrates that the computer code used to select cooling coil design is valid in defining the heat removal rates of plate-finned tube cooling coil assemblies of Reactor Containment Fan Cooler Systems. Therefore, these test demonstrate that Westinghouse fan cooler designs which are selected by this computer program will perform as required in the post-accident containment environment.

Containment Spray

When a spray drop enters the hot saturated steam-air environment, the vapor pressure of the water at its surface is much less than the partial pressure of the steam in the atmosphere. Hence, there will be diffusion of steam to the drop surface and condensation on the drop. This mass flow will carry energy to the drop. Simultaneously the temperature difference between the atmosphere and the drop will cause a heat flow to the drop. Both of these mechanisms will cause the drop temperature and vapor pressure to rise. The vapor pressure of the drop will eventually become equal to the partial pressure of the steam and the condensation will cease. The temperature of the drop will be essentially equal to the temperature of the steam-air mixture.

The terminal velocity of the drop can be calculated using the formula given by Weinberg⁽⁷⁾ where the drag coefficient C_D is a function of the Reynolds number:*

$$V^2 = \frac{4Dg (\rho - \rho_m)}{3C_D \rho_m} \quad (1)$$

For the 700 micron drop size expected from the nozzles, the terminal velocity is less than 7 ft/sec. For a 1000 micron drop, the velocity would be less than 10 ft/sec. The Nusselt number for heat transfer, Nu , and the Nusselt number for mass transfer, Nu' (Sherwood Number), can be calculated from the empirical relations given by Ranz and Marshall.⁽⁸⁾

$$Nu = 2 + 0.6 (Re)^{1/2} (Pr)^{1/3} \quad (2)$$

$$Nu' = 2 + 0.6 (Re)^{1/2} (Sc)^{1/3} \quad (3)$$

* Nomenclature used is given at the end of this discussion.

The Prandtl number and the Schmidt number for the conditions assumed are approximately 0.7 and 0.6 respectively. Both of these are sufficiently independent of pressure, temperature and composition to be assumed constant under containment conditions.^(9,10) The coefficients of heat transfer (h_c) and mass transfer (k_G) are calculated from Nu and Nu' respectively. The equations describing the temperature rise of a falling drop are:

$$\frac{d}{dt} (Mu) = m h_g + q \quad (4)$$

$$\frac{d}{dt} (M) = m \quad (5)$$

where

$$q = h_c A (T_s - T) \quad (6)$$

$$m = k_G A (P_s - P_v) \quad (7)$$

These equations can be integrated numerically to find the internal energy and mass of the drop as a function of time as it falls through the atmosphere. Analysis shows that the liquid drop temperature rises to the steam-air mixture temperature in less than 0.5 seconds, which occurs before the drop has fallen 5 feet. These results demonstrate that the spray will be 100% effective in removing heat from the atmosphere.

Nomenclature

A	area
C_D	drag coefficient
D	droplet diameter
g	acceleration of gravity
h_c	coefficient of heat transfer
h_s	steam enthalpy
k_G	coefficient of mass transfer
M	droplet mass
m	diffusion rate
Nu	Nusselt number for heat transfer
Nu'	Nusselt number for mass transfer
P_s	steam partial pressure
P_v	droplet vapor pressure
Pr	Prandtl number
q	heat flow rate
Re	Reynolds number
Sc	Schmidt number
T	droplet temperature
T_s	steam temperature
t	time
u	droplet internal energy
V	velocity
ρ	droplet density
ρ_m	steam-air mixture density

Containment Pressure Transients

The containment pressure was calculated for a range of large area ruptures of the Reactor Coolant System. The rupture sizes considered were:

- a. Double Ended Rupture
- b. 6 ft² break
- c. 3 ft² break
- d. .5 ft² break

Figure 14.3.4-2 presents the results of the transients. For all cases a pressure peak of less than 37.8 psig was calculated. Since the design pressure for the containment is 42 psig, a margin more than 11% above the conservative value of the blowdown peaks, is available.

In the transients one spray pump and two fans starting at 60 seconds were assumed. These acted to quickly reduce the pressure after the peak pressures were reached.

The following paragraphs are a summary of the energy sources and sinks used in the calculation.

Energy Sources

The energy sources presented in Table 14.3.4-2 are potentially available to be transferred to the containment during the blowdown time.

In the above energy summation all sensible energy sources are referenced to the datum of saturated water at containment design pressure, which is the maximum amount of energy that can be transferred from the metal to the coolant.

The integrated energy balance at the end of blowdown is presented in the Table 14.3.4-3. The values were determined by the FLASH R Code.

In this calculation all energy generated by the core during blowdown is transferred to the coolant as it is generated. The sensible energy sources are transferred to the coolant as a function of time, and for longer blowdown times more sensible energy is absorbed. For the very large breaks very little energy is transferred to the steam generators, because of the rapid uncovering of the tubes, while for smaller breaks the tubes do not uncover as rapidly and significant heat transfer results.

A negligible amount of energy is transferred from the reactor vessel during the relatively fast blowdown.

Energy Sinks

Figure 14.3.4-3 presents the energy absorption capability within the 2.1×10^6 ft³ free volume of the containment.

The integrated containment energy balance at the end of blowdown is given by:

$$U_f = U_i + \sum (mh)_{in} + \sum Q_{in} - \sum Q_{out}$$

Where

U_f = Final internal energy in the containment

U_i = Initial external energy in the containment

$\sum (mh)_{in}$ = Enthalpy added by blowdown sources

$\sum Q_{in}$ = Energy added directly to containment atmosphere
by hydrogen-oxygen recombination

$\sum Q_{out}$ = Heat removal by containment structures and
cooling system.

The internal energy is made up of three sources: air, steam, and sump water. Only the air-steam mixture with their respective partial pressures contribute to the containment total pressure. The internal energy for the initial assumed containment conditions, 120°F and 15 psia, is as follows:

$$\begin{array}{llll}
 \text{Steam (m) (u)} & = & (2110) (1077) & = 2.27 \times 10^6 \text{ Btu} \\
 \text{Air (m) (Cr) (T)} & = & (1.51 \times 10^6) (0.172) (120) & = 3.12 \times 10^6 \text{ Btu} \\
 \text{Sump (m) (u)} & = & (1.23 \times 10^4) (87.9) & = \underline{1.06 \times 10^6 \text{ Btu}} \\
 & & & 6.45 \times 10^6 \text{ Btu}
 \end{array}$$

The internal energy balance at the end of blowdown is given in the Table 14.3.4-4. All entries are in millions of Btu's.

The difference between the internal energies given by the energy balance equation and by the COCO program represents an error of less than $\pm 1\%$ in the calculation.

Figure 14.3.4-4 shows the heat transfer coefficients calculated for the various break sizes.

Containment Margin Evaluation

Evaluation of the capability of the reactor containment and containment cooling systems to absorb energy additions without exceeding the containment design pressure requires consideration of two periods of time following a postulated large area rupture of the reactor coolant system.

The first period is the blowdown phase. Since blowdown occurs too rapidly for the containment cooling systems to be activated, there must be sufficient energy absorption capability in the free volume of the containment (with due credit for energy absorption in the containment structures) to limit the resulting pressure below design.

The second period is the post-blowdown period where the containment cooling systems must be able to absorb any postulated post-blowdown energy additions and continue to limit the containment pressure below design.

Margin - Blowdown Peak to Design Pressure

Point A in Figure 14.3.4-5 corresponds to the internal energy at the end of a DE break blowdown, 200×10^6 Btu. In order for the pressure to increase to design pressure (42 psig) the internal energy must be increased to 222×10^6 Btu (Point B). The allowed energy addition is therefore 22×10^6 Btu. Since energy transferred to the containment from the core is in the form of steam the total transferred core energy corresponding to allowed energy addition is as follows:

$$Q_{\text{core}} = \frac{h_{fg}}{h_g} Q_{\text{allowed}} = 22 \times 10^6 \times \frac{917.9}{1176.6} = 17.4 \times 10^6 \text{ Btu}$$

This allowable value of energy which could be transferred from the core to the containment without increasing the transient containment pressure to design pressure can be compared to the energy stored in the reactor vessel and transferred to the steam generator during blowdown for the double ended break. The thick metal of the reactor vessel was not considered since a negligible amount of this energy can be transferred in the short blowdown time.

Stored in the core	15.0×10^6 Btu
Core internals Metal	0.3×10^6 Btu
Transferred to Steam Generators	<u>1.4×10^6 Btu</u>
	16.7×10^6 Btu

Thus, the containment has the capability to limit containment pressure below design even if all of the available energy sources were transferred to the containment at the end of blowdown. This would also include no credit for energy absorption in the steam generator. For this to occur an extremely high core to coolant heat transfer coefficient is necessary. This would result in the core and internals being completely subcooled and limit the potential for release of fission products.

Additional Energy Added as Superheat

Line A to C on Figure 14.3.4-5 represents a constant mass line extended into the superheated region. Comparison of the energy addition allowable for the superheated case relative to the saturated case shows a lesser ability of the containment to absorb an equivalent amount of energy as superheat. An addition of 5.5×10^6 Btu of energy after blowdown would cause the containment pressure to increase to design. The recombination of hydrogen and oxygen from a 6.2% Zr-H₂O reaction completed before the end of blowdown would be required to generate 5.5×10^6 Btu's of energy. For the case analyzed, the core was assumed to be in a subcooled state, and no Zr-H₂O reaction would be possible. In order for Zr-H₂O reaction to occur before the end of blowdown all of the stored initial energy must remain in the core. If this occurred a blowdown peak containment pressure of only 33.5 psig would be reached instead of 37.8 psig in the case analyzed. Lines D and E on Figure 14.3.4-5 represent the superheat energy addition required to increase the pressure to the design pressure and this corresponds to the hydrogen oxygen recombination energy from a 11.2% Zr-H₂O reaction.

It is, therefore, concluded that the containment has the capability to absorb the maximum energy addition from any loss-of-coolant accident without reliance on the containment cooling system. In addition, a substantial margin exists for energy additions from arbitrary energy sources much greater than any possible.

Margin - Post Blowdown Energy Additions

The Safety Injection System is designed to rapidly cool the core and stop significant addition of mass and energy to the containment.

However, the following cases are presented to demonstrate the capability of the containment to withstand post accident energy additions without credit for core cooling.

Case 1. Blowdown from a large area rupture with continued addition of the core residual energy and hot metal energy to the containment as steam.

Case 2. Same as Case 1 but with the energy addition from a maximum Zirconium - water reaction.

Figure 14.3.4-6 presents the containment pressure transient for Case 1. For this case the decay heat generated for a 2300 MWt core operated for an infinite time is conservatively assumed. This decay heat is added to the containment in the form of steam by the boiling off of water in the reactor vessel. For this case injection water merely serves as a mechanism to transfer the residual energy to the containment as it is produced. Injection water is in effect throttled at the required rate.

In addition, all the stored energy in the core and internals which is calculated to remain at the end of blow down is added in the same way during the time interval between 12.7 and 36.5 seconds (corresponds to accumulator injection time). Also all the sensible heat of the reactor vessel is added as steam exponentially over 2000 seconds time interval.

The containment cooling system capability assumed in the analysis was one of two available containment spray pumps and two of four available containment fan coolers. This is the minimum equipment available considering the single failure criterion in the emergency power system, the spray system and the fan cooler system.

The containment heat removal capability started at 60 seconds exceeds the energy addition rate and the pressure does not exceed the initial blowdown value. An extended depressurization time results due to the increased heat load on the containment coolers.

It should be emphasized that this situation is highly unrealistic in that continued addition of steam to the containment after blowdown could not occur. The accumulator and Safety Injection System acts to rapidly reflood and cool the core.

Figure 14.3.4-7 presents the containment pressure transient for Case 2. To realistically account for the energy necessary to cause a metal-water reaction, sufficient energy must be stored in the core. Storing the energy in the core rather than transferring it to the coolant causes a decrease in the blowdown peak.

The reaction was calculated using the parabolic rate equation developed by Baker and assuming that the clad continues to reactor until zirconium oxide melting temperature of 4800°F is reached. An additional 10% reaction of the unreacted clad is assumed when the oxide melting temperature is reached. A total reaction of 32.3% has occurred after 1000 seconds. If the reactions were to be steam limited, they could result in a higher total reaction but at a much later time. The reaction provided by the parabolic rate equation therefore, imposes the greatest load on the containment cooling system.

As in Case 2, the residual heat and sensible heat is added to the containment as steam. The energy from the $\text{Zr-H}_2\text{O}$ reaction is added to the containment as it is produced. The hydrogen was assumed to burn as it entered the containment from the break.

The blowdown peak was reduced to 33.5 psig and a peak pressure of 40.5 psig was reached at 900 seconds. At this time the heat removal capability of the containment cooling system assumed to be operating (one containment spray pump and two fan coolers) exceeded the energy addition from all sources.

For comparison the containment pressure transients for Cases 1, 2 and the double ended blowdown are replotted in Figure 14.3.4-8. It is concluded that operation of the minimum containment cooling system equipment provides the capability of limiting the containment pressure below its design pressure with the addition of all available energy sources and without credit for the cooling effect from the safety injection system.

Discussion of Energy Sources Used in Cases 1 and 2

The following is a summary of the energy sources and the containment heat removal capacities used in the containment capability study. Figure 14.3.4-9 presents the rate of energy addition from core decay heat, $\text{Zr-H}_2\text{O}$ reaction energy, and the hydrogen-oxygen recombination energy. The heat removal capability for the partial containment cooling (one spray pump and two fan coolers) is also presented. These heat removal values are for operation with the containment at design pressure.

The integrated heat additions and heat removals for Cases 1 and 2 are plotted in Figures 14.3.4-10 and 14.3.4-11, respectively. These curves are presented in a manner that demonstrates the capability of the containment and the cooling systems to absorb energy. The integrated heat removal capacity is started at the internal energy corresponding to design pressure, while the integrated heat additions begin from the internal energy calculated at the end of blowdown for each case. The upper line on each curve is the containment structures and containment cooling systems capability to absorb energy additions without exceeding design pressure. The lower curve for each are the energy addition curves, and since these energy additions are the maximum possible with no credit for core cooling, there is more than adequate capability to absorb arbitrary additions.

The curves in Figures 14.3.4-12 and 14.3.4-13 present the individual contribution of the heat removal and heat addition source, respectively.

Evaluation of Long Term Fan Cooler Capability

The ability of the fan coolers to limit containment pressure following loss of the component cooling system has been examined. If the component cooling loop were lost for any reason during long term recirculation, core subcooling could be lost and boiling in the core would begin. Since the fan cooling units are cooled by service water, the energy from the core would be removed from the containment via the fans. The following table summarizes the maximum pressure the containment could reach for assumed times of component cooling system failure.

	<u>3 Fans</u>	<u>2 Fans</u>
C.C. Failure at 12 hours	9.5	27
C.C. Failure at 1 day	7.0	16
C.C. Failure at 1 week	2.0	4.5

3

Evaluation of Containment Internal Structures

The crane wall has been designed for several pressures as the volume within it is compartmentalized into three compartments each housing one loop of the RCS. The compartments are separated from each other by the refueling canal, missile shield walls and the in-core instrumentation room which restricts venting of the steam resulting from the loss of coolant accident. The plan location of the compartments are shown on Figure 14.3.4-14. The pressures for which each compartment is designed are listed below:

<u>Compartment</u>	<u>Design Pressure</u>
Northeast	16 psig
Southeast	13.5 psig
Northwest	22 psig

The primary shield was designed for an internal pressure of 80 psig.

The peak pressures in each compartment were determined by a digital computer code, COMCO, which was developed to analyze the pressure build-up in the reactor coolant loop compartments. The COMCO code is largely an extension of the COCO Code in that a separation of the two phase blowdown into steam and water is calculated and the pressure build-up of the steam-air mixture in the compartment is determined. Each compartment has a vent opening to the free volume of the containment.

3

The main calculation performed is a mass energy balance within the control volume of a compartment. The pressure builds up in the compartment until a mass and energy relief through the vent exceeds the mass and energy entering the compartment from the break. The reactor coolant loop compartments are designed for the maximum calculated differential pressure resulting from an instantaneous double ended rupture of the reactor coolant pipe.

REFERENCES

- 1) Tagami, Takaski, "Interim Report on Safety Assessments and Facilities Establishment Project in Japan for Period Ending June 1965 (no. 1)."
- 2) Kolflat, A., and Chittenden, W. A., "A New Approach to the Design of Containment Shells for Atomic Power Plants." Proc. of Amer. Power Conf., 1957 p. 651-9.
- 3) Eckert, E.R.G., & Drake, P.M.J., Heat and Mass Transfer, McGraw-Hill Book Co., Inc., New York (1959)
- 4) Kern, D.Q., Process Heat Transfer, McGraw-Hill Book Co., Inc., New York, (1950)
- 5) McAdams, W.H., Heat Transmission, 3rd Edition, McGraw-Hill Book Co., Inc., New York, (1954)
- 6) Chilton, T.H., and Colburn, A.P., "Mass Transfer (Absorption) Coefficients Prediction from Data on Heat Transfer and Fluid Friction," Ind. Eng. Chem., 26, (1934), pp. 1183-87.
- 7) S. Weinberg, Proc. Inst. Mech. Engr., 164, pp. 240-258, 1952.
- 8) W. Ranz and W. Marshall, Chem, Engr., Prog. 48, 3, pp. 141-146 and 48, 4, pp. 173-180, 1952.
- 9) J. Perry, "Chemical Engineers Handbook," 3rd Ed. McGraw-Hill, 1950.
- 10) E. Eckert and J. Gross, "Introduction to Heat and Mass Transfer," McGraw-Hill, 1963.

TABLE 14.3.4-1

STRUCTURAL HEAT SINKS

HEAT SINK	MATERIAL	AREA FT ²	THICKNESS FT	DENSITY LB/FT ³	HEAT CAPACITY BTU/LB °F	CONDUCTIVITY BTU/HR.FT °F
Containment cylinder	steel lined concrete	47,500	0.03	486	0.11	29.5
Containment dome	steel lined concrete	26,600	0.04	486	0.11	29.5
Containment floor	unlined concrete	29,500	1.,0.4,0.3	144	0.186	1.05
Refueling canal	lined concrete	4,140	0.02	486	0.11	29.5
Misc. concrete structure	unlined concrete	29,100	1.	144	0.186	1.05
Misc. steel structure	steel	48,300	0.05	486	0.11	29.5
Insulation	vinylcol	57,000	0.104	4.	0.75	0.037

TABLE 14.3.4-2

ENERGY SOURCES

1	Reactor coolant system internal energy	240 x 10 ⁶ BTU
2	Accumulator internal energy (2)	8.4 x 10 ⁶ BTU
3	Initial core stored energy	26.4 x 10 ⁶ BTU
4	Core internals metal energy	7.4 x 10 ⁶ BTU
5	Reactor vessel metal (below nozzles)	<u>11.9 x 10⁶ BTU</u>
	Sub total	294.1 x 10 ⁶ BTU
6.	Core power generation during blowdown	
	a - Double ended (12.7 sec)	4.6 x 10 ⁶ BTU
	b - 6 ft ² (16 sec)	5.3 x 10 ⁶ BTU
	c - 3 ft ² (22.5 sec)	6.5 x 10 ⁶ BTU
	d - 0.5 ft ² (106.0)	15.2 x 10 ⁶ BTU
7.	Z _r -H ₂ O reaction	~ 0.0
Totals:		
	a - Double ended	298.7 x 10 ⁶ BTU
	b - 6 ft ²	299.4 x 10 ⁶ BTU
	c - 3 ft ²	300.6 x 10 ⁶ BTU
	d - 0.5 ft ²	309.3 x 10 ⁶ BTU

TABLE 14.3.4-3

INTEGRATED ENERGY BALANCE AT END OF BLOWDOWN
BTU x 10⁻⁶

Outside reactor coolant system - control volume	DE	6 FT ²	3 FT ²	0.5 FT ²
1 - Blowdown enthalpy	260.	260.8	260.	251.4
2 - Transferred to steam generator	1.4	1.7	4.6	22.1
Inside reactor coolant system - control volume				
1 - Reactor coolant internal energy (water remaining in vessel plus accumulator addition)	6.	7.3	5.9	17.8
2 - Stored in core	15.	12.6	11.	2.5
3 - Core internal metal	0.3	0.4	0.9	0.7
4 - Reactor vessel metal	11.9	11.9	11.9	11.9
5 - Internal energy of water remaining in accumulator (injection not complete)	6.1	5.8	6.3	3.7
	<hr/>	<hr/>	<hr/>	<hr/>
	39.3	38.0	36.0	36.6
	<hr/>	<hr/>	<hr/>	<hr/>
	300.7	300.5	300.6	310.2

TABLE 14.3.4-4

INTERNAL ENERGY BALANCE AT END OF BLOWDOWN
BTU $\times 10^{-6}$

	<u>DE</u>	<u>6 FT²</u>	<u>3 FT²</u>	<u>0.5 FT²</u>
U_i	6.5	6.5	6.5	6.5
$\Sigma(mh)_{in}$	260.0	260.8	260.	251.4
ΣQ_{in}	0.0	20	20	20
ΣQ out struct	-11.8	-13.2	-14.5	-20.
fans	0.0	0.	0.	-0.74
spray	0.0	0.	0.	-0.66
Total U_f	<u>254.7</u>	<u>254.1</u>	<u>252.0</u>	<u>236.5</u>

From CoCo the final condition
are

steam	194.0	187.1	192.7	177.7
air	6.4	6.3	6.4	6.4
sump	54.3	60.2	53.4	53.2
	<u>254.7</u>	<u>253.6</u>	<u>252.5</u>	<u>237.4</u>

FAN COOLER HEAT REMOVAL AS A FUNCTION
OF CONTAINMENT PRESSURE

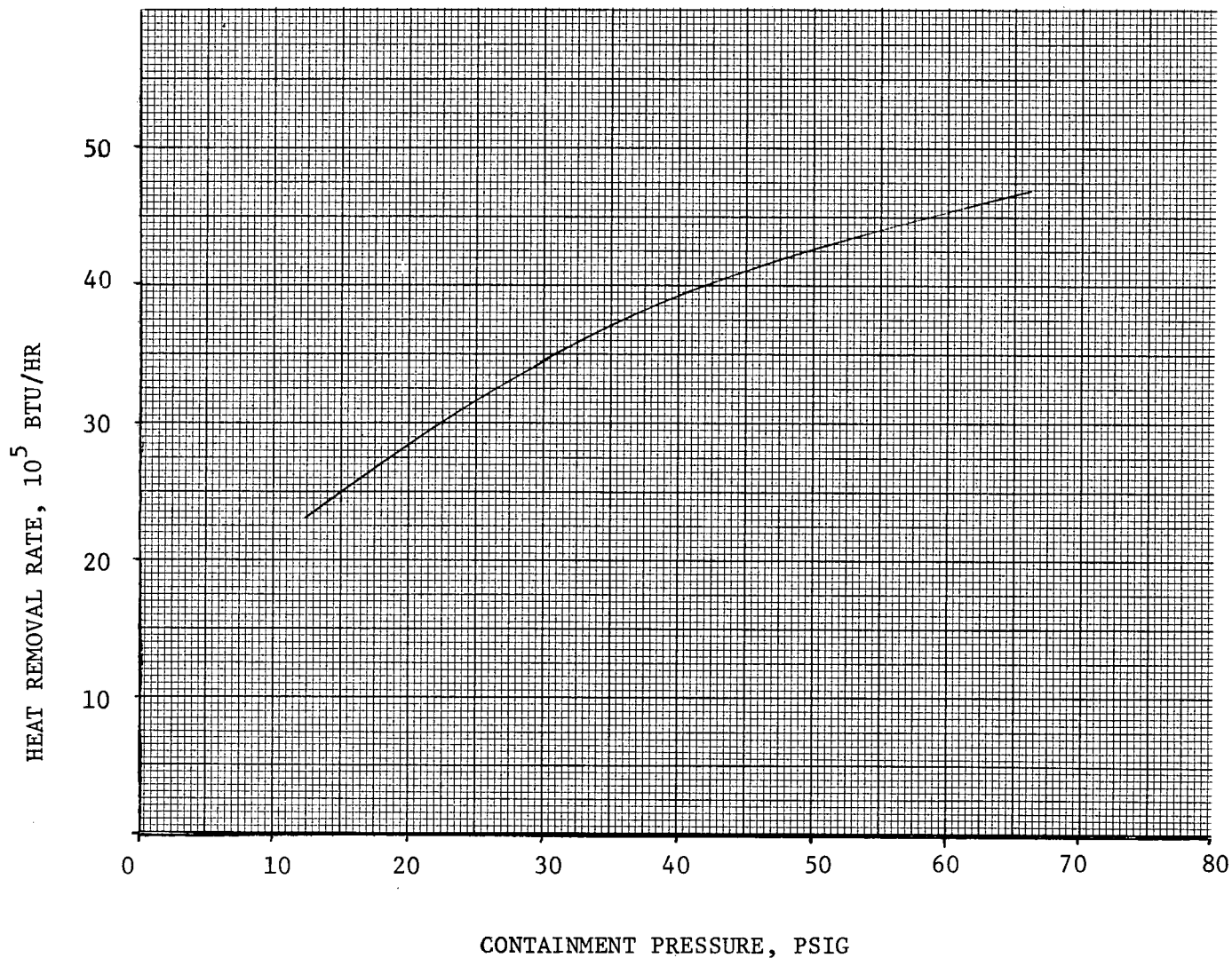


FIGURE 14.3.4-1

CONTAINMENT PRESSURE TRANSIENTS FOR A RANGE OF BREAK SIZES (MIN, SAFETY FEATURES OPERATING)

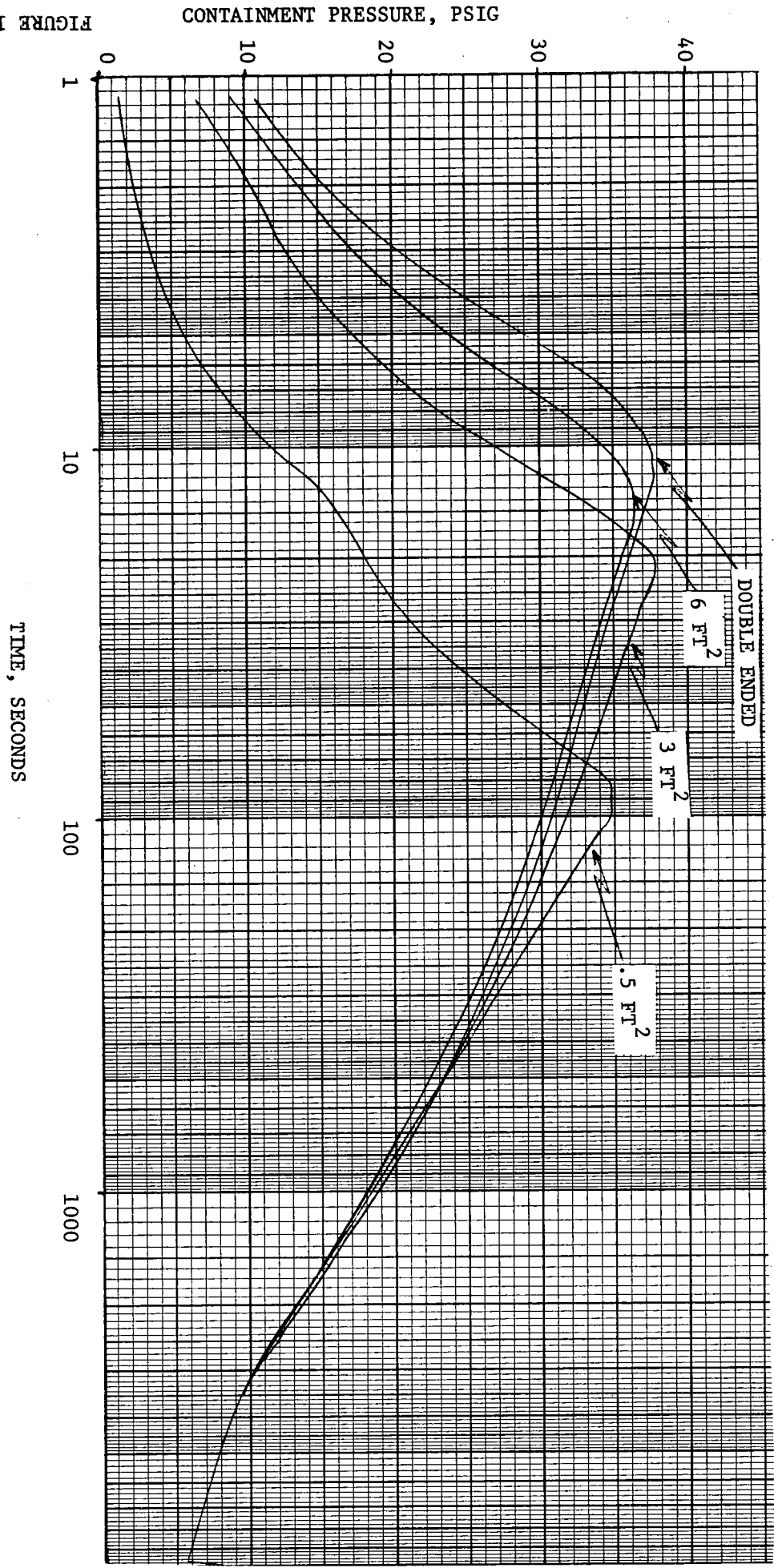


FIGURE 14.3.4-2

CONTAINMENT CAPABILITY STUDY
CONTAINMENT PRESSURE VS. STEAM-AIR INTERNAL ENERGY
Volume: $2.1 \times 10^6 \text{ FT}^3$

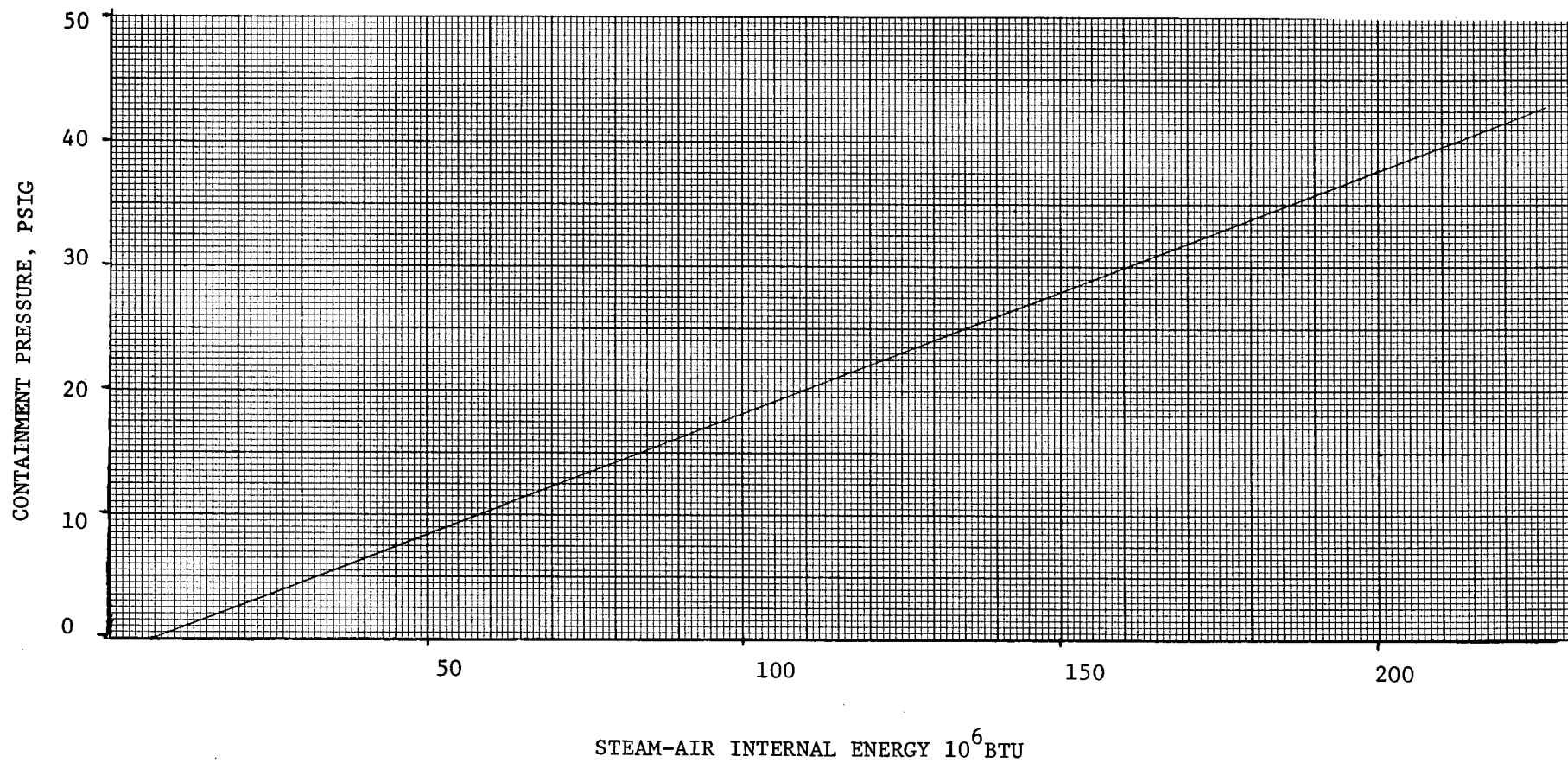


FIGURE 14.3.4-3

STRUCTURAL HEAT TRANSFER COEFFICIENT

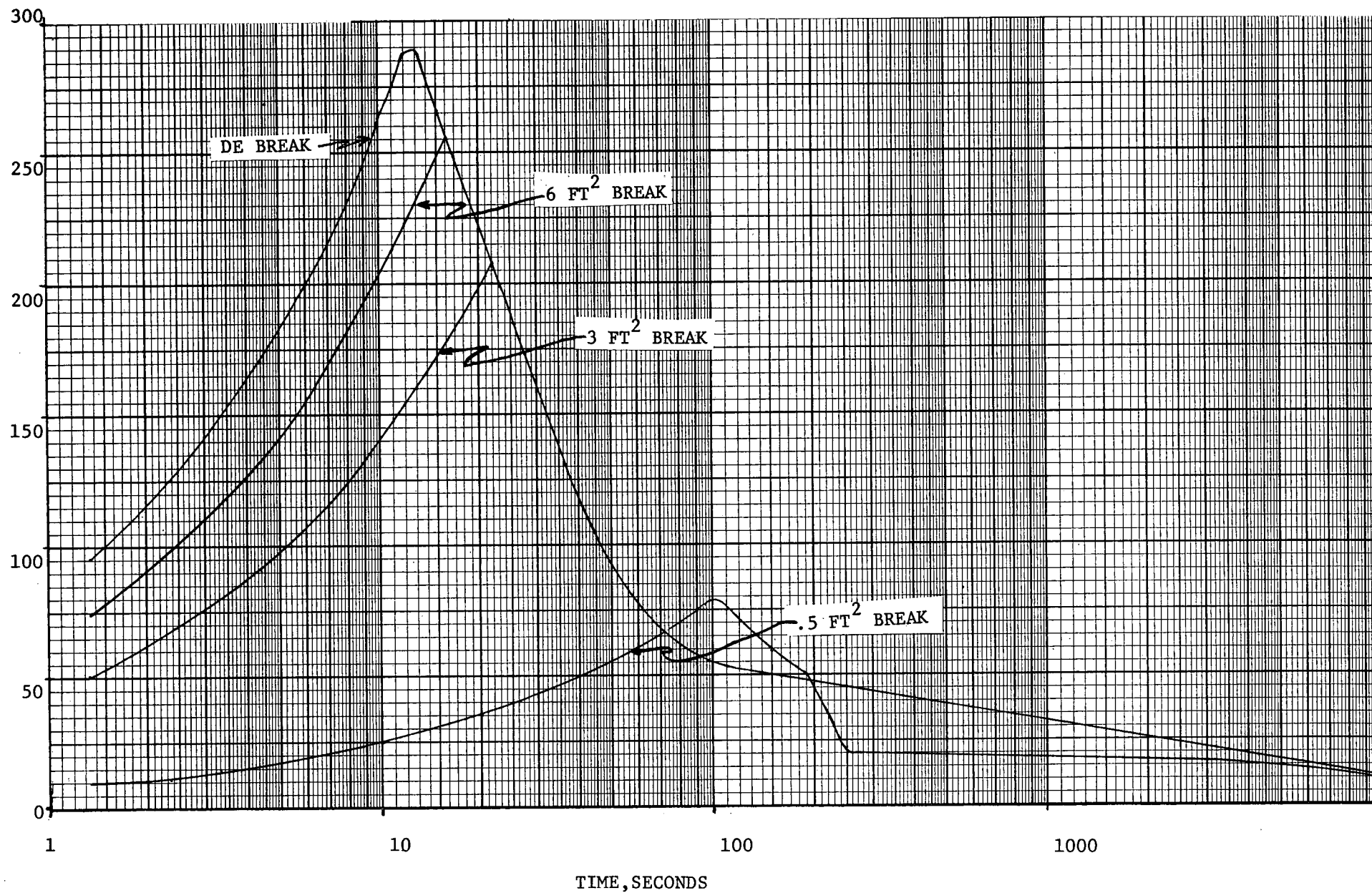


FIGURE 14.3.4-4

CONTAINMENT CAPABILITY STUDY
CONTAINMENT PRESSURE VS. STEAM AIR INTERNAL ENERGY

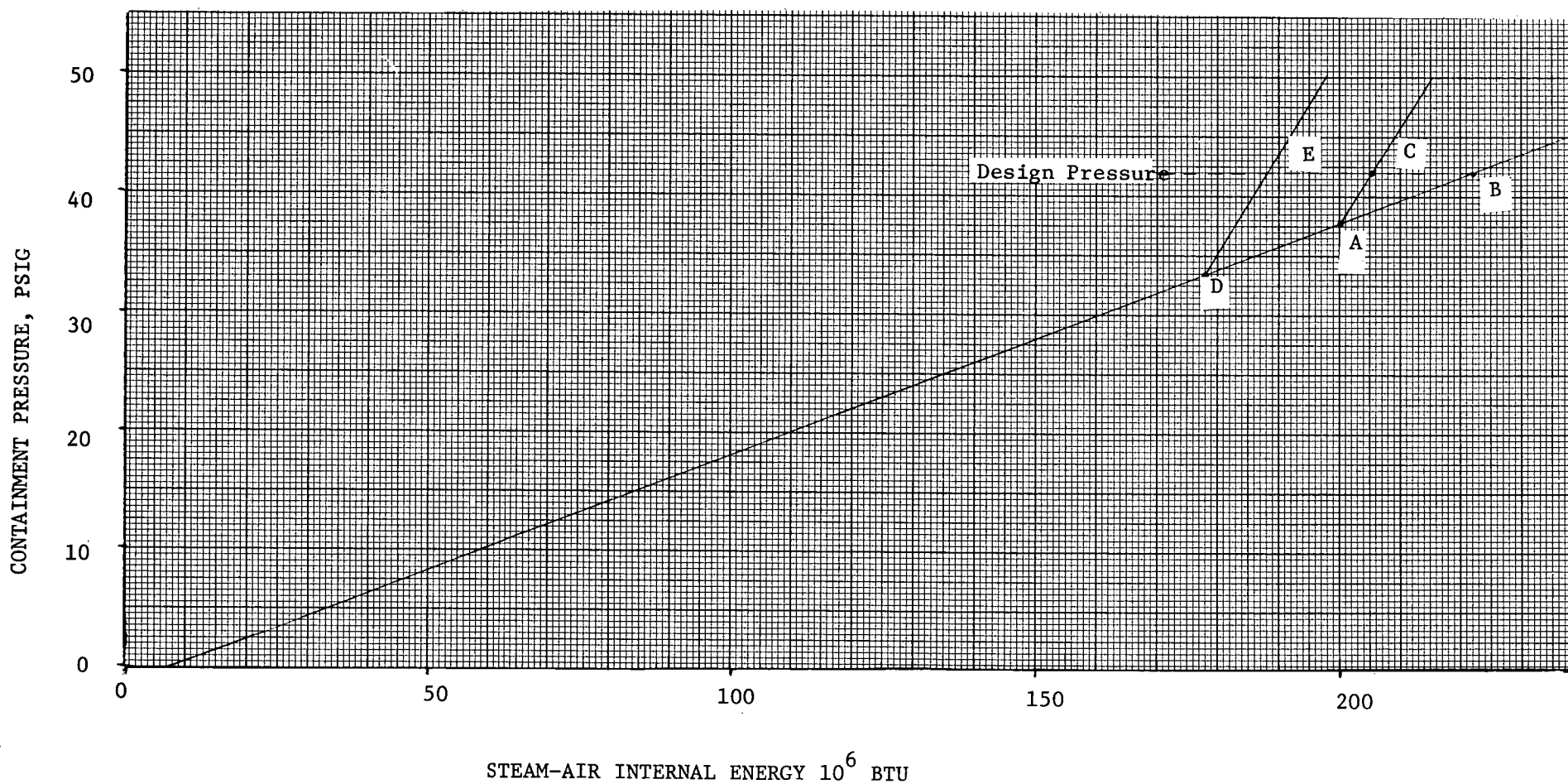


FIGURE 14.3.4-5

CONTAINMENT CAPABILITY STUDY

ALL AVAILABLE ENERGY

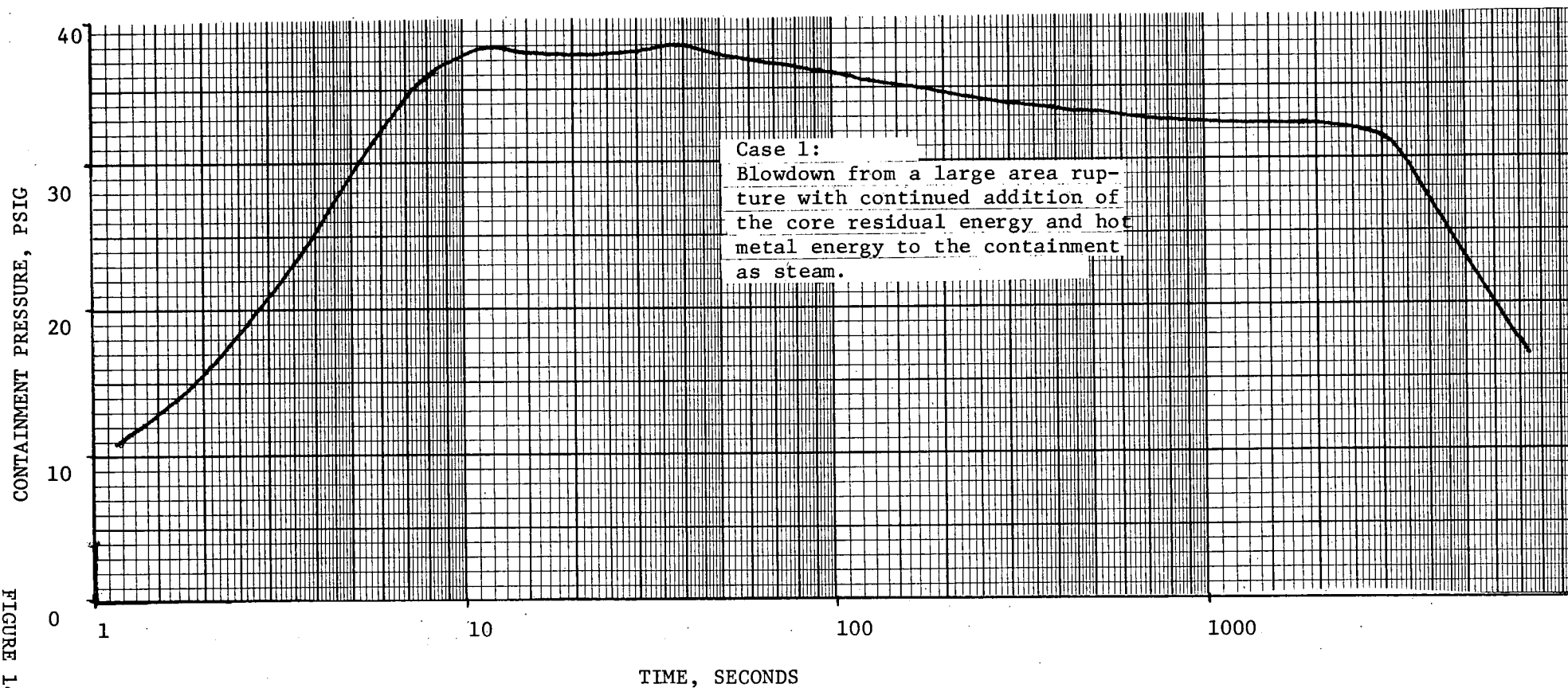


FIGURE 14.3.4-6

CONTAINMENT CAPABILITY STUDY

ZR-WATER REACTION

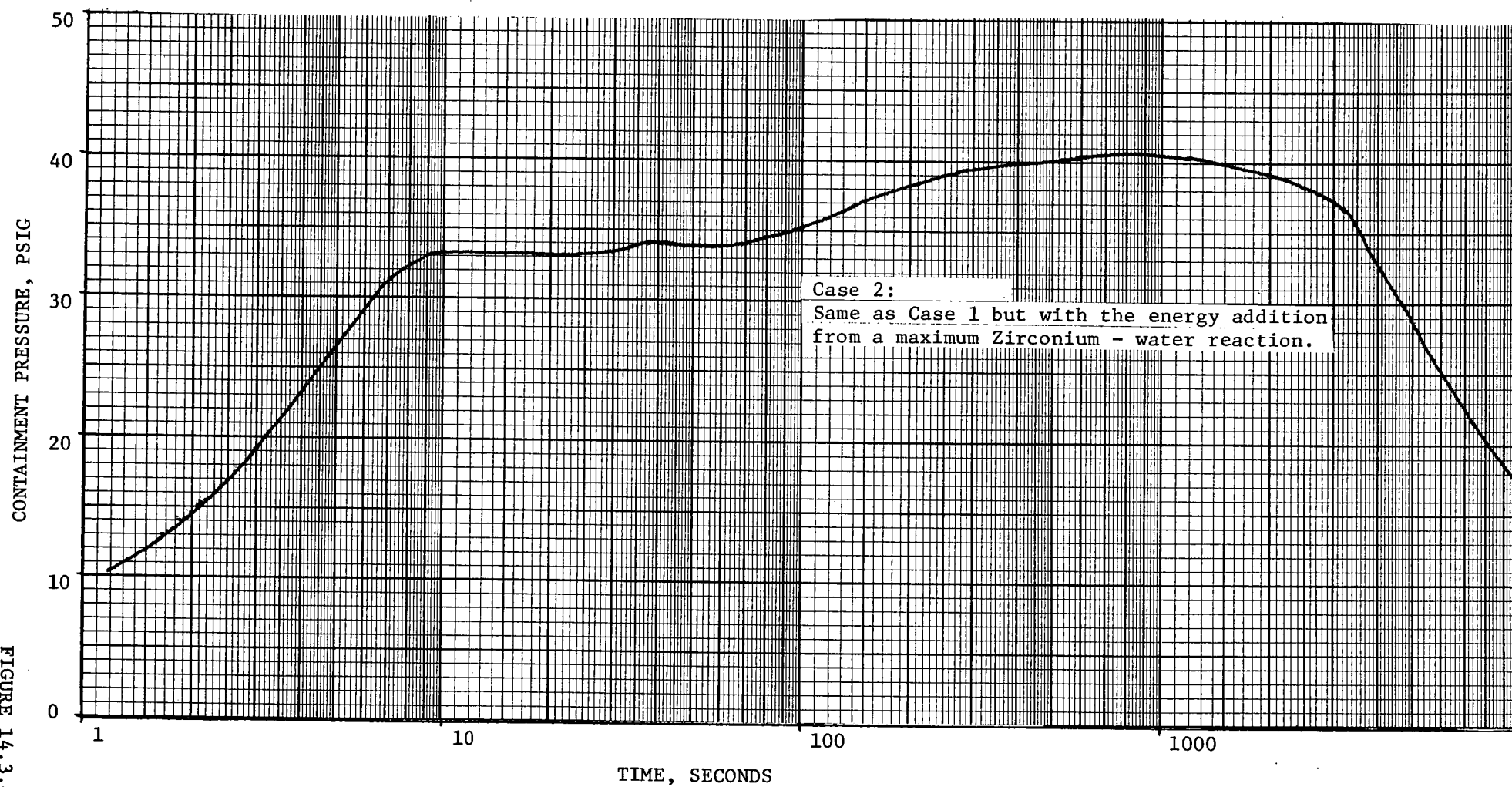


FIGURE 14.3.4-7

CONTAINMENT CAPABILITY STUDY
COMPARISON OF PRESSURE TRANSIENTS
DOUBLE-ENDED BREAK

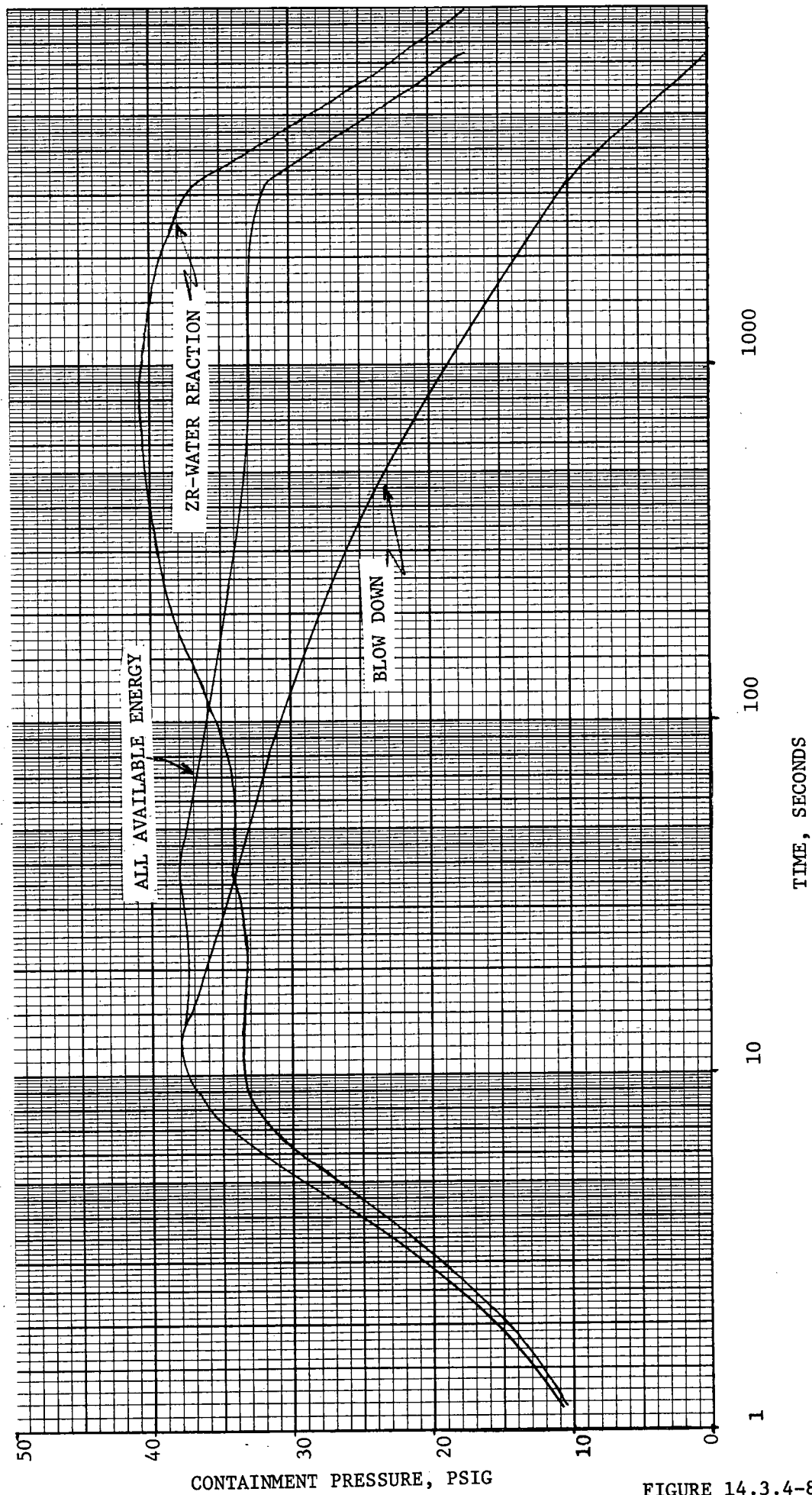
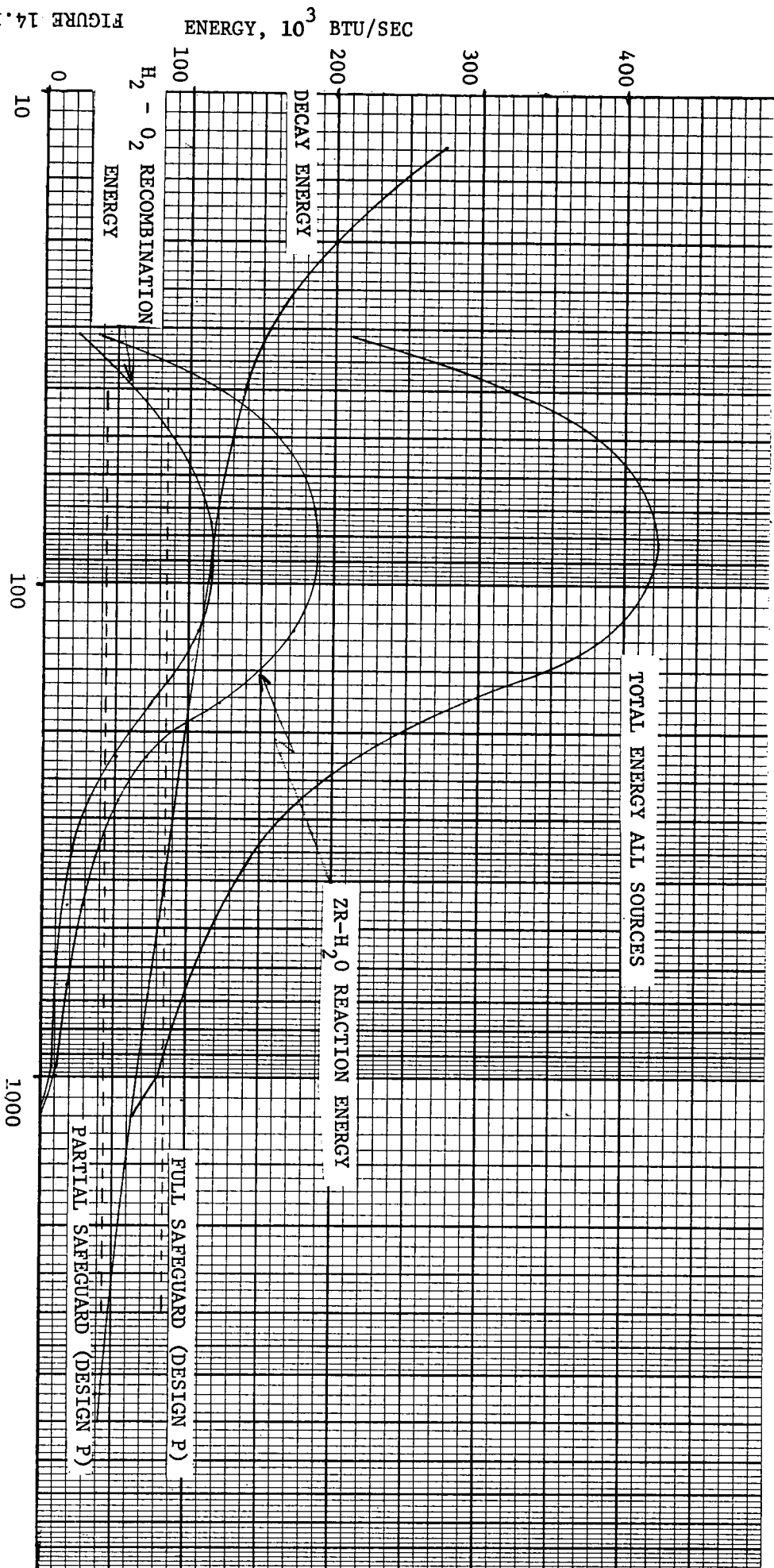


FIGURE 14.3.4-8

CONTAINMENT CAPABILITY STUDY RATE OF ENERGY ADDITION



CONTAINMENT CAPABILITY

CASE 1

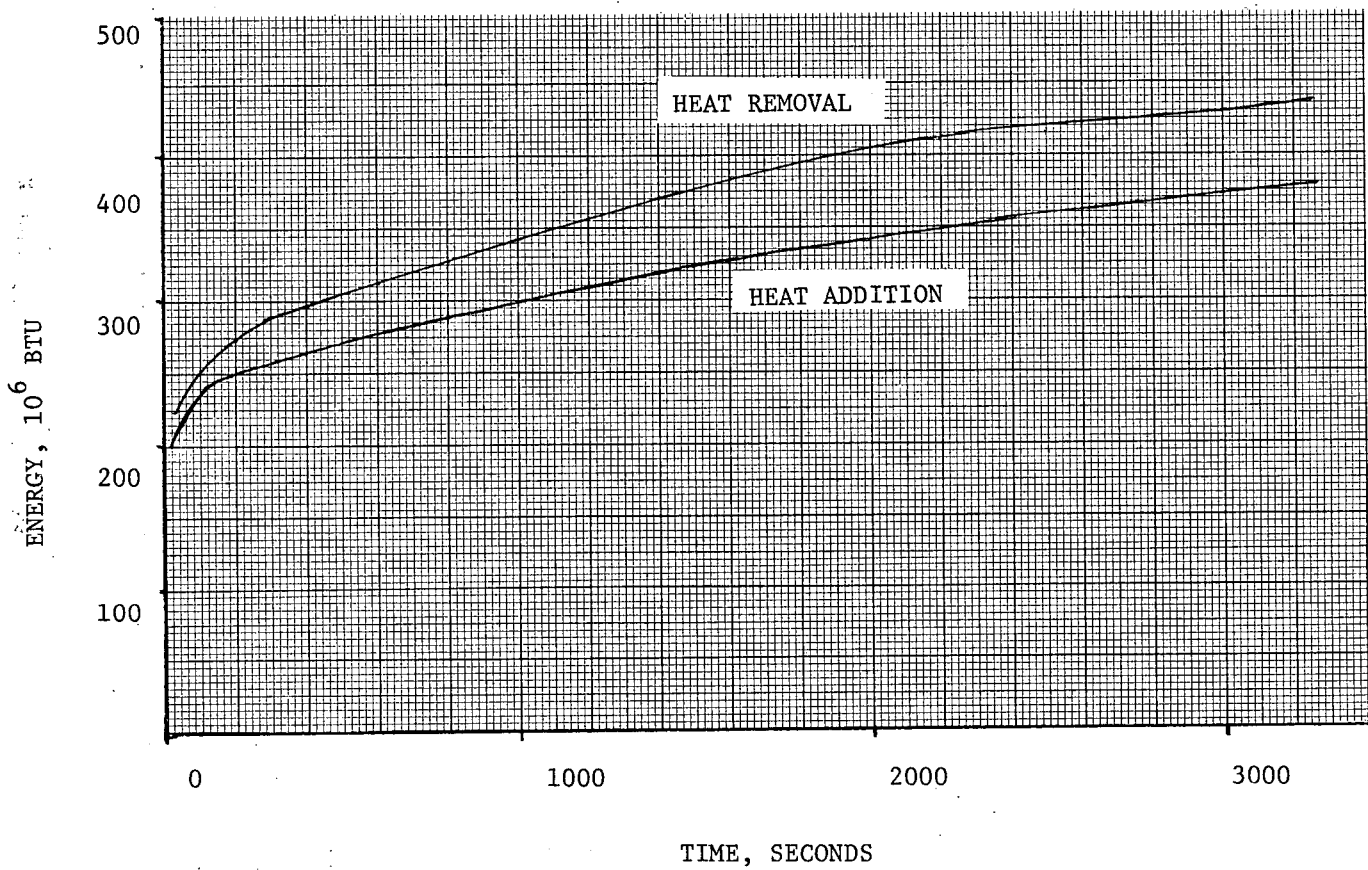


FIGURE 14.3.4-10

CONTAINMENT CAPABILITY
CASE 2

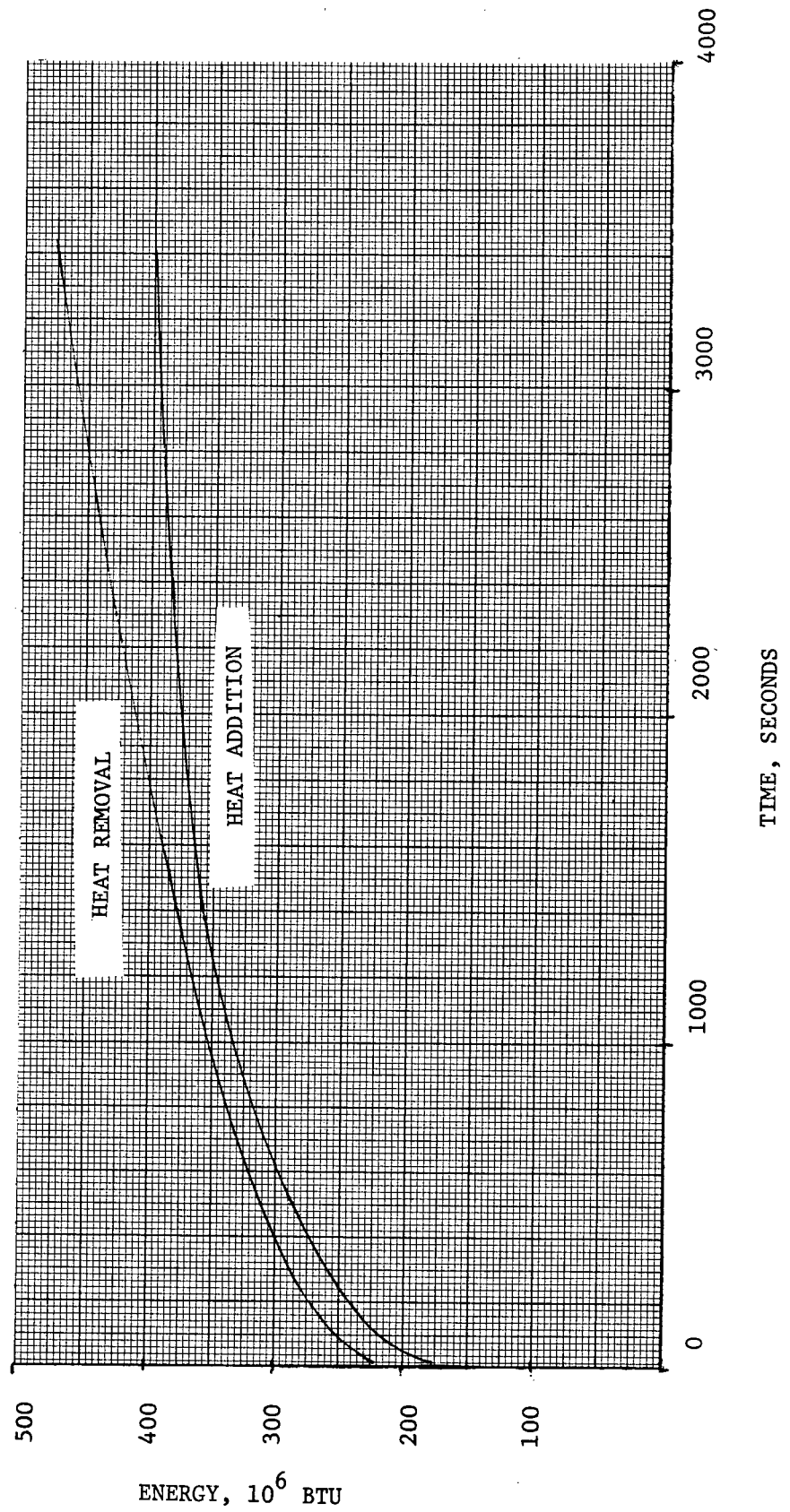


FIGURE 14.3.4-11

CONTAINMENT CAPABILITY STUDY HEAT REMOVAL

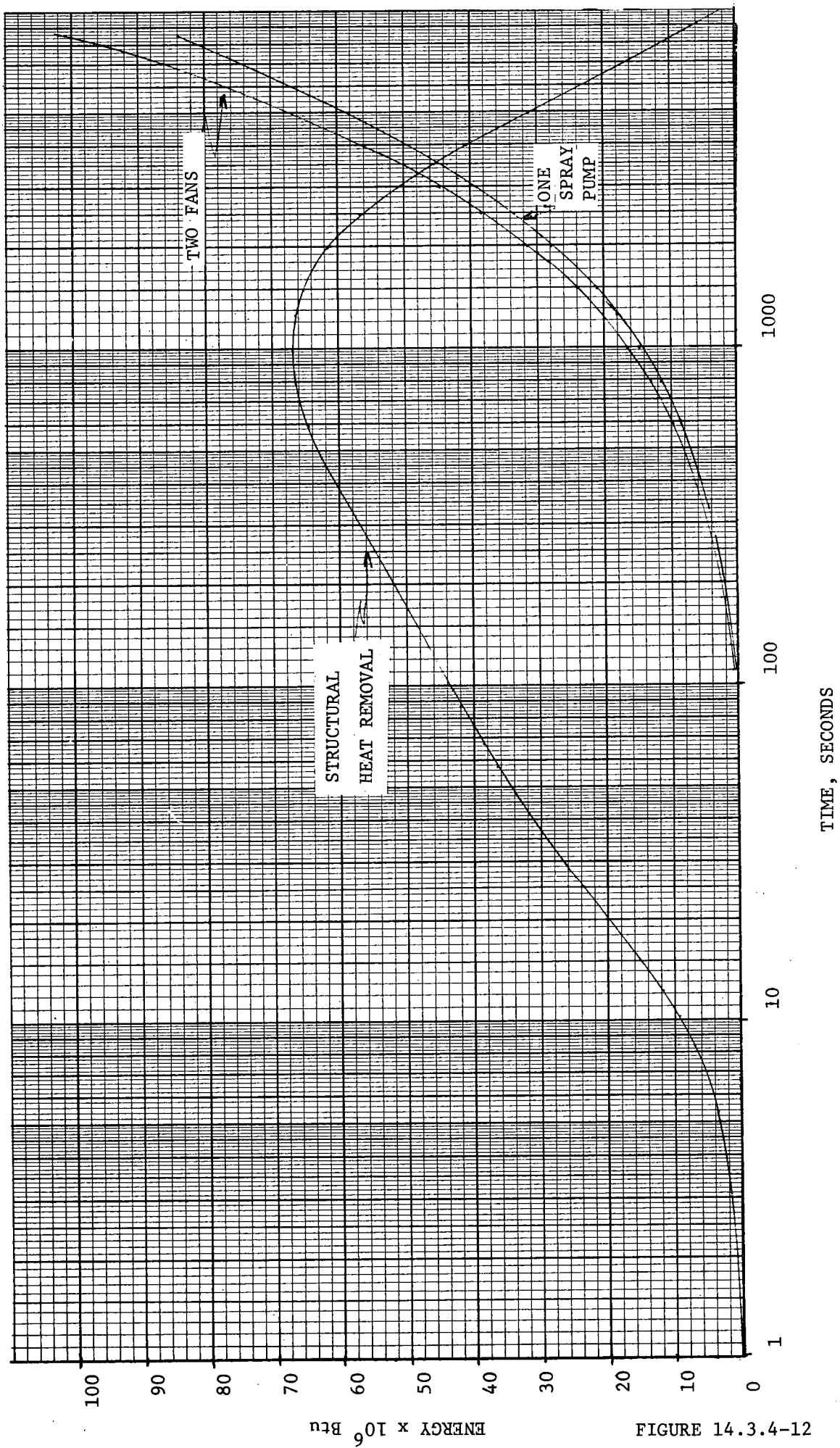


FIGURE 14.3.4-12

ENERGY $\times 10^6$ Btu

TIME, SECONDS

CONTAINMENT CAPABILITY STUDY HEAT SOURCE

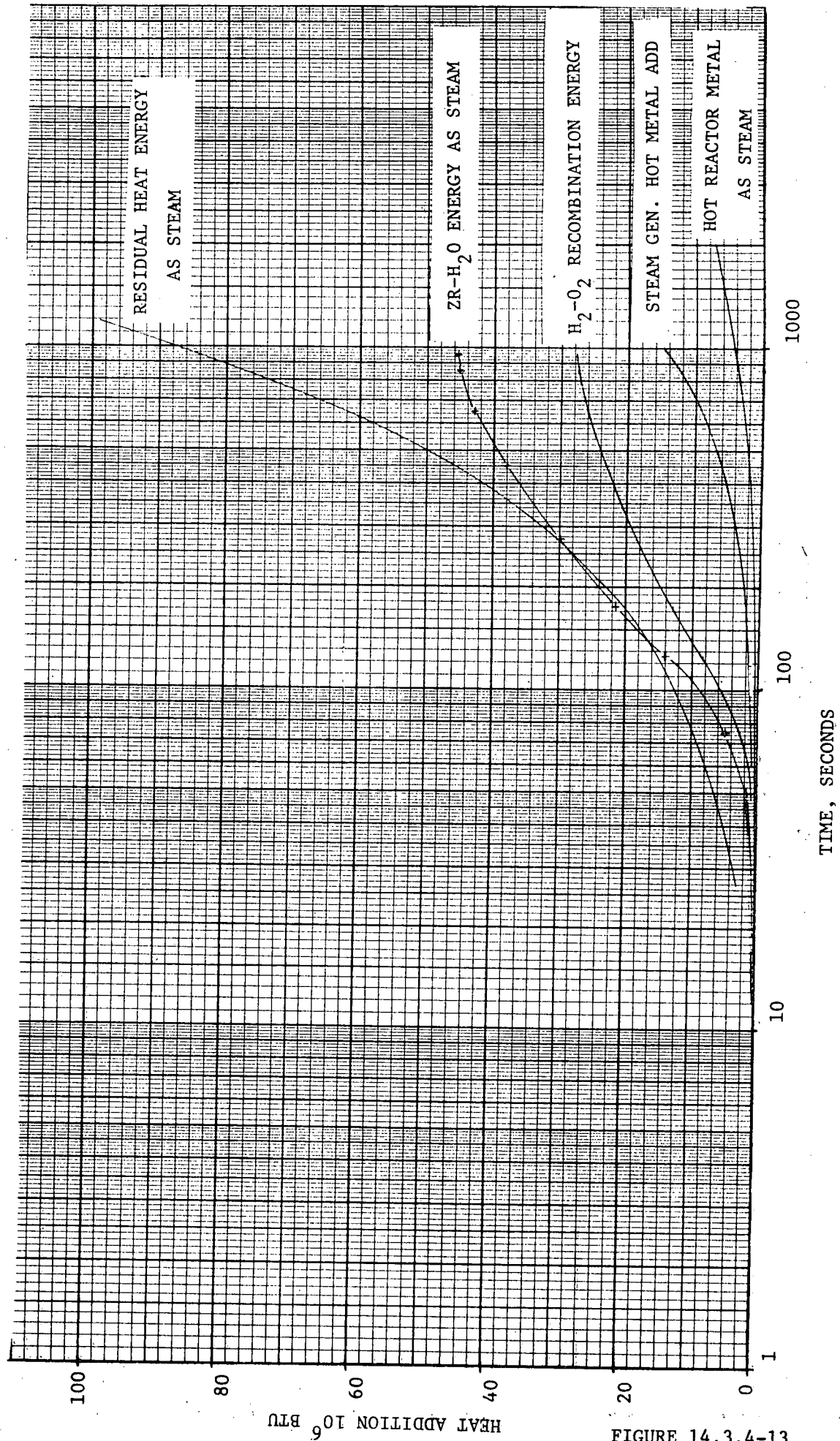


FIGURE 14.3.4-13

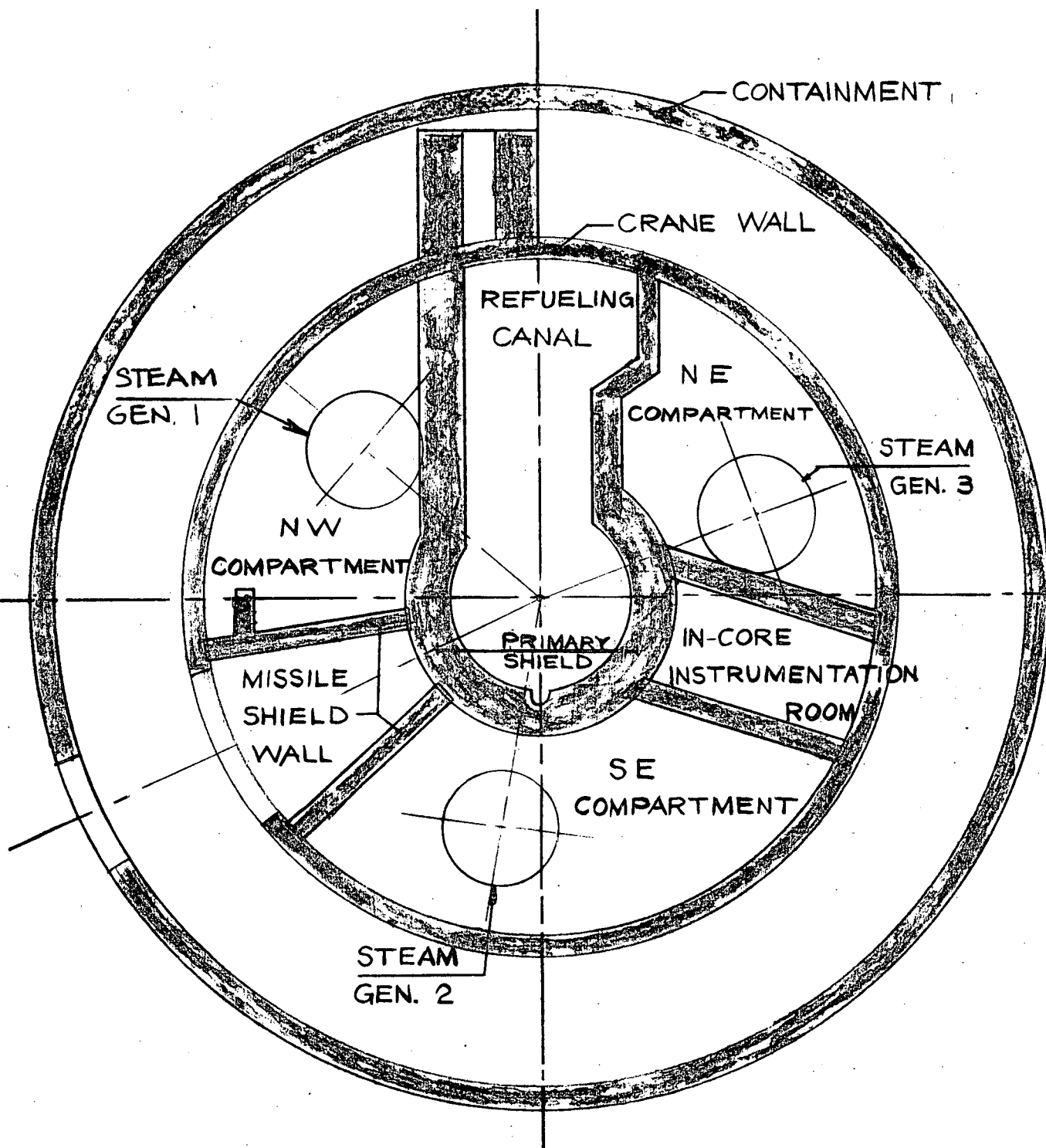


FIG. 14.3.4-14

AMENDMENT 3

14.3.5 ENVIRONMENTAL CONSEQUENCES OF LOSS-OF-COOLANT ACCIDENT

The results of analyses presented in this section demonstrate that the amounts of radioactivity released to the environment in the event of a loss-of-coolant accident do not exceed the limits specified in 10 CFR 100. The calculated inhalation doses are summarized in Table 14.3.5-2.

Basic Events and Release Fractions

The event causing the postulated releases is a double-ended rupture of a reactor coolant pipe, with subsequent blowdown, as described in Section 14.3.4. As demonstrated by the analysis in Section 14.3.2, the Emergency Core Cooling System, using emergency power, keeps cladding temperatures well below melting and limits zirconium - water reactions to an insignificant level, assuring that the core remains intact and in place. As a result of the increase in cladding temperature and the rapid depressurization of the core, however, some cladding failure may occur in the hottest regions of the core.

The off-site doses have been analyzed for two cases. In the first case, the design basis accident, it has been assumed that the entire inventory of volatile fission products contained in the pellet-cladding gap is released during the time the core is being flooded by the Emergency Core Cooling System. Of this gap inventory, 50% of the halogens and 100% of the noble gases are considered to be released to the containment atmosphere. It has also been assumed that 2.5% of the halogens originally present in the gaps are available for leakage from the containment in organic forms, and are not subject to plate-out. The remaining 47.5% of the gap inventory is considered to be in elemental form, and is assumed to be subject to condensation and plate-out on the containment surfaces at the rate of 1.0 hr^{-1} . After two hours, no further decrease is assumed to occur due to condensation or plate-out. The basic inventories, release fractions, and initial activities in the containment atmosphere used in the analysis of this case are listed in Table 14.3.5-1.

3 In the second case, the off-site doses resulting from a hypothetical accident assuming larger activity releases have been analyzed. Activity releases of these magnitudes have a considerably lower probability than those associated with design basis accident. For the analysis of the hypothetical case, it has been assumed that 50% of the core inventory of halogens and 100% of the core inventory of noble gases are released to the containment atmosphere. It has also been assumed that 2.5% of the halogens originally present in the core are available for leakage from the containment in organic forms, and are not subject to plate-out. The remaining 47.5% of the core inventory is considered to be in elemental form, and is assumed to be subject to plate-out and condensation on the containment surfaces at the rate of 1.0 hr^{-1} for the first two hours. The basic inventories, release fractions, and initial activities in the containment atmosphere used in the analysis of this case are listed in Table 14.3.5-2.

The calculations of total core inventories were consistent with the methods used in TID-14844⁽¹⁾ and data from ORNL-2127.⁽²⁾ Operation of the core at 2300 MWt for 500 days was assumed. The inventories present in the fuel rod gap resulting from diffusion through the pellet material were calculated using the following expression for the diffusion coefficient.

$$D(T) = D(1673) \exp \left[-\frac{E}{R} \left(\frac{1}{T} - \frac{1}{1673} \right) \right]$$

The quantities E and R are the activation energy and the gas constant, respectively, and the temperature (T) is in degrees Kelvin. This relationship is valid for temperatures above 1100°C, and below 1100°C. The diffusion coefficient was assumed constant at the 1100°C value.

A conservative value of $1.0 \times 10^{-11} \text{ sec}^{-1}$ for $D(1673)$, based on data at burnups greater than 10^{19} fissions/cc, was used to account for other possible mechanisms of release, such as pellet cracking. The diffusion coefficient for iodine was assumed to be the same as that for xenon and krypton. Toner and Scott⁽³⁾ observed that iodine diffuses at about the same rate in UO_2 as xenon and krypton, and data surveyed and reported by Belle⁽⁴⁾ indicated that iodine diffuses at a slightly slower rate.

In determining the gap inventories, the fuel pellets were grouped into five concentric rings, each having a release rate dependent upon the mean fuel temperature in the ring. Results show that less than 3% of the core iodine inventory (dose - weighted) will be released to the gap, and that about 2.5% of the core inventory of noble gases reaches the gap. The gap inventories of Kr - 85m, Kr - 87, and Kr - 88 are negligible, since the half-lives for natural decay are short compared to the times required for diffusion to the pellet surfaces.

It is not expected that a significant amount of organic iodine would be liberated from the fuel as a result of a loss-of-coolant accident. This conclusion is based on the results of fuel meltdown experiments conducted by the Oak Ridge National Laboratory. The fraction of the total iodine which is released in organic forms is expected to be on the order of 0.2 per cent, or less, since the rate of thermal radiolytic decomposition would exceed the rate of production.

Organic compounds of iodine can be formed by reaction of absorbed elemental iodine on contaminated surfaces of the containment vessel. Recent experiments have shown that the rate of formation is dependent on specific test conditions such as the concentrations of iodine and impurities, radiation levels, pressures, temperatures, and relative humidity. The rate of conversion of airborne iodine is proportional to the surface to volume ratio of the enclosure, whether the process is limited by diffusion to the surface or by the reaction rate of the absorbed iodine. The yields of organic iodine observed as a function of aging time in various test enclosures were extrapolated to determine the values for the H. B. Robinson containment vessel, using the variation of the surface to volume ratios. The iodine conversion rates predicted in this manner did not exceed 0.0035 per cent of the atmospheric iodine per hour.

Containment Release Rate

The maximum acceptable leak rate for the containment vessel is 0.1 per cent per day, at the containment design pressure, and without the

benefit of the Isolation Valve Seal Water System or the Penetration Pressurization System. All penetrations are constructed with a double barrier, and the intermediate space is maintained at a pressure above the containment design pressure during reactor operation. The Isolation Valve Seal Water System, described in Section 5, provides a water seal in pipelines during accident conditions. The containment vessel release rates used in the dose calculations were based on the blowdown curves presented in Figures 14.3.4-2 through 14.3.4-8. The design leak rate of 0.1% per day ($1.16 \times 10^{-8} \text{ sec}^{-1}$) was assumed to be maintained throughout the first 24 hours, and a leak rate of 0.045% per day ($0.52 \times 10^{-8} \text{ sec}^{-1}$) was maintained for the remainder of the 30 day period. These leak rates are based on figures 14.3.5-1 and 14.3.5-2.

Methods of Analysis

The quantities of activity released from the containment were calculated with the PREL digital computer code, which solves the following first order linear differential equation for each isotope.

$$\frac{dC(I)}{dt} = -\lambda(I) C(I)$$

Where:

$C(I)$ = containment inventory if isotope I at any time, curies
 $\lambda(I)$ = total removal rate of isotope I, hr^{-1}
 t = time, hr

The total removal rate $\lambda(I)$, is the sum of the rates of reduction of the containment inventory due to natural decay, leakage, plate-out and sprays. The code uses values of $\lambda(I)$ which are constant for each of the several time periods in a computation. The initial inventories used in this analysis are listed in Tables 14.3.5-1 and 14.3.5-2. The removal rates used for each process are discussed in Appendix A. The total activity of each isotope released from the containment for each time period is computed with the relationship:

$$Q(I,T) = \lambda_L(I) \int_{t_1}^{t_2} C(I) dt$$

where:

$Q(I,T)$ = activity of isotope I released in time $t_2 - t_1$, curies

$\lambda_L(I)$ = containment leak rate, hr^{-1}

The resulting activity releases are used in the WEDOSE digital code to calculate the off-site inhalation and whole body doses. The WEDOSE code used the following standard relationship for the inhalation dose from each isotope for each time period:

$$D(I, T) = Q(I, T) \cdot DCF(I) \cdot B(T) \cdot \frac{X}{Q}(x, T)$$

where the undefined terms are:

$D(I,T)$ = inhalation dose from isotope I during period T, rems

$DCF(I)$ = inhalation dose conversion factor for isotope I, rem/curie

$B(T)$ = breathing rate, m^3/sec

$\frac{X}{Q}(x,T)$ = atmospheric dilution factor, sec/m^3

For the computation of the whole body doses from cloud immersion, the equation for the semi-infinite spherical model was used, as follows:

$$D(I, T) = 0.246 Q(I, T) \cdot E(I) \cdot \frac{X}{Q}(x, T)$$

The values of average energy per disintegration, $E(I)$, the decay constants, and the dose conversion factors used are listed in Table 14.3.5-3. Values of the atmospheric dilution factor for the site boundary and low population zone distances were presented in Section 2 and are listed along with the breathing rates in Table 14.3.5-4. The contribution to the whole body dose from direct radiation from the containment was found to be negligible.

Spray System Iodine Removal Rates

The effectiveness of the spray system for elemental iodine removal is discussed in Appendix 6A. For the H. B. Robinson plant, a three loop design, an iodine removal coefficient of 18.7 hr^{-1} was calculated.

3

Discussion of Resulting Doses

As shown in Table 14.3.5-5, all doses resulting from the accidents studied are below the guideline levels given in 10CFR100. Because of the combination of independent conservative assumptions, the doses actually expected following the occurrence of any of these accidents would be much lower than the values tabulated.

References

1. DiNunno, J. J., et. al., Calculation of Distance Factors for Power and Test Reactor Sites, AEC Report Number TID-14844, March 23, 1962.
2. Blomeke, J. O., and Todd, M. F., Uranium - 235 Fission - Product Production as a Function of Thermal Neutron Flux, Irradiation Time, and Decay Time, AEC Report Number ORNL-2127, August 19, 1957.
3. Toner, D. F., and Scott, J. S., Fission Product Release from UO₂ Nuclear Safety, Vol. 3, No. 2, December, 1961.
4. Belle, J., Uranium Dioxide: Properties and Nuclear Applications, Naval Reactor, DRD of USAEC, 1961.
5. Perkins, J. F., and King, R. W., Energy Release from the Decay of Fission Products; Nuclear Science and Engineering, 3, 1958.

References

1. DiNunno, J. J., et. al., Calculation of Distance Factors for Power and Test Reactor Sites, AEC Report Number TID-14844, March 23, 1962.
2. Blomeke, J. O., and Todd, M. F., Uranium - 235 Fission - Product Production as a Function of Thermal Neutron Flux, Irradiation Time, and Decay Time, AEC Report Number ORNL-2127, August 19, 1957.
3. Toner, D. F., and Scott, J. S., Fission Product Release From UO_2 , Nuclear Safety, Vol. 3, No. 2, December, 1961.
4. Belle, J., Uranium Dioxide: Properties and Nuclear Applications, Naval Reactors, DRD of USAEC, 1961.

TABLE 14.3.5-1

ISOTOPE INVENTORIES - DESIGN BASIS ACCIDENT

Isotope	Gap Inventory (Curies)	Fraction Available for Leakage from Containment	Initial Containment Inventory (Curies)
I-131 (inorg.)	12.9×10^5	0.475	6.13×10^5
I-132 (inorg.)	2.24×10^5	0.475	1.06×10^5
I-133 (inorg.)	10.2×10^5	0.475	4.84×10^5
I-135 (inorg.)	5.08×10^5	0.475	2.41×10^5
I-131 (org.)	0.0	0.025	3.23×10^4
I-132 (org.)	0.0	0.025	5.6×10^3
I-133 (org.)	0.0	0.025	2.55×10^4
I-135 (org.)	0.0	0.025	1.27×10^4
Xe-133	24.5×10^5	1.00	24.5×10^5
Xe-133m	0.39×10^5	1.00	0.39×10^5
Xe-135	0.56×10^5	1.00	0.56×10^5
Xe-135m	0.0	1.00	0.0
Kr-85	1.41×10^5	1.00	1.41×10^5
Kr-85m	0.0	1.00	0.0
Kr-87	0.0	1.00	0.0
Kr-88	0.0	1.00	0.0

TABLE 14.3.5-2

ISOTOPE INVENTORIES - HYPOTHETICAL ACCIDENT

Isotope	Core Inventory (Curies)	Fraction Available for Leakage from Containment	Initial Containment Inventory (Curies)
I-131 (inorg.)	5.6×10^7	0.475	2.66×10^7
I-132 (inorg.)	8.62×10^7	0.475	4.09×10^7
I-133 (inorg.)	12.9×10^7	0.475	6.13×10^7
I-135 (inorg.)	11.8×10^7	0.475	5.61×10^7
I-131 (org.)	0.0	0.025	1.40×10^6
I-132 (org.)	0.0	0.025	2.16×10^6
I-133 (org.)	0.0	0.025	3.23×10^6
I-135 (org.)	0.0	0.025	2.95×10^6
Xe-133	12.9×10^7	1.00	12.9×10^7
Xe-133m	0.31×10^7	1.00	0.31×10^7
Xe-135	6.32×10^7	1.00	6.32×10^7
Xe-135m	0.0	1.00	0.0
Kr-85	0.083×10^7	1.00	0.083×10^7
Kr-85m	2.53×10^7	1.00	2.53×10^7
Kr-87	4.89×10^7	1.00	4.89×10^7
Kr-88	7.03×10^7	1.00	7.03×10^7

TABLE 14.3.5-3

PHYSICAL DATA FOR ISOTOPES

Isotope	Decay Constant* (Hr ⁻¹)	Beta Energy** (Mev/Dis.)	Gamma Energy** (Mev/Dis.)	Dose Conversion Factor* (Rem/Curie)
I-131	0.358×10^{-2}	1.83×10^{-1}	3.92×10^{-1}	$1.48 \times 10^{+6}$
I-132	$0.297 \times 10^{+0}$	4.85×10^{-1}	2.13×10^0	5.35×10^4
I-133	0.331×10^{-1}	4.93×10^{-1}	5.65×10^{-1}	4.00×10^5
I-135	$0.102 \times 10^{+0}$	3.16×10^{-1}	1.68×10^0	1.24×10^5
Xe-133	5.47×10^{-3}	1.55×10^{-1}	2.70×10^{-2}	-
Xe-133m	1.26×10^{-2}	2.07×10^{-1}	2.60×10^{-2}	-
Xe-135	7.60×10^{-2}	3.04×10^{-1}	2.61×10^{-1}	-
Xe-135m	1.03×10^{-1}	1.04×10^{-1}	4.16×10^{-1}	-
Kr-85	7.95×10^{-6}	2.21×10^{-1}	4.00×10^{-3}	-
Kr-85m	1.59×10^{-1}	2.52×10^{-1}	1.57×10^{-1}	-
Kr-87	5.33×10^{-1}	1.34×10^0	1.59×10^0	-
Kr-88	2.50×10^{-1}	3.72×10^{-1}	1.92×10^0	-

* Reference 1.

** Reference 5.

TABLE 14.3.5-4

ATMOSPHERIC DILUTION FACTORS

Time Period (Hours)	Site Boundary (425 m)	Low Population Zone (7242 m)
0 - 12	7.1×10^{-4}	4.0×10^{-5}
12 - 24	1.8×10^{-4}	7.2×10^{-6}
24 - 720	3.0×10^{-5}	8.0×10^{-7}

Time Period (Hours)	Breathing Rates (M ³ /sec)
0 - 8	3.47×10^{-4}
8 - 24	1.75×10^{-4}
24 - 720	2.32×10^{-4}

Table 14.3.5-5

SUMMARY OF OFF-SITE DOSES FROM
LOSS-OF-COOLANT ACCIDENT

THYROID DOSES - REM

	Site Boundary - 2 Hours	LPZ - 30 Days
10CFR100 Guidelines	300	300
Design Basis Accident	1.8	0.45
Hypothetical Accident	116	26

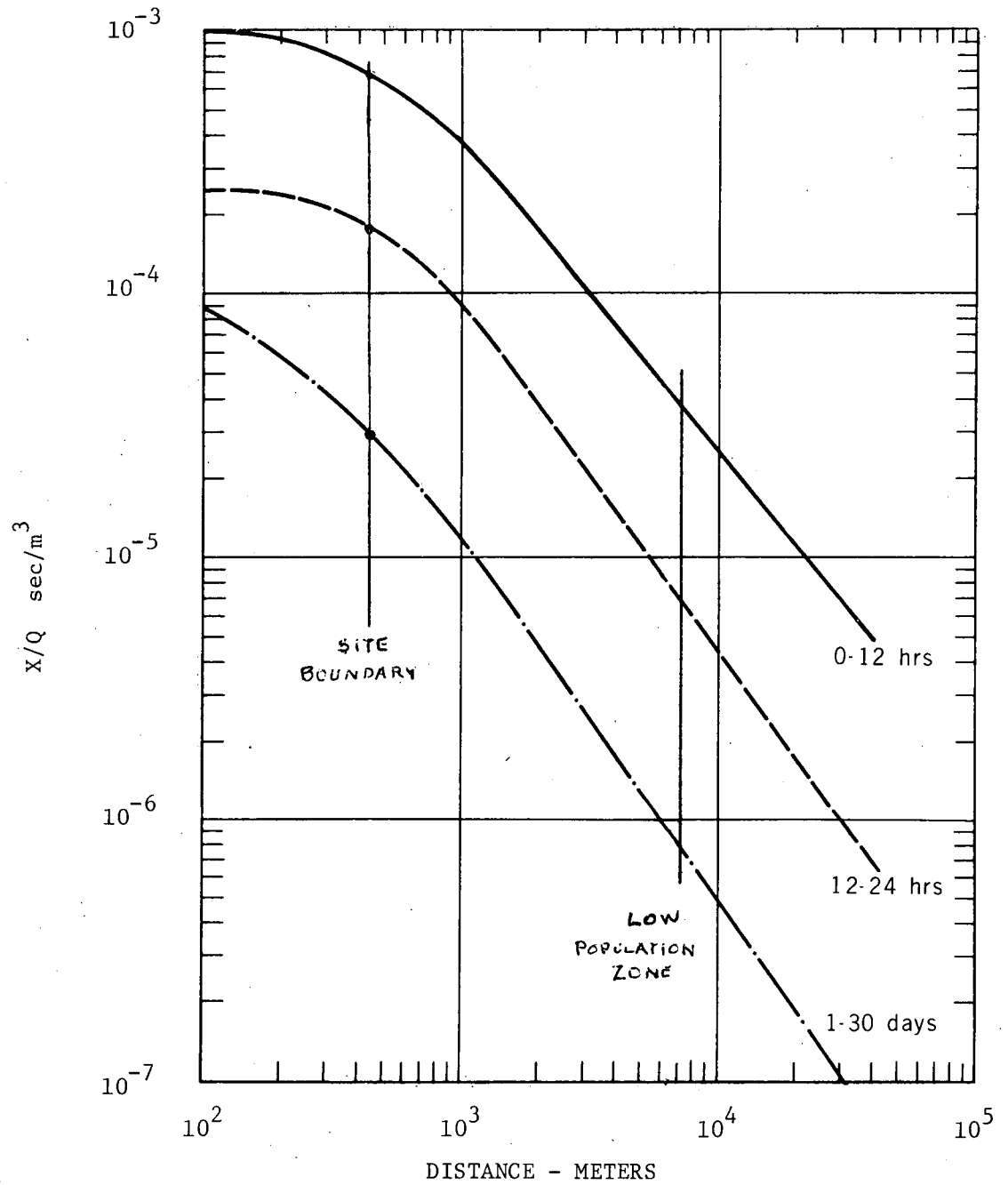
WHOLE BODY DOSES - REM

	Site Boundary - 2 Hours	LPZ - 30 Days
10CFR100 Guidelines	25	25
Design Basis Accident	0.009	0.004
Hypothetical Accident	4	0.7

BASED ON SITE DATA

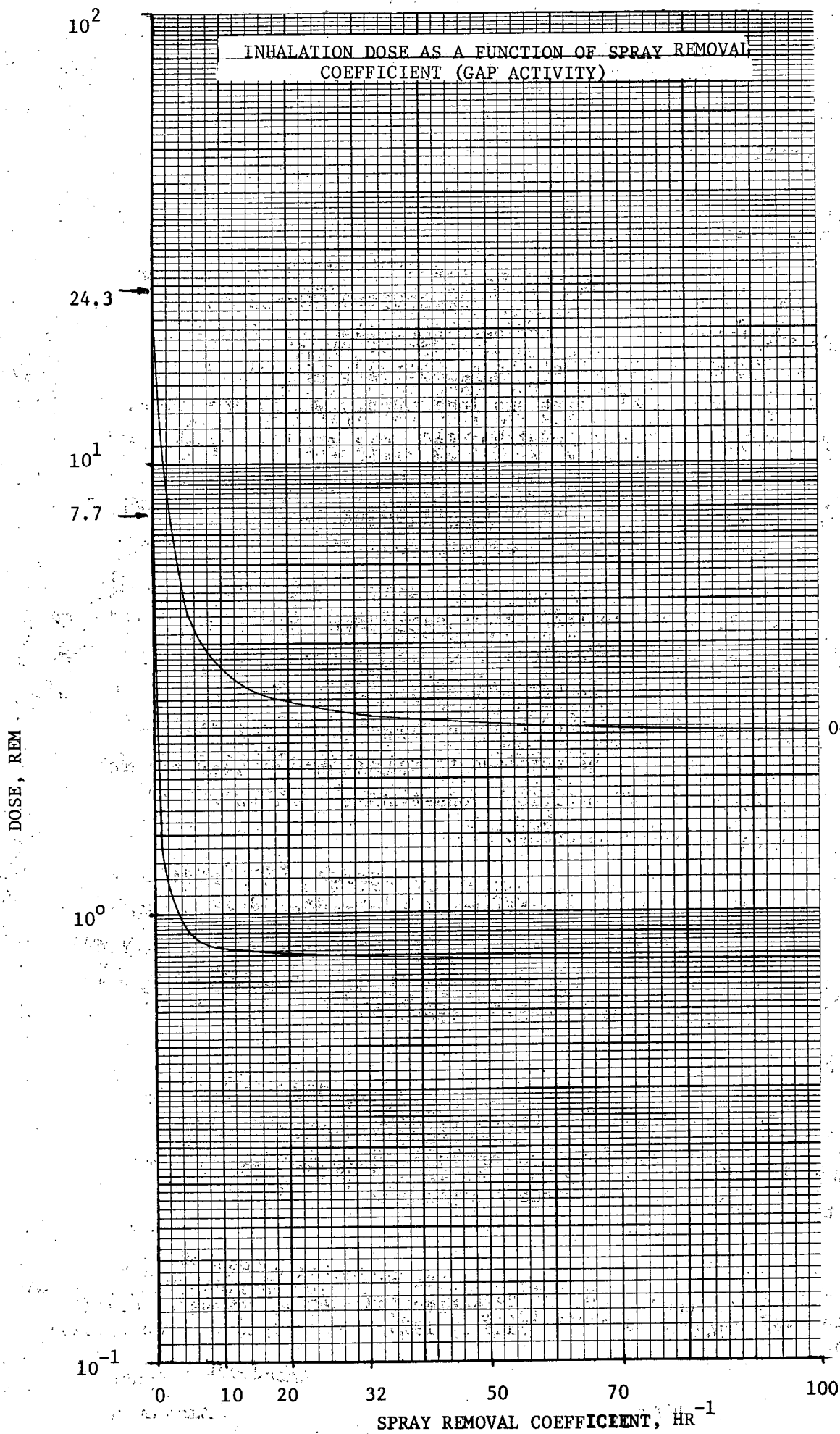
4/67 - 4/68

BLDG. WAKE $C = 1/2$, $A = 2000 \text{ m}^2$



SITE DISPERSION FACTORS

FIGURE 14.3.5-1



0-2 HR
SB

0-30 DAY
LPZ

FIGURE 14.3.5-2

APPENDIX 14A

H. B. Robinson Unit No. 2 Supplement

The FSAR for the H. B. Robinson Unit No. 2 plant presented a complete analysis for the loss-of-coolant accident (14.3.2) at a peak kw/ft of 19.1, which corresponds to 102% of the maximum calculated thermal rating of 2300 MWt. The conservatisms inherent in this analysis were discussed on page 14.3.2-12. A maximum clad temperature of 2450°F was predicted to occur for the double ended cold leg break. At a peak kw/ft of 18.3, which corresponds to 102% of the initial rating of 2200 MWt, the predicted peak clad temperature would be reduced to a value of 2280°F.

In Amendment 13 Tab IX to the FSAR it was shown that the design peak clad temperature and metal water reactions calculated were substantially below acceptable values as determined by the Westinghouse Experimental Rod Quench Tests. It was therefore concluded that the quench mechanism during the reflooding phase of a LOCA does not lead to rod shattering or loss of integrity over the range of conditions conservatively estimated for the H. B. Robinson Unit No. 2 LOCA analysis.

It has been suggested that the capability of Emergency Core Cooling System should be increased to reduce the maximum clad temperatures. It should be emphasized that additional margins are available by virtue of the conservatisms in the analysis. Any changes to the Emergency Core Cooling System are therefore unwarranted.

Improved analytical models, which have been developed and experimentally verified,⁽¹⁾ now make it possible to quantify the additional conservatism that is claimed in the design of the Emergency Core Cooling System.

(1) J. W. Dorrycott and J. Shefcheck "PWR Core Behavior Following a Loss of Coolant Accident", WCAP 7422-L, January 1970. (Westinghouse Proprietary)

1. Mass flow rate, coolant quality, pressure and power parameters are determined by the SATAN-V code.
2. The assumption that stable film boiling occurs immediately following DNB is no longer used. Credit is taken for the higher heat transfer coefficients which exist during the transition and film boiling periods after the occurrence of DNB.
3. During the reflooding phase of the accident, the film heat transfer coefficient as calculated by the dispersed flow correlation is allowed to increase as more of the core is reflooded. This is a change from the analysis presented in the FSAR where a constant value of $25 \text{ Btu/hr-ft}^2\text{-}^\circ\text{F}$ is assumed.

The double ended cold leg break was analyzed using this improved but still conservative treatment of the core thermal transient. This break was selected because it experienced the highest peak clad temperature in the

FSAR analysis. The power distribution (maximum power density of 19.1 kw/ft) was used in the analysis. The power level was 102% of the 2300 MWt maximum calculated thermal rating to account for possible errors in the steam cycle calorimeter measurements.

The analysis resulted in a peak maximum clad temperature of 1790°F which occurred 28.6 seconds after the accident. It should be noted that an additional 28 seconds could be tolerated before any fuel clad melt would be reached.

Figures 1 and 2 present the important results of this analysis. Figure 1 presents the core flow, pressure, and heat transfer coefficient vs. time. Figure 2 presents the clad temperature vs. time.

Inherent in the design of the Emergency Core Cooling System for H. B. Robinson Unit #2 is the additional margin between the results presented in the FSAR and those evaluated above with improved analytical methods.

DOUBLE ENDED COLD LEG BREAK

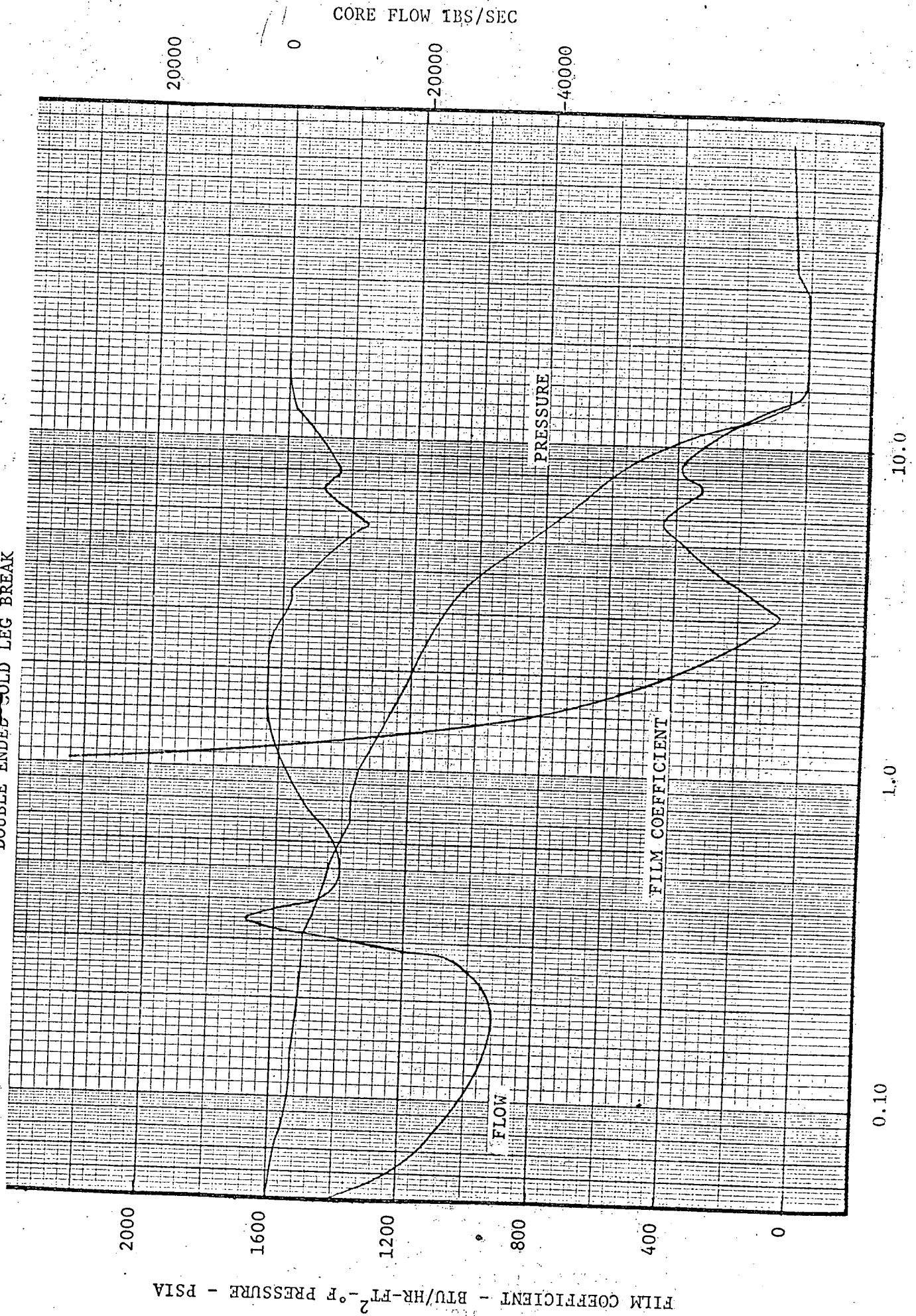
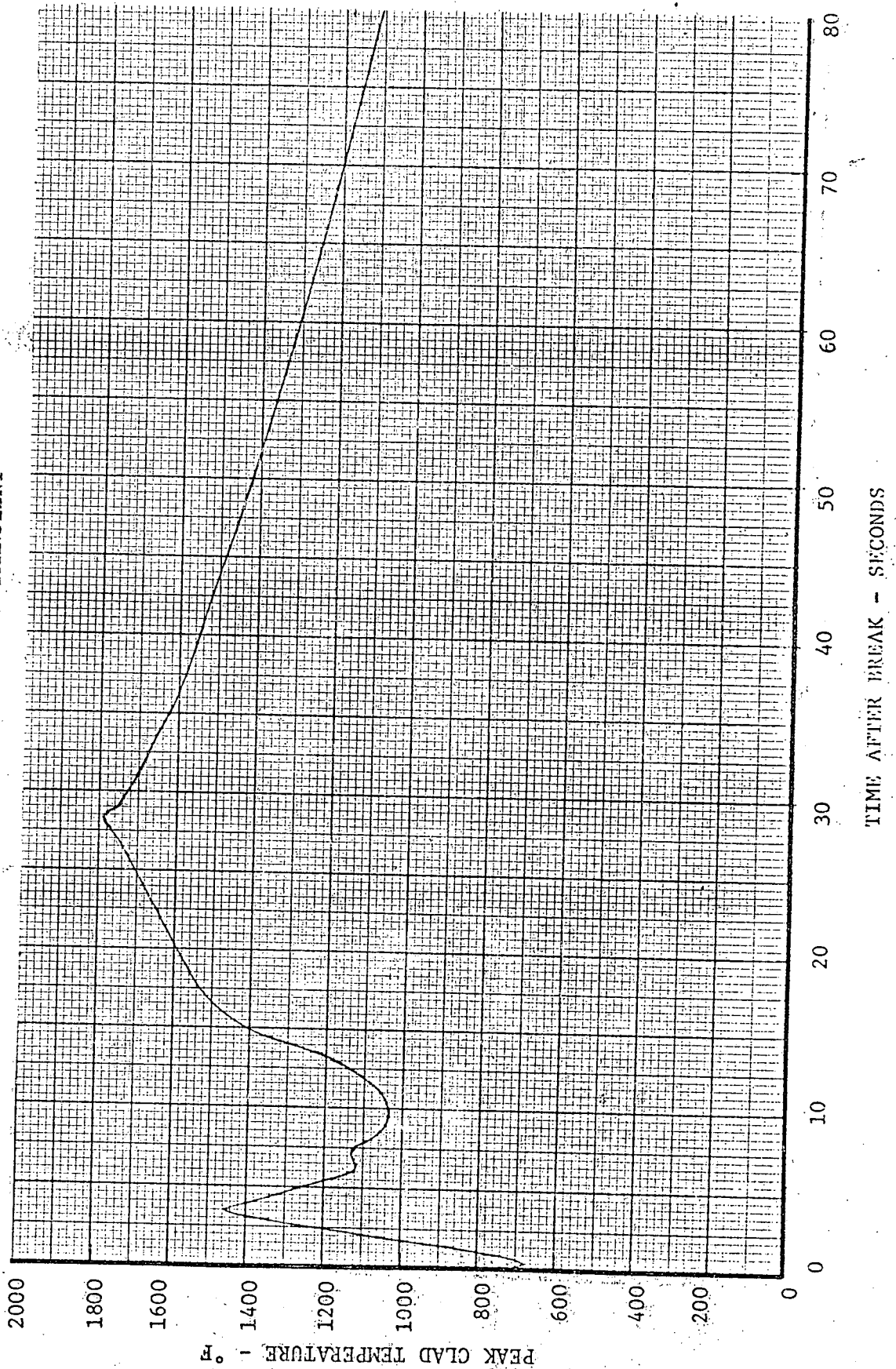


Figure 1

DOUBLE ENDED COLD LEG BREAK
CLAD TEMPERATURE TRANSIENT



APPENDIX 14B

STEAM GENERATOR TUBE RUPTURE

Justification of 70,000 Pounds Carryover to the Secondary Side

The break flow following a complete tube failure is calculated to be approximately 80 lbs per second at a pressure differential of 1500 psi between the primary and secondary systems, and it is assumed that as the pressure varies the resultant flow is proportional to the square root of the pressure differential. Immediately after the postulated accident, pressurizer pressure and level will decrease until the reactor trip point is reached in about 3 minutes. During this period the average break flow is about 74 lbs per second corresponding to the reduced primary to secondary pressure differential and the total mass transfer in the first 3 minutes is therefore 13,300 lbs.

Following reactor trip, the pressurizer level will fall rapidly and the safety injection actuation signal will be generated leading to actuation of the safety injection pumps. In the first two or three minutes after plant trip, the primary system pressure will dip through a minimum and eventually reach stability at the pressure where the flow through the break is balanced by incoming safety injection flow. This flow is about 270 gpm or 37 lbs/second. Since the reactor pressure passes through a minimum before reaching equilibrium at 1400 psia, the 37 lbs/second is the average break flow in the twenty-seven minute interval subsequent to plant trip. The total mass transfer in this interval is therefore 60,000 lbs.

Thus, in the absence of any Operator action, approximately 73,300 lbs of primary system fluid could be transferred to the secondary system in the 30 minute period after the accident and prior to the time the faulty steam generator is isolated.

The mass transfer estimated above is pessimistic in two respects. First, no consideration is given to the fact that the safety injection pump would

be regulated when water level returns in the pressurizer, as suggested in the Emergency Operating Instructions. This would result in an average break flow of less than the 37 lbs/second assumed above. Secondly, as decay heat and core stored heat sources gradually reduce after plant trip, the reactor coolant temperature will gradually decrease. Therefore in order to maintain an equilibrium pressure, the break flow will be less than the incoming safety injection flow during the twenty-seven minutes subsequent to plant trip.

Thus the 70,000 pounds was taken as a conservative mass carryover for this postulated accident.